

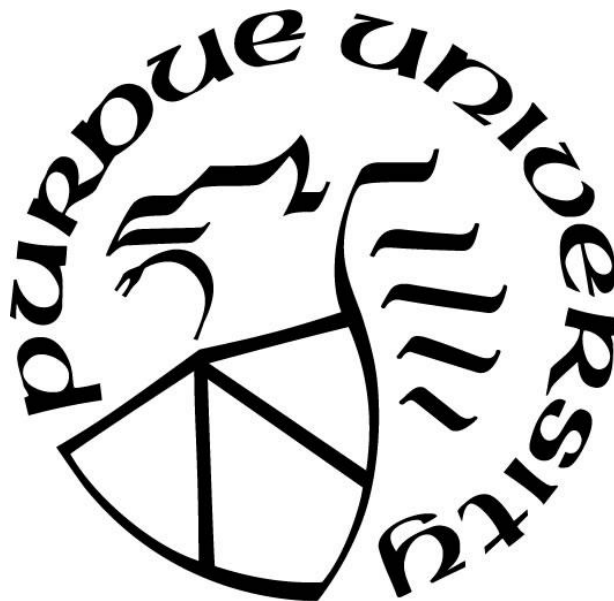
**INTEGRATED MODELING FRAMEWORK FOR DYNAMIC  
INFORMATION FLOW AND TRAFFIC FLOW UNDER VEHICLE-TO-  
VEHICLE COMMUNICATIONS: THEORETICAL ANALYSIS AND  
APPLICATION**

by  
**Yong Hoon Kim**

**A Dissertation**

*Submitted to the Faculty of Purdue University  
In Partial Fulfillment of the Requirements for the degree of*

**Doctor of Philosophy**



Lyles School of Civil Engineering  
West Lafayette, Indiana  
December 2019

**THE PURDUE UNIVERSITY GRADUATE SCHOOL  
STATEMENT OF COMMITTEE APPROVAL**

**Dr. Srinivas Peeta, Chair**

School of Civil and Environmental Engineering  
Georgia Institute of Technology

**Dr. Kumares Sinha**

Lyles School of Civil Engineering

**Dr. Daniel A. DeLaurentis**

School of Aeronautics and Astronautics

**Dr. Fred L. Mannering**

Department of Civil and Environmental Engineering  
University of South Florida

**Approved by:**

Dr. Dulcy M. Abraham, Chair, Burke Graduate Program,  
Lyles School of Civil Engineering

*To my family*

## ACKNOWLEDGMENTS

I would first like to express my thanks to my Ph.D. advisor, Dr. Srinivas Peeta, for his technical and philosophical guidance, as well as his constant encouragement throughout my time as a student. His devotion and enthusiasm for education and research have been and will always be an inspiration in my life.

I would like to thank all my committees to, Dr. Kumares C. Sinha, Dr. Fred L. Mannering, Dr. Daniel A. DeLaurentis, and Dr. Samuel Labi for their guidance towards excellence. Besides, I thank the rest of the faculty in Transportation and Infrastructure Systems Engineering throughout my stay at Purdue University. I would also like to thank Dr. Xiaozheng He for his constructive comments and collaboration. Many thanks to Dr. Lili Du, Dr. Salvador Hernandez, Dr. Georgios Kalafatas, Dr. Yu-Ting Hsu and Dr. Amit Kumar for their help and collaborations in my academic career. Many thanks to every member of NEXTRANS Center for supporting me and making my stay at Purdue University a memorable one.

Finally, my heartfelt gratitude goes to my parents, parents-in-law, and my family whose wholehearted support, encouragement, love and affection make this accomplishment possible for me.

# TABLE OF CONTENTS

LIST OF TABLES .....	11
LIST OF FIGURES .....	12
ABSTRACT .....	15
1. INTRODUCTION .....	18
1.1 Background .....	18
1.2 Objectives of the dissertation .....	20
1.3 Organization of the dissertation .....	23
2. GRAPH-BASED MODELING OF INFORMATION FLOW EVOLUTION AND PROPAGATION UNDER V2V COMMUNICATIONS BASED ADVANCED TRAVELER INFORMATION SYSTEMS .....	25
2.1 Introduction .....	25
2.2 Preliminaries .....	29
2.2.1 The integrated multi-layer network framework .....	29
2.2.1.1 Notation .....	30
2.2.2 Physical traffic network .....	32
2.2.3 Virtual inter-vehicle communication network .....	33
2.2.4 Graph-based representation of information flow network .....	35
2.2.4.1 Information flow generation/deletion .....	37
2.2.4.2 Information flow evolution and propagation .....	38
2.2.5 Graph structure and reverse search algorithm for vehicle knowledge identification .....	41
2.3 Retrospective modeling capability in the graph-based framework .....	42
2.3.1 Vehicle knowledge update in simulation-based approach .....	42
2.3.2 Retrospective modeling capabilities .....	44
2.3.2.1 Retrospective modeling of the integrated multi-layer network .....	44
2.3.2.2 Information propagation chain .....	44
2.3.3 Efficiency of the graph database .....	49
2.3.3.1 Graph database in the graph-based approach .....	49
2.3.3.2 Memory usage efficiency .....	50
2.3.3.3 Computational efficiency .....	50

2.4	Numerical experiments .....	52
2.4.1	Experiment design .....	52
2.4.2	Information flow network size and construction time .....	53
2.4.3	Performance evaluation .....	53
2.4.3.1	Memory usage efficiency .....	53
2.4.3.2	Computational efficiency .....	55
2.4.4	Key insights for V2V-based ATIS .....	57
2.5	Summary and discussion.....	58
3.	AN ANALYTICAL MODEL TO CHARACTERIZE THE SPATIOTEMPORAL PROPAGATION OF INFORMATION UNDER VEHICLE-TO-VEHICLE COMMUNICATIONS .....	60
3.1	Introduction.....	60
3.2	Preliminaries .....	64
3.2.1	Epidemic model.....	64
3.2.2	Traffic flow model.....	66
3.3	Mathematic modeling of the spatiotemporal propagation of information .....	67
3.3.1	Modeling heterogeneous traffic flows .....	67
3.3.2	Modeling information flow propagation .....	68
3.3.3	Modeling the force of communication .....	69
3.3.4	Estimation of success rate of V2V communication.....	71
3.3.5	Deriving analytical formula for the wave speed of the information flow propagation . .....	74
3.4	Numerical experiments .....	76
3.4.1	Experiment Design .....	76
3.4.2	Uni-directional highway .....	77
3.4.3	Bi-directional highway .....	79
3.4.4	Uni-directional highway under different market penetration rates.....	81
3.4.5	Comparison of analytical and numerical results.....	82
3.4.6	Bi-directional highway with incident .....	83
3.5	Summary and discussion.....	85

4. MODELING THE INFORMATION FLOW PROPAGATION WAVE UNDER VEHICLE-TO-VEHICLE COMMUNICATIONS.....	86
4.1 Introduction.....	86
4.1.1 Background.....	86
4.1.2 Information flow propagation wave (IFPW).....	89
4.2 Modeling the spatiotemporal propagation of information flow.....	93
4.2.1 Modeling framework.....	93
4.2.2 Characteristics of V2V communication.....	95
4.2.3 Spatial susceptible-informed model.....	97
4.2.4 Traffic flow model.....	98
4.2.5 Solutions for homogeneous and heterogeneous conditions.....	99
4.3 Closed-form solution of IFPW speed for homogeneous traffic conditions.....	101
4.3.1 Information dissemination wave speed.....	101
4.3.2 Traffic flow propagation wave speed.....	104
4.4 Numerical solution of IFPW speed for heterogeneous traffic conditions.....	105
4.4.1 Framework of numerical solution for heterogeneous conditions.....	105
4.4.2 Numerical method for SI model.....	106
4.4.3 Numerical method for single class traffic flow model.....	107
4.4.4 Intermediate component to connect the lower and upper layers.....	108
4.5 Numerical experiments.....	109
4.5.1 Experiment design.....	109
4.5.2 Parameter calibration of communication kernel.....	110
4.5.3 Comparison of the IFPW speeds of the closed-form and numerical solutions.....	114
4.5.3.1 IFPW speed under homogeneous traffic conditions and unidirectional flow.....	114
4.5.4 Shape of the IFPW and its asymptotic speed.....	117
4.5.5 IFPW under bidirectional flow and/or heterogeneous traffic conditions.....	119
4.5.5.1 Bidirectional flow.....	119
4.5.5.2 One-lane unidirectional highway with incident.....	120
4.6 Concluding comments.....	122
5. COUPLED HIDDEN MARKOV MODEL FOR TWO-STAGE MANEUVER-BASED MULTI-ANTICIPATIVE FORWARD COLLISION WARNING SYSTEM.....	124

5.1	Introduction.....	124
5.2	Two-stage MBMAM model-based FCW system .....	128
5.2.1	V2V communications for the MBMAM model .....	128
5.2.2	Capability enabled by the MBMAM model .....	129
5.2.3	MBMAM model-based FCW system.....	131
5.2.3.1	Conceptual modeling of driver maneuver intention.....	132
5.2.3.2	Proposed coupled HMM.....	135
5.2.3.3	Trajectory estimation using Gipps' car-following model.....	140
5.2.4	Two-stage criticality assessment .....	140
5.3	Experiment design .....	142
5.3.1	Experiment scenario .....	142
5.3.2	NGSIM data.....	142
5.3.3	Generation of driver maneuver states using NGSIM data.....	145
5.3.4	The two benchmark FCW systems .....	146
5.3.4.1	A single-stage FCW embedded with Knippling model.....	146
5.3.5	NHTSA physics-based motion model based two-stage FCW system.....	147
5.4	Numerical experiments .....	148
5.4.1	Performance index .....	148
5.4.2	Performance comparison .....	149
5.4.3	Timing of warnings.....	150
5.5	Concluding comments .....	151
6.	MODELING OF THE DYNAMIC FLOW PROPAGATION OF MULTIPLE UNITS OF INFORMATION UNDER V2V COMMUNICATIONS BASED ADVANCED TRAVELLER INFORMATION SYSTEMS .....	153
6.1	Introduction.....	153
6.2	The physical traffic flow and inter-vehicle communication layers .....	158
6.2.1	Physical traffic flow layer.....	158
6.2.2	Inter-vehicle communication layer .....	161
6.3	Information flow layer .....	164
6.3.1	Information flow network construction .....	164
6.3.2	Information flow generation/deletion .....	166

6.3.3	Information flow evolution and propagation.....	167
6.4	Characterizing the information flow dynamics.....	170
6.4.1	Graph structure of information flow network and the forward search algorithm to track the information flow propagation .....	170
6.4.2	Identification of information forward/backward propagation wave.....	171
6.5	Numerical experiments .....	172
6.5.1	Experiment setup .....	172
6.5.2	Interaction between the traffic flow and inter-vehicle communication layers .....	173
6.5.3	Information forward propagation wave .....	175
6.5.4	Spatiotemporal characteristics of vehicle knowledge.....	177
6.6	Summary and discussion.....	179
7.	<b>EVALUATION OF DECENTRALIZED VEHICLE-TO-VEHICLE COMMUNICATIONS-BASED ADVANCED TRAVELER INFORMATION SYSTEM .....</b>	<b>181</b>
7.1	Introduction.....	181
7.2	Decentralized V2V-based ATIS modeling framework.....	184
7.3	Modeling of the decentralized V2V-based ATIS components.....	186
7.3.1	Multi-layer framework for network-level interactions .....	186
7.3.1.1	Physical traffic flow network .....	186
7.3.1.2	V2V communications network.....	186
7.3.1.3	Graph-based representation of information flow network .....	188
7.3.2	Vehicle-level computations .....	189
7.3.2.1	Information processing .....	189
7.3.2.2	Routing decisions .....	191
7.4	Case study .....	192
7.4.1	Experiment setup .....	192
7.4.2	Test network and characteristics.....	192
7.4.3	Historical database for link travel time distribution .....	194
7.4.4	Baseline and system optimal scenarios.....	194
7.5	Results.....	194
7.5.1	V2V communications efficiency and vehicle-level knowledge .....	194
7.5.2	Baseline and SO scenarios.....	197

7.5.3	Incident-free scenario .....	197
7.5.3.1	Analysis of network performance.....	197
7.5.3.2	Analysis of individual vehicle performance.....	199
7.5.4	Incident scenario.....	200
7.6	Concluding comment.....	201
8.	CONCLUSIONS .....	203
8.1	Summary and conclusions .....	203
8.2	Research Contributions.....	204
8.3	Future Research .....	206
	REFERENCES .....	208

## LIST OF TABLES

Table 2-1 Information flow network size and construction time under different scenarios .....	54
Table 2-2 Memory usage to update vehicle knowledge .....	55
Table 2-3 Computation time to determine vehicle knowledge for all vehicles .....	55
Table 3-1 Conceptual analogy between epidemiological and V2V communications systems ....	65
Table 3-2 Cell characteristics of the study network.....	76
Table 4-1 Cell characteristics of the study network, and experiment parameters .....	110
Table 4-2 Calibrated communication kernel parameters for various densities, and the market penetration rate of 50% .....	113
Table 5-1 Discrete trajectory-related observations .....	137
Table 5-2 Confusion matrix .....	149
Table 5-3 Performance indices .....	149
Table 5-4 Missed alarm rates .....	149
Table 5-5 False alarm rates .....	149
Table 5-6 Timing of warnings .....	151
Table 6-1 Notation to represent variables in the information flow layer.....	165
Table 7-1 Comparison to baseline and SO scenarios.....	197
Table 7-2 V2V-equipped vehicles changing routes en route for different MPRs .....	198

## LIST OF FIGURES

Figure 1-1 Components of a V2V-based traffic system .....	19
Figure 2-1 Conceptual framework of the integrated multi-layer network framework .....	30
Figure 2-2 Interference among vehicles .....	34
Figure 2-3 Vehicle knowledge evolution.....	36
Figure 2-4 Travel experience data nodes in the information flow network corresponding to events of travel experience data generation in the physical traffic network .....	38
Figure 2-5 Representation of information flow evolution and propagation .....	40
Figure 2-6 Implementation of the graph-based reverse search algorithm .....	41
Figure 2-7 Vehicle knowledge update in the simulation-based approach .....	43
Figure 2-8 Multi-layer network analysis and evolution of vehicle knowledge .....	46
Figure 2-9 Comparison of spatiotemporal tracking capabilities.....	47
Figure 2-10 Dynamic information flow evolution and propagation under different market penetration rates .....	48
Figure 2-11 Study network .....	52
Figure 3-1 Conceptual framework of cell-based information flow propagation model .....	62
Figure 3-2 V2V communication range .....	70
Figure 3-3 V2V communication range and interference among vehicles in simulation-based experiment.....	72
Figure 3-4 Estimation of success rate of V2V communication ( $\mu$ ).....	73
Figure 3-5 Force of communication ( $P_i^t$ ).....	73
Figure 3-6 Forward and backward propagation wave speeds of information flow under the uni-directional traffic scenario .....	78
Figure 3-7 Information flow wave speed variation relative to density under the uni-directional traffic scenario .....	79
Figure 3-8 Forward and backward propagation wave speeds of information flow under the bi-directional traffic scenario .....	80
Figure 3-9 Information flow wave speed variation relative to density under the bi-directional traffic scenario .....	80

Figure 3-10 Information flow wave speed variation under the different market penetration rates ( $\alpha$ ) in a uni-directional traffic scenario.....	81
Figure 3-11 Comparison between predicted and simulated information flow wave speeds under the uni-directional traffic scenario.....	82
Figure 3-12 Comparison between predicted and simulated information flow wave speeds under the bi-directional traffic scenario.....	83
Figure 3-13 Contours of traffic density and informed vehicle density.....	84
Figure 4-1 Components of a V2V-based traffic system.....	87
Figure 4-2 Illustration of the information flow propagation wave.....	90
Figure 4-3 Two-layer structure of the proposed model.....	93
Figure 4-4 The IFPW modeling framework.....	94
Figure 4-5 Characteristics of V2V communications.....	96
Figure 4-6 Impacts of traffic flow dynamics on the IFPW under homogeneous and heterogeneous conditions.....	101
Figure 4-7 Framework of numerical solution for heterogeneous conditions.....	105
Figure 4-8 Framework of the intermediate component to connect the upper and lower layers .	108
Figure 4-9 Parameter calibration for communication kernel (density: 50 veh./km, and market penetration rate: 50%).....	112
Figure 4-10 Speed of IFPWs under various densities (one-lane highway).....	115
Figure 4-11 Speed of IFPWs under various densities (two-lane highway).....	116
Figure 4-12 IFPW speeds for different market penetration rates.....	117
Figure 4-13 IFPWs under various densities.....	118
Figure 4-14 Illustration of asymptotic speed.....	119
Figure 4-15 Speed of IFPWs under various densities (bidirectional two-lane highway).....	120
Figure 4-16 Contours of traffic density and information density.....	121
Figure 5-1 Conceptual comparison of the proposed approach with the current approaches.....	127
Figure 5-2 Capability of the MBMAM model to provide an earlier early warning.....	130
Figure 5-3 Framework of the MBMAM-based FCW system.....	132
Figure 5-4 Set of the lead-vehicle driver's current maneuver intention ( $qt$ ) states.....	134
Figure 5-5 Graphical representation of the proposed coupled HMM.....	139
Figure 5-6 Illustration of the two-stage criticality assessment.....	142

Figure 5-7 NGSIM acceleration data pre-processing .....	144
Figure 5-8 NGSIM speed data pre-processing.....	145
Figure 5-9 Estimation of maneuver states .....	146
Figure 6-1 Conceptual overview of the multi-layer framework .....	157
Figure 6-2 The travel experience data generation, and interactions among the vehicles .....	160
Figure 6-3 Interference among vehicles .....	163
Figure 6-4 Estimation of cumulative success rate of V2V communication ( $Z(q)$ ) .....	164
Figure 6-5 TED nodes in $G^1$ corresponding to events of travel experience data generation ....	167
Figure 6-6 Information flow evolution and propagation .....	169
Figure 6-7 Subgraph of information flow network ( $G^1$ ) indicating information flow propagation .....	171
Figure 6-8 Illustration of the information forward propagation wave.....	172
Figure 6-9 Study traffic network and traffic density contours.....	173
Figure 6-10 Heat map showing inter-vehicle communication frequency.....	174
Figure 6-11 Trajectories of information forward propagation wave front .....	176
Figure 6-12 Information flow propagation speed .....	176
Figure 6-13 Illustration of the time-dependent knowledge of vehicles located on link 4 .....	178
Figure 6-14 Illustration of the knowledge of vehicles located at link 4 at a given time point ...	179
Figure 7-1 Elements of a decentralized V2V-based ATIS .....	185
Figure 7-2 Illustration of V2V communications-related constraints .....	188
Figure 7-3 Study network and associated characteristics .....	193
Figure 7-4 Efficiency of V2V communications under different MPR .....	195
Figure 7-5 Number of obtained travel experience data during trips .....	196
Figure 7-6 Number of obtained travel experience data during trips for different MPRs .....	196
Figure 7-7 Effects of MPR on average travel time under the incident-free scenario .....	199
Figure 7-9 Distribution of travel time differences for different trip time (under 25% MPR) ....	200
Figure 7-10 Effects of MPR on average travel time under incident scenario.....	201

## ABSTRACT

Author: Kim, Yon Hoon. PhD

Institution: Purdue University

Degree Received: December 2019

Title: Integrated Modeling Framework for Dynamic Information Flow and Traffic Flow under Vehicle-to-Vehicle Communications: Theoretical Analysis and Application

Major Professor: Srinivas Peeta

Advances in information and communication technologies enable new paradigms for connectivity involving vehicles, infrastructure, and the broader road transportation system environment. Vehicle-to-vehicle (V2V) communications under the aegis of the connected vehicle are being leveraged for novel applications related to traffic safety, management, and control, which lead to a V2V-based traffic system. Within the framework of a V2V-based traffic system, this study proposes an integrated modeling framework to model the dynamics of a V2V-based traffic system that entails spatiotemporal interdependencies among the traffic flow dynamics, V2V communication constraints, the dynamics of information flow propagation, and V2V-based application. The proposed framework systematically exploits their spatiotemporal interdependencies by theoretical and computational approaches.

First, a graph-based multi-layer framework is proposed to model the V2V-based advanced traveler information system (ATIS) as a complex system which is comprised of coupled network layers. This framework addresses the dynamics of each physical vehicular traffic flow, inter-vehicle communication, and information flow propagation components within a layer, while capturing their interactions among layers. This enables the capabilities to transparently understand the spatiotemporal evolution of information flow propagation through a graph structure. A novel contribution is the systematic modeling of an evolving information flow network that is characterized as the manifestation of spatiotemporal events in the other two networks to enhance the understanding of the information flow evolution by capturing the dynamics of the interactions involving the traffic flow and the inter-vehicle communication layers. The graph-based approach enables the computationally efficient tracking of information propagation using a simple graph-based search algorithm and the computationally efficient storage of information through a single graph database.

Second, this dissertation proposes analytical approaches that enable theoretical investigation into the qualitative properties of information flow propagation speed. The proposed analytical models, motivated from spatiotemporal epidemiology, introduce the concept of an information flow propagation wave (IFPW) to facilitate the analysis of the information propagation characteristics and impacts of traffic dynamics at a macroscopic level. The first model consists of a system of difference equations in the discrete-space and discrete-time domains where an information dissemination is described in the upper layer and a vehicular traffic flow is modeled in the lower layer. This study further proposes a continuous-space and continuous-time analytical model that can provide a closed-form solution for the IFPW speed to establish an analytical relationship between the IFPW speed and the underlying traffic flow dynamics. It can incorporate the effects of congested traffic, such as the backward traffic propagation wave, on information flow propagation. Thereby, it illustrates the linkage between information flow propagation and the underlying traffic dynamics. Further, it captures V2V communication constraints in a realistic manner using a probabilistic communication kernel (which captures the probability).

Third, within the integrated modeling framework, this dissertation captures the impact of information flow propagation on traffic safety and control applications. The proposed multi-anticipative forward collision warning system predicts the driver's maneuver intention using a coupled hidden Markov model, which is one of statistical machine learning techniques. It significantly reduces the false alarm rates by addressing the uncertainty associated with the performance of the future motion prediction, while currently available sensor-based kinematic models for addressing the uncertainty associated with the future motion prediction. A network-level simulation framework is developed to investigate a V2V-based ATIS in a large-scale network by capturing its inter-dependencies and feedback loop. This modeling framework provides the understanding of the relationship between the travelers' routing decisions and information flow propagation.

This thesis provides a holistic understanding of information flow propagation characteristics in space and time by characterizing interactions among information flow propagation, and underlying traffic flow, and V2V communications characteristics. The proposed models and the closed-form solution of IFPW speed can help in designing effective V2V-based traffic systems, without relying on computationally expensive numerical methods. An innovative aspect of this approach represents a building block to develop both descriptive capabilities and prescriptive

strategies related to propagating the flow of useful information efficiently and synergistically generating routing mechanisms that enhance the traffic network performance. Given the lack of appropriate methodologies to characterize the information flow propagation, this thesis expects to make a novel and significant contribution to understanding the characteristics of V2V-based traffic systems and their analysis.

# 1. INTRODUCTION

## 1.1 Background

The connectivity provided to the transportation system through dedicated short range communication (DSRC) is enabling new paradigms involving vehicles (V2V), infrastructure (V2I) and the broader road transportation system environment (V2X). These capabilities can provide a data-rich environment and enhanced range of awareness of traffic conditions for a V2V-based traffic system. Therefore, the communication capabilities have potential to develop innovative solutions for enhancing traffic safety and mobility, and sustainable solutions from the perspectives of energy usage and the environment.

The success of the V2V-based traffic systems is dependent on the timely and reliable dissemination of information. However, the real-world environment for implementing a V2V-based application can be constrained by the characteristics and phenomena associated with the interactions involving traffic flow dynamics and V2V communication constraints. Hence, a critical question is how information propagation is impacted by the traffic flow dynamics and V2V communication constraints. While widely-used analytical and simulation-based models exist to characterize the influencing factors in the communication and transportation domains, there are currently limited methodologies that allow us to integrate the underlying components for modeling of the information flow propagation in space and time and investigating effects of emergent phenomena associated with communication connectivity.

Modeling the propagation of multiple units of information in space and time and determining how the information flow dynamics can be mapped from the traffic flow dynamics and the inter-vehicle communication constraints are not trivial. This is because a V2V-based traffic system consists of the vehicular traffic flow, inter-vehicle communication, spatiotemporal information flow, and V2V-based applications. Further, the relationship between these components is characterized by non-linearity, interdependencies, and feedback loop as illustrated in Figure 1.1.

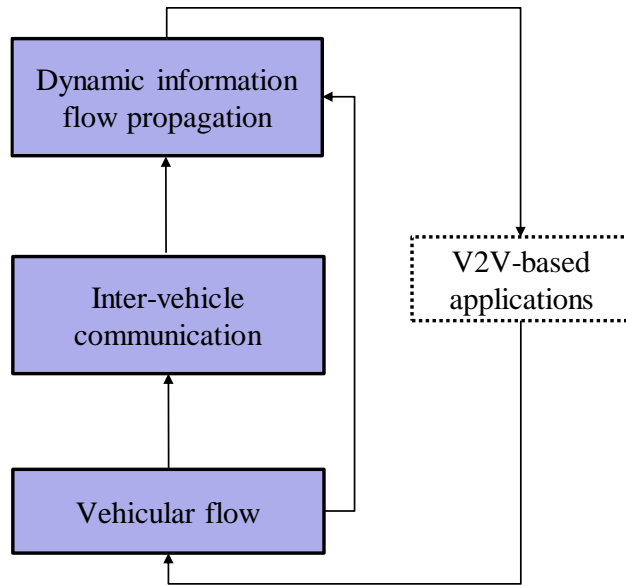


Figure 1-1 Components of a V2V-based traffic system

This dissertation focuses on developing the integrated modeling framework that incorporates these underlying components to address their dynamics within a layer and the interactions among layers. The proposed graph-based multi-layer network framework not only models the impacts from traffic flow dynamics and V2V communication constraints but also provides a retrospective capability to track the spatiotemporal characteristics of multiple units of information flow and evolution of vehicle knowledge explicitly across the network. This systematic modeling and understanding of the information flow propagation in a V2V-based traffic system are critical to leverage its use to develop driver route guidance strategies and system operator strategies for the efficient spread of useful information. Hence, the proposed multi-layer framework serves as a building block for the design of a new generation of information flow routing and vehicular route guidance strategies to manage traffic conditions in congested networks.

The proposed dissertation proposes macroscopic approaches that enable theoretical investigation into the qualitative properties of information flow propagation speed. To do so, this study introduces the concept of an information flow propagation wave (IFPW) to facilitate the analysis of the information propagation characteristics and impacts of traffic dynamics at an aggregate level. It constructs a two-layer model consisting of an information dissemination model in the upper layer and a traffic flow model in the lower layer. First, a system of difference equations in the discrete space and time domain is proposed. Second, it further proposes a continuous-timing

and continuous-space analytical model that can provide a closed-form solution for the IFPW speed to establish an analytical relationship between the IFPW speed and the underlying traffic flow dynamics. The closed-form solution and analytical model can be used to predict the IFPW speed and the position of the IFPW front under diverse vehicular environments (in terms of density and topology) and V2V communication network parameters (such as data communication frequency, transmission power, etc.). Further, it can incorporate the effects of congested traffic, such as the backward traffic propagation wave, on information flow propagation. Thereby, it illustrates the linkage between information flow propagation and the underlying traffic dynamics.

From the traffic safety application perspective, the comprehensive coverage enabled by V2V communications bring a possible benefit that information of multiple vehicles ahead can be used as a priori knowledge to provide the early warning by predicting the collision risk associated with a lead-vehicle. The problem is that the earlier a warning is provided, the less certain that the situation will require the driver to act to a collision. This dissertation develops a coupled Hidden Markov model that synergistically combines the multiple vehicles information to predict the potential risk of collision. From the traffic management and control application perspective, the successful V2V-based advanced traveler information system (ATIS) is dependent on the individual vehicle's accurate estimation of prevailing traffic conditions. Therefore, the characteristic of dynamic vehicle knowledge must be considered in the formulation of the guidance solutions. This dissertation proposes a simulation-based framework to analyze a fully decentralized ATIS system, in which the guidance is continuously updated for V2V-equipped vehicles based on both on historical information stored in the vehicle-level database and time-dependent vehicle knowledge that is updated through V2V communications. Hence, an understanding of the relationship between V2V-based ATIS performance and dynamic knowledge of vehicle provides insights into the design of robust V2V-based ATIS architecture. It seeks to evaluate an impact assessment of V2V-based system for the application domains in the perspectives of network-level and feedback loop.

## **1.2 Objectives of the dissertation**

The fundamental objective of this dissertation is to develop a systematic model that integrates the physical traffic flow, inter-vehicle communication, information flow propagation, V2V application for a V2V-based system. The specific tasks that address these objectives are:

- (i) Propose a graph-based multi-layer network framework to model the V2V-based system as a complex system which is comprised of three coupled network layers: a physical traffic flow network, and virtual inter-vehicle communication and information flow networks. To determine the occurrence of V2V communication, the inter-vehicle communication layer is first constructed using the time-dependent locations of vehicles in the traffic flow layer and inter-vehicle communication related constraints. Then an information flow network is constructed based on events in the traffic and inter-vehicle communication networks. The graph structure of this information flow network enables the efficient tracking of the time-dependent vehicle knowledge of the traffic network conditions using a simple graph-based reverse search algorithm and the storage of the information flow network as a single graph database. The development of multi-layer framework enables to consider explicitly these interdependencies and to track the spatiotemporal characteristics of information flow propagation in the analytical framework. This proposed graph-based multi-layer network framework provides an explicit retrospective modeling capability to articulate how information flow evolves and propagates beyond the current descriptive capability afforded by simulation-based approaches.
- (ii) Develop a system of difference equations in the discrete space and time domain to model the dynamic information flow propagation. We propose a cell-based heterogeneous traffic flow model, where the information flow propagation mechanism is consistent with an epidemic model. Vehicle movement in the traffic layer satisfies the classical traffic flow theory characterized by the cell transmission model in this study. The upper layer describes the information dissemination among the equipped vehicles. It captures the dynamics of IFPW that can characterize how the density, speed, and locations of the vehicles lead to the dynamics of information flow.
- (iii) Develop a macroscopic model to characterize the IFPW. The proposed information dissemination model constructs a continuous-timing and continuous-space analytical model that can provide a closed-form solution for the IFPW speed under certain conditions. It establishes an analytical relationship between the IFPW speed and the underlying traffic flow dynamics. It uses a probability communication kernel function to represent the strength of communication of nearby vehicles compared with distant

ones under a fixed V2V-equipped vehicle density level. The dynamics of traffic flow propagation are described through a macroscopic hydrodynamic model of traffic flow originated with the first order LWR model.

- (iv) Develops a multi-anticipative forward collision warning system that synergistically combines V2V communication technologies to predict the potential risk. There are currently limited methodologies that allow us to incorporate these multiple vehicle kinematic data to predict the motion of the lead-vehicle and assess the associated risk. A coupled hidden Markov model is developed, motivated by a statistical machine learning technique, for predicting the motion of lead-vehicle trajectory. The coupled HMM offers a mathematically sound basis for making inference under uncertainty. It breaks down each maneuver into a chain of consecutive events. The proposed model can reduce the false/nuisance significantly.
- (v) Models the dynamic flow propagation of multiple units of information using an analytical multi-layer framework that captures the dynamics of interacting layers. The traffic flow dynamics are captured using a cell transmission model in the vehicular traffic flow layer. The inter-vehicle communication layer uses the time-dependent locations of vehicles and the density of the V2V-equipped vehicles as inputs for an aggregate analytical function of the inter-vehicle communication success rate. Then, the information flow evolution and propagation is modeled using a graph-based representation. The proposed analytical modeling framework enables capturing the information flow dynamics (in terms of the information forward/backward propagation waves, spatial propagation fronts, spatiotemporal vehicular knowledge characteristics, etc.) using the traffic flow dynamics (in terms of traffic forward/backward propagating waves and traffic flow variables) and the inter-vehicle communication events.
- (vi) Proposes a simulation-based framework to investigate a V2V-based ATIS in a large-scale network. In this system, each individual vehicle can potentially gain knowledge on travel-related information and utilize the associated knowledge to revise vehicle-level routing decisions. Hence, an understanding of the relationship between the travelers' routing decisions and information flow propagation provides insights into the design of robust V2V-based ATIS architecture. This approach is intended to improve guidance quality with the ability of the decentralized architecture to respond rapidly to

random incidents. The results show that the proposed model provides potential benefits both for travelers with such equipment as well as for a whole system are demonstrated.

### **1.3 Organization of the dissertation**

This dissertation consists of eight chapters. Chapter 2 proposes a multi-layer framework that models the information flow propagation based on a dynamic graph structure. The performance of the graph structure is compared with that of the simulation-based approaches to investigate the capabilities of the proposed model to transparently track information generation and propagation in both time and space. The associated experiments highlight the potential benefits of the retrospective capability of the graph-based modeling of the information flow propagation to identify the spatiotemporal characteristics of vehicle knowledge.

Chapter 3 discusses the concept of IFPW and develops a descriptive analytical model that illustrates the IFPW. Results from computational experiments demonstrate its ability to describe the dynamic characteristics of information flow propagation along with the traffic flow dynamics.

Chapter 4 develops a macroscopic model to characterize the information flow propagation wave (IFPW). A closed-form solution is derived for the IFPW speed under homogeneous traffic conditions. The IFPW speed is numerically determined for heterogeneous traffic conditions. Numerical experiments illustrate the influence of traffic density heterogeneity on the IFPW speed. The proposed model can capture the spatiotemporal interactions between the traffic and V2V communication layers, and aid in the design of novel information propagation strategies to manage traffic conditions.

Chapter 5 develops a multi-anticipative forward collision warning (FCW) system. It balances the trade-off between false/nuisance and missed alarms. The proposed model can alert a driver of the potential risk in advance and can give enough response time, helping to avoid a collision. Results from computational experiments demonstrate the effectiveness of the proposed model and its ability to predict the potential risk of collision using dissemination of information through V2V communication.

Chapter 6 models the dynamic propagation of multiple units of information using an analytical multi-layer framework that captures the dynamics of the three interacting layers. The proposed framework describes how the dynamic flow propagation of multiple units of information can be mapped from the traffic flow dynamics and the inter-vehicle communication constraints. Synthetic

experiments analyze the interactions between the traffic flow dynamics and inter-vehicle communication constraints, and the flow propagation characteristics of multiple units of information. They illustrate that the proposed analytical multi-layer framework enables the integration of the traffic flow dynamics and inter-vehicle communication constraints to generate insights on the flow propagation of multiple units of information. Also, they indicate that it can be extended to incorporate the dynamic flow propagation characteristics of multiple units of information into the design of robust V2V-based ATIS architectures.

Chapter 7 develops a simulation-based framework to evaluate a V2V-based ATIS in a large-scale network. The routing decisions are subsequently revised by V2V-equipped vehicles based on both on historical data stored in the vehicle-level database and on real-time information obtained through V2V communications. An information updating process and online stochastic routing scheme are processed on vehicle-level computation. Using simulation-based experiments, potential benefits for V2V-equipped vehicles as well as for unequipped vehicles are demonstrated. The experiments illustrate that a higher market penetration rate of V2V-equipped vehicles does not guarantee better performance for a V2V-based ATIS. It highlights the value of considering some level of coordination of decision-making across vehicles to enhance network-level traffic performance, and points to the need for a new generation of hybrid traffic management strategies that leverage such emerging technologies.

Chapter 8 concludes this dissertation with a summary of the overall insights from the research. Novelties and significant contributions are identified. Finally, the potential directions for future research are discussed.

## **2. GRAPH-BASED MODELING OF INFORMATION FLOW EVOLUTION AND PROPAGATION UNDER V2V COMMUNICATIONS BASED ADVANCED TRAVELER INFORMATION SYSTEMS**

### **2.1 Introduction**

Communications technologies enable technological advances to be integrated into the transportation system and vehicles to foster objectives such as congestion mitigation, safety improvement, and traffic network performance enhancement. In this context, vehicle-to-vehicle (V2V) communications can be leveraged in an advanced traveler information system (ATIS) to allow vehicles to accumulate their own travel experience data and communicate with other vehicles within communication range to exchange travel experience data without any central coordination. Hence, V2V communications capabilities in an ATIS can provide a data-rich environment for travelers based on information transmitted anonymously from vehicles without the requirement of additional infrastructure. Thereby, it can potentially provide an enhanced range of awareness of traffic conditions to travelers.

The dynamics of vehicular traffic flow, inter-vehicle communication, and traffic information flow are the three underlying factors that shape a V2V-based ATIS. A complex characteristic of this system is that these factors themselves interact with each other. Due to these interactions, a V2V-based ATIS can be viewed as consisting of coupled layers involving traffic flow, inter-vehicle communication, and information flow, in which events in the different layers are interdependent. In this study, we use the term “information flow” to denote the flow of the information on the time-dependent link travel time experienced by a vehicle, and refer it as “a unit of information”. This information is not processed for congestion or incident detection (Yang and Recker 2008), and/or other applications through data fusion/update. The analysis of the propagation of a single unit of descriptive information has been proposed by various analytical approaches (Kim et al. 2014; Wang 2007; Wu et al. 2005a). By contrast, as vehicles generate their own link travel time experience data over time and space, a V2V-based ATIS entails the propagation of multiple units of information. The set of travel experience data on an equipped

vehicle, based on own experience or obtained through inter-vehicle communication, is referred to as the “vehicle knowledge.”

Due to the highly-decentralized nature of the V2V-based ATIS in the absence of centralized coordination of information provision, and the dynamics associated with the traffic and information flows, different vehicles may have different time-dependent knowledge of the network traffic conditions. In this context, this study focuses on modeling the information flow evolution and propagation that lead to the dynamics of vehicle knowledge in V2V-based ATIS as a building block to develop coordinated information provision strategies that additionally would require an understanding of how the vehicle knowledge would affect the driver actions. This is because the estimated network traffic conditions based on a vehicle’s time-dependent knowledge can be used by its driver for route choice decisions. The route choice decisions of V2V-equipped vehicles would then lead to the traffic network flow evolution and influence the dynamics of the information flow due to their interactions. To reiterate, this study does not intend to determine the driver route choices based on the information content in the time-dependent vehicle knowledge. Thus, the identification of the time-dependent vehicle knowledge addressed here is a sub-problem of the broader V2V-based ATIS that seeks to address user/system objectives in congested traffic networks, possibly in coordinated control settings. This aspect is reinforced further when discussing the conceptual framework in Figure 2-1.

Several studies (Gupta and Kumar 2000; Jinyang Li et al. 2001; Vuyyuru and Oguchi 2007) originating from the communications domain primarily focus on how the vehicle dynamics affect the inter-vehicle communication effectiveness between vehicles; for example, at different speeds. Hence, these studies have sought to address the integration of the dynamics of the traffic flow and the inter-vehicle communication. Other studies (Fitzgibbons et al. 2004; Schroth et al. 2005; Wu et al. 2005b) propose frameworks that incorporate a traffic flow simulator (such as Paramics and CORSIM) and a wireless (inter-vehicle communication) network simulator (such as NS-2 and Qualnet, or a simple analytical model) to derive some descriptive insights on the interactions between the traffic flow movement and the inter-vehicle communication.

However, the aforementioned studies focus primarily on the feasibility and the reliability of the V2V communication system for practical applications, and do not explicitly address the modeling

of the dynamics of the traffic information flow in the V2V-based ATIS context. Thereby, they address only two of the three coupled layers identified heretofore.

Motivated by the need to analyze the dynamics of the interactions among the traffic flow, inter-vehicle communication, and information flow at the network level, recent simulation-based studies (Eichler et al. 2005; Schmidt-Eisenlohr et al. 2007; Wu et al. 2005b) in the transportation domain seek to estimate the dynamic traffic conditions through simple data update mechanisms so that travelers can use this information to make routing decisions under V2V communication systems. They incorporate a microscopic traffic flow model and a set of inter-vehicle communication constraints to determine vehicle knowledge. Thereby, these simulation-based approaches entail a descriptive capability to identify the time-dependent knowledge of each vehicle in terms of their own travel experience data and such data obtained from other vehicles through V2V communication.

However, these approaches do not have a retrospective capability to articulate explicitly how information flow evolves and propagates, particularly in terms of its linkage to the interactions with the traffic flow and inter-vehicle communication dynamics. That is, they cannot track when and from whom a specific unit of V2V communication-based travel experience data located in a certain vehicle's knowledge reaches it, and when and to whom it propagates from it. Such spatiotemporal capabilities are critical to develop strategies for both the rapid flow of useful information and traffic routing to enhance network performance.

The lack an explicit model for the information flow layer at the network level in simulation-based and analytical approaches precludes an understanding of the fundamental relationships between the dynamic interactions among the three layers, and the evolution of equipped vehicles' knowledge in time and space. This is critical for three real-world objectives: (i) to identify and/or design information flow strategies/paradigms that lead to the rapid propagation of useful information (in the sense of enhancing the traffic network performance), (ii) to develop targeted V2V-based routing strategies to manage traffic network conditions, and (iii) to design a V2V-based ATIS so that such communications are reliable and successful. This paper seeks to fill this key gap in the literature by proposing an integrated graph-based multi-layer network framework to model the V2V-based ATIS as a complex system which is comprised of three coupled network layers: traffic flow network, inter-vehicle communication network, and information flow network.

The proposed graph-based framework provides an explicit retrospective modeling capability to articulate how information flow evolves and propagates beyond the current descriptive capability afforded by simulation-based approaches. To do so, the framework is modeled as a set of interacting networks in which information flow occurs as a result of events in the traffic flow and inter-vehicle communication networks. These events are the travel experience data generation in the traffic flow network, and the V2V communication occurrences in the inter-vehicle communication network. In particular, the dynamics of traffic flow are represented in terms of the spatiotemporal vehicle trajectories in the traffic network, and the feasibility of inter-vehicle communication among vehicles is captured in the inter-vehicle communication network using constraints. Hence, to simulate the information flow evolution and propagation that characterize the vehicle knowledge in a V2V traffic system, the following are assumed to be known: (i) “travel experience data” from the physical traffic network, which represents the actual travel experiences of vehicles (in terms of the time a vehicle enters a link and its experienced travel time on that link) along their route trajectories, and (ii) the inter-vehicle communication constraints arising from the communications network technology (in terms of the communication range, interference and bandwidth).

Based on the known entities in the V2V-based ATIS, the study first constructs the virtual inter-vehicle communication layer that illustrates inter-vehicle communication events determined by the known locations of the vehicles and the technological constraints. Then, it constructs the information flow network layer based on the events in the other two layers. Finally, it seeks to identify the vehicle knowledge of all vehicles in space and time to explain what information is obtained by each equipped vehicle. Through these modeling processes, the graph-based approach provides a retrospective capability to explicitly illustrate how information flow evolves and propagates, particularly in terms of the linkage to the interactions with the traffic flow and inter-vehicle communication dynamics.

The proposed information flow network has two key modeling characteristics. First, it has a graph structure that illustrates the information flow evolution and propagation. This enables the efficient use of a graph-based search algorithm to obtain a vehicle’s travel experience data based on its traversing a connected subgraph of the information flow network. Second, it stores data using an efficient graph database. Graph databases (Robinson et al. 2013) use the graph as a data

structure that is optimized for the efficient storing and processing of dense, interrelated datasets. Akin to other studies that involve graph databases such as social, citation, and biological networks, an information flow network employs a graph database by assembling nodes and links into a single graph structure. Thus, the information flow network eliminates data representation redundancies so that the same piece of data is not stored in more than one place, and information flow evolution and propagation is represented using directed links. Also, since a graph-based search algorithm to characterize in the information flow network performs a local search and is not concerned with the network size, adapting a graph database enables the development of computationally efficient solution methodologies.

## **2.2 Preliminaries**

### **2.2.1 The integrated multi-layer network framework**

As illustrated by Figure 2-1, the V2V-based ATIS can be viewed as an integrated multi-layer network framework consisting of three network layers: traffic flow network, inter-vehicle communication network, and information flow network. Their structures are determined based on the physical traffic network. Hence, the three network layers have interactions. For example, the inter-vehicle communication network evolution is linked to the traffic flow network through dynamic vehicle trajectories and inter-vehicle communication constraints.

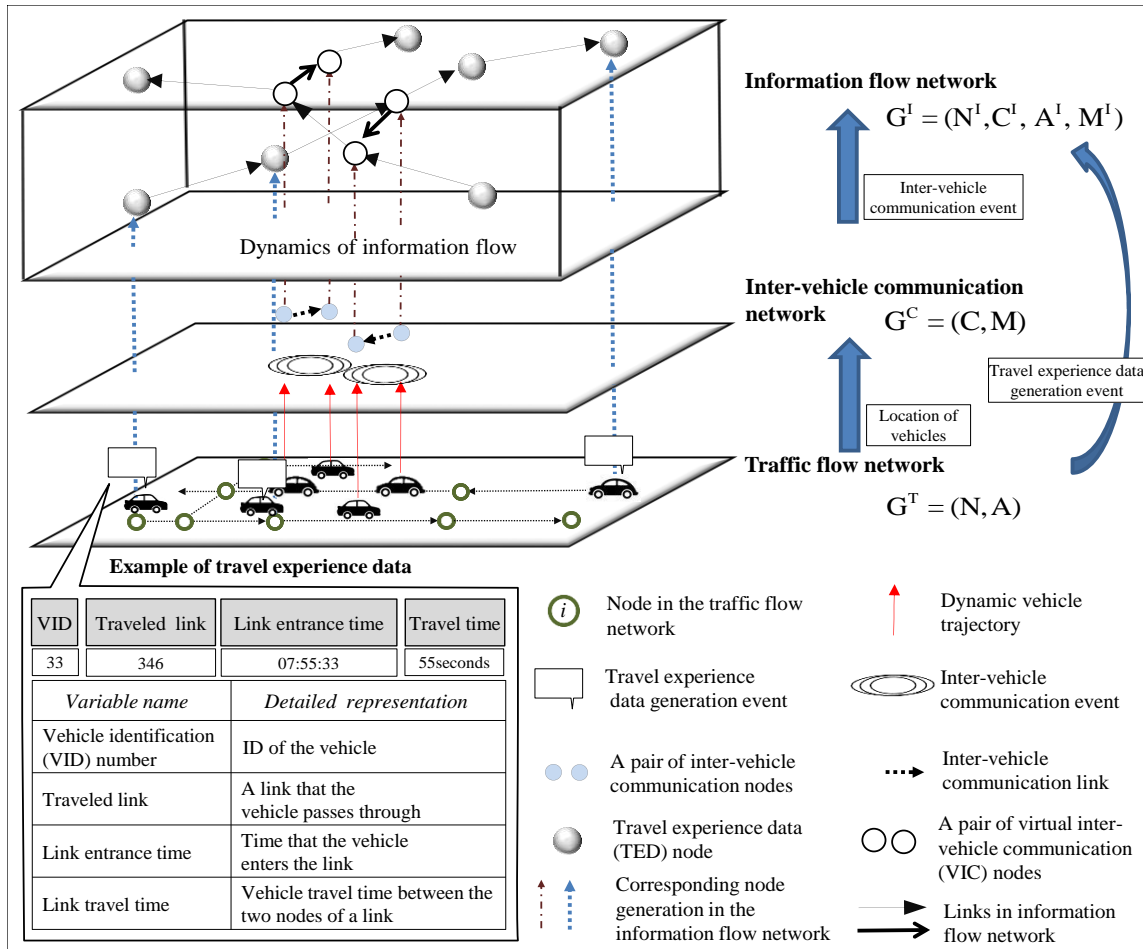


Figure 2-1 Conceptual framework of the integrated multi-layer network framework

The information flow network is dependent on the other two layers through events in them; specifically, through the travel experience data generation in the traffic flow network and the V2V communications in the inter-vehicle communication network. Thereby, the information flow evolution and propagation can be depicted as a network whose nodes correspond to events that occur in the traffic flow and inter-vehicle communication networks, and whose links indicate the direction of information flow propagation. This facilitates the analysis of their spatiotemporal interactions through shared structural characteristics.

### 2.2.1.1 Notation

The following notation is used to represent variables in the integrated multi-layer network framework.

Traffic flow network  $G^T = (N, A)$

$N$  : the set of physical nodes

$A$  : the set of physical links

$X$  : the set of vehicles

$x$  : subscript for a vehicle,  $x \in X$

$T$  : the duration of interest in the V2V-based ATIS

$t$  : superscript for (continuous) the time of interest,  $t \in [0, T]$

$i$  : a physical node in the network,  $i \in N$

$(i, j)$  : a physical link in the network,  $(i, j) \in A$

Inter-vehicle communication network  $G^C = (C, M)$

$C$  : the set of inter-vehicle communication nodes

$M$  : the set of inter-vehicle communication links

$\lambda_x$  : broadcasting inter-vehicle communication nodes for vehicle  $x$ ,  $\lambda_x \in C$

$\bar{\lambda}_y$  : receiving inter-vehicle communication nodes for vehicle  $y$ ,  $\bar{\lambda}_y \in C$

$(\lambda_x, \bar{\lambda}_y)$  : inter-vehicle communication link from vehicle  $x$  to vehicle  $y$ ,  $(\lambda_x, \bar{\lambda}_y) \in M$

**Information flow network**  $G^I = (N^I, C^I, A^I, M^I)$

$N^I$  : the set of travel experience data (TED) nodes

$C^I$  : the set of virtual inter-vehicle communication (VIC) nodes

$P^I$  : the set of nodes in the information flow network,  $P^I = \{N^I, C^I\}$ ,  $N^I \cap C^I = \emptyset$

$A^I$  : the set of information flow propagation trajectory links (T-link) indicating the vehicle trajectory direction based on the traffic flow

$M^I$  : the set of inter-vehicle communication based information flow propagation links (I-link) denoting the direction of information flow based on the inter-vehicle communication

$i_x^t$  : travel experience data (TED) node indicating a travel experience data generated by vehicle  $x$  at node  $i$  at time  $t$ ,  $\forall x \in X$ ,  $\forall i \in N$ ,  $i_x^t \in N^I$

$\lambda_x^t$  : virtual inter-vehicle communication (VIC) node denoting that vehicle  $x$  broadcasts travel experience data at time  $t$ ,  $\lambda_x^t \in C^I$

$\bar{\lambda}_y^t$  : virtual inter-vehicle communication (VIC) node denoting that vehicle  $y$  receives travel experience data at time  $t$ ,  $\bar{\lambda}_y^t \in \mathbf{C}^I$

$p_x^t, q_x^t$  : nodes in the information flow network associated with vehicle  $x$  at time  $t$ ;  $p_x^t, q_x^t \in \mathbf{P}^I$

$(p_x^{t_1}, q_x^{t_2})$ : information flow propagation trajectory link associated with the trajectory direction of vehicle  $x$  from time  $t_1$  to time  $t_2$ ,  $p_x^{t_1}, q_x^{t_2} \in \mathbf{P}^I, \forall x \in \mathbf{X}, t_1 < t_2$

$(\lambda_x^{t_1}, \bar{\lambda}_y^{t_2})$ : inter-vehicle communication based information flow propagation link representing the direction of information flow (from vehicle  $x$  to vehicle  $y$ ),  $(\lambda_x^{t_1}, \bar{\lambda}_y^{t_2}) \in \mathbf{C}^I, x \neq y, t_1 = t_2$

### 2.2.2 Physical traffic network

Under V2V-based ATIS, the equipped vehicles generate data on their travel experiences using a global positioning system (GPS) and a digital network mapping. Thereby, when a vehicle reaches the end of the link (that is, the associated downstream node in the traffic network), it generates travel experience data. As shown in Figure 2-1, the travel experience data of a vehicle includes its vehicle identification (VID) number, the identification number of the link traversed, the link entrance time, and the link travel time. Since the traffic flow network is a physical entity, we assume that the generation of travel experience data based on vehicle trajectories are observable, and given in the study.

Let  $G^T = (\mathbf{N}, \mathbf{A})$  denote a traffic flow network in which vehicles have an ability to communicate with each other. A set  $\mathbf{N}$  of nodes corresponds to physical intersections or designated points in the traffic flow network, and a set  $\mathbf{A}$  of directed links corresponds to road links. This layer captures the spatiotemporal interactions among vehicles through their trajectories. The time-dependent locations of vehicles determine the events of interest; the travel experience data generation in the traffic flow network, and the feasibility of inter-vehicle communication based on relevant technical constraints in the inter-vehicle communication network. The travel experience data generated in the physical traffic network represent one of the components used to construct the information flow network.

### 2.2.3 Virtual inter-vehicle communication network

The known time-dependent locations of vehicles in the traffic flow network and the inter-vehicle communication constraints are used to construct the inter-vehicle communication network.

An inter-vehicle communication event is viewed as a one-way transfer from a broadcasting vehicle to a receiving vehicle. The transfer of information through inter-vehicle communication creates a virtual communication node set  $C$  and a directed communication link set  $M$ , leading to the inter-vehicle communication network  $G^C = (C, M)$ . The virtual inter-vehicle communication network represents the characteristics of the inter-vehicle communication events (that is, which vehicle broadcasts and which vehicle receives the information in a given event), as illustrated in Figure 2-1. Based on the occurrence of events in the inter-vehicle communication network, information flow propagation takes place between vehicles.

The communication range illustrates the physical distance within which V2V communication can potentially occur. The communication signal power decreases with distance. Hence, it is assumed that V2V communication will not occur outside the specified range. Two equipped vehicles can potentially communicate with each other when physical distance is less than a predefined communication range  $r$ . However, multiple transmissions from vehicles within communication range leads to interference, which may result in the failure of receiving information from other vehicle. The interference rate is defined as follows (Gupta and Kumar, 2000):

$$\frac{T_x}{|\theta_x - \theta_y|^2} / (E + \sum_{\substack{z \in X \\ z \neq x}} \frac{T_z}{|\theta_z - \theta_y|^2}) \geq \beta \quad (1)$$

where,  $\theta_z$  is defined as the GPS location coordinate of an equipped vehicle  $z$  within communication range,  $z \in X$ . We assume that the power levels of vehicles ( $T_x$  and  $T_z$ ) are identical and the ambient noise power level ( $E$ ) is zero. Signal power decays with distance and the vehicle  $y$  will successfully receive the information from vehicle  $x$  if it satisfies the minimum signal-to-interference ratio of  $\beta$  (the study experiments use  $\beta = 2$  based on Gupta and Kumar, (2000)). Specifically, all equipped vehicles' positions within communication range of vehicle  $y$  in the traffic network are tracked. The time interval of V2V communication is set to 0.5 seconds and the accomplishment of inter-vehicle communication between  $y$  and those vehicles is checked every



vehicle communication constraints in terms of capturing the randomness related to the V2V communication.

#### **2.2.4 Graph-based representation of information flow network**

Under a V2V-based ATIS, a vehicle continuously updates its knowledge using its own experience and the anonymously obtained travel experience data of other vehicles. These travel experience data are stored in the temporary memory on board the vehicle's system, and duplicate (spatiotemporal data of the same vehicle) and/or older (data older than 30 minutes in the study experiments) data are discarded.

Figure 2-3 illustrates the vehicle knowledge evolution due to travel experience data generation and inter-vehicle communication, and details of the associated data packet configuration. Figure 2-3(a) shows the details of the vehicle knowledge of vehicles 33 and 25, and the associated travel experience data. Figure 2-3(b) illustrates how events (generation of travel experience data, and inter-vehicle communication) impact the evolution of vehicle knowledge in Figure 2-3(a). For example, the vehicle knowledge of vehicle 33 consists of sets of data that it generates and stores, and receives from other vehicles (vehicle 17 in Figure 2-3).

The information flow network, whose flows are a set of travel experience data, is constructed using nodes and links to map what/when/where information is generated and how it propagates. It illustrates the dynamic nature of the information flow evolution and propagation, and the associated evolution of vehicle knowledge.

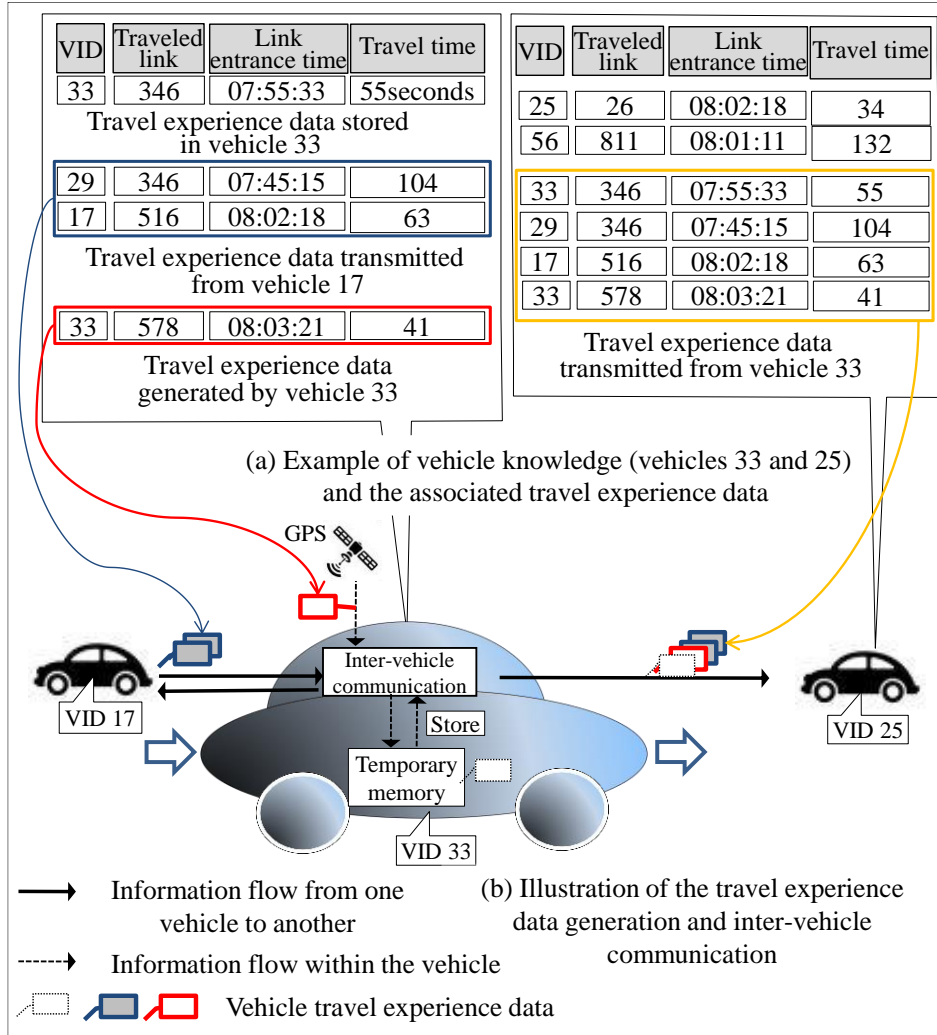


Figure 2-3 Vehicle knowledge evolution

The information flow network  $G^I = (N^I, C^I, A^I, M^I)$  has two types of nodes: a “travel experience data (TED)” node  $\in N^I$  generated by the corresponding each event of travel experience data generation in  $G^T$ , and ii) a pair of “virtual inter-vehicle communication (VIC)” nodes (one for broadcast and the other for receiving)  $\in C^I$  representing the corresponding each event of inter-vehicle communication in  $G^C$ , as illustrated in Figure 2-1.

Two sets of links represent the dynamics of information flow evolution and propagation. The directed information flow propagation trajectory links (T-link)  $\in A^I$  denotes the spatiotemporal trajectories of the same vehicles through TED-TED, TED-VIC, VIC-TED or VIC-VIC node

connections. The inter-vehicle communication based information flow propagation links (I-link)  $\in M^I$  connect each pair of nodes (VIC-VIC) corresponding to inter-vehicle communication events between two vehicles.

#### 2.2.4.1 Information flow generation/deletion

When a V2V-equipped vehicle reaches a physical intersection, it generates data on the travel time experienced on the link just traversed. This event is denoted by a TED node, denoted as  $i_x^t \in N^I$ . It represents the travel experience data generated by vehicle  $x \in X$  at node  $i$  at time  $t$ . As illustrated in Figure 2-3, the travel experience data consists of the vehicle identification number, the link entrance time, and the experienced link travel time. Figure 2-4 shows the route trajectory of vehicle  $x \in X$ , and the corresponding TED nodes  $i_x^{t_1}$  and  $j_x^{t_2}$  generation in the information flow network. They share the same topology of the physical nodes  $i \in N$  and  $j \in N$ , but at time points  $t_1$  and  $t_2$ , respectively.

Since the TED nodes are generated based on vehicles' time-dependent locations in the traffic flow network, the TED node can characterize the spatiotemporal dynamics of traffic flow. Thus,  $i_x^{t_1}$  also characterizes the spatiotemporal vehicle trajectory for vehicle  $x \in X$  located at node  $i$  at time  $t$ . Therefore, in Figure 2-4, the TED node  $j_x^{t_2}$  in the information flow network denotes the travel experience data that is generated by  $x$  at the physical node  $j \in N$  at time  $t_2$ .

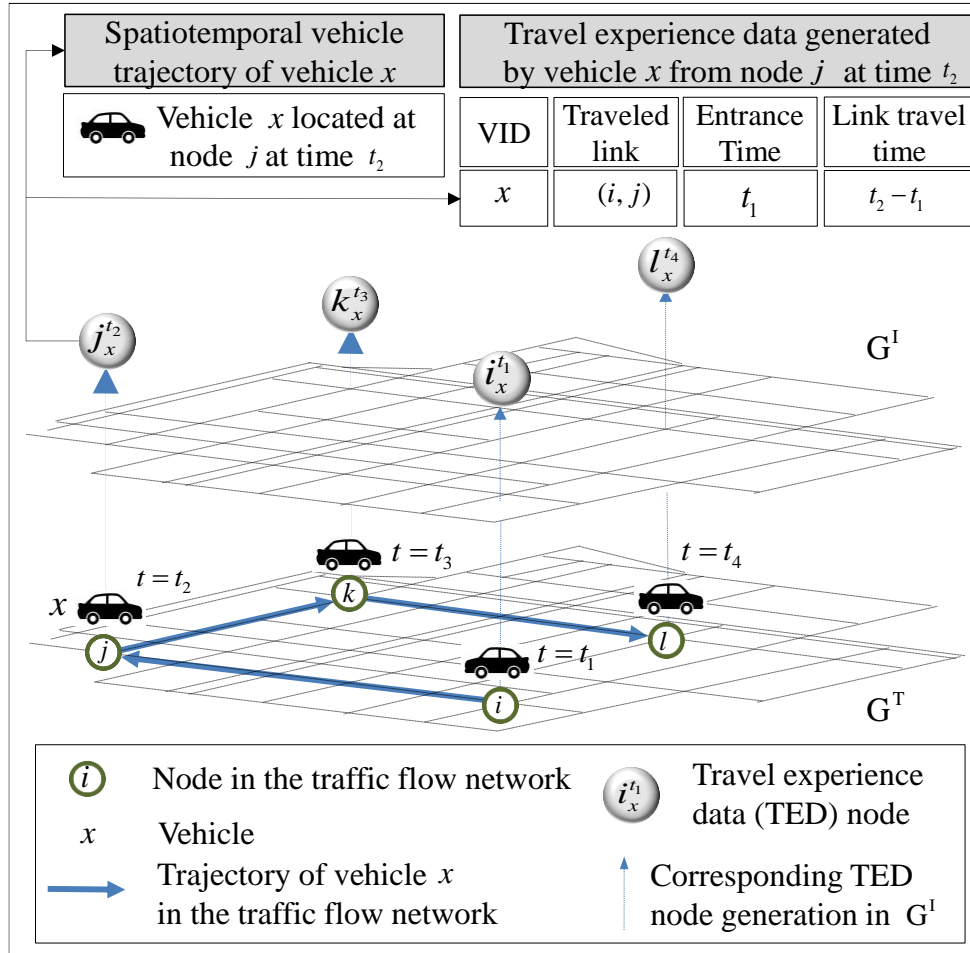


Figure 2-4 Travel experience data nodes in the information flow network corresponding to events of travel experience data generation in the physical traffic network

As discussed earlier, if the data stored in a vehicle’s onboard memory storage becomes large, it can burden the inter-vehicle communication of data and lead to failure in terms of communicating that data. To avoid this issue, older data is removed from the vehicle’s onboard memory storage by designating  $\delta$  as the maximum data storage time interval (for example, 30 minutes in the study experiments).

#### 2.2.4.2 Information flow evolution and propagation

We construct the VIC nodes and the directed links (T-links and I-links) in the information flow network to represent how information flow evolves and propagates. When vehicle  $x$  broadcasts its

travel experience data to vehicle  $y$ , a pair of VIC nodes  $\lambda_x^{t_1}$  and  $\bar{\lambda}_y^{t_2} \in C^I$  is generated in  $G^I$  corresponding to the inter-vehicle communication nodes ( $\lambda_x$  and  $\bar{\lambda}_y$ ) of  $G^C$ . The VIC node pairs consist of the broadcasting VIC node  $C_b^I$  and the receiving VIC node  $C_r^I$  ( $C_b^I, C_r^I \subset C^I$ ).

Each pair of VIC nodes is connected by an inter-vehicle communication based information flow propagation link (I-link),  $(\lambda_x^{t_1}, \bar{\lambda}_y^{t_2}) \in M^I$  in  $G^I$ , which is defined as follows:

$$M^I = \{(\lambda_x^{t_1}, \bar{\lambda}_y^{t_2}) \in C_b^I \times C_r^I \mid x \neq y, t_1 = t_2\} \quad (2)$$

A directed I-link connects a pair of VIC nodes from the broadcasting VIC node  $\lambda_x^t \in C_b^I$  to the receiving VIC node  $\bar{\lambda}_y^t \in C_r^I$ . This representation stores the corresponding information flow propagation through the inter-vehicle communication. We assume that the broadcasting and receiving of information start at the same time.

Figure 2-5 illustrates the generation of the VIC nodes and I-links in the information flow network corresponding to the inter-vehicle communication. For example, the occurrence of the inter-vehicle communication from vehicle  $y$  to vehicle  $x$  at time  $t_7$  is represented as the pair of broadcasting VIC node  $\lambda_y^{t_7}$  and receiving VIC node  $\bar{\lambda}_x^{t_7}$ , and the directed I-link  $(\lambda_y^{t_7}, \bar{\lambda}_x^{t_7})$ . These VIC nodes and I-links can map when/where information propagates from one vehicle to another vehicle.

We define a set of information flow propagation trajectory links (T-links)  $\in A^I$  as follows:

$$A^I = \{(p_x^{t_1}, q_x^{t_2}) \in (P^I \times P^I) \mid \forall x \in X, t_1 < t_2\} \quad (3)$$

As the TED and VIC nodes for a vehicle occur along with its trajectory, a directed T-link connects TED-TED, TED-VIC, VIC-TED or VIC-VIC nodes based on the trajectory of vehicle  $X$  from time  $t_1$  to time  $t_2$  ( $t_1 < t_2$ ). Hence, a set of T-links represents the associated spatiotemporal traffic flow dynamics. Figure 2-5 illustrates that the directed T-links  $(i_x^{t_1}, j_x^{t_2})$ ,  $(j_x^{t_2}, \bar{\lambda}_x^{t_3})$  and  $(\bar{\lambda}_x^{t_3}, \lambda_x^{t_4})$  connect the TED-TED, TED-VIC, and VIC-VIC nodes based on the vehicle  $x$  trajectory direction. These T-links explain how information flow propagates along with this vehicle's trajectory.

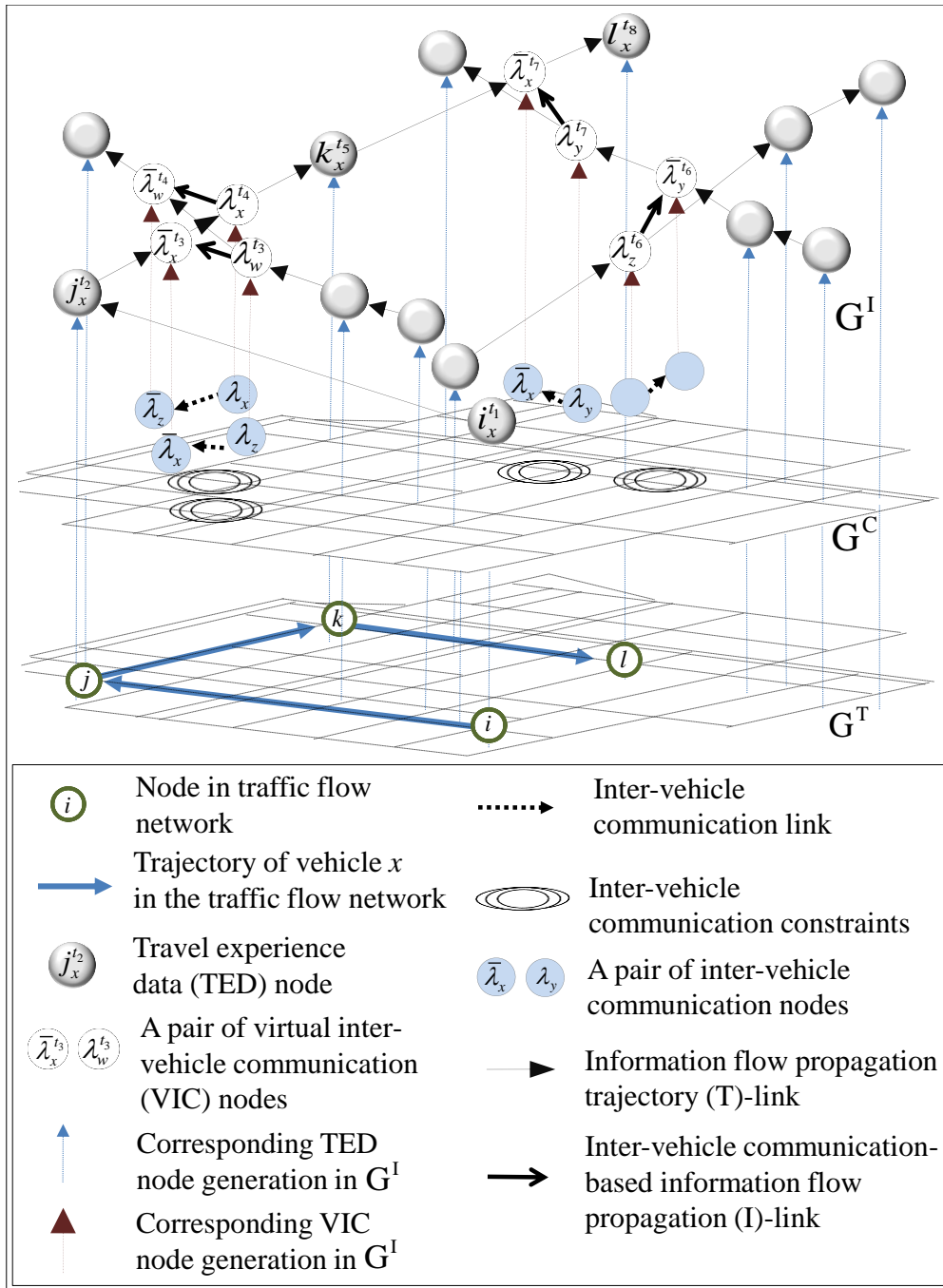


Figure 2-5 Representation of information flow evolution and propagation

### 2.2.5 Graph structure and reverse search algorithm for vehicle knowledge identification

The time-dependent knowledge of a vehicle at a particular location (indicated by a specific TED node) is represented by a connected group of TED nodes (interpreted as travel experience data) and the associated directed links in the graph structure of the information flow network. Thereby, determining a subgraph that is connected to a specific node in the information flow network identifies the vehicle knowledge of interest. We formulate this process as a searching problem. A graph-based reverse search algorithm (Ahuja et al., 1993) tracks the flow of information using a backtracking logic from the specific node, by tracing the direction opposite to that of the directed link and identifying each source of information (that is, each TED node).

```
begin
    Unmark all nodes in  $G^1$ ;
    Mark node  $s$  ;
    List:={ $s$ };
    while List  $\neq \emptyset$  do
        begin
            select a node  $j$  in List;
            while there is an admissible link  $(i, j)$ 
                that is incident to node  $j$  do
                begin
                    mark node  $i$ ;
                    add node  $i$  to List;
                    add node  $i$  to Travel Data;
                end;
            delete node  $j$  from List;
        end;
    end;
```

Figure 2-6 Implementation of the graph-based reverse search algorithm

The time-dependent knowledge of a vehicle located at a TED node can be identified by identifying all nodes that can reach it along directed paths. Figure 2-6 illustrates the procedure to implement the reverse search algorithm to identify the vehicle knowledge. In the initialization step, every

node is set as “unmarked”, and “Travel Data”, which collects all nodes that are reachable from a specific node  $s$  (vehicle location), is set to empty. Here, a node  $l$  is “reachable” from another node  $k$  if there is a directed path from  $k$  to  $l$ .

A specific node  $j = s$  is marked initially and added to the empty list “List”. We fan out from  $j$  to identify nodes that can reach it. To do so, we search for admissible links that are incident to  $j$ . A link  $(i, j)$  is referred to as admissible if node  $i$  is unmarked and node  $j$  is marked. For each admissible link, we designate its unmarked node  $i$  as visited and tag it as marked. Node  $i$  is added to “List” and “Travel Data”. After all admissible links for  $j$  are scanned, remove  $j$  from “List”. Go to the next node in “List” and repeat the algorithmic process until there are no nodes in “List”. When the algorithm terminates, each TED node in “Travel Data” indicates a generated travel experience data and each VIC node explains how it is obtained through inter-vehicle communication.

## **2.3 Retrospective modeling capability in the graph-based framework**

### **2.3.1 Vehicle knowledge update in simulation-based approach**

Modeling a large-scale V2V-based ATIS is inherently complex. Hence, a simulation-based approaches has typically been used to identify vehicle knowledge in V2V-based ATIS studies. Past studies (Wu et al., 2005; Kim et al., 2009; Kim, 2010) use traffic simulators as the traffic flow layer, and inter-vehicle communication constraints govern data exchange based on each equipped vehicle’s location information in each simulation time step. Thereby, in each time step of the simulation-based approach, each vehicle’s knowledge is updated using traffic data received from other vehicles as well as the data generated by the vehicle itself. In an update process, each vehicle’s knowledge after a relevant event is copied to an individual memory location (for that vehicle) which stores its previous vehicle knowledge; this is illustrated in Figure 2-7 for two time steps ( $t_1$  and  $t_2$ ). While this is an intuitive approach that mimics the individual vehicles’ onboard memory storage and copies the travel experience data from one vehicle to another, it lacks retrospective modeling capabilities to articulate explicitly how information flow evolves and propagates. Further, as explained in Section 2.3.3, an extensive update process is required to update each vehicle’s knowledge under this approach.

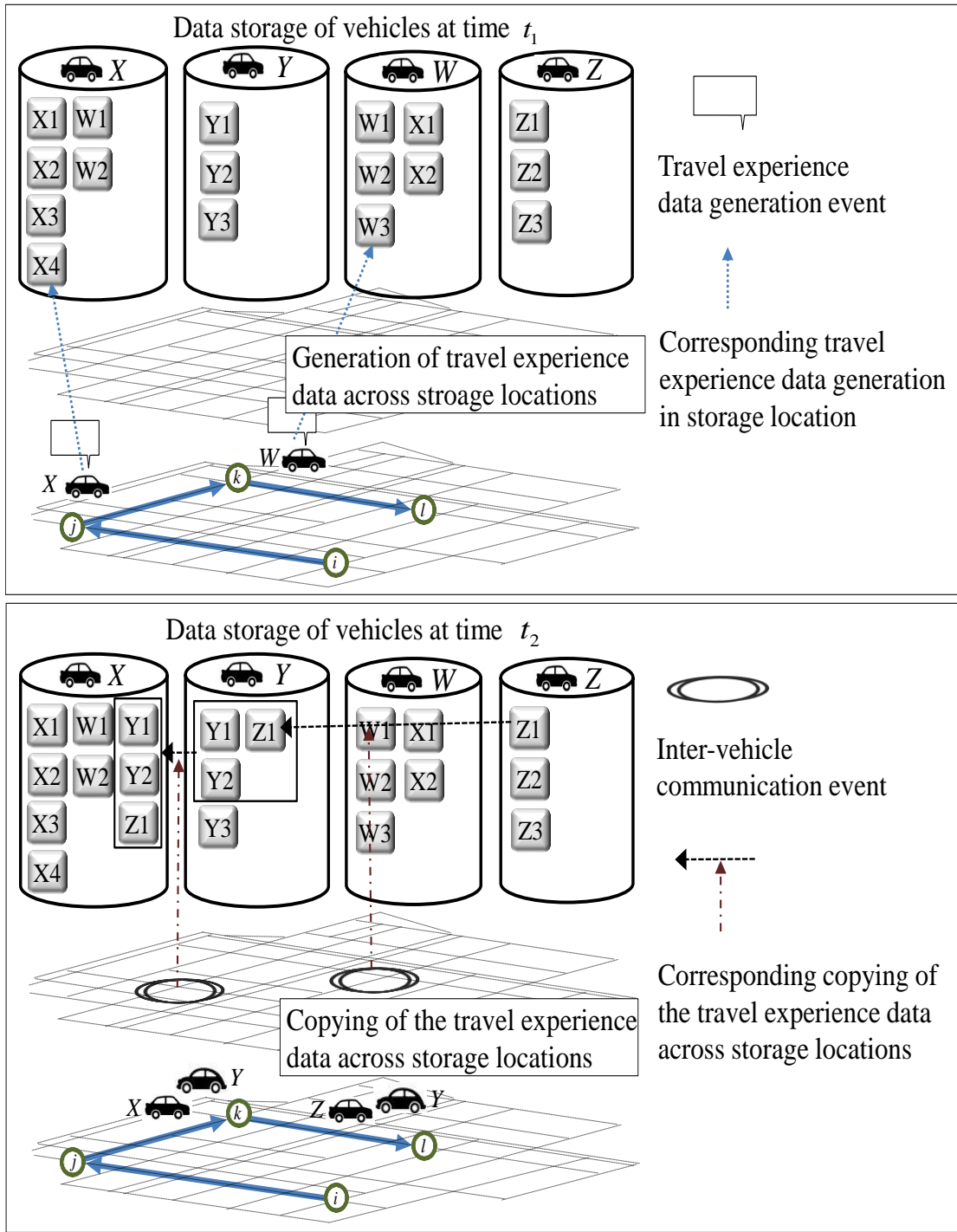


Figure 2-7 Vehicle knowledge update in the simulation-based approach

## **2.3.2 Retrospective modeling capabilities**

### **2.3.2.1 Retrospective modeling of the integrated multi-layer network**

There is a need to understand and model the dynamics of information flow explicitly at the multi-layer network level. However, the integration of the information flow evolution and propagation with the traffic flow dynamics and inter-vehicle communication introduces significant complexity for two reasons. First, the need to track vehicles from the perspective of information flow evolution and propagation in addition to the physics of vehicular interactions requires a multi-layer network approach. Second, since information is exchanged by vehicles continuously, there is a need to ensure consistency in information flow propagation over space and time. In this context, the evolution of vehicle knowledge can be analyzed in the multi-layer network framework through the information flow network by linking the TED nodes to events in the traffic flow network and VIC nodes to the events in the inter-vehicle communication network, thereby illustrating the dynamics of traffic flow and the occurrence of the inter-vehicle communication, respectively.

Figure 2-8 (a) shows an example to track the evolution of knowledge of two vehicles with similar routes based on the dynamics of traffic flow and the inter-vehicle communication events. By understanding what inter-vehicle communication occurs with whom, when vehicles communicate, and what vehicle knowledge is transmitted over space and time, insights can be generated on the interaction of events that influence the evolution of vehicle knowledge. Figure 2-8 (b) illustrates a spatiotemporal analysis of the knowledge of two vehicles shown in Figure 2-8 (a) in space and time. It illustrates that dynamic vehicle knowledge entails the following aspects: dynamic spatiotemporal coverage, time delay (different color shades imply different time delays), quality and quantity of travel experience data (thickness of line indicates the number of travel experience data for a corresponding link), and the relevance of data for its trip (based on current location and destination). These observations illustrate the need for a systematic understanding of vehicle knowledge characteristics to leverage its use to develop driver route guidance strategies, and system operator strategies for the efficient spread of useful information.

### **2.3.2.2 Information propagation chain**

The graph structure of the information flow network provides retrospective information related to how information evolves and vehicle knowledge is updated. This provides a capability to track

the spatiotemporal characteristics of information flow evolution and propagation directly through a connected graph structure and generate a fundamental understanding of how events affect the evolution of the information flow network. Figure 2-9 (a) illustrates an example of an information flow network using the graph-based representation and a subgraph of  $G^I$  indicating vehicle knowledge. The vehicle knowledge of this vehicle consists of a set of subgraphs that it generates or receives from other vehicles (from vehicle  $y$  and  $w$ ) through inter-vehicle communication. Therefore, the evolution of vehicle knowledge of interest can be tracked from any point using a graph-based search algorithm. A subgraph connected to a VIC node represents vehicle knowledge received from another vehicle through each inter-vehicle communication. As shown in Figure 2-9 (a), the vehicle knowledge of vehicle  $y$  (represented by a subgraph using dotted lines) is transmitted to vehicle  $x$  through the inter-vehicle communication from vehicle  $y$  to vehicle  $x$ . Figure 2-9 (b) illustrates the “Travel Data” obtained using the graph-based search algorithm.

The algorithm fans out from the node in the shaded circle in Figure 2-9 (a) in sequence, identifying the reachable nodes in “Travel Data”. VIC nodes in “Travel Data” form an information propagation chain which can address the following: (1) which vehicle contributes to propagating the travel experience data of vehicle  $z$  to vehicle  $x$ ?, and (2) what is the time required to propagate information to the target vehicle  $x$  through inter-vehicle communication?.

Figure 2-9 (c) shows each vehicle’s knowledge at the end of the simulation based on the same events as in Figure 2-9 (a). As can be seen, unlike in Figure 2-9 (b), the simulation-based approach is limited in its ability to illustrate the information flow evolution and propagation. That is, Figure 2-9(c) shows the vehicle knowledge without indicating the time dimension and the information propagation chain. It cannot easily infer which vehicle contributes to propagating the travel experience data  $z$  in the shaded square and when this experience data is obtained by vehicle  $x$ .

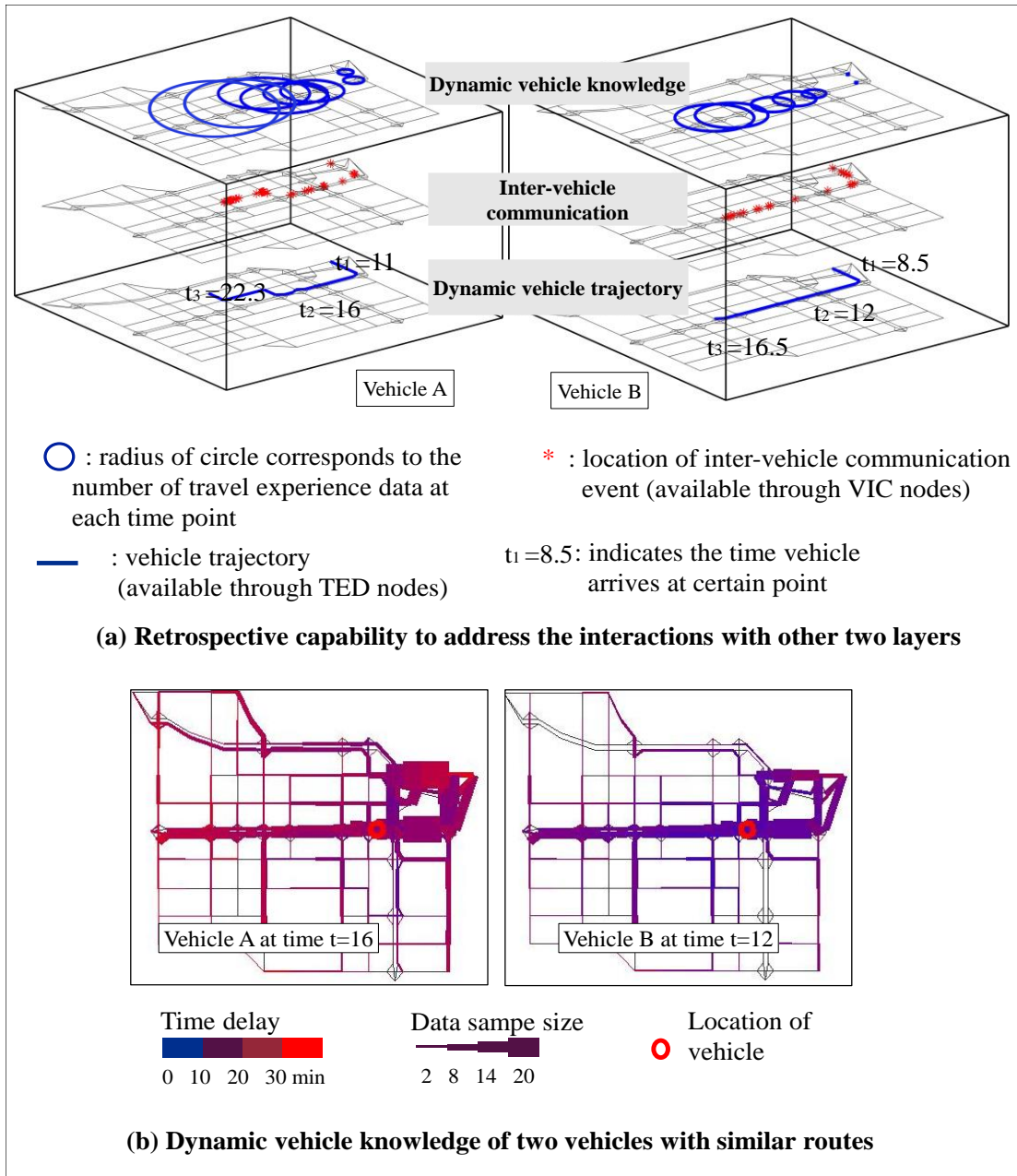


Figure 2-8 Multi-layer network analysis and evolution of vehicle knowledge

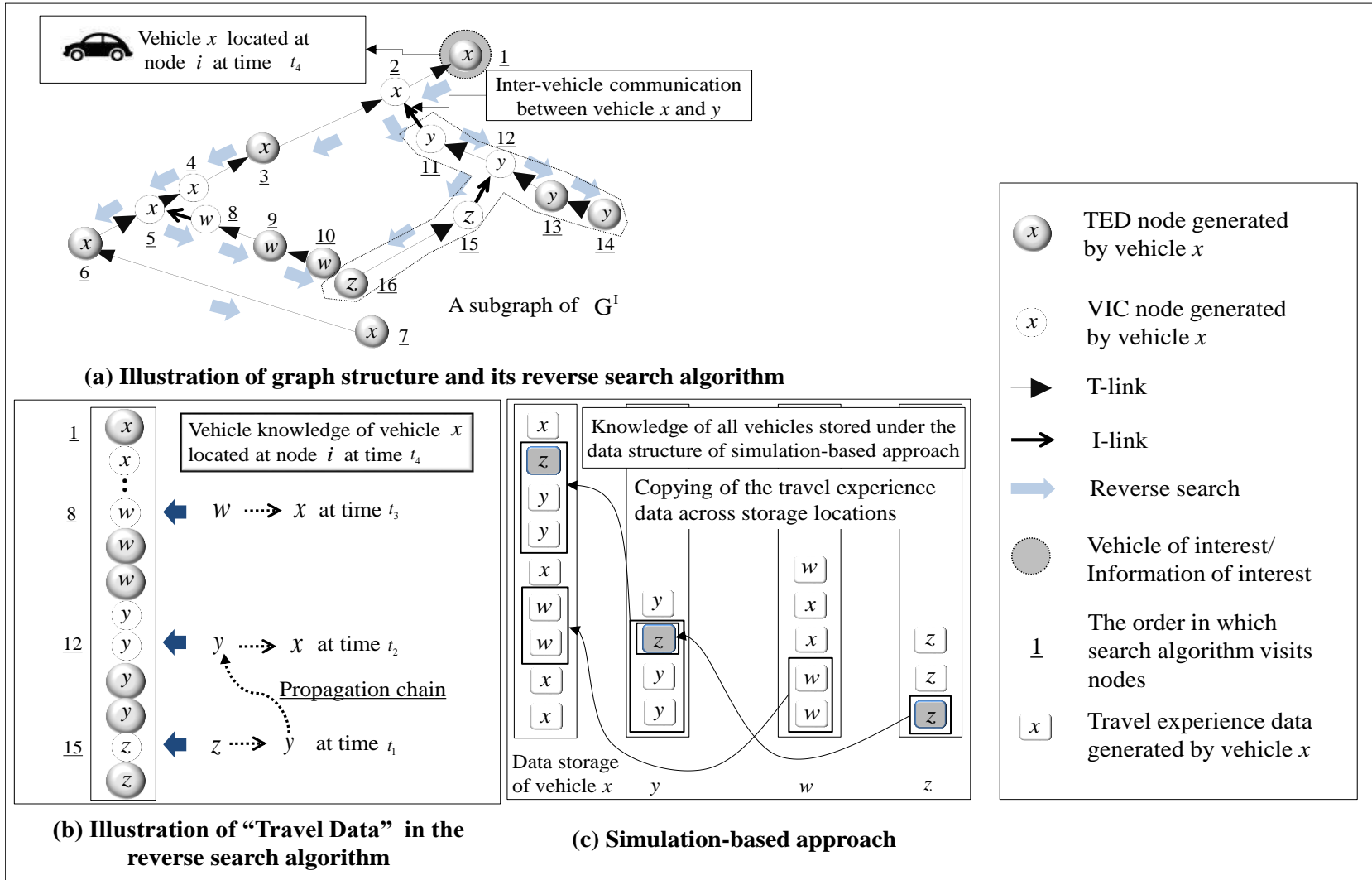


Figure 2-9 Comparison of spatiotemporal tracking capabilities

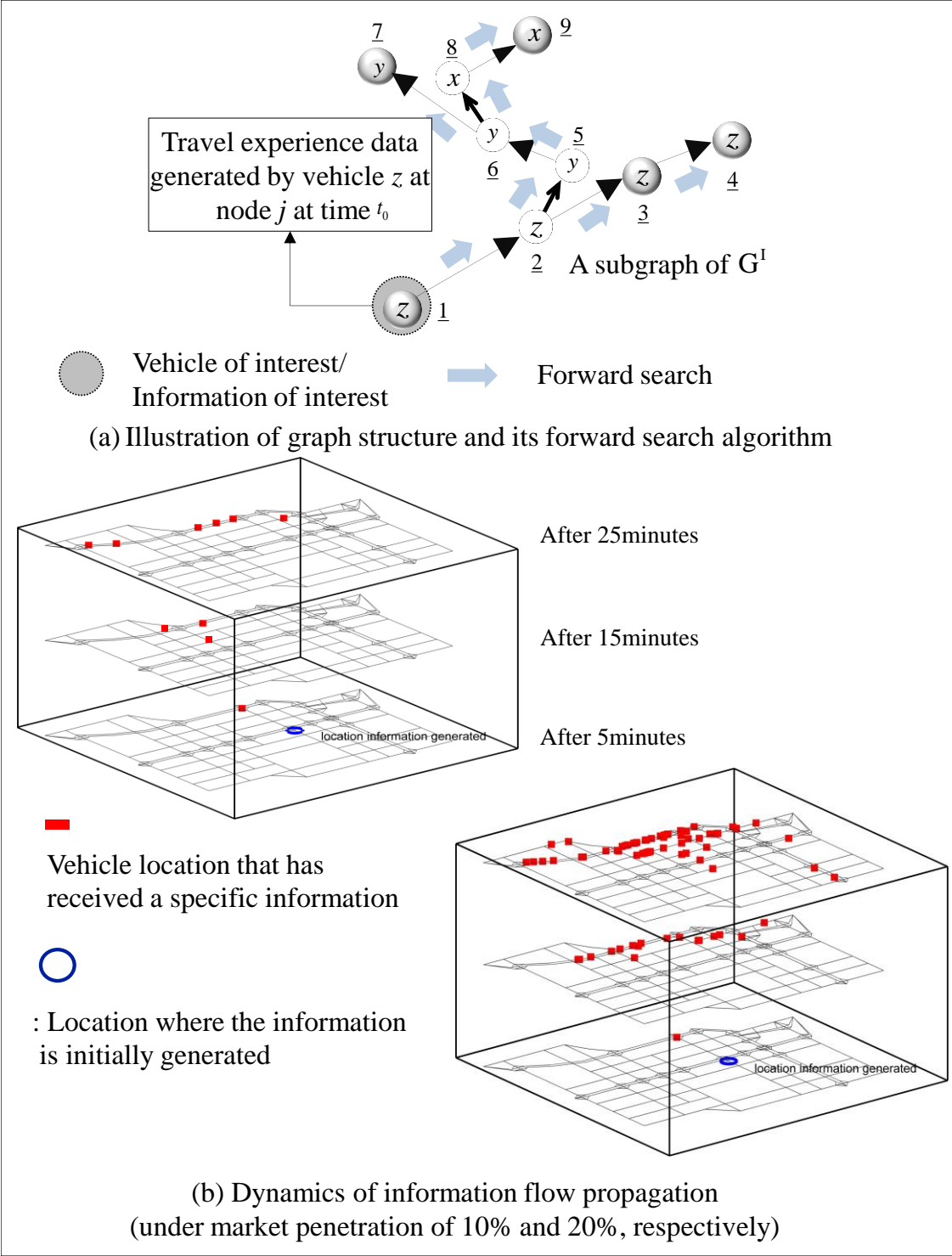


Figure 2-10 Dynamic information flow evolution and propagation under different market penetration rates

This is because the simulation-based approach copies data from the vehicle knowledge of one vehicle to another without explicitly indicating which vehicle is involved in the inter-vehicle communication. Therefore, tracking the spatiotemporal characteristics of the inter-vehicle communication requires the tagging of when such communications occur and which vehicles are involved in such communication, which can be computationally expensive. Figure 2-10 (a) illustrates a subgraph of  $G^1$  indicating the propagation of a single unit of information. A subgraph can explicitly address when and to whom a specific unit of information propagates. For example, travel experience data generated by vehicle  $z$  at time  $t_o$  propagates to vehicle  $y$  and  $x$  through the inter-vehicle communication, and the event locations can be tracked using the TED node as discussed in Section 2.3.2.1.

Therefore, the graph structure transparently provides a direct link to track the information flow evolution and propagation from one vehicle to another using the graph-based search algorithm from a TED node (which indicates a specific travel experience data). By contrast, the simulation-based approach requires a scan of the knowledge of all vehicles stored using the data structure in Figure 2-7 to determine whether it has a particular travel experience data of interest, which can be computationally expensive. Figure 2-10 (b) shows the propagation of a travel experience data from a vehicle in terms of the dynamics of traffic flow and inter-vehicle communication events. It shows which vehicle receives this information over time (5, 15, and 25 minutes after it is first generated) under different market penetration rates (10% and 20%).

### **2.3.3 Efficiency of the graph database**

#### **2.3.3.1 Graph database in the graph-based approach**

In contrast to the data storage mechanism of the simulation-based approach illustrated in Section 3.1, the graph database used in this study shares data in a single memory to represent the knowledge of all vehicles through interconnected nodes and links, and uses a local search to identify the vehicle knowledge of any vehicle. A reverse graph-based search algorithm leverages this structure to traverse the graph in a direction opposite to that of the information flow propagation from the current location of a vehicle to determine the current vehicle knowledge. More details on graph databases can be found in Robinson et al. (2013) and Sakr and Pardede (2012).

### 2.3.3.2 Memory usage efficiency

By sharing the nodes and links to represent the knowledge of vehicles in the information flow network, the graph database leads to memory size efficiency compared to a simulation-based approach which needs to store the vehicle knowledge separately for each vehicle to update the knowledge of other vehicles. The reverse search algorithm for each vehicle of interest identifies the subgraph of the information flow network that denotes its knowledge. Thereby, the proposed graph database is efficient and eliminates the need to store vehicle knowledge for each vehicle.

By contrast, the simulation-based approach adapts an update mechanism which copies data from the most recent vehicle knowledge of the broadcasting vehicle to the receiving vehicle at the time of inter-vehicle communication, as seen in Figure 2-7. Thus, the simulation-based approach must memorize all vehicles' knowledge individually to compute other vehicles' knowledge. This leads to an exponential increase in memory size usage for large scale real-world traffic networks.

Let  $|X|$  be the number of equipped vehicles in V2V-based ATIS, and  $|N^1|$ ,  $|C^1|$ ,  $|A^1|$ , and  $|M^1|$ , the number of elements in  $N^1$ ,  $C^1$ ,  $A^1$ , and  $M^1$ , respectively. Since the graph database of the information flow network is stored as a single graph, there is no duplication of nodes. Hence, the memory usage for representing the information flow network can be bounded by  $(|N^1| + |C^1| + |A^1| + |M^1|)$ . However, the memory usage for the simulation-based approach requires up to  $(|N^1| \cdot |X|)$ . This is because it stores all vehicles' knowledge individually to compute other vehicles' knowledge. That is, each of the  $|X|$  vehicles can have a maximum of  $|N^1|$  travel experience data nodes.

### 2.3.3.3 Computational efficiency

In the graph database, the vehicle knowledge of any vehicle can be identified by visiting only connected subgraph of information flow network. Therefore, it does not require an update of the knowledge of all vehicles to identify a specific vehicle's knowledge. In addition to addressing the three real-world objectives identified in Section 2-1, this provides a significant practical benefit in terms of the ability to track the spatiotemporal evolution of information for a specific class of vehicles. Further, traversing from one node to another is a constant time operation. Thus, the search time is defined solely by the number of nodes and links identified by the local search. This is irrespective of the size/topology of the information flow network as a whole. The time it takes to

search is determined by the local topology of the subgraph surrounding the particular node being traversed from.

Thus, the graph-based approach can identify a vehicle's knowledge with complexity  $O(|A^1| + |M^1|)$ . In the reverse search algorithm in Figure 2-6, the admissible links are identified and new nodes are marked and added to "List" and "Travel Data". The effort spent in identifying the admissible links from each node  $j$  in the information flow network is equal to the number of adjacent links to  $j$ , indicated by the link adjacency list of  $j$ . Hence, the graph-based approach for a vehicle of interest at a specific location has the order of the total number of links in  $G^1$ ;  $O(|A^1| + |M^1|)$ . Then, for a specific class of vehicles (such as vehicles in a certain geographical area or vehicles exposed to a certain variable message sign), the algorithm has an order  $O((|A^1| + |M^1|) \cdot |K|)$ , where  $|K|$  is the number of vehicles of the specific class  $K$ .

By contrast, to track the knowledge of a specific class of vehicles, the simulation-based approach relies on updating all processes starting from the first time interval to update the knowledge of a vehicle. Thus, the simulation-based approach in Figure 2-7 can identify a vehicle's knowledge of interest only when all processes of copying the travel experience data across storage locations are completed. Therefore, the execution time to identify the knowledge of a single vehicle is the same as that for identifying the knowledge of all vehicles.

The computational complexity is determined as follows. For each vehicle, each travel experience data is added to its storage location. Since there are  $|N^1|$  such travel experience data generated, the computational time to store all such data has an order  $O(|N^1|)$ . When inter-vehicle communication takes place, the vehicle knowledge is copied from the broadcasting vehicle storage location to the receiving vehicle storage location. Since the maximum size of vehicle knowledge has an order  $O(|N^1|)$ , the copy operation computational time for each inter-vehicle communication has an order  $O(|N^1|)$ . As the number of inter-vehicle communications is  $|N^1|$ , the time complexity of updating all vehicles' knowledge in the simulation-based approach is  $O(|N^1| + |N^1| \cdot |M^1|)$ . Since  $|M^1|$  can be really large, this approach is less efficient compared to the graph-based approach.

Further, the travel experience data are stored in the temporary memory on board the vehicle's system, and duplicate data from many other vehicles are processed and discarded. In this context, the simulation-based approach copies the travel experience data across storage locations and executes the process to filter duplicate data. However, in the graph database, each travel experience

data is represented by a node only once and its propagation is captured through the link representation, eliminating these filtering processes. This observation is important to further illustrate the efficiency of the graph-based approach.

## 2.4 Numerical experiments

### 2.4.1 Experiment design

The Borman Expressway network in northern Indiana, which includes interstates 80/94 and 65, and the surrounding arterials, is used as the study network. It consists of 197 nodes and 460 links, and has a size 11.3miles×8.5miles. Different demand levels (low: 11,074 vehicles; medium: 43,988 vehicles; high: 88,123 vehicles) and market penetration rates (1%, 5%, 10% and 20%) that denote percentage of V2V-equipped vehicles, are considered for analysis over a 90-minute period of interest. Figure 2-11 shows the Borman Expressway network.

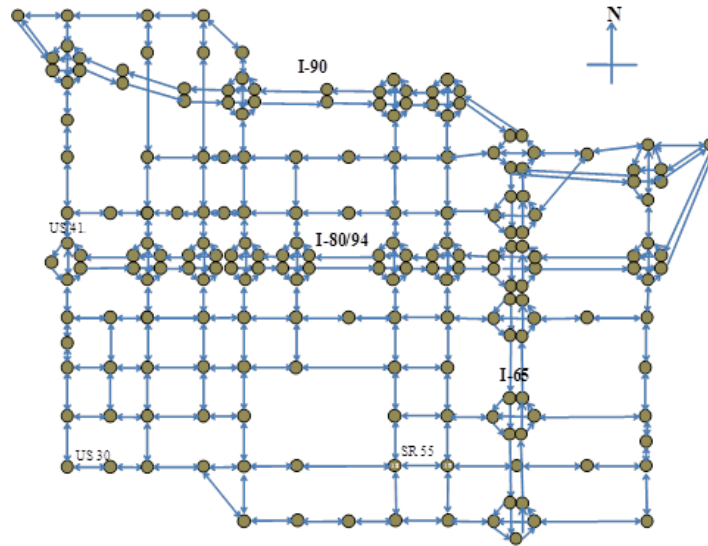


Figure 2-11 Study network

Of the three layers of the V2V-based ATIS, the traffic flow layer is replicated using a mesoscopic vehicular traffic simulator, DYNASMART-P, to represent the flow dynamics in the traffic network. To ensure consistency in comparison, both the graph-based and simulation-based approaches use the corresponding trajectories of the V2V-equipped vehicles in the traffic flow layer for a 90-minute time horizon of interest, and the inter-vehicle communication constraints, to determine the vehicle knowledge. The following inter-vehicle communication constraints are used: the inter-vehicle communication range (250m), interference rate (Equation (1)), and bandwidth

(2Mbps). Since the graph-based representation of the information flow network does not store the travel experience data in disparate storage locations, to calculate the data packet size of a vehicle the bandwidth constraint is applied by restricting the number of travel experience data (12,500 TED nodes) to be searched from a specific node in the information flow network. Correspondingly, for consistency, the simulation-based approach is allowed to copy only a maximum number of 12,500 such travel experience data for each inter-vehicle communication. The performance of the two approaches to identify the vehicle knowledge under various scenarios is examined in terms of memory usage efficiency and computational efficiency. In all scenarios, demand is loaded during the first 90 minutes of analysis. We examine twelve scenarios that represent combinations of three demand levels (low, medium, and high) and four market penetration rates (1%, 5%, 10%, and 20%).

## **2.4.2 Information flow network size and construction time**

Given events in the traffic flow and inter-vehicle communication networks, the information flow network is constructed in the graph-based approach by adding new nodes and links. The sizes of the information flow network under the 250m communication range, and different scenarios of demand and market penetration levels are summarized in Table 2-1 in terms of the number of equipped vehicles  $N$  and the number of network components, including TED nodes  $N_{TED}$ , VIC nodes  $N_{VIC}$ , T-links  $L_{T}$ , and I-links  $L_{I}$ . Here,  $N$  increases with the number of equipped vehicles  $N$ . As vehicles are more likely to exchange information under higher demand and market penetration rates, the associated number of nodes  $N_{TED}$ , and links  $L_{T}$  and  $L_{I}$  increase rapidly. The time to construct in terms of generating the node-link adjacency matrix of the information flow network is also shown in Table 2-1. Given the information flow network for each scenario, the graph-based approach identifies the spatiotemporal characteristics of vehicle knowledge using the graph-based reverse search algorithm.

## **2.4.3 Performance evaluation**

### **2.4.3.1 Memory usage efficiency**

Table 2-1 compares the memory usage of the graph-based information flow network and the simulation-based approach. For example, for the high demand scenario with market penetration

20%, the memory usage to store the knowledge of all vehicles requires 2.9 MB for the graph-based representation and 1.45 GB for the simulation-based approach.

Table 2-1 Information flow network size and construction time under different scenarios

Scenario*	Size of the information flow network					Network construction <i>time</i> (unit: seconds)
	$ X $	$ N^I $	$ C^I $	$ A^I $	$ M^I $	
L-1	111	1,082	174	1,145	87	0.04
L-5	543	5,060	4,146	8,663	2,073	0.06
L-10	1,091	10,324	15,936	25,169	7,968	0.53
L-20	2,173	20,763	62,280	80,870	31,140	1.4
M-1	372	3,490	2,488	5,606	1,244	0.25
M-5	1,834	16,885	54,464	69,515	27,232	1.15
M-10	3,682	33,995	202,806	233,119	101,403	4.2
M-20	7,354	67,729	689,358	749,733	344,679	15.1
H-1	601	4,959	8,260	12,618	4,130	0.4
H-5	2,986	24,898	174,082	195,994	87,041	2.8
H-10	5,953	49,895	589,180	633,122	294,590	13.2
H-20	11,953	99,947	1,945,198	2,033,192	972,599	42.3

\*L: low demand, M: medium demand, H: high demand; 1,5,10, and 20: market penetration rate (in percent)

The associated ratios of the memory usage of the simulation-based and graph-based approaches are shown in the last column. As the number of inter-vehicle communication events increases rapidly with higher demand and market penetration rates, the memory required to store the knowledge of all vehicles individually tends to increase exponentially.

As discussed earlier, the superior memory usage efficiency under the graph-based approach is due to the sharing of nodes and links to represent vehicle knowledge rather than duplicating the travel experience data when information propagation occurs.

### 2.4.3.2 Computational efficiency

Table 2-3 compares the computational times of the graph-based and the simulation-based approaches to determine the vehicle knowledge of all vehicles at their destinations to ensure consistency in comparison, as the simulation-based approach can determine their vehicle knowledge only at the end of the horizon of interest (90 minutes in the study experiments).

Table 2-2 Memory usage to update vehicle knowledge

Scenario*	Memory usage (unit: Megabytes)		
	Graph-based approach	Simulation-based approach	Comparison ratio
L-1	0.025	0.1	4
L-5	0.1	2.5	25
L-10	0.2	13.3	67
L-20	0.4	54	135
M-1	0.1	0.6	6
M-5	0.3	28.2	94
M-10	0.7	130	185
M-20	1.4	543	387
H-1	0.1	1.2	12
H-5	0.5	49	98
H-10	1.1	477	433
H-20	2.9	1,454	501

\*L: low demand, M: medium demand, H: high demand; 1,5,10, and 20: market penetration rate (in percent)

Table 2-3 Computation time to determine vehicle knowledge for all vehicles

Scenario*	Graph-based approach for the vehicle knowledge identification			Simulation-based approach
	Number of equipped vehicles  X	Average execution time of the search algorithm (seconds)	Time to determine the knowledge of all vehicles (seconds)	Time to determine the knowledge of all vehicles (seconds)
L-1	111	0.0018	0.2	0.3
L-5	543	0.0030	1.6	2.0
L-10	1,091	0.0046	5.0	7.2
L-20	2,173	0.0075	16.3	38.8
M-1	372	0.0024	0.9	1.4
M-5	1,834	0.0074	13.6	26.7
M-10	3,682	0.0169	62	310
M-20	7,354	0.0567	417	2,552
H-1	601	0.0031	1.9	4.4
H-5	2,986	0.0175	52	166
H-10	5,953	0.0502	299	1,147
H-20	11,953	0.1715	2,050	9,212

\*L: low demand, M: medium demand, H: high demand; 1,5,10, and 20: market penetration rate (in percent)

The number of equipped vehicles |X|, shown in the second column, represents the number of times that the reverse search algorithm is executed. Since the graph-based approach can identify the knowledge of a vehicle of interest without updating the other vehicles' knowledge, the associated average computational times across the vehicles in column 2 are shown in the third column. The computational times to determine the knowledge of all vehicles are shown in the fourth column (as the product of the second and third columns). The computational times to

determine the knowledge of all vehicles under the simulation-based approach are shown in last column.

In summary, an explicit modeling of the information flow network as a graph database leads to memory efficiency due to the circumvention of redundant storage of the travel experience data. Further, the local searching of only reachable nodes, which are a subgraph of the information flow network, enables the computational efficiency.

#### **2.4.4 Key insights for V2V-based ATIS**

As illustrated in Sections 2-3 and 2-4, a primary benefit of the graph-based approach is its capability to track the spatiotemporal characteristics of vehicle knowledge explicitly. Further, the proposed graph-based multi-layer network framework provides an explicit modeling capability to articulate how information flow evolves and propagates. It can link it to the interactions with traffic flow and inter-vehicle communication dynamics. The graph-based multi-layer framework also provides the important capability to determine the vehicle knowledge of any vehicle in space and time in a computationally efficient manner. By contrast, simulation-based approaches need to update the knowledge of all vehicles so as to track the knowledge of any vehicle or subset of vehicles of interest, and this can be computationally exhaustive and expensive. These capabilities of the graph-based approach are fundamental to illustrating the significance of this study. Information-based control and/or management of highly congested traffic networks, especially under random incidents (such as accidents), entails a detailed understanding of the information flow dynamics under V2V-based ATIS. Such an understanding is critical to develop strategies for the active control of congested traffic networks and the rapid flow of useful information. Hence, the proposed graph-based framework serves as a building block for the design of a new generation of information flow routing and vehicular route guidance strategies to manage traffic conditions in congested networks. That is, the proposed approach can pave the way to develop a range of graph-based and/or analytical models/strategies that can entail theoretical properties and illustrate spatiotemporal phenomena transparently. These aspects, and the capabilities to generate prescriptive solutions for both information flow and traffic flow, enable the proposed graph-based multi-layer network framework to foster advances significantly beyond the current simulation-based approaches for V2V-based ATIS.

While the proposed framework does not require public infrastructure, it may be beneficial to install public infrastructure along roads to promote the propagation of information for system-level applications. This vehicle-to-infrastructure (V2I) context is particularly useful: (i) during the initial deployment stages when the penetration rate of V2V communication devices is low, (ii) for a situation where the information collection is not smooth/adequate in certain locations of the network due to insufficient traffic flow, or (iii) for system-level traffic control strategies.

## **2.5 Summary and discussion**

The need to understand the information flow evolution and propagation, and spatiotemporal characteristics of the vehicle knowledge, is a core problem for a V2V-based ATIS, especially in the context of information-based decision-making by travelers and control by system operators. This study models the information flow evolution and propagation based on a dynamic graph structure in the form of a virtual information flow network emerging from the spatiotemporal events in the other two layers of the proposed integrated multi-layer network framework. The graph structure of the information flow network provides a key capability to track the complex spatiotemporal characteristics of information flow, and analyze the underlying fundamental relationships among the dynamics of the traffic flow network, inter-vehicle communication network, and the information flow network.

The graph structure of the information flow network enables the leveraging of well-known graph algorithms and properties to develop efficient approaches to explicitly elicit the information flow evolution and propagation aspects that characterize the dynamic vehicle knowledge. These capabilities are critical to develop strategies for the rapid flow of useful information and traffic routing to enhance network performance, and for the design of V2V-based ATIS so that such communications are reliable and successful. The proposed graph-based framework provides capabilities to transparently track information generation and propagation in both time and space. Thereby, individual vehicles can be tracked at any point in time or space to identify their current knowledge. The graph-based approach is compared to a simulation-based approach to determine vehicle knowledge. It illustrates the potential benefits of the retrospective capability of the graph-based modeling of the information flow evolution and propagation to identify the spatiotemporal characteristics of vehicle knowledge. Hence, a graph-based modeling of the information flow

evolution and propagation can provide powerful capabilities to leverage efficient graph-based methods and algorithms.

Synthetic experiments illustrate memory efficiency through the use of a graph database and computational efficiency through the use of a simple reverse search algorithm to update the vehicle knowledge by traversing a connected subgraph of the information flow network. Hence, graph-based modeling to identify vehicle knowledge can provide powerful capabilities to leverage efficient graph-based methods and algorithms.

The proposed multi-layer network framework represents a building block to develop both descriptive capabilities and prescriptive strategies related to propagating the flow of useful information efficiently, and synergistically generating routing mechanisms that enhance the traffic network performance. Hence, an important practical implication of the proposed methodology is the ability to generate effective traffic control strategies under V2V-based ATIS. The proposed methodology can serve as a platform to address several other applications and modeling needs related to V2V-based ATIS; they include routing strategies for specific classes of vehicles, targeted information propagation strategies to alleviate local traffic situations, rapid information communication strategies to address emergent safety problems, seamless communication of pricing strategies, etc.

Ongoing work by the authors seeks to leverage the graph-based multi-layer network framework in various ways. First, the inter-vehicle communication layer in the proposed framework assumes a deterministic framework. A stochastic modeling capability to generate greater realism is being incorporated. Second, we are developing V2V communications based route guidance strategies that link vehicle knowledge to driver decision-making, thereby completing the interactions loop in Figure 2-1 by linking the information flow network dynamics to the traffic flow network dynamics.

### **3. AN ANALYTICAL MODEL TO CHARACTERIZE THE SPATIOTEMPORAL PROPAGATION OF INFORMATION UNDER VEHICLE-TO-VEHICLE COMMUNICATIONS**

#### **3.1 Introduction**

Understanding and modeling the spatiotemporal characteristics of information flow propagation is a core problem for a vehicle-to-vehicle (V2V) communications based traffic system. For example, a forward collision warning system based on V2V communications can allow drivers to receive a safety warning from other vehicles when a vehicle traveling far ahead detects an impending rear-end collision (Biswas et al. 2006a; Palazzi et al. 2010). A cooperative system enables drivers to be continuously aware of each other and adjust their driving speed, so that the level of service and stability of traffic flow can be improved (Leontiadis et al. 2011; Monteil et al. 2013). An important issue that arises in the aforementioned V2V communication based traffic systems is how far and quickly information can propagate to other vehicles in the network.

In a traffic system with V2V communications, the dynamics of information flow propagation is shaped by the traffic flow dynamics and the V2V communication events. Hence, the modeling of information flow propagation entails the integration of dynamic traffic flow and V2V communication events.

An integrated multi-layer framework is required to describe the interdependencies among information flow, traffic flow, and the V2V communication events, each of which would represent a network layer in this framework (Kim and Peeta 2015). Due to inherent complexities introduced by the integration of traffic flow dynamics and V2V communications, information flow propagation is typically analyzed using simulation-based approaches, most of which integrate two simulators: a traffic flow simulator and a communication simulator (Kim 2007; Yang and Recker 2005, 2006). A detailed review on simulation-based approaches can be found in Spaho et al. (2011). The simulation-based approaches can adequately capture the non-linear interactions between traffic flow, V2V communications, and information flow. However, their major disadvantage is the lack of a rigorous mathematical formulation that precludes theoretical insights. Thereby, while traffic flow and V2V communication phenomena have been investigated using the simulation-based approaches, the applications developed therein are tailored to the specific problem.

In contrast to simulation-based approaches, an analytical approach can provide theoretical insights by integrating the dynamics of traffic flow and information flow into a multi-layer framework. However, existing analytical approaches have limitations to characterize the spatiotemporal propagation of information, as discussed hereafter.

First, most existing analytical approaches (Briesemeister et al. 2000; Ukkusuri and Du 2008; Wang 2007; Yang and Recker 2008) assume that information propagates instantaneously through a multi-hop process. A few studies (Kesting et al. 2010; Ng and Travis Waller 2010; Wu et al. 2005a) discuss the limitations of instantaneous information propagation which restricts the information hopping only to the spatial dimension. They propose models in which information is stored and relayed to other vehicles with time delay to relax the assumption of instantaneous propagation. However, traffic flow in these models is largely simplified as a static flow that relies on a statistical distribution of the spatial headway to derive analytical probability distributions for message transmission times and propagation speeds. A recent study (Du and Dao 2015) proposes models that assume precise vehicle movement trajectories are available, and does not include a traffic flow model. Hence, existing models cannot analytically describe the comprehensive interactions between the information flow propagation and the traffic flow dynamics, especially under congested traffic conditions. Second, to capture the information propagation in temporal dimension, some analytical approaches rely on the independent vehicle mobility assumption (Wu et al. 2004, 2009). Thereby, congestion phenomena are absent at medium to high densities, and the impacts from spatiotemporal vehicle movements, such as traffic propagation waves and queues, are not captured. As a result, the fundamental role of traffic flow in information flow propagation has largely been ignored in these models. It is significant because the traffic dynamics lead to spatiotemporal changes of vehicle position and equipped vehicles density within communication range, both of which constrain V2V communications. In the literature, Choffnes and Bustamante (2005) shows that the success rate of V2V communications based on the random waypoint model significantly differs from that based on a realistic traffic flow model.

Third, V2V communication constraints are not well captured in existing analytical approaches. Most of them only factor the communication range constraint. However, in the real world, the occurrence of V2V communication is also subject to other technical constraints, such as interference and bandwidth.

Fourth, to our knowledge, no existing analytical approach considers an information flow propagation wave that can be used to describe the interactions between the information flow and the underlying traffic flow. If equipped vehicles are distributed across a network and information is generated from a vehicle, information flow propagation waves can occur indicating the potential for a sudden variation of information density, similar to the traveling waves in epidemiology (Grenfell et al. 2001; Mollison 1977). In this regard, a wide variety of phenomena related to spatiotemporal information spread can be characterized by information flow propagation waves, which describe how the density, speed, and locations of the vehicles lead to the dynamics of information flow.

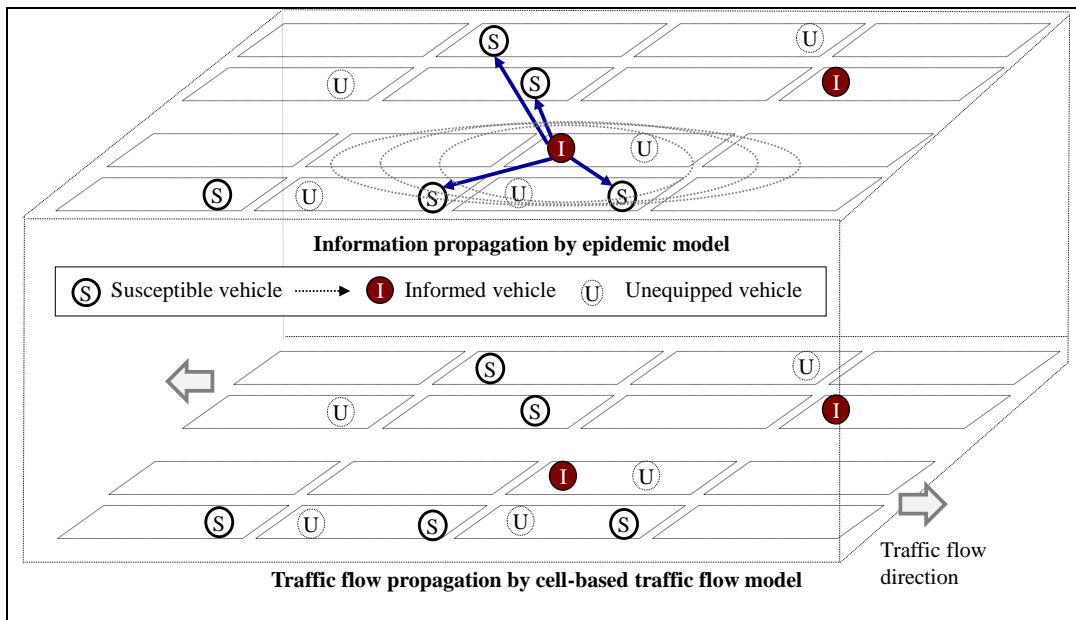


Figure 3-1 Conceptual framework of cell-based information flow propagation model

To bridge the methodological gaps in the existing literature, this study seeks to develop a descriptive analytical model that illustrates the information flow propagation. We propose a cell-based heterogeneous traffic flow model, where the information flow propagation mechanism is consistent with an epidemic model. Figure 3-1 illustrates a conceptual framework of the proposed model.

The model formulates the dynamics of traffic flow and information flow in a two-layer structure. The lower layer in Figure 3-1 describes the traffic flow propagation, where vehicles are considered as heterogeneous flows according to their status as follows. The set of vehicles in the transportation network, denoted by  $M$ , is divided into two disjoint subsets, i.e.,  $M = \{G, U\}$ ,

where  $G$  represents the set of vehicle equipped with a V2V communications capability and  $U$  represents the set of unequipped vehicles. The equipped vehicles (i.e., set  $G$ ) are further divided into two disjoint subsets,  $S$  and  $I$ , to represent the susceptible and informed vehicles, respectively. Informed vehicles already have the information, while susceptible vehicles do not yet have that information, but have the potential to receive that information. Vehicle movement in the traffic layer satisfies the classical traffic flow theory characterized by the cell transmission model (CTM) (Daganzo 1994) in this study.

The upper layer in Figure 3-1 describes the information dissemination among the equipped vehicles. A classical epidemic model is adapted to formulate the information dissemination process due to the similarity between the information transmission under V2V communications and disease transmission. At any time instant, all equipped vehicles attempt to communicate with other equipped vehicles within the communication range. If a susceptible vehicle successfully communicates with an informed vehicle, then that vehicle changes its status from susceptible to informed, similar to getting infected in epidemiology.

Following the two-layer structure, the proposed model provides capabilities to: (i) describe the characteristics of information flow wave built upon the traffic flow dynamics, (ii) factor the impacts from congested traffic, such as the backward traffic propagation wave, in information flow propagation, (iii) capture V2V communication constraints, and (iv) illustrate the dependency between the information flow propagation and the underlying traffic flow. These capabilities lead to a better understanding of the fundamental relationship between traffic flow dynamics and information flow propagation and enable a broader development of applications based on V2V communications.

The remainder of this paper is structured as follows. The next section introduces the fundamentals of epidemiology and the CTM. Section 3-3 presents the detailed model which integrates information flow propagation and traffic flow dynamics. This is followed by numerical experiments and the associated results in Section 3-4. The final section summarizes the main findings and future research directions.

## **3.2 Preliminaries**

### **3.2.1 Epidemic model**

In a V2V communications system, once an equipped vehicle generates traffic information (such as travel time on a link), the information continuously propagates to other vehicles through V2V communications. In this study, we use the term “information flow” to denote the flow of raw data between equipped vehicles, and data processing or data fusion/update.

There is a broad analogy between the information flow propagation among equipped vehicles and the transmission of an infectious disease between individuals, though the fundamental assumptions of standard epidemic models need to be revised to account for the unique characteristics of V2V communications due to their high mobility and V2V communication constraints. Table 3-1 summarizes the analogy between a V2V communications system and an epidemiological system, and the terminology that will be used in the study.

Applying an epidemic model to information flow propagation can aid in describing the underlying transmission mechanism of information. The complexity of information flow propagation in a V2V communications system precludes the formulation of the dynamics of information flow propagation using a simple equation. An epidemiological model bridges the microscopic description (the role of an infectious individual) to the macroscopic behavior of disease spread through a population. Hence, mathematical epidemic models provide a tool to formulate information flow propagation at the macroscopic level.

Table 3-1 Conceptual analogy between epidemiological and V2V communications systems

Notation	Epidemiology	V2V communications system
$G_i^t$	Set of individuals in community $i$ at time $t$	Set of equipped vehicles in cell $i$ at time $t$
$S_i^t$	Set of susceptible individuals in community $i$ at time $t$	Set of vehicles that can potentially receive the information in cell $i$ at time $t$
$I_i^t$	Set of infectious individuals in community $i$ at time $t$	Set of vehicles who have the information in cell $i$ at time $t$
$P_i^t$	<b>Force of infection:</b> Probability that a susceptible individual in community $i$ becomes infected between $t$ and $t+1$	<b>Force of communication:</b> Probability that a susceptible vehicle becomes informed in cell $i$ between $t$ and $t+1$
$\mu$	Success rate of the infection	Success rate of V2V communications

In classical epidemic models, the population is divided into two disjoint groups of individuals: the susceptible group (denoted by  $S_i^t$ ) and the infected group (denoted by  $I_i^t$ ). Let  $S_x^t$  and  $I_x^t$  denote the densities of vehicles that are susceptible and informed, respectively, and located at  $x$  at time  $t$ . Then the spread of infection can be governed by the following differential equations (Mollison 1977):

$$\frac{\partial S}{\partial t} = -\lambda q S I, \quad (1)$$

$$\frac{\partial I}{\partial t} = \lambda q S I, \quad (2)$$

with initial condition  $S(0) = S_0 > 0$  and  $I(0) = I_0 > 0$ . Here,  $\lambda > 0$  is the average contact rate, and  $q > 0$  known as the success rate of infection. The above formulation is also known as a Susceptible-Infected model, which can be approximated by difference equations.

Several previous studies (Chen and Robert 2004; Chen et al. 2003; Cole et al. 2005) in computer science and recent studies (Khelil et al. 2002; Nekovee 2006; Trullols-Cruces et al. 2013) in information spreading have modeled the propagation of a computer virus or malicious information in a network. For example, Trullols-Cruces et al. (2013) evaluates the dynamics of a vehicular malware epidemic in a large-scale road network. However, the applicability of an

epidemic model for a V2V communication system with traffic flow dynamics has not been numerically validated previously.

An analogy of the Susceptible-Infected model under V2V communications is the Susceptible-Informed (SI) model. However, the SI model cannot address the underlying traffic dynamics that affect the information flow propagation. The inclusion of an traffic flow model is a key ingredient in the modeling of the spatiotemporal propagation of information under V2V communications.

### 3.2.2 Traffic flow model

Daganzo (1994 and 1995) introduced the cell transmission model (CTM) as a continuous-to-discrete transformation of the LWR model (Lighthill and Whitham 1955; Richards 1956). The key advantages of the CTM are: (i) its low computation requirements compared to micro simulation models, (ii) a simpler structure that can model traffic propagation without the assumption of a link performance function or an exit function, and (iii) the ease with which it can be empirically calibrated in practice (Lin and Ahanotu 1995; Muñoz et al. 2004). The CTM captures several key phenomena of real-world traffic flow such as kinematic waves, and queue formation and dissipation, in an explicit manner, making it a suitable platform for modeling dynamic traffic.

The CTM can be constructed as follows. The road network is represented by the set of cells  $C$  with a length equal to the distance traveled at free flow speed in one time interval  $\Delta t$ , and the set of cell connectors  $E$ . Let  $\Gamma^+(i)$  denote the set of successors of cell  $i \in C$  and  $\Gamma^-(i)$  denote the set of predecessors of cell  $i \in C$ . The maximum occupancy of a cell  $i \in C$  at time point  $t \in T$  is  $N_i^t$ , and the maximum inflow or outflow is  $Q_i^t$  for time step  $t \in T$ . For cell  $i \in C$  in time step  $t \in T$ , the free-flow speed is  $v_i^t$ , the traffic backward wave propagation speed is  $r_i^t$ , and the ratio  $\delta_i^t = r_i^t / v_i^t$ .

Further, denote  $x_i^t$  as the number of vehicles in cell  $i \in C$  at time point  $t \in T$ ,  $y_{ij}^t$  the number of vehicles routed by cell connector  $(i, j) \in E$ , in time interval  $(t, t+1)$ . These two sets of variables are the decision variables in the CTM. Other notation will be defined when first introduced. In the CTM, vehicles moving from an upstream cell to a downstream cell satisfy two main constraints on flow conservation and flow restriction:

$$x_i^t = x_i^{t-1} + \sum_{k \in \Gamma^-(i)} y_{ki}^{t-1} - \sum_{j \in \Gamma^+(i)} y_{ij}^{t-1}, \quad \forall i \in C, t \in T, \quad (3)$$

$$y_{ij}^t = \min \left\{ x_i^t, q_i^t, q_j^t, \delta_j^t (N_j^t - x_j^t) \right\}, \quad \forall i \in C, j \in \Gamma^+(i), t \in T. \quad (4)$$

Equation (3) indicates the flow conservation. Equation (4) represents flow propagation that is restricted by the three traffic conditions of the underlying trapezoidal flow density relationship: (i) free flow, (ii) saturated, and (iii) congested.

The CTM is a difference equation system, where traffic dynamics are examined at discrete time steps. Discrete-time models are especially appealing for the description of vehicle traffic movement as well as the information flow propagation process, since such a process can be conceptualized as evolving through a set of discrete-time epochs rather than continuously. In addition, most available simulation-based or field data are discrete in nature (e.g., success or information transmission rates for a given time interval). The integration of the epidemic model and the CTM is illustrated in next section.

### 3.3 Mathematic modeling of the spatiotemporal propagation of information

The proposed model, named CTM-SI model, is a system of difference equations in the discrete space and discrete time domains. The difference equations system prescribes the V2V communications as well as the traffic flow dynamics.

#### 3.3.1 Modeling heterogeneous traffic flows

In the proposed CTM-SI model, vehicles are classified into groups depending on their status S, I, and U with regard to the information of interest. All variables in the CTM are first expanded to S-I-U subgroups. Classical infectious disease propagation models in epidemiology are based on the status change of disease in a population. Here, two groups of vehicles, S and I, are used to describe information flow propagation. Once a susceptible vehicle receives the information, it moves into the informed group. Only informed vehicles can transmit the information. An informed vehicle is assumed to keep carrying and broadcasting the information.

Heterogeneous traffic flow movement in the CTM-SI model satisfies the flow conservation constraint (5) for each group of vehicles as follows:

$$\hat{x}_{i,g}^t = x_{i,g}^{t-1} + \sum_{k \in \Gamma^-(i)} y_{ki,g}^{t-1} - \sum_{j \in \Gamma^+(i)} y_{ij,g}^{t-1} \quad (5)$$

where subscript  $g \in M = \{S, I, U\}$  denotes each group of vehicles and  $y_{ij,g}^t$  represents the total number of vehicles in group  $g$  advancing from upstream cell  $i$  to downstream cell  $j$  during time interval  $(t-1, t)$ . Note that the road capacity is shared by all groups of vehicles. Based on the proportional movement assumption that is used for multi-class vehicle movement in the CTM (Han et al. 2011), the vehicular flow restriction constraint (4) has a corresponding reformulation for each group of vehicles  $g \in M$ , as follows:

$$y_{ij,g}^t = \frac{x_{i,g}^{t-1}}{\sum_{g \in M} x_{i,g}^{t-1}} \cdot \min \left\{ x_i^t, q_i^t, q_j^t, \delta_j^t (N_j^t - x_j^t) \right\}, \quad \forall g \in M, \quad (6)$$

where  $\sum_{g \in M} x_{i,g}^{t-1} = x_i^{t-1}$  represents the total number of vehicles in cell  $i$  at time  $t-1$ . The group-specified flow restriction constraint (6) shows that each group of vehicles proportionally advances to the downstream cell.

In the CTM-SI model, equations (5) and (6) are used as an intermediate step to update the heterogeneous traffic flow dynamics due to the V2V communications. The intermediate step allows the factoring of the traffic flow dynamics into the V2V communication constraints. It should be noted here that since V2V events can occur within a time interval, time discretization can lead to approximation, especially as the interval length increases. The details of information flow propagation are presented in the next section.

### 3.3.2 Modeling information flow propagation

Determining the rate at which the susceptible vehicles become informed is the core part of the proposed CTM-SI model and is critical to determining the information flow propagation waves. Without loss of generality, the study assumes that the information hopping distance in one-time interval is equal to one cell length due to the communication constraints.

Based on the intermediate step, a fraction of vehicles that belong to susceptible group  $S$  in cell  $i$  at time  $t$  have received the information during time interval  $(t-1, t)$  depending on the V2V communication constraints. This fraction is determined by the force of communication  $P_i^t$ , which

is the probability that the information is received by a susceptible vehicle during a time interval. Then, the susceptible group of vehicles in cell  $i$  at time  $t$  is updated as:

$$x_{i,S}^t = (1 - P_i^t) \cdot \hat{x}_{i,S}^t \quad (7)$$

where  $\hat{x}_{i,S}^t$  is determined by equation (5). As a result, the informed group  $I$  in cell  $i$  at time  $t$  can be updated as:

$$x_{i,I}^t = \hat{x}_{i,I}^t + P_i^t \cdot \hat{x}_{i,S}^t . \quad (8)$$

The unequipped vehicle in group  $U$  would not change its status; that is:

$$x_{i,R}^t = \hat{x}_{i,R}^t . \quad (9)$$

Note that equations (7) - (9) ensure flow conservation, that is,  $x_{i,S}^t + x_{i,I}^t + x_{i,U}^t = \hat{x}_{i,S}^t + \hat{x}_{i,I}^t + \hat{x}_{i,U}^t$ .

The next section focuses on the determination of  $P_i^t$ .

### 3.3.3 Modeling the force of communication

The force of communication corresponds to the force of infection in epidemiology, which denotes the probability per unit time that a susceptible individual becomes infected. The classical epidemic models (Keeling and Rohani 2008; Kermack and McKendrick 1927; Rvachev and Longini 1985) assume homogeneous mixing in a large population size, meaning that the individuals with whom a susceptible individual has contact are proportional to the prevalence of the infectious individuals. This assumption allows the use of nonlinear differential equations to describe the rates of change for the respective groups. However, this assumption of homogeneous mixing may not hold for V2V communications, due to the communication range constraints.

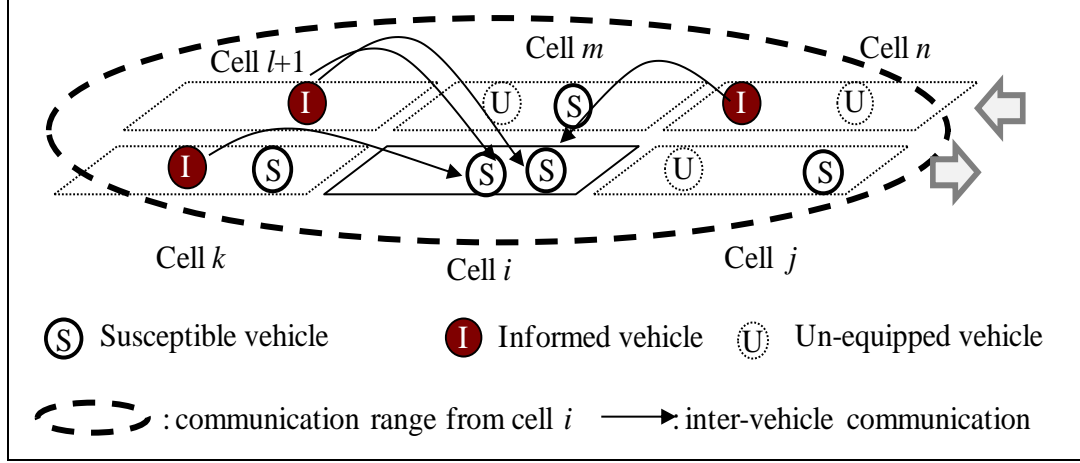


Figure 3-2 V2V communication range

The communication range constraint is defined as follows. Any pair of vehicles whose distance is less than a predefined communication range may communicate with each other at any time through V2V communications as shown in Figure 3-2. Note that all susceptible vehicles within communication range have the same probability to be informed vehicles.

The force of communication,  $P_i^t$ , varies in each cell  $i$  and at each time  $t$ , as the force of infection in modeling the disease spread on a social network (Newman 2002). Consider a susceptible vehicle inside cell  $i$  at time  $t$ , and let  $z_{i,I}^t$  denote the number of informed vehicles within its communication range. Let the success rate of V2V communications between any pair of equipped vehicles be  $\mu$ . Then,  $P_i^t$  is determined by:

$$P_i^t = 1 - (1 - \mu)^{z_{i,I}^t}. \quad (10)$$

In general,  $z_{i,I}^t$  varies across cells, determined by  $z_{i,I}^t = \sum_{j \in C(i)} x_{j,I}^t$ , where  $C(i)$  denotes the set of cells within the communication range of cell  $i$ .

Note that the success rate of the infection  $\mu$  in the classical epidemic model is assumed to be constant (Kermack and McKendrick 1927). It may not be the case for V2V communications, as the success rate of V2V communications also depends on the interference which is based on the number of equipped vehicles within the communication range. It is reasonable to assume that the success rate of V2V communications is a decreasing function of the equipped vehicle density, where a large number of equipped vehicles lead to an increase of interference. Therefore, the success rate  $\mu$  abstracts the V2V communication constraints for information transmission.

Although the lack of real world data makes it difficult to measure success rate precisely, it is possible to estimate the success rate through a simulation-based approach. The next section describes the estimation of the success rate of V2V communications.

### 3.3.4 Estimation of success rate of V2V communication

The goal of estimation is to use an equation to describe the relationship between the success rate of V2V communications,  $\mu$  and the density of equipped vehicle. An integrated simulation-based approach is used to estimate  $\mu$ , where a traffic flow simulator DYNASMART (Mahmassani et al. 1998) describes the traffic flow dynamics and V2V communication constraints are considered, including wireless communication range, the interference rate and bandwidth. We first generate the traffic flows under various scenarios with different demand levels and market penetration rates ( $\alpha$ ) that denote the percentages of V2V-equipped vehicles, and track the trajectories of all equipped vehicles. Then, we compute whether vehicles succeed or fail to communicate with each other along the locations/trajectories traveled by equipped vehicles in the presence of interference. For simplicity, the information propagation mechanism in this study assumes that the V2V communications can occur successfully up to a predefined distance (200 meters) representing the communication range, and none beyond it. Thereby, the effect of the communication success rate decay with distance is ignored. The communication frequency are set to be 0.5 seconds. For the communication from equipped vehicle  $b$  to equipped vehicle  $a$ , the interference rate is defined as (Gupta and Kumar 2000):

$$\frac{T_a}{\|\theta_a - \theta_b\|^2} / \sum_{\substack{k \in G \\ k \neq a}} \frac{T_k}{\|\theta_k - \theta_b\|^2} \geq \beta \quad (11)$$

where  $\theta_k$  denotes the coordinates of an equipped vehicle  $k$  within communication range of equipped vehicle  $a$ . A simultaneous broadcasting at some time instant from a subset of equipped vehicles within the communication range leads to possible interference. The signal power decays with distance from a broadcasting vehicle  $k$  as  $1/\|\theta_k - \theta_b\|^2$ . The transmitted information from vehicle  $b$  is successfully received by vehicle  $a$  if it satisfies the minimum signal-to-interference ratio of  $\beta$  (the study experiments use  $\beta = 2$ ) as shown in Figure 3-3. The signal power level of vehicle  $a$  ( $T_a$ ) and of all vehicles ( $T_k$ ) is identical in this study. The accomplishment of V2V communications between a pair of equipped vehicles is checked every 0.5 seconds. Also, we

assume that vehicles transmit a packet size that is less than 1 kilobyte at the data rate of 3Mbit/s. When the density of equipped vehicles is less than a critical value, the V2V communications under the assumptions would not exceed the available bandwidth capacity. Hence, when the density of equipped vehicles exceeds the critical value, it would cause communication irregularities (Killat and Hartenstein 2009) that are not addressed by our model.

Then, the success rate  $\mu$  is calculated based on simulation results as follows:

$$\mu(w) = s(w) / (s(w) + f(w)), \quad (12)$$

where  $s(w)$  is the number of vehicles who successfully receive information,  $f(w)$  is the number of vehicles who fail to receive information due to the communication constraints, and  $w$  denotes the total number of equipped vehicles within the V2V communication range.

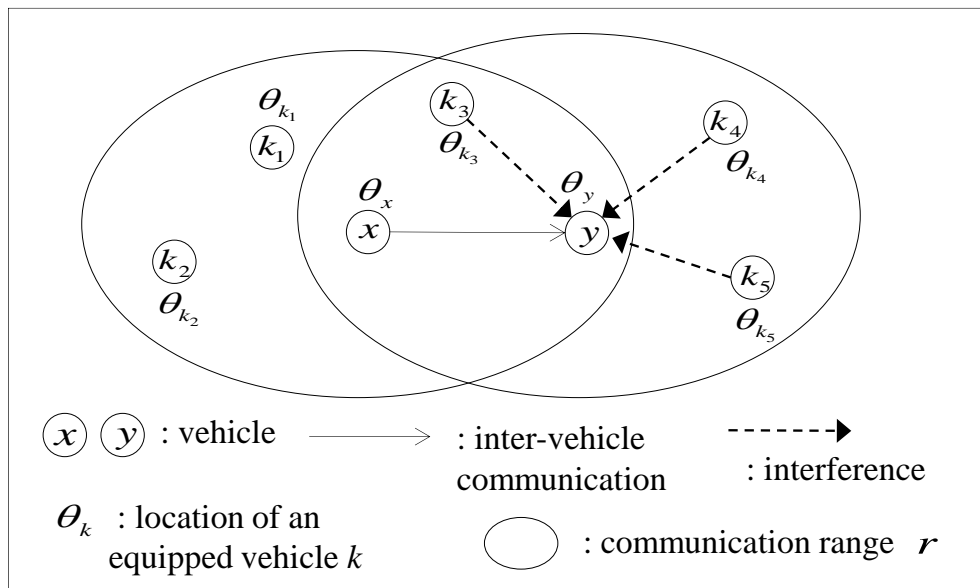


Figure 3-3 V2V communication range and interference among vehicles in simulation-based experiment

The values of  $\mu$  for different numbers of equipped vehicles are shown in Figure 3-4. The Least Sum of Squared Errors (LSSE) was applied to estimate the function  $\mu$ . The estimation result indicates that the success rate of V2V communications is a negative exponential function of the density of equipped vehicles within V2V communication range. It means that a larger number of equipped vehicles in communication range increase the potential interference.

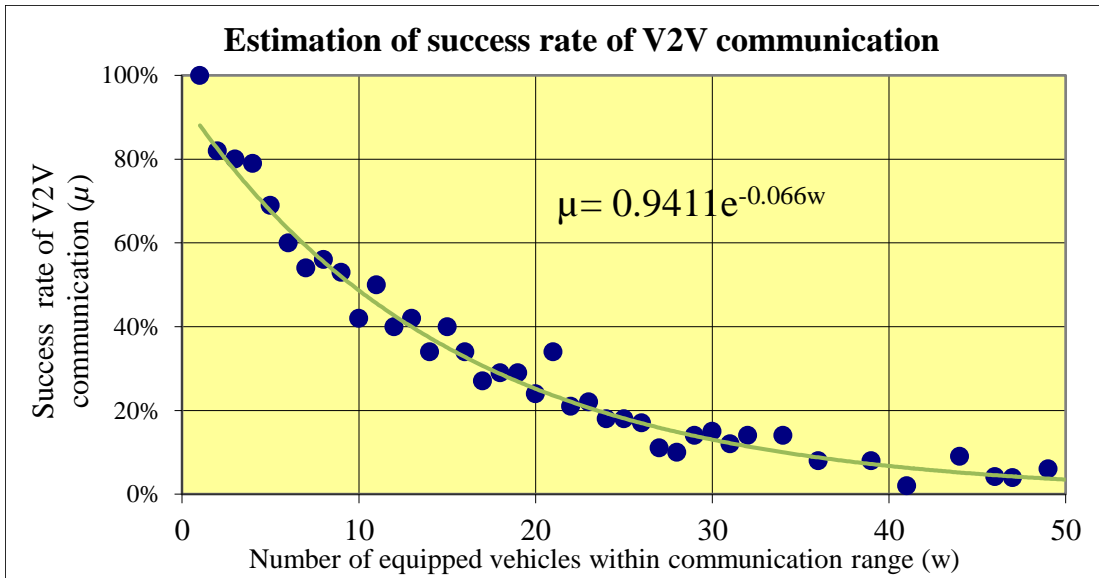


Figure 3-4 Estimation of success rate of V2V communication ( $\mu$ )

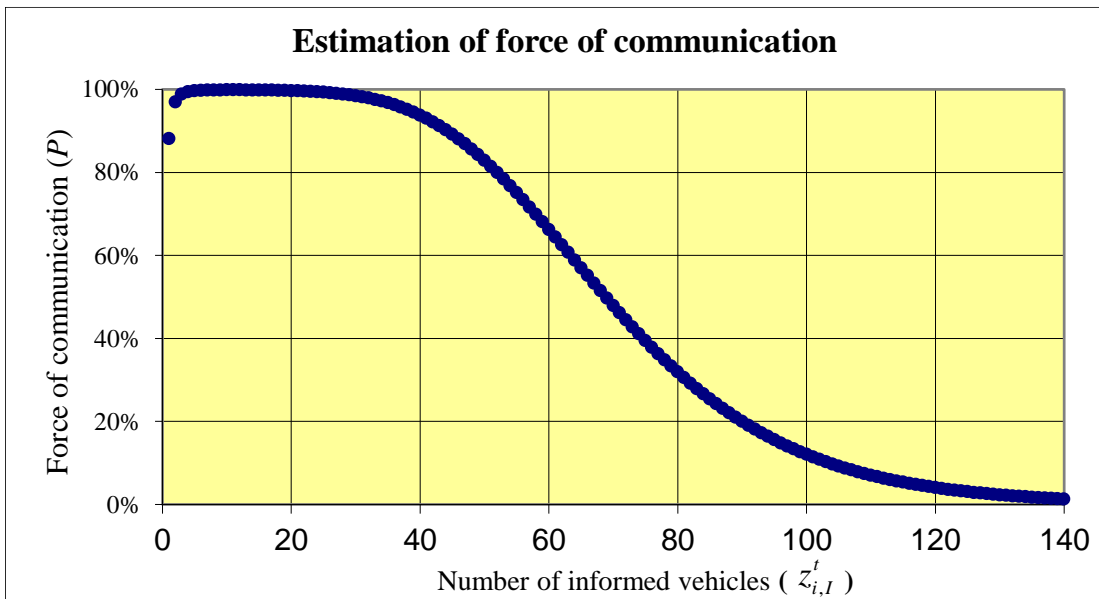


Figure 3-5 Force of communication ( $P_i^t$ )

Using the estimated function  $\mu(w)$ , the corresponding force of communication  $P_i^t$  can be calculated as shown in Figure 3-5.  $P_i^t$  reaches and maintains 100% when the density level of informed vehicles  $z_{i,l}^t$  is below 22 vehicles within communication range. It decreases with higher density levels of informed vehicles. It indicates that while a larger number of equipped vehicles imply the potential to communicate with more vehicles, it simultaneously increases the

interference as well. Consequently, the number of vehicles that successfully communicate decreases with higher density of informed vehicles due to the increased interference rate.

### 3.3.5 Deriving analytical formula for the wave speed of the information flow propagation

When the information is spreading, an information flow propagation wave separates the traffic flow into the informed and uninformed regions and moves towards the uninformed region with a certain speed. The aim of this section is to derive the analytical formulation of the wave speed of information flow propagation, which is a function of traffic density and market penetration rate ( $\alpha$ ).

We label the wave speed of information flow propagation in the direction of vehicular traversal as the forward propagation wave speed ( $v_f$ ). The wave speed of information flow propagation opposite to the direction of vehicular traversal is defined as the backward propagation wave speed ( $v_b$ ). We consider a uniform stream of traffic on a highway whose density is  $\rho$ .

The wave speed of information flow propagation consists of three parts: (i) information hopping speed ( $v_i$ ) through V2V communications, (ii) traffic flow speed ( $v_t$ ), and (iii) adjusted speed ( $v_a$ ) due to the temporal and spatial discretization in the CTM.

The information hopping speed can be estimated as:

$$V_i = v_i^t \times (1 - (1 - \mu(w))^{z_{i,t}^t}) \approx v_i^t \times (1 - (1 - \mu(w))^{w/3}) \quad (13)$$

where  $v_i^t$  is free flow speed,  $w$  is the number of equipped vehicles within communication range, and  $z_{i,t}^t$  is the number of informed vehicles within communication range of cell  $i$ . Equation (13) represents that the information hopping speed depends on the force of communication. However,  $z_{i,t}^t$  varies across space and time, and this precludes the derivation of a close-form formulation. We approximate  $z_{i,t}^t$  based on the scenario that the equipped vehicles in the adjacent upstream cell  $k$  are informed and those in cell  $i$  and in the adjacent downstream cell  $j$  are susceptible. In this scenario, all informed vehicles that can communicate with the susceptible vehicles in cell  $i$  are in cell  $k$ . Therefore, the number of informed vehicles within the communication range of cell  $i$ , i.e.,  $z_{i,t}^t$ , can be estimated as  $w/3$  under a uniform stream of traffic flow. As information is assumed

to propagate only to the adjacent cells in one time interval, the maximum information hopping speed is equal to the free flow speed  $v_i^t$ .

The traffic flow speed,  $v_T$ , is determined by the fundamental diagram which implies a speed-density relationship. This study adopts a trapezoid fundamental diagram in the CTM where the traffic speed can be expressed by (Jin and Recker 2010):

$$V_T = \begin{cases} v_i^t, & 0 \leq \rho < \rho_c \\ \frac{Q_i^t}{\rho}, & \rho_c \leq \rho < \rho_k \\ \frac{\rho_k \cdot (\rho_j - \rho)}{(\rho_j - \rho_k) \cdot \rho} \cdot \frac{Q_i^t}{\rho_k}, & \rho_k \leq \rho \end{cases} \quad (14)$$

where,  $Q_i^t$  is maximum flow for time step,  $\rho_c$  is the critical density,  $\rho_k$  is equal to  $\rho_j - \rho_c$ , and  $\rho_j$  is the jam density.

In addition, temporal and spatial discretization in the CTM model can lead one fraction of vehicles to advance to downstream cells and the other fraction of vehicles to remain in the current cell under saturated and congested traffic conditions, if there are no spillbacks downstream. Under these conditions, the ‘‘leading forward front’’ vehicles for the forward propagation wave are defined as the informed vehicles inside the leading forward front cell (that separates the informed and uninformed regions) that advance to the downstream cell in the next time step. For the backward propagation wave, the ‘‘trailing backward front’’ vehicles are defined as those informed vehicles inside the trailing backward front cell (that separates the informed and uninformed regions) that remain in that cell in the next time step. From the information flow propagation perspective, the front vehicles determine the forward and backward propagation wave speeds. This observation motivates the derivation of the adjusted speed to account for the front vehicle speed differences for forward and backward propagation waves under saturated and congested traffic conditions. The adjusted speed  $v_A$  is as follows:

$$V_A = (V_k - V_T) \times (1 - \mu(w))^{A(\rho)} \quad (15)$$

where  $V_k$  is the front vehicle speed and  $A(\rho)$  is the number of front vehicles. The term  $(V_k - V_T)$  represents difference between the front vehicle and average vehicle speed. Here, we use free flow speed as the speed of the leading forward front vehicles and zero as the speed of the trailing

backward front vehicles to be consistent with the CTM-SI model. The number of front vehicles  $A(\rho)$  is defined as  $y_{ij}^t / \alpha$  and  $(x_i^t - y_{ij}^t) / \alpha$  for the forward and backward propagation wave speed, respectively. The term  $(1 - \mu(w))^{A(\rho)}$  represents the probability that a susceptible vehicle in a downstream cell will receive information through a leading forward front vehicle, or in an upstream cell through a trailing backward front vehicle. Finally,  $v_F$  and  $v_B$  are defined as:

$$V_F = V_I + V_T + V_A \quad (16)$$

$$V_B = V_I - V_T + V_A \quad (17)$$

Note that though the derivation of equations (16) and (17) is based on uni-directional traffic flow, the formulation holds for bi-directional traffic flow as well. Under the bi-directional traffic flow case, the backward propagation wave speed of one direction is determined by the forward propagation wave speed of its opposite direction.

### 3.4 Numerical experiments

#### 3.4.1 Experiment Design

The network consists of 200 cells and 199 cell connectors, which are equivalent to 22 miles of highway length. Different levels of demand and a pre-defined market penetration (50%) are used to generate various traffic conditions. The cell parameters are provided in Table 3-2 using CTM terminology. Note that all cells have homogeneous characteristics. The study focus is on the spatiotemporal information flow propagation along with the traffic flow dynamics. In this sense, a uniform stream of traffic with density  $\rho$  on a long highway is considered. To describe the relationship between the traffic flow dynamics and spatiotemporal information flow propagation, the inflow rates are assumed constant.

Table 3-2 Cell characteristics of the study network

Free flow speed (mph)	65
Time interval (seconds)	6
Cell length (miles)	0.11
Number of lanes	3
Number of cells	200
Maximum link flow (vehicle/hr/lane)	2,350
Maximum cell flow (vehicle/time interval)	12
Maximum number of vehicles per cell	60

### 3.4.2 Uni-directional highway

First, the results on uni-directional traffic flow streams are illustrated. The forward and backward propagation wave speeds of information flow are shown in Figure 3-6. Note that since vehicles carry the information, and the information can leap forward through V2V communications, forward propagation wave speed of information flow is always greater than or equal to a vehicle's speed.

As shown in Figure 3-6 and Figure 3-7, under low density case (Case 1:  $\rho = 7$ ), the forward propagation wave speed of information flow is close to the free flow traffic speed because the opportunity for V2V communications is limited. As the density increases, the opportunity for V2V communications increases. The maximum forward propagation wave speed of information flow reaches (Case 2:  $\rho = 27$ ), while the traffic flow speed does not change. As the density level increases further, the traffic flow speed decreases, so does the forward propagation wave speed of information flow (Case 3:  $\rho = 80$  and case 4:  $\rho = 160$ ) due to the reduced traffic flow speed and the reduced success rate of V2V communications under high densities.

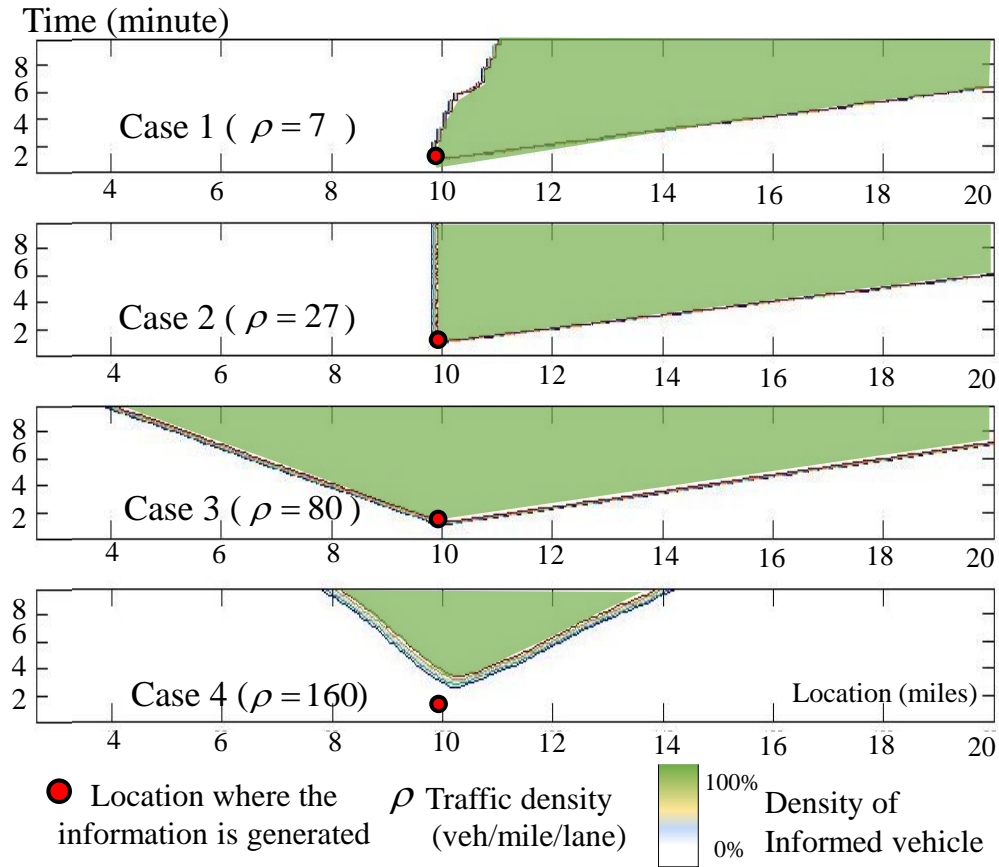


Figure 3-6 Forward and backward propagation wave speeds of information flow under the uni-directional traffic scenario

Similarly, the backward propagation wave speed of information flow can be analyzed. Under very low density, backward propagation wave of information flow may not occur, due to the limited opportunity for V2V communications (Cases 1 and 2). As the density level increases, the backward propagation wave of information flow occurs and gradually reaches its maximum speed (Case 3) due to the increased opportunity for V2V communications and slower traffic flow speed. However, as the density level increases to more than 80 veh/mile/lane, the backward propagation wave speed of information flow reduces (Case 4) due to the much higher impact of interference than the effect of the reduced traffic speed.

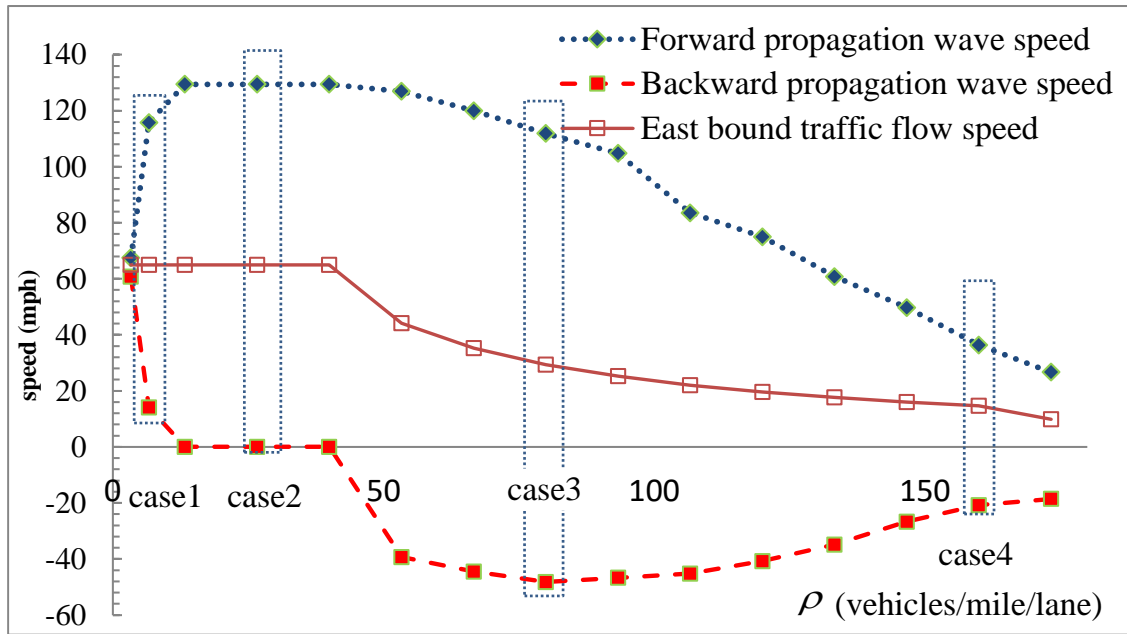


Figure 3-7 Information flow wave speed variation relative to density under the uni-directional traffic scenario

### 3.4.3 Bi-directional highway

In the bi-directional highway case, the opposite direction traffic is set as a uniform stream with fixed density (50 veh/mile/lane) and fixed speed (57 mph). Unlike the uni-directional traffic flow stream, for the bi-directional traffic flow stream, two more factors affect the forward and backward propagation wave speeds of information flow: (i) the interference from the opposite direction traffic, and (ii) the information carried by equipped vehicles in the opposite direction.

Comparing Figure 3-9 with Figure 3-7, it can be observed that the pattern of forward propagation wave speed of information flow is similar to that of the uni-directional highway case, and the overall speed is lower because the vehicles in the opposite direction may introduce additional interference. By contrast, the backward propagation wave speed of information flow in the bi-directional traffic case is much faster than that of the uni-directional highway case. The reason is because the opposite direction vehicles carry and propagate the information.

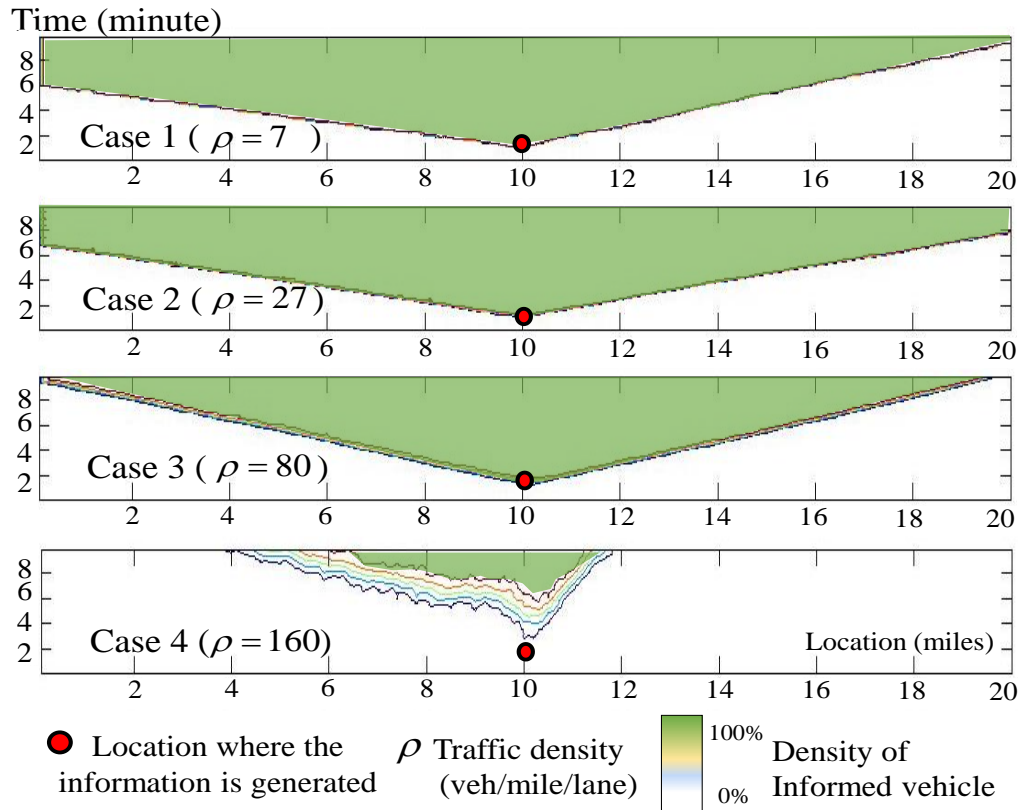


Figure 3-8 Forward and backward propagation wave speeds of information flow under the bi-directional traffic scenario

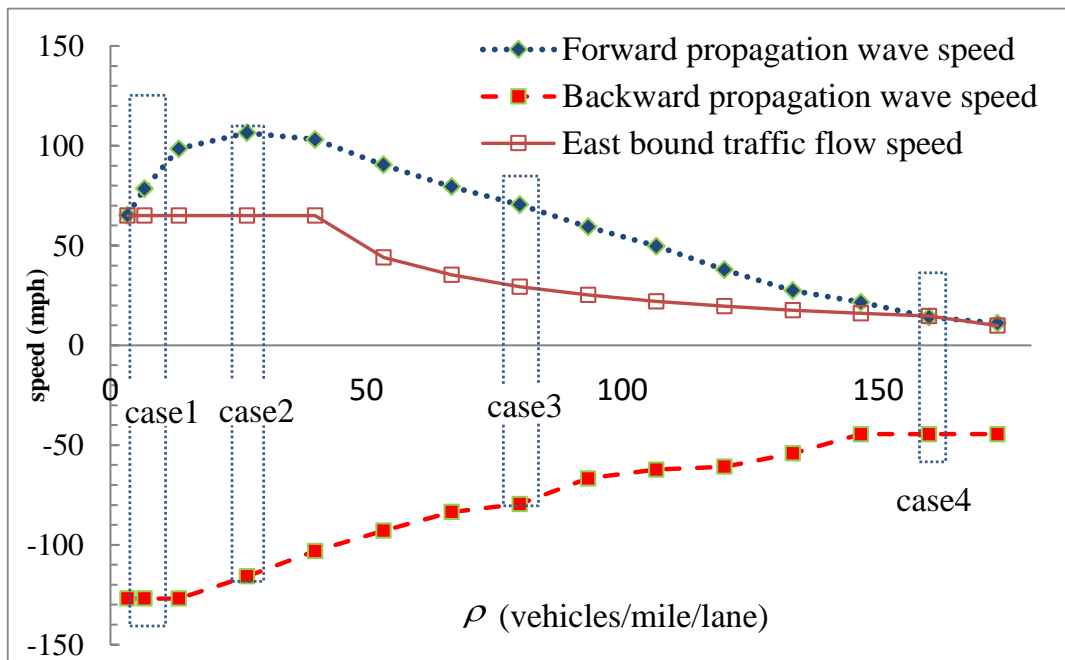


Figure 3-9 Information flow wave speed variation relative to density under the bi-directional traffic scenario

It should be noted here that these results are based on the assumption that the information propagates only to the cells within communication range in a given time interval. The proposed CTM-SI model uses cells to simulate the evolution of traffic flow and information spreading, whose length is equal to the distance traveled by a free-flowing vehicle in one time step. This implies that the accuracy of the propagation wave speed of information flow can be improved by adjusting the cell characteristics.

### 3.4.4 Uni-directional highway under different market penetration rates

We examine the sensitivity of the information flow propagation wave speed to the market penetration rate ( $\alpha$ ). The traffic density is set as a uniform stream with fixed density (80 veh./mile/lane) and fixed speed (29.4 mph). The forward and backward propagation wave speeds of information flow are illustrated in Figure 3-10.

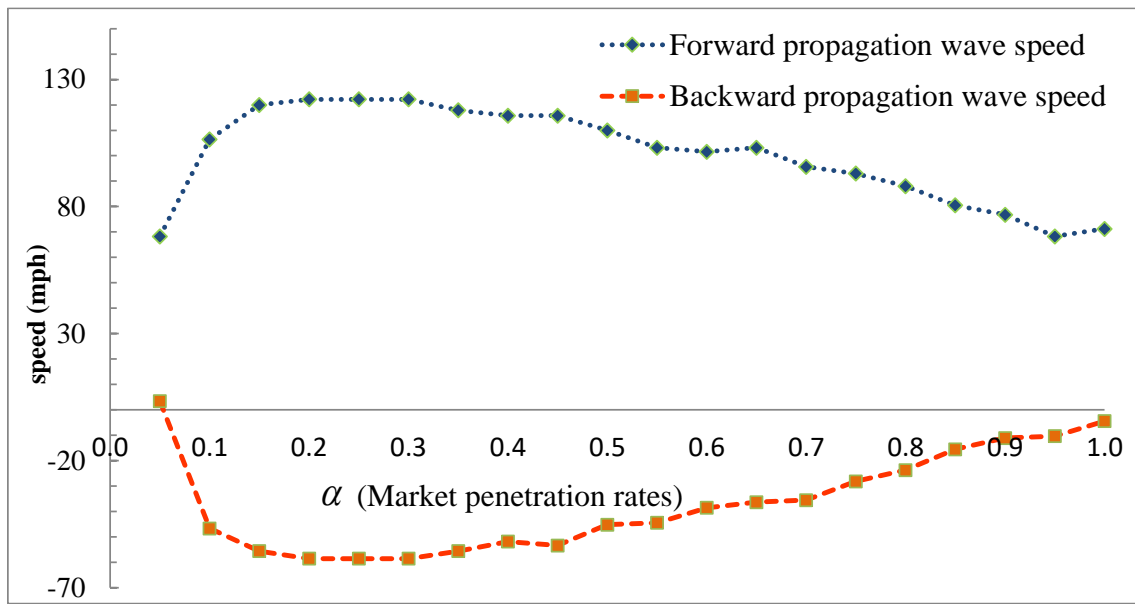


Figure 3-10 Information flow wave speed variation under the different market penetration rates ( $\alpha$ ) in a uni-directional traffic scenario

As the traffic flow speed remains unchanged, the wave speed of information flow propagation varies due to the information hopping speed under different values of  $\alpha$ . The speed variation pattern is symmetric for the forward and backward wave speeds. Up to  $\alpha$  of 0.2, both wave speeds of information flow increase due to the increased opportunity for information hopping under V2V communications. Beyond  $\alpha$  of 0.3, both wave speeds decrease due to the increased interference.

This is consistent with the trends identified in the previous sections that show a non-linear relationship between the different interference rates and the propagation wave speed of information flow.

### 3.4.5 Comparison of analytical and numerical results

We analyze the analytical formulation of the propagation wave speeds of information flow by comparing the results from equations (13-17) to the numerical experiments from equations (5-10). Figure 3-11 and 12 show that the analytical formulation can predict the relationship between the density of traffic flow and the propagation wave speed of information flow accurately, except for the case with low traffic flow density.

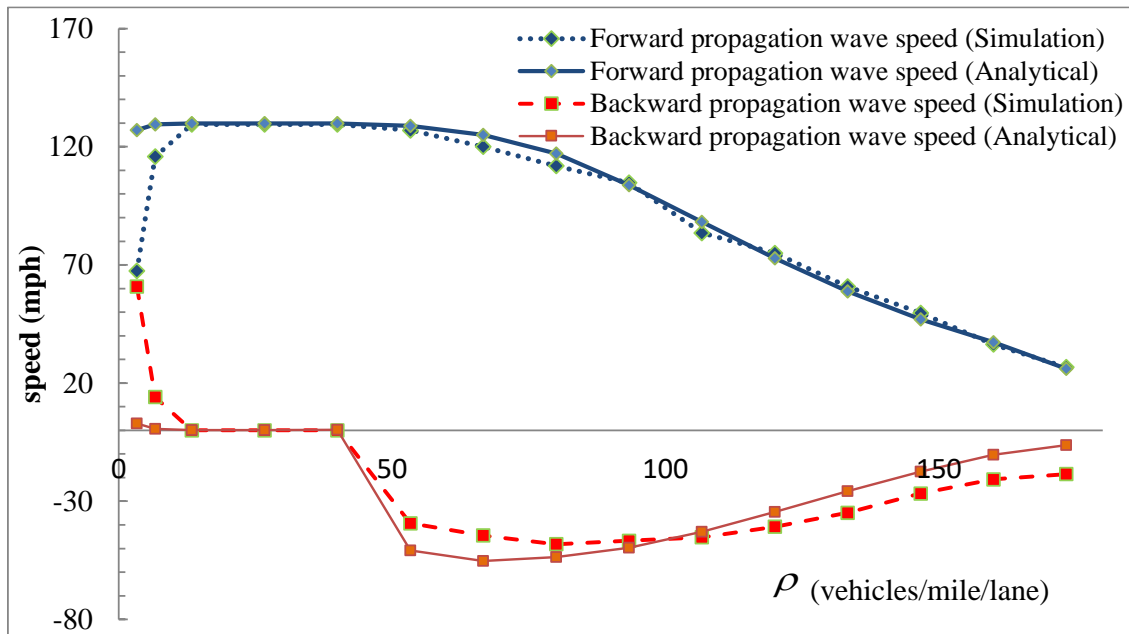


Figure 3-11 Comparison between predicted and simulated information flow wave speeds under the uni-directional traffic scenario

For the low density case, the numerical result is able to capture the stochastic nature of V2V communications in that information hopping may not occur, due to the limited number of vehicles to propagate the information. However, the analytical formulation is constructed based on non-discrete numbers of vehicles in equation (13), resulting in the overestimation of the propagation wave speed of information flow in the low density case.

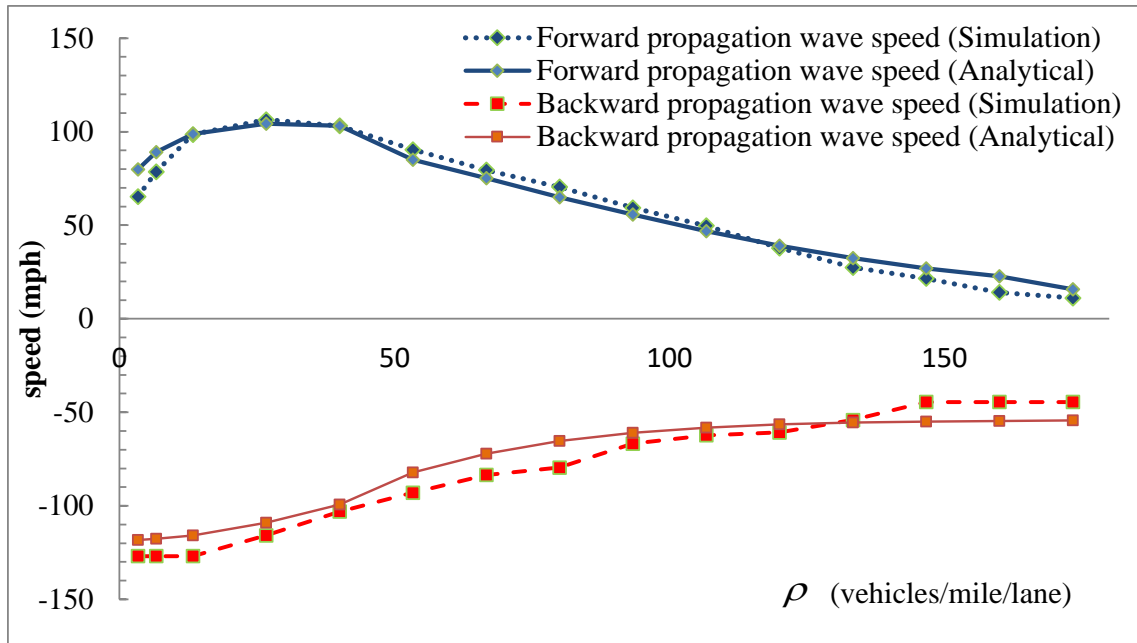


Figure 3-12 Comparison between predicted and simulated information flow wave speeds under the bi-directional traffic scenario

### 3.4.6 Bi-directional highway with incident

Here, we consider a non-uniform traffic stream on a bi-directional highway. Initially, the EB (vehicles moving to the right in Figure 3-13) traffic density is 80 veh./mile/lane and the WB density is 50 veh./mile/lane. As illustrated in Figure 3-13(a), an incident occurs at location A at 5 time units and reduces the highway capacity by 1/3 of its initial value. Highway capacity is recovered to capacity at 4.5 minutes (at point B in Figure 3-13(a)). Point C in Figure 3-13 (a) shows the location where the discharging flow departing from the congested area catches the tail of downstream flow traffic.

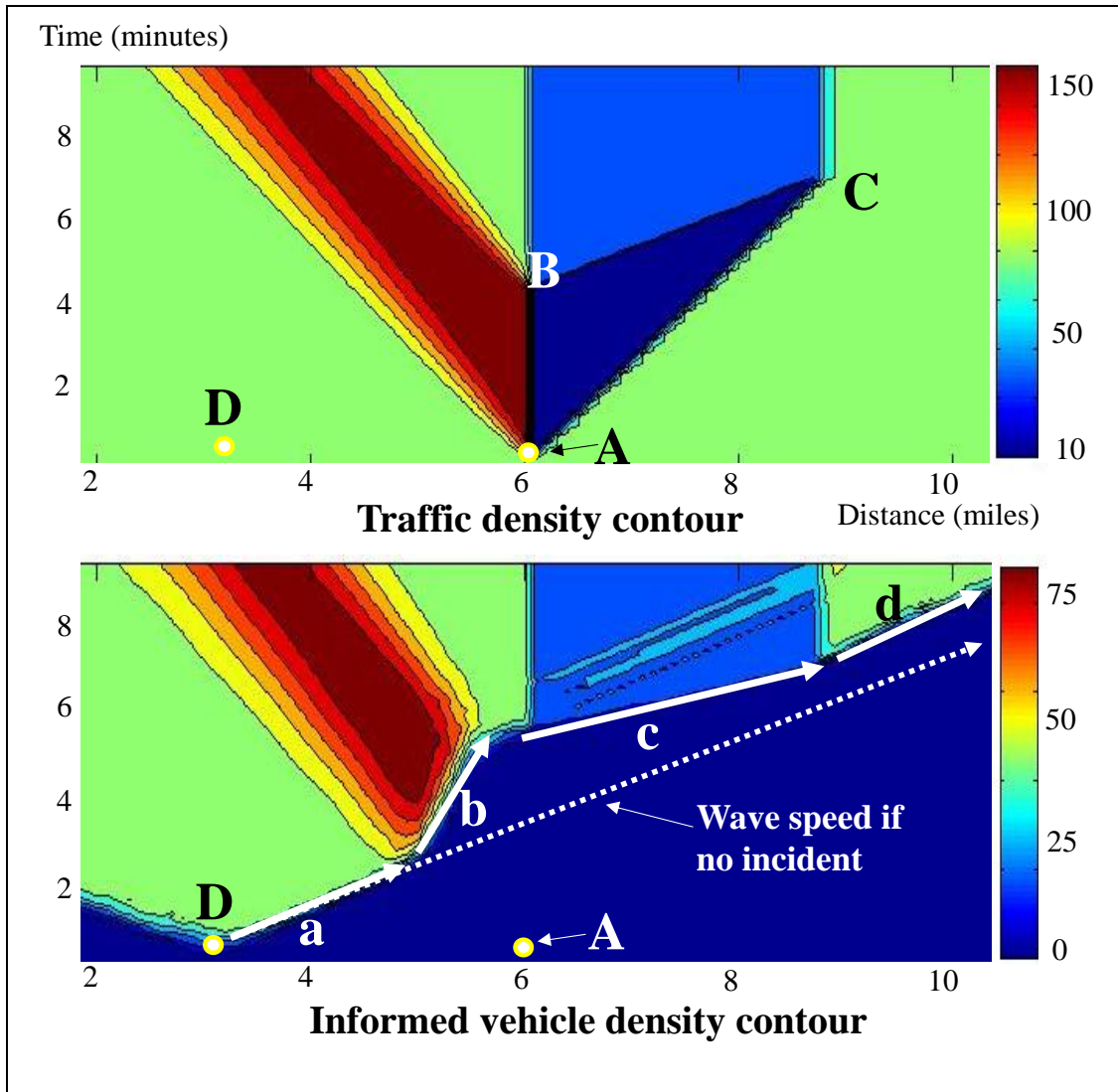


Figure 3-13 Contours of traffic density and informed vehicle density

The information is generated at 10 time units (1 minute) at point D by an equipped vehicle. In Figure 3-13(b), forward propagation wave speed of information flow varies as the downstream traffic density changes. Note the arrows a, b, c, and d in Figure 3-13(b) represent the forward propagation wave speeds of information flow corresponding to downstream densities.

As shown in Figure 3-13(b), the forward propagation wave speed of information flow reduces after encountering the underlying traffic shock wave, since higher vehicle density implies higher interference and lower likelihood of V2V communications. By contrast, at the queue dissipation area, forward propagation wave speed of information flow is faster than that of the other cases, since traffic is at free flow speed and V2V communication takes place more frequently. After the

information propagates through the congested traffic area, the overall information flow propagation is delayed as measured by the difference between the solid arrow and dash arrow, which shows the forward propagation wave of information flow if no incident occurs. The observation of the different information flow propagation speeds at different density levels is consistent with the results summarized in Figures 3-7 and 3-9.

### **3.5 Summary and discussion**

To account for the limitations arising from existing analytical approaches based on instantaneous information flow propagation, this study develops a discrete analytical model to track dynamic information flow propagation by integrating a traffic flow model and an epidemic model. The main contributions of this study are as follows. First, the proposed model can describe the network-wide spatiotemporal propagation of information while factoring the constraints arising from traffic flow dynamics and V2V communications. Second, with the integrated multi-layer framework, the proposed model can describe the interdependencies among information flow, traffic flow and V2V communication events by simultaneously tracking the dynamics of information flow and traffic flow. Third, it captures information flow propagation wave that can characterize how the density, speed, and locations of the vehicles lead to the dynamics of information flow.

The study offers the possibility of developing more sophisticated information flow propagation models. First, this model can be extended to the multiple information flow propagation context which has issues such as information quality and reliability. Second, more detailed epidemic models can be adopted. Third, a stochastic modeling capability to generate greater realism can be incorporated.

## **4. MODELING THE INFORMATION FLOW PROPAGATION WAVE UNDER VEHICLE-TO-VEHICLE COMMUNICATIONS**

### **4.1 Introduction**

#### **4.1.1 Background**

Advances in information and communication technologies enable new paradigms for connectivity involving vehicles, infrastructure, and the broader road transportation system environment. They provide the potential for developing innovative and sustainable solutions to enhance traffic safety and mobility. In this context, vehicle-to-vehicle (V2V) communications under the aegis of the connected vehicle are being leveraged for novel applications related to traffic safety, management, and control, which lead to a V2V-based traffic system. For example, traffic safety applications (Benedetto et al. 2015; Biswas et al. 2006a; Palazzi et al. 2010) primarily provide advisories and warning for drivers to avoid potential collisions. Traffic management and control applications (Leontiadis et al. 2011; Monteil et al. 2013) focus on improving mobility by assisting the driver to manage speed for smooth driving or fostering informed decision-making by providing information on alternate routes. These applications can be developed based on vehicle operational information (such as vehicle position, speed, and direction) and road condition information (such as hazardous locations on roads, slippery sections, and potholes).

A V2V-based traffic system consists of the vehicular traffic flow, inter-vehicle communication, spatiotemporal information flow, and V2V-based applications. The relationships between these components are characterized by nonlinearity, interdependencies, and a feedback loop, as illustrated in Figure 4-1. In this study, we use the term “information flow” to denote the flow of a single unit of traffic data (for example, traffic condition information or safety alert information) between vehicles. The dynamics of the vehicular traffic flow (such as the travel direction, location, speed, and the density of equipped vehicles) determine the occurrences of inter-vehicle communication. The traffic flow dynamics and the communication occurrences lead to the dynamics of information flow propagation. Based on the information propagated, a V2V-based application provides an audio or visual message to a driver, which he/she uses to determine the

future speed or an alternative route to take. This impacts the traffic dynamics, as illustrated by the feedback loop in Figure 4-1.

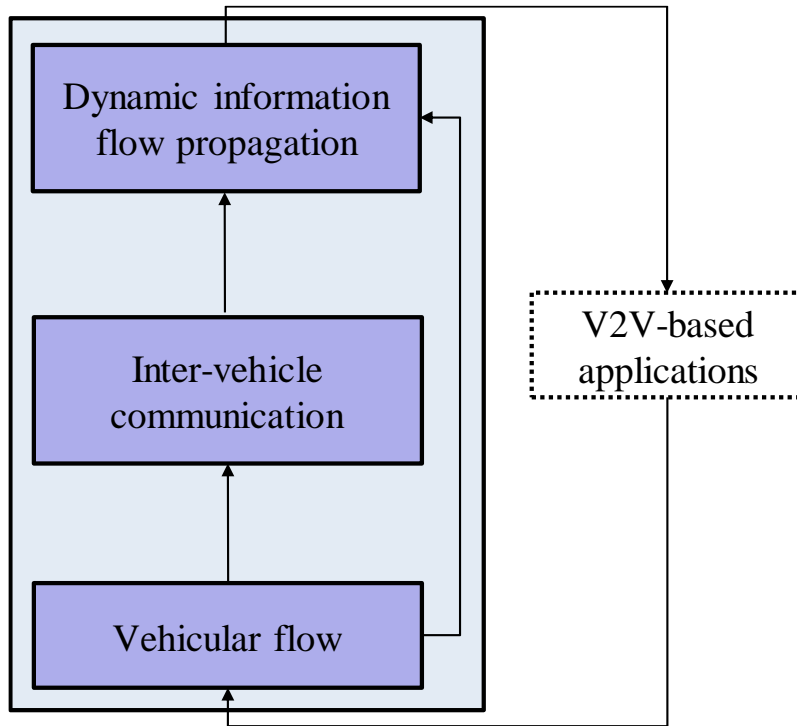


Figure 4-1 Components of a V2V-based traffic system

Within the proposed V2V-based traffic system framework, this study focuses on understanding how information propagates in space and time, as highlighted by the shaded box in Figure 4-1. This is because V2V-based applications require timely and reliable information delivery. However, the real-world environment for implementing a V2V-based application can be constrained by the characteristics and phenomena associated with the interactions involving traffic flow dynamics and V2V communication constraints. Hence, a critical question is how information propagation is impacted by the traffic flow dynamics and V2V communication constraints.

To address the aforementioned question, there is the key need to develop realistic models that can: (i) capture the relationship between traffic flow and information flow propagation, (ii) incorporate realistic V2V communication constraints related to range, data communication frequency, and transmission power, and (iii) generate closed-form solutions for the information flow propagation speed, so as to provide insights on its qualitative properties.

This paper seeks to develop an analytical model, which characterizes the relationship between V2V communications and traffic flow dynamics, to determine the information flow propagation speed. In this context, we derive a closed-form solution of the information flow propagation speed under certain traffic conditions. Reliable knowledge of the information flow propagation, and corresponding closed-form solutions, serve as the enabling foundation for the reliable and practical design of V2V-based applications. This underlines the importance of developing realistic, yet easy-to-use, models to capture the dynamics of information flow propagation.

Previously, analytical microscopic models have been developed to describe the dynamics of information flow propagation. These models can be classified into two groups based on the underlying assumption of V2V communications. The first group of analytical models (Han et al. 2011; Jin and Recker 2006; Li and Wang 2007; Wang et al. 2012; Yin et al. 2013) rely on the assumption of instantaneous multi-hop to characterize the propagation of information flow. They assume that information propagation is instantaneous with respect to vehicle movement based on the existence of an end-to-end multi-hop communication path between vehicles. Based on this, the probabilities for information to travel to and beyond a vehicle are computed (Jin and Recker 2006).

The second group of studies (Du and Dao 2015; Jacquet et al. 2010; Wu et al. 2009; Zhang and Peeta 2011) are based on a store-and-forward scheme, also referred to as a delay-tolerant network. Vehicles are partitioned into a number of clusters, where a cluster is a maximal set of vehicles in which every pair of vehicles is connected by an instantaneous multi-hop communication path. Due to the dynamics of vehicular flow, these clusters may split and merge over time. The information is stored in moving vehicles and propagated when the head vehicle of a cluster communicates with the tail vehicle of another cluster. Therefore, the entire information flow propagation process consists of a catch-up process, followed by a forwarding process.

The aforementioned analytical models have several realism issues in the context of a V2V-based traffic system. First, the instantaneous multi-hop assumption restricts the information hopping only to the spatial dimension. It precludes the analysis of the time delay of information to reach a certain location. In a traffic safety application, it is important to analyze a stringent delivery delay requirement in order to provide timely emergency warnings to drivers. Second, these models rely on the Poisson or uniform distribution of equipped vehicles and ignore interactions between vehicles. They do not allow for traffic dynamics such as kinematic waves, and queue formation

and dissipation, and the consequent dynamics in the propagation of information flow. Third, they do not capture the relationships between the dynamics of traffic flow and V2V communications. While Jin and Recker (2010) introduce a continuous traffic stream to capture the dynamics of traffic flow, traffic density is used only to calculate the geometric communication distance between vehicles. However, from a communication perspective, diverse traffic situations in terms of vehicular density may affect the success rate of V2V communications due to the interference caused by transmissions of other equipped vehicles within communication range. Fourth, as distance between equipped vehicles is used as the only communication constraint in most of the aforementioned models (except in Du and Dao (2015)), all equipped vehicles are assumed to be connected if the traffic density reaches a certain critical level such that the distance between vehicles is shorter than the communication range. Therefore, these models can possibly be applied only to situations of low vehicle density, low market penetration rate (the proportion of V2V-equipped vehicles), and large spatial gaps in traffic flow that temporarily delay the propagation of information.

Further, the microscopic nature of the aforementioned models leads to three major difficulties in terms of their applicability to a V2V-based traffic system. First, it is analytically challenging to properly account for the traffic flow dynamics and communication constraints at a disaggregate level. Second, the integration of traffic flow dynamics and V2V communications entails large computational burden for microscopic models. Third, it is difficult to generalize the findings in a meaningful manner, as the evaluation involves a microscopic model with specific settings related to market penetration rates, and road traffic and network topological conditions.

#### **4.1.2 Information flow propagation wave (IFPW)**

In contrast to the microscopic models, macroscopic models can be derived from the knowledge of disaggregate microscopic behavior at a high level of aggregation without distinguishing between individual vehicles. A key advantage of macroscopic models is that they can quantify the characteristics of information flow propagation using analytical formulations. Very few studies develop macroscopic approaches to describe information flow propagation. Indrakanti et al. (2012) propose a macroscopic analytical model to predict the number of vehicles in a region that receive a specific unit of information over time, by adopting an epidemic Susceptible-Infected-Removed

model from epidemiology. However, they do not consider the spatial structure to describe the propagation of information in space. The spatial structure plays an important role in information propagation, not only because the spread of information relies on communication between spatially-distributed equipped vehicles, but also because these vehicles carry information and move in space. We propose a spatially-structured macroscopic model that treats space and time explicitly.

From a macroscopic perspective, as a unit of information spreads in a V2V-based traffic system, an information flow propagation wave (IFPW) front forms a moving boundary that separates the traffic flow into informed and uninformed regions, and moves towards the uninformed region (Kim et al., 2016), as shown in Figure 4-2. Thereby, the IFPW is characterized by the direction and speed of the moving boundary. As illustrated in the figure, this wave can move in the forward and backward directions; the speed of the wave in each direction depends on the traffic flow dynamics and V2V communication constraints. Hence, the quantification of the IFPW speed and the position of the IFPW front are fundamental to determining how information flow propagates in a V2V-based traffic system.

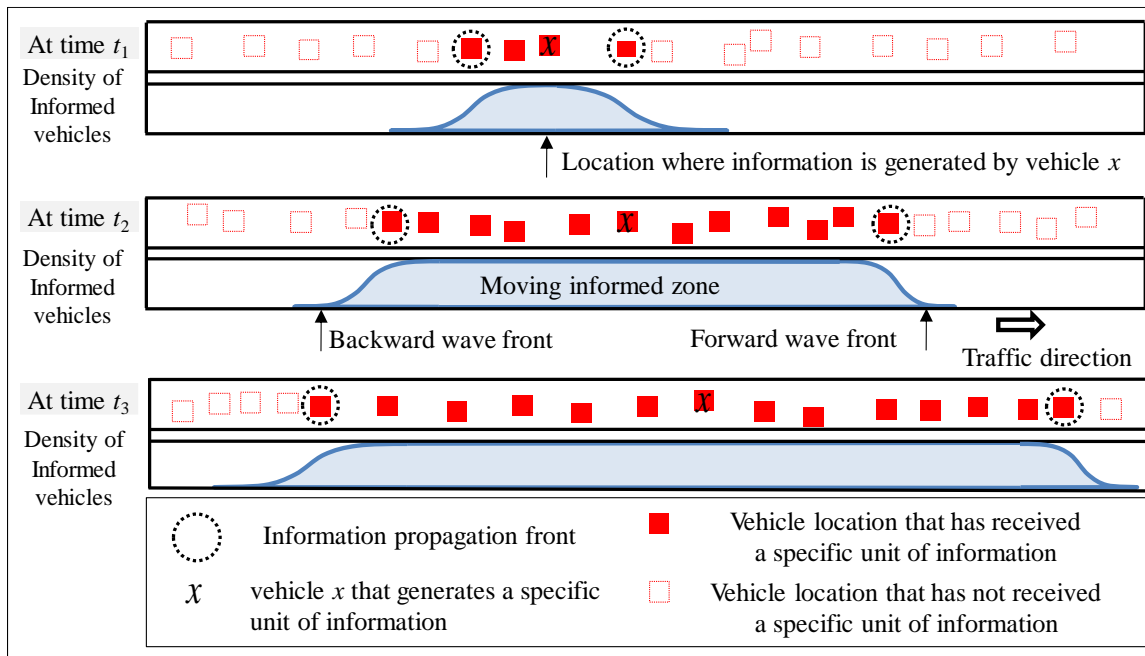


Figure 4-2 Illustration of the information flow propagation wave

A recent study by the authors (Kim et al., 2016) proposes a system of difference equations in the discrete space and time domain to track the dynamic information flow propagation. However, the associated analytical formulation estimates the IFPW speed based on the numerical solution of traffic flow dynamics using a cell transmission model (Daganzo, 1995 (a)). Hence, it lacks a closed-form solution that can establish an analytical relationship between the IFPW speed and the underlying traffic flow dynamics. This motivates the current study which constructs a continuous-time, continuous-space analytical model that can provide a closed-form solution for the IFPW speed under certain traffic conditions. The closed-form solution and analytical model can be used to predict the IFPW speed and the position of the IFPW front under diverse vehicular environments (in terms of density and topology) and V2V communication network parameters (such as data communication frequency, transmission power, etc.). Such an understanding of the IFPW characteristics is critical to designing strategies to propagate information (e.g., safety alert or work zone message) to appropriate locations in a timely manner, and effective traffic control strategies that leverage V2V-based capabilities.

This paper proposes a macroscopic model to characterize the IFPW. As illustrated in Figure 4-3, the proposed model has a two-layer structure in which V2V communications and vehicle movements are assumed to occur continuously. The IFPW consists of two waves: traffic flow propagation wave in the lower layer and information dissemination wave in the upper layer. The traffic flow propagation is formulated in the lower layer as a system of partial differential equations (PDEs) based on the Lighthill-Whitham-Richards (LWR) model (Lighthill and Whitham, 1955; Richard; 1956). The upper layer adapts and modifies the spatial epidemic Susceptible-Infected (SI) model from epidemiology to describe the information dissemination among equipped vehicles, using a probabilistic communication model (labeled “communication kernel”) to indicate the communication strength with distance. The communication kernel can capture the traffic randomness and V2V communication range in representing real-world V2V communication characteristics, as will be discussed in Section 5.2. The multi-hop information dissemination process is formulated as integro-differential equations (IDEs). These two layers are coupled, in that the traffic flow dynamics in the lower layer affect the V2V communication in the upper layer.

When traffic density is uniform and traffic flow is unidirectional, the impacts of the traffic flow dynamics on the IFPW speed are uniform in space and time in the sense that the traffic flow dynamics do not change the density of informed vehicles. We refer to this situation as *homogeneous* conditions in this study. Under homogeneous conditions, the proposed two-layer model provides a closed-form solution of the IFPW speed. However, when traffic density is not uniform and/or traffic flow is bidirectional, the impacts of traffic flow dynamics on the IFPW speed are not uniform in space and time, and this situation is referred to as *heterogeneous* conditions in this study. Under heterogeneous conditions, we propose a numerical method for the proposed two-layer model. Section 2.5 discusses homogeneous and heterogeneous conditions in more detail (see Fig. 6), and the rationale for the solutions for the two-layer model under homogeneous and heterogeneous conditions.

Through the concept of the IFPW, the proposed model provides capabilities to: (i) derive a closed-form solution of the IFPW speed for homogeneous traffic conditions (constant density) and unidirectional flow, (ii) propose a numerical method for the IFPW speed for heterogeneous traffic conditions, (iii) factor the impacts from congested traffic, such as the backward traffic propagation wave, on information flow propagation, (iv) capture V2V communication constraints in a realistic manner through the communication kernel, and (v) illustrate the dependency between the information flow propagation and the underlying traffic flow. These capabilities lead to a better understanding of the fundamental relationship between traffic flow dynamics and information flow propagation and enable traffic management and safety applications based on V2V communications.

The primary contributions of this study can be summarized as follows. First, it models the multi-hop process of information flow propagation based on the broadcast method rather than the assumption of instantaneous multi-hop propagation. Second, it characterizes the success rate of single-hop V2V communication as a probabilistic function to reflect the impact and details of V2V communication constraints. This provides significant flexibility for the traffic modeler in terms of testing different communication models to characterize the evolution of the IFPW speed. Third, it leverages a well-developed mathematical model from epidemiology and ecology to describe the information flow propagation. To the best of our knowledge, this work is the first attempt to consider the impact of V2V communication constraints on the characteristics of information flow propagation wave.

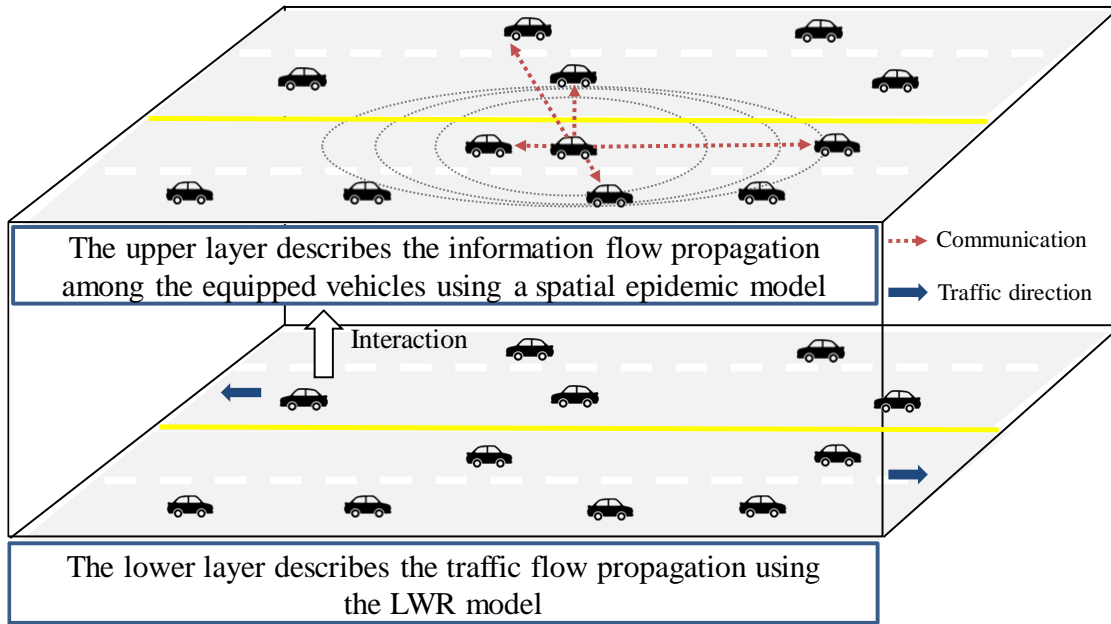


Figure 4-3 Two-layer structure of the proposed model

The remainder of this paper is organized as follows. The next section discusses the macroscopic model for the IFPW, including the modeling framework, the IDEs for information flow propagation using the SI model, and the PDEs for the traffic flow propagation using the LWR model. Then, the linearization of the IDEs is used to generate a closed-form solution of the IFPW speed under homogeneous traffic conditions. Next, for heterogeneous traffic conditions, a numerical method is presented to numerically solve the proposed model using the fast Fourier Transform and the Runge-Kutta method for the IDEs, and finite difference equations for the PDEs. This is followed by a discussion of the numerical experiments, the parameter calibration for the proposed communication kernel, and the associated insights. The final section summarizes the main findings and future research directions.

## 4.2 Modeling the spatiotemporal propagation of information flow

### 4.2.1 Modeling framework

Figure 4-4 illustrates the proposed modeling framework to determine the IFPW. The dynamics of traffic flow propagation in the lower layer are described using a macroscopic hydrodynamic model based on the first-order LWR model. The LWR model has been used extensively in the field of traffic flow theory due to its capability for capturing key real-world traffic flow phenomena,

such as shock waves and spillbacks. The traffic flow propagation is formulated as a system of PDEs. The traffic flow propagation layer is coupled with the information dissemination layer through the density of equipped vehicles. As shown in Figure 4-4, while the equipped vehicles are associated with both information dissemination (through the communication success rate) and traffic flow dynamics, the unequipped vehicles are directly associated only with the traffic flow dynamics.

To describe the information dissemination among equipped vehicles, the upper layer adapts a probabilistic communication model that incorporates the success rate of single-hop communication based on the distance between equipped vehicles. As illustrated in Figure 4-4, the density of the equipped vehicles, transmission power, data communication frequency, and environmental factors (such as weather, urban or rural area, etc.) determine the success rate of single-hop communication with distance, which is represented as a probability function labeled the communication kernel. The communication kernel is then used to formulate the process of multi-hop information dissemination as a system of IDEs. These PDEs and IDEs in the two layers determine the IFPW characteristics. A detailed description of the communication kernel and the multi-hop information dissemination process is provided in the next section.

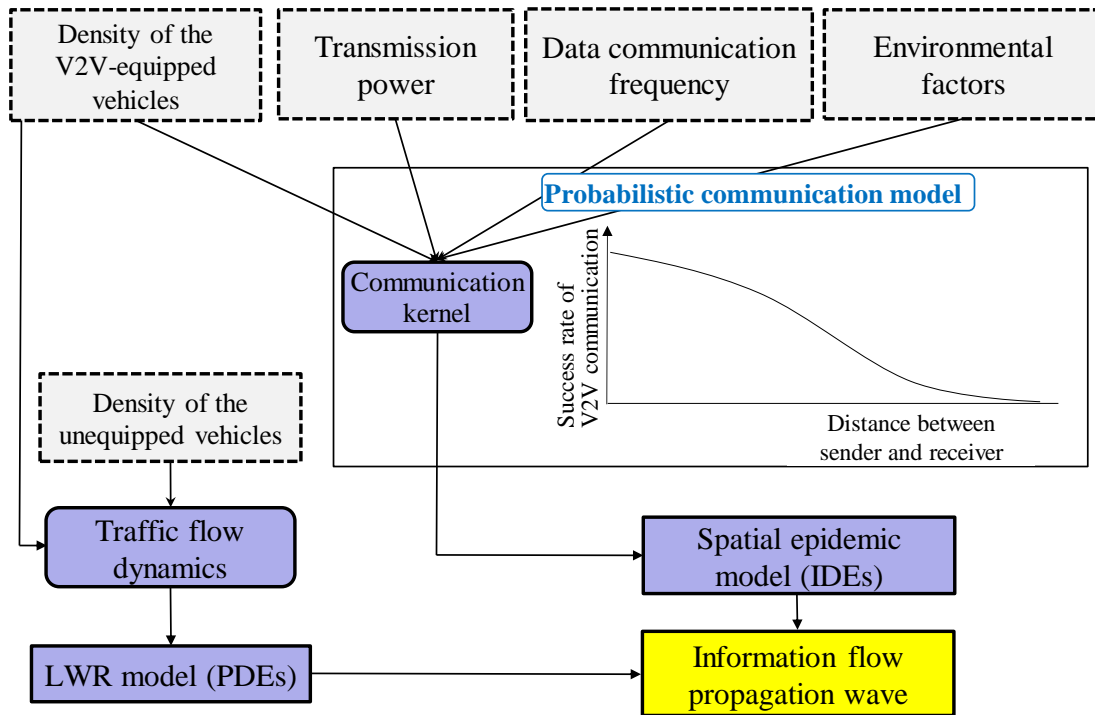


Figure 4-4 The IFPW modeling framework

#### 4.2.2 Characteristics of V2V communication

The success rate of V2V communication decays over distance due to the fading effects of the signal amplitudes. This signal fading significantly affects the efficiency of information propagation in a V2V-based traffic system, especially when multiple vehicles frequently exchange or disseminate information simultaneously.

Real-world measurements (Jiang et al. 2008; Torrent-Moreno et al. 2009) and simulation studies (Killat and Hartenstein 2009) show that the distance between sender and receiver vehicles, and the mutual interference from equipped vehicles, have a significant effect on packet reception. However, deterministic models of communication success rate assume that V2V communication can occur with a 100% success rate up to a predefined communication range, and that no V2V communications can take place beyond that distance (Killat and Hartenstein, 2009). Hence, deterministic models lack realism, and may provide only an upper bound on the information flow propagation wave speed. By contrast, our study models the success rate of V2V communication as a probabilistic function due to the effects of interference caused by multiple transmissions in the network. In IEEE 802.11p networks, interference can cause failure of the reception of V2V communication.

The V2V communication constraints related to range, data communication frequency, and transmission power and density of V2V-equipped vehicles influence the rate of interference. Successful or unsuccessful reception of transmitted information is determined using the signal to interference and noise ratio (SINR) while considering the sum of all ongoing transmissions as the cumulative interference.

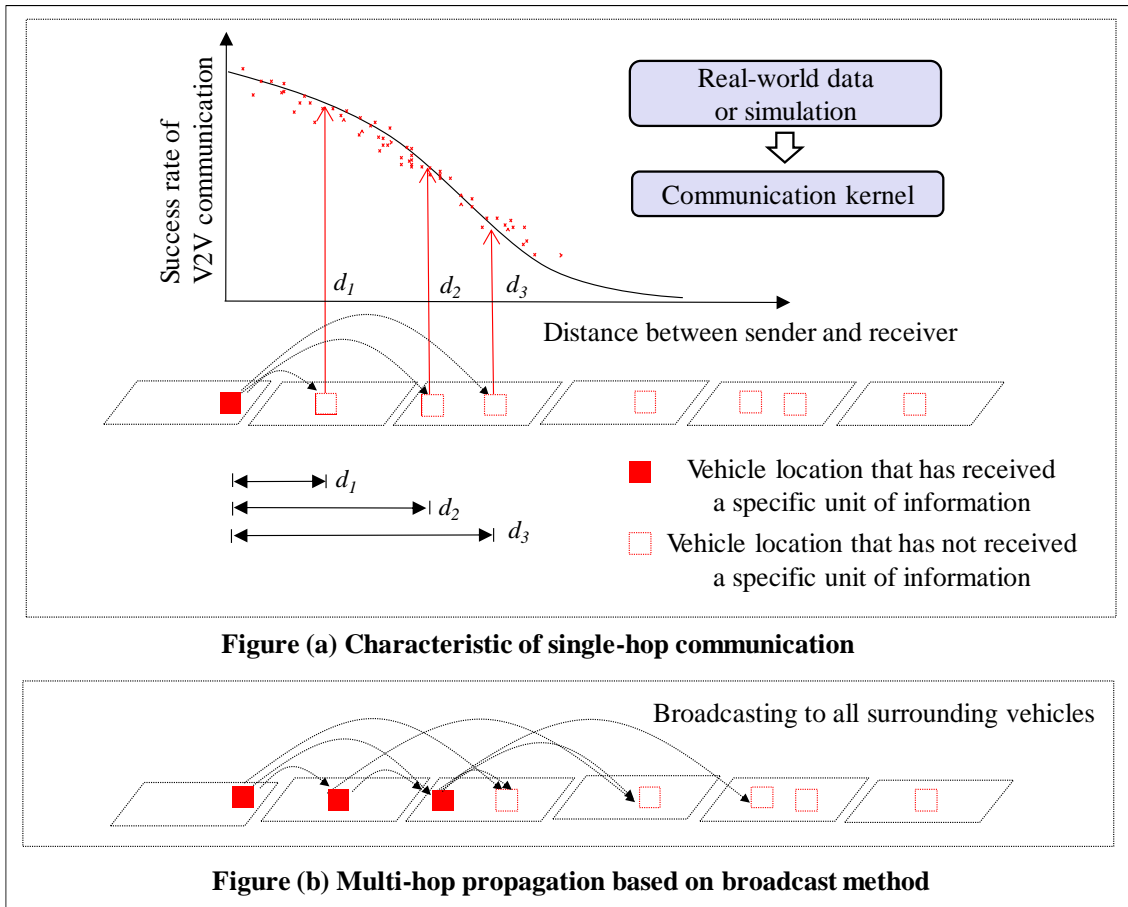


Figure 4-5 Characteristics of V2V communications

Figure 4-5 (a) illustrates the probability of successful communication over distance (communication kernel). The parameters of the communication kernel can be calibrated using real-world data or simulated data. Section 5.2 provides a detailed discussion related to SINR-based simulation.

Further, in V2V-based applications, information should be provided to all surrounding vehicles, motivating the need for a broadcast method (Karagiannis et al. 2011). A vehicle that receives the information can forward information again using a broadcast communication. Thus, information propagates by being relayed from one vehicle to another (multi-hop information dissemination process), as shown in Figure 4-5 (b). The formulation of the multi-hop information dissemination process, where the success rate of single-hop communication corresponds to the communication kernel, is discussed next.

### 4.2.3 Spatial susceptible-informed model

This study leverages modeling capabilities from epidemiology and ecology to study the IFPW in a V2V-based traffic system. The upper layer adapts and modifies a spatial SI epidemic model to describe information dissemination between equipped vehicles as a spatial “susceptible-informed” model. Conceptual similarities exist in terms of propagation of information and disease in space and time. First, the spread of both disease and information relies on contacts between spatially-distributed entities (individuals for disease and equipped vehicles for information). Second, based on their spatial positions, nearby individuals/vehicles interact more strongly. In this sense, well-developed mathematical theory in epidemiology and ecology (Hastings 1996; Mollison 1972 a; b) to describe traveling frontal waves of a disease spread provides a conceptual platform that can be adapted to describe the dynamics of information flow propagation in terms of the forward/backward IFPWs, and spatial propagation fronts.

Key differences should be noted when adapting an epidemic model to the V2V-based traffic system context. First, while a specific disease may spread in all directions through airborne transmission, road network is geographically constrained. Second, unlike the fixed infection rate for a specific disease, communication success rate varies with the density of equipped vehicles. Third, individuals can be assumed to be stationary or moving randomly in the context of disease spread. However, since drivers interact with each other in a traffic stream, the positions of vehicles and their mobility are not independent. Fourth, while the objective in epidemiology is to regulate disease spread, V2V-based traffic systems typically seek the fast propagation and widespread dissemination of information.

We now describe the proposed spatial susceptible-informed model. In a V2V-based traffic system, vehicles can be grouped into mutually exclusive classes: equipped vehicles  $E$  and unequipped vehicles  $U$ . Equipped vehicles can be further classified into susceptible and informed vehicle classes based on their status in space  $x$  and time  $t$ . Let  $S(x,t)$  denote the density of susceptible vehicles located at  $x$  at time  $t$ , that is, those vehicles that are equipped to receive information, but are not yet informed. Let  $I(x,t)$  denote the density of informed vehicles, that is, vehicles that have received information and can transmit it to any susceptible vehicle within communication range. Hence, the model has three classes of vehicles:  $S$ ,  $I$  and  $U$ . The susceptible-informed model is constructed upon the following assumptions: (i) a single unit of information

propagates to other vehicles; (ii) susceptible vehicles can receive information from any informed vehicle that is within communication range; and (iii) unequipped vehicles are not involved in the information propagation process but affect the traffic flow dynamics.

Assume that an equipped vehicle generates information at time zero. The probability that a susceptible vehicle located at point  $x$  at time  $t$  becomes an informed vehicle can be represented as a rate proportional to the product of the local density of susceptible vehicles  $S(x,t)$ , and a communication kernel-weighted integral of the density of informed vehicles,  $I(y,t)$ , over the spatial domain  $\Omega$  ( $y \in \Omega$ ) within V2V communication range from  $x$ . Due to flow conservation, we have the following IDEs:

$$\frac{\partial S}{\partial t} = -\beta \cdot \left( \int_{\Omega} K(x,y) \cdot I(y,t) dy \right) \cdot S(x,t) \quad (1-a)$$

$$\frac{\partial I}{\partial t} = \beta \cdot \left( \int_{\Omega} K(x,y) \cdot I(y,t) dy \right) \cdot S(x,t), \quad (1-b)$$

where contact rate  $\beta$  represents the frequency of communication. Due to their tractability in mathematical analysis, the Laplace, Gaussian and Exponential distributions are widely used (Kot, 1992) to represent the communication kernel  $K(x,y)$  which is an integrable function satisfying  $K(x,y) \geq 0$ . The differentials in the IDEs are evolution equations that specify how the system will evolve with time through multi-hop broadcast communications.

#### 4.2.4 Traffic flow model

The lower layer describes the dynamics of traffic flow propagation using a first-order LWR model. The mathematical form of the LWR model is a PDE describing the spatiotemporal evolution of density and flow. It assumes that the behavior of traffic at a given point in space and time is only affected by the state of the system in a neighborhood of that point (Daganzo, 1995b). The model consists of the flow conservation law and an explicit density-flow relationship known as the fundamental diagram of traffic flow. The flow conservation law and the fundamental diagram can be expressed as follows:

$$\frac{\partial}{\partial t} k(x,t) + \frac{\partial}{\partial x} q(x,t) = 0 \quad (2)$$

$$u(x,t) = F(k, x, t), \quad (3)$$

where  $k(x,t)$  denotes the traffic density for cell  $x$  at time  $t$ ,  $q(x,t)$  is the instantaneous flow,  $u(x,t)$  is the average speed, and  $F(k, x, t)$  is the fundamental diagram in which  $k(x,t)$  and  $u(x,t)$  are related by a continuous and piecewise differential equation. The PDE model allows small perturbations to the system to propagate forward when traffic is light, and backward when traffic is heavy (Daganzo, 1995b). The spatiotemporal change of the equipped-vehicle density in the lower layer affects the success rate of V2V communication due to the effects of interference, where the success rate is specified by the probabilistic communication kernel function discussed in Section 4.2.2. This spatiotemporal coupling between the traffic flow dynamics and the V2V communication constraints can capture the impacts of congested traffic (such as the backward traffic propagation wave) on information flow propagation. It is important to note here that  $k(x,t)$  in equation (2) of the lower layer is the same as  $S(x,t) + I(x,t) + U(x,t)$  in equation (1) of the upper layer. This illustrates the linkage between the two layers of the proposed model.

#### 4.2.5 Solutions for homogeneous and heterogeneous conditions

For the proposed two-layer model (Sections 4.2.3 and 4.2.4), the traffic flow layer (Section 4.2.4) is a single class traffic flow model which is sufficient to represent the impacts of traffic flow dynamics on the IFPW for homogeneous conditions. This is because while the traffic flow dynamics shift the IFPW towards the direction of traffic flow, they do not change the density of informed vehicles. Figure 4-6 illustrates the impact of the traffic flow dynamics on the IFPW under homogeneous and heterogeneous conditions. Figure 4- 6(a) shows the location and shape of the IFPW at time  $t_1$ . Figure 4-6(b) shows that the traffic flow dynamics only shift the IFPW to the direction of traffic flow with constant speed but do not change the density of informed vehicles under homogeneous conditions. Therefore, the two layers are part of a coupled system in which dynamics occur in each system simultaneously, consisting of the information dissemination dynamics in the upper layer and the traffic flow dynamics in the lower layer. The information dissemination process is an overlay to the traffic flow that progresses in the same direction under homogeneous conditions. Both of these dynamics are addressed in a continuous time setting simultaneously. As discussed next, different approaches are needed to obtain solutions for the two-layer model under homogeneous (Section 4.3) and heterogeneous (Section 4.4) conditions. A

simultaneous approach and continuous time settings suffice for homogeneous conditions, while a sequential approach and discrete time settings are required for heterogeneous conditions.

Section 4.3, which determines a closed-form solution for the IFPW speed under homogeneous conditions, uses the two-layer model to determine the solution by simultaneously capturing the interactions involving the two layers. Hence, the single class traffic flow model and a continuous time setting are sufficient to obtain a closed-form solution under homogeneous conditions due to the ability to use the simultaneous approach.

By contrast, as will be discussed in Section 4.4, under heterogeneous conditions, the impacts of traffic flow dynamics on the IFPW are not uniform in space and time. Figure 4-6(c) shows the spatiotemporal change of the informed vehicle density under heterogeneous conditions. Figure 4-6(d) illustrates the effects of bidirectional flow on the IFPW in that the density of informed vehicles is changed in space. This makes it necessary to track the density of informed vehicles in each cell in the lower layer (which was not necessary under homogeneous conditions). This requires discretizing the problem, unlike in Sections 4.2 and 4.3 where continuous time settings suffice due to the simultaneous approach. To do so, an intermediate component is introduced in Section 4.4.4 that consists of a set of steps to connect the upper and lower layers consistently in terms of the number of vehicles by vehicle class. The intermediate component uses a discretized multi-class traffic flow model and outcomes from a discretized SI model. We propose a numerical solution to capture the interactions between the upper and lower layers sequentially using discretized time intervals.

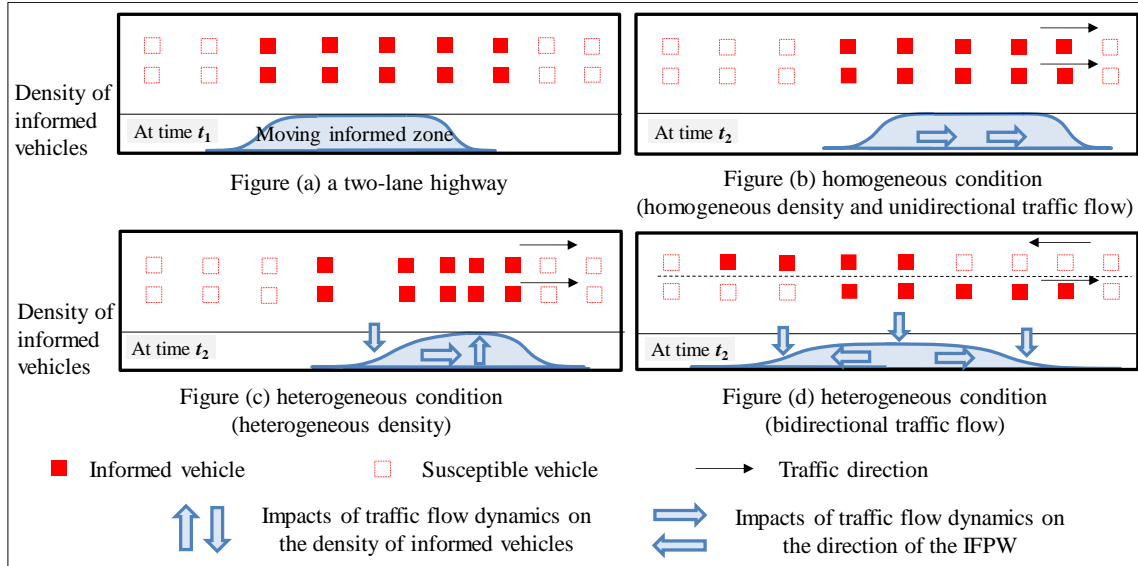


Figure 4-6 Impacts of traffic flow dynamics on the IFPW under homogeneous and heterogeneous conditions

### 4.3 Closed-form solution of IFPW speed for homogeneous traffic conditions

One of the main advantages of the model [(1), (5)] proposed to characterize the IFPW, is that it can be used to derive a closed-form solution of the IFPW speed under homogeneous traffic conditions, thereby circumventing the need for a more complex numerical solution. We now derive the closed-form solution for the IFPW speed, obtained as the summation of the information dissemination wave speed ( $\bar{c}_I$ ) and traffic flow propagation wave speed ( $c_T$ ).

#### 4.3.1 Information dissemination wave speed

The proposed susceptible-informed model using IDEs identifies an information dissemination wave whose speed quickly converges to a finite asymptotic speed  $c_I$  (Weinberger, 1978; Kot, 1992; Hart and Gardner, 1997). Equation (1) is not amenable to obtaining a closed-form solution for the traveling wave speed. However, there is compelling empirical evidence (Kot, 1992; Hart and Gardner, 1997) that the asymptotic speed ( $c_I$ ) of the IDEs for the SI model is equal to the minimum wave speed,  $\bar{c}_I$ , of a linearized version of the model obtained by satisfying a linear conjecture (Mollison, 1991; Kot, 1996; Medlock and Kot, 2003). In the V2V-based traffic system

context, the linear conjecture would be satisfied if: (i) the success rate of communication per informed vehicle is a non-increasing function of the number of informed vehicles, so that the maximum per capita communication rate occurs at the wave front, and (ii) the influence of a vehicle beyond its communication range is negligible. Both these conditions are satisfied in the V2V-based traffic system.

To linearize equation (1), the last term in its integral,  $S(x,t)$ , is replaced by  $E(x,t) - I(x,t)$  (by definition), and then the negative term  $-I(x,t)$  is removed based on the linear conjecture. Under homogeneous traffic conditions,  $E(x,t) \equiv E > 0$ ; hence, equation (1) can be linearized as:

$$\frac{\partial S}{\partial t} = -\beta \cdot \left( \int_{\Omega} K(x,y) \cdot I(y,t) dy \right) \cdot E \quad (6-a)$$

$$\frac{\partial I}{\partial t} = \beta \cdot \left( \int_{\Omega} K(x,y) \cdot I(y,t) dy \right) \cdot E. \quad (6-b)$$

Since the negative term is ignored in the linearized model (6),  $E$  overestimates  $S(x,t)$  in (6-a) and (6-b). Hence, in (6-a), the rate of decrease of susceptible vehicles is overestimated, and similarly, in (6-b), the rate of increase of informed vehicles is overestimated. Therefore, the solution of model (1) is bounded above by the solution of its linear approximation (6). Then, by the linear conjecture, the minimum wave speed of equation (6),  $\bar{c}_I$ , is equal to the asymptotic wave speed of equation (1). We will now solve equation (6) to obtain the information dissemination wave speed.

As the traffic density is constant under homogeneous conditions, the communication kernel  $K$  depends only on the absolute value of the magnitude of the distance between the vehicle located at  $x$  and any vehicle located at any  $y$  within communication range,  $|x-y|$ , and not the locations themselves. This enables the communication kernel to be of convolution type, i.e.,  $K(x,y) = K(|x-y|) = K(v)$ , where  $v = |x-y|$ . In particular, this study adopts the Gaussian exponentially bounded kernel,  $K(v) \leq A \cdot e^{-\theta|v|}$  with positive parameters  $A$  and  $\theta$ , which has the following moment generating function:

$$M(\theta) = \int_{\Omega} e^{\theta \cdot v} \cdot K(v) \cdot dv. \quad (7)$$

The moment generating function  $M(\theta)$  has a strictly positive radius, and its integral converges to a finite value (Medlock and Kot, 2003). Studies (Kot, 1996; Medlock and Kot, 2003) for SI

epidemic models illustrate analytically that Gaussian kernels produce constant traveling wave speeds. Hence, the information dissemination wave in the proposed V2V-based traffic system context has a constant asymptotic speed.

The basic technique for determining traveling wave solutions of equation (6) is by using the form  $I(x,t) = A \cdot e^{-\theta(x-\bar{c}_t)}$  (Mollison, 1991). We now define a new variable  $I^*(x,t) = I(x-\bar{c}_t \cdot t)$  that shifts the reference coordinates to speed  $\bar{c}_t$ . Thus, the density  $I(x,t)$  at  $x$  at time  $t$  will be exactly the same as the density at  $x+\bar{c}_t$  at time  $t+1$ . This allows us to derive a closed-form solution for equation (6). Based on equation (6-b), we obtain the characteristic equation:

$$\theta \cdot \bar{c}_t \cdot A \cdot e^{-\theta(x-\bar{c}_t t)} = \beta \cdot E \cdot \int_{\Omega} K(v) \cdot A \cdot e^{-\theta(y-\bar{c}_t t)} dy . \quad (8)$$

Canceling common factors,  $A \cdot e^{\theta \bar{c}_t t}$  gives:

$$\theta \cdot \bar{c}_t = \beta \cdot E \cdot \left( \int_{\Omega} e^{\theta v} \cdot K(v) dv \right) = \beta \cdot E \cdot M(\theta) . \quad (9)$$

Equation (9) shows that  $\bar{c}_t$  is function of  $\theta$ . Minimizing  $\bar{c}_t(\theta)$  for all  $\theta > 0$  provides the asymptotic speed ( $c_t$ ):

$$\bar{c}_t(\theta) = \beta \cdot E \cdot \inf_{\theta > 0} \frac{M(\theta)}{\theta} . \quad (10)$$

To find  $\bar{c}_t$ , we set the derivative of  $M(\theta)/\theta$  to zero based on the first-order optimality condition.

Then,

$$\bar{c}_t = \beta \cdot E \cdot M'(\theta^*) , \quad (11)$$

where  $\theta^*$  satisfies the first-order optimality condition:

$$M(\theta^*) = \theta^* M'(\theta^*) . \quad (12)$$

Using the Gaussian communication kernel  $K(v) = \frac{\lambda}{\alpha \cdot \sqrt{\pi}} \cdot e^{-v^2/\alpha^2}$ , where  $\alpha$  and  $\lambda$  are constants,

the moment generating function is given by:

$$M(\theta) = \lambda \cdot e^{\frac{\alpha^2 \theta^2}{4}} , \quad (13)$$

Equations (11)-(13) together determine the minimum wave speed  $\bar{c}_t$  as:

$$\bar{c}_t = \sqrt{\frac{e}{2}} \cdot \alpha \cdot \beta \cdot \lambda \cdot E . \quad (14)$$

Equation (14) illustrates a simple, but important relationship between the communication kernel parameters ( $\alpha$ ,  $\lambda$ ), the data communication frequency ( $\beta$ ), the density of the equipped vehicles ( $E$ ), and the information dissemination wave speed ( $\bar{c}_I$ ). It shows that the proposed model can leverage the success rate of V2V communication to illustrate the information dissemination wave speed using the communication kernel parameters. Therefore, it provides significant flexibility to test various communication models to characterize the evolution of the IFPW speed. Also, the equipped-vehicle density and data communication frequency illustrate a linear relationship with the IFPW speed.

### 4.3.2 Traffic flow propagation wave speed

The traffic flow propagation wave speed ( $c_T$ ) is determined by the fundamental diagram which is a continuous and a non-increasing function defined on  $[0, k_j]$ , where  $k_j$  is the jam density. Since the fundamental diagram is identical across the three vehicle classes, each class has the same speed at a given location and time. This study adopts the following triangular fundamental diagram (Jin and Recker, 2006):

$$c_T = \begin{cases} u_f, & 0 \leq k < k_c \\ \frac{k_c \cdot (k_j - k)}{(k_j - k_c) \cdot k} \cdot u_f, & k_c \leq k \leq k_j \end{cases} \quad (15)$$

where,  $u_f$  is the free flow speed, and  $k_c$  is the critical density. The IFPW speed depends on the information dissemination wave speed and the traffic flow propagation wave speed. For a single straight road corridor, the IFPW speed is the sum of two speeds ( $\bar{c}_I + c_T$ ), since the information dissemination wave is an overlay to the traffic flow propagation wave that progresses in the same direction. Correspondingly, the backward IFPW is opposite to the traffic flow, and hence the backward IFPW speed is ( $\bar{c}_I - c_T$ ). To illustrate the closed-form solution, the experiments in Section 4-5 are also conducted for this topology. However, the numerical solution approach, discussed next for heterogeneous conditions, is applicable to any network topology.

#### 4.4 Numerical solution of IFPW speed for heterogeneous traffic conditions

The closed-form solution for the IFPW speed derived in the previous section is applicable only for homogeneous conditions (which occur under constant density and unidirectional traffic flow). In this section, a numerical solution is proposed for heterogeneous conditions.

##### 4.4.1 Framework of numerical solution for heterogeneous conditions

The conceptual framework of the numerical solution is illustrated in Figure 4-7. As discussed in Section 2.5, the numerical solution for heterogeneous conditions requires the discretization of the two-layer model. The continuous SI model in the upper layer consists of IDEs (equation 1) that involves both integrals (spatial domain) and differentials (time domain) of a function. The fast Fourier Transform (FFT) is used for the spatial discretization of the integral part of the IDE equations. The Runge-Kutta method is used for the temporal discretization of the differential part of the IDE equations (Medlock and Kot, 2003). The mathematical form of the LWR model (PDEs, equations (2)-(3)) in the lower layer is discretized using the generalized cell transmission finite difference equations (FDEs) that approximate the PDEs (Daganzo, 1995b).

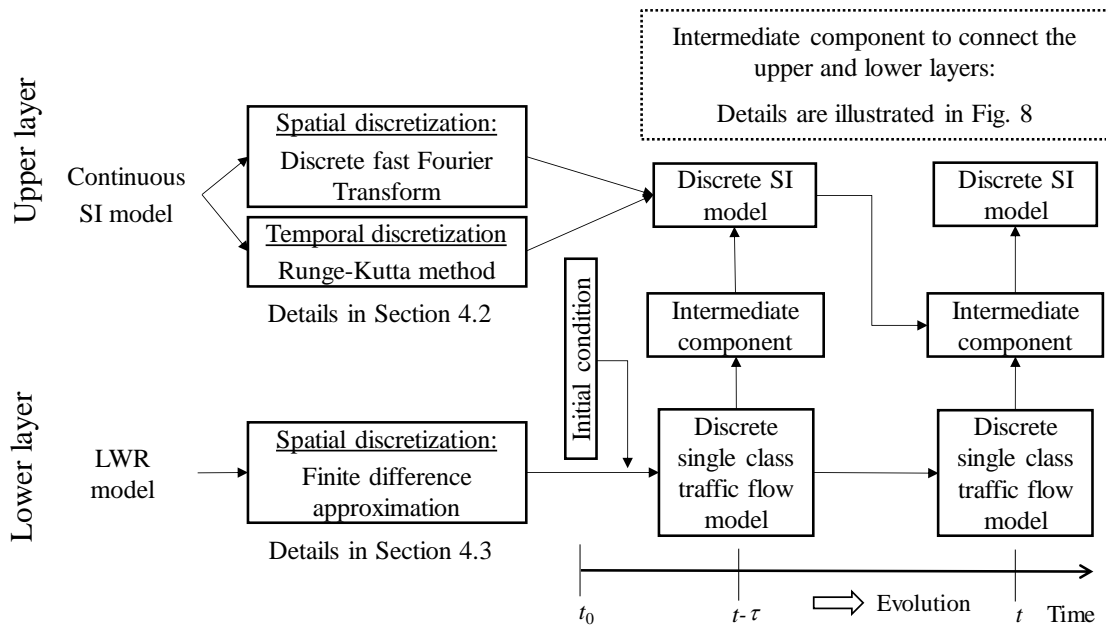


Figure 4-7 Framework of numerical solution for heterogeneous conditions

Sections 4.4.2 and 4.4.3 provide a detailed discussion related to the numerical solution framework for the upper and lower layers, respectively. The numerical solution starts by defining an initial condition in which the information unit is generated in the middle of the single straight road corridor, and propagates in both directions. Then, the upper and the lower layers are sequentially solved for by using the discretized SI model and the FDEs, respectively. An intermediate component is introduced in Section 4.4.4 that consists of a set of steps to connect the upper and lower layers consistently in terms of the number of vehicles by vehicle class. At time  $t$ , the discrete single class traffic flow in the lower layer is solved first. Then, the outcomes of the discrete single class traffic flow model at time  $t$  and the outcomes of the discretized SI model at time  $t - \tau$  are used to update the number of vehicles by vehicle class in the intermediate component. The outcomes of the intermediate component are used to solve the discretized SI model at time  $t$  in the upper layer. Then, the numerical solution moves to next time interval  $(t + \tau)$ . Therefore, the system evolves in time by solving the lower layer, intermediate component, and the upper layer, sequentially and iteratively.

#### 4.4.2 Numerical method for SI model

The FFT is used to solve the integral part of equation (1),  $\int_{\Omega} K(x, y) \cdot I(y, t) dy$  (Medlock and Kot, 2003). Space and time are discretized into cells with length  $(\Delta x)$  and time interval  $(\tau)$ , respectively. We assume that  $\Delta x = u_f \cdot \tau$ , based on Daganzo (1995a). We note an important property of the FFT; that the FFT of the convolution of two functions is the product of their individual FFTs. Therefore, the FFT of the convolution of the  $\int_{\Omega} K(|x - y|) \cdot I(y, t) dy = f * g(w)$  is as follows:

$$\overline{f * g(w)} = \frac{2L}{N} \overline{f(w)} \cdot \overline{g(w)}, \quad (14)$$

where  $L$  represents communication range and  $N$  represents the number of cells within communication range in the two directions. We use the discrete FFT:

$$\overline{f(w)} = \sum_{j=-N/2}^{N/2} f(j\Delta x) \cdot e^{2\pi i \cdot w \cdot j \Delta x}, \quad (15)$$

where function  $f$  is defined on the interval  $w \in [0,1]$  and  $i$  is the imaginary unit that satisfies  $i^2 = -1$ . Note that  $2L$  in equation (14) allows for a change in the length of the interval from 1 to  $2L$ . Finally, the inversion of FFT provides  $f * g(w)$  which is the value of the right-side of IDEs (1).

With the solution of the FFT which provides the value of the right-side of IDEs (1), the original IDEs can be treated as an initial value problem. The Runge-Kutta method is used to solve this initial value problem. Then, the number of vehicles by vehicle class in cell  $x$  and at time  $t$  through information dissemination process are updated. The updated proportion of vehicles by vehicle class are used in the intermediate component for the next time interval.

#### 4.4.3 Numerical method for single class traffic flow model

The single class traffic flow model (PDE equations (2) and (3)) is reformulated into the discrete single class traffic flow model (equations (16) and (17)). Same as the upper layer, space and time are discretized into cells with length ( $\Delta x$ ) and time interval ( $\tau$ ), and  $\Delta x = u_f \cdot \tau$ . The continuous single class traffic flow conservation law (equation (2)) is discretized as follows:

$$k(x, t + \tau) / \tau - k(x, t) / \tau = q(x - \Delta x, t) / \Delta x - q(x, t) / \Delta x . \quad (16)$$

The fundamental diagram of traffic flow (equation (3)) is discretized as (Daganzo, 1995b):

$$q(x, t) = \min \{ T(k(x, t)), R(k_j - k(x + \Delta x, t)) \} \quad (17)$$

where a “sending” function  $T$  specifies the maximum flow from the cell that can be sent to a downstream cell, and a “receiving” function  $R$  specifies the maximum flow that can be received by the downstream cell. The functions  $T$  and  $R$  are continuous, piecewise differentiable, and non-decreasing functions defined in the interval  $[0, k_j]$ , and such that  $T(0)=R(0)=0$ . In FDE approximation, the sending and receiving functions correspond to the increasing and decreasing branches of the flow-density curve. In an uncongested region of time-space, the outflow of a cell is  $T(k(x, t))$ . Similarly, in a congested region the outflow of a cell is  $R(k_j - k(x + \Delta x, t))$ . Hence, the outflow from a cell,  $q(x, t)$ , is the largest value that does not exceed the number of vehicles that can be sent by the cell or received by its downstream cell (Daganzo, 1995b). The updated total number of advancing vehicles in cell  $x$  and at time  $t$  is used to update the upper layer through the intermediate component.

#### 4.4.4 Intermediate component to connect the lower and upper layers

At each location  $x$  and time  $t$ , numerical solutions are obtained for the discrete SI and the discrete single class traffic flow model. We introduce an intermediate component to connect the upper and lower layers consistently in terms of the number of vehicles by vehicle class. The sequence of numerical solutions and the intermediate component are illustrated in Figure 4-8. The single class outflow of a cell at location  $x$  and time  $t$ ,  $q(x,t)$ , is decomposed into the multi-class outflow using the previous time interval's proportion of vehicles by vehicle class in the upper layer. Then, the discrete multi-class traffic flow conservation equation is used to update the number of vehicles by vehicle class of each cell. The steps of the intermediate component are as follows:

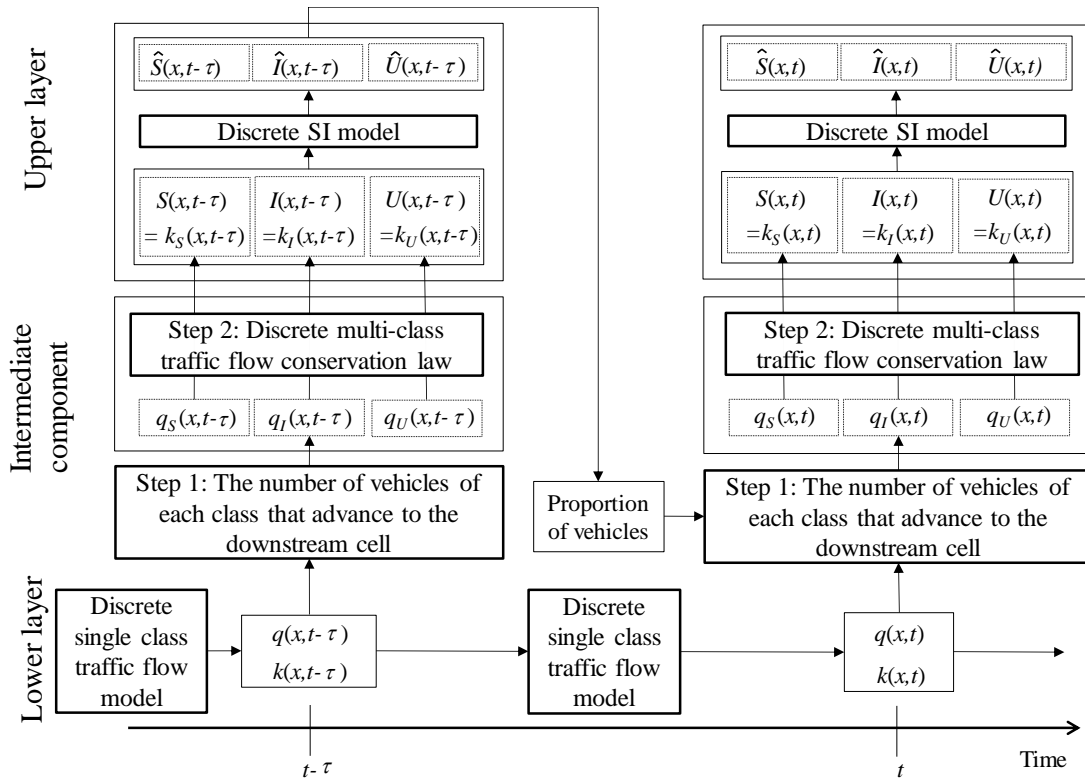


Figure 4-8 Framework of the intermediate component to connect the upper and lower layers

Step 1 determines the number of vehicles of each class  $z$ , where  $z \in \{S, I, U\}$ , that advance to the downstream cell using the outcomes of the lower layer (equations (16)-(17)) and the proportion of upper layer in previous time interval in the upper layer, as follows:

$$\begin{aligned}
q_s(x,t) &= \frac{\hat{S}(x,t-\tau)}{k(x,t-\tau)} \cdot q(x,t) \\
q_I(x,t) &= \frac{\hat{I}(x,t-\tau)}{k(x,t-\tau)} \cdot q(x,t) \\
q_U(x,t) &= \frac{\hat{U}(x,t-\tau)}{k(x,t-\tau)} \cdot q(x,t)
\end{aligned} \tag{18}$$

where  $q_z(x,t)$  is the number of vehicles of each class that leave cell  $x$  during time interval  $\tau$  and  $\hat{S}(x,t)$ ,  $\hat{I}(x,t)$ ,  $\hat{U}(x,t)$  are variables that describe the updated number of vehicles of each class in cell  $x$  at time  $t$  in the discrete SI model. Equation (18) indicates that the number of vehicles of each class that advance to the downstream cell is proportional to the previous time interval's proportion of vehicles by vehicle class in the upper layer (equations (14)-(15) and the Runge-Kutta method).

Step 2 updates the number of vehicles by vehicle class in each cell of the upper layer using the discrete multi-class flow conservation law, as follows:

$$k_z(x,t+\tau) - k_z(x,t) = q_z(x-\Delta x,t) - q_z(x,t). \tag{19}$$

It is important to note here that  $k_s(x,t)$ ,  $k_I(x,t)$ ,  $k_U(x,t)$  in equation (19) are the same as  $S(x,t)$ ,  $I(x,t)$ ,  $U(x,t)$  that describe the number of vehicles of each class in the upper layer, respectively. At each location  $x$  and time  $t$ , two layer's numerical solutions are obtained sequentially to update the evolution of the IFPW.

## 4.5 Numerical experiments

This section first discusses the design of numerical experiments and the parameter calibration for the proposed communication kernel. Then, it provides numerical examples for the IFPW speed under homogeneous and heterogeneous traffic conditions.

### 4.5.1 Experiment design

The study network consists of 2,000 grid cells, which is equivalent to 30 km of highway length. Consistent with the data communication frequency (2Hz), the time interval  $\tau$  for updating is set to 0.5 seconds. Different demand levels and a pre-defined market penetration rate (50%) are used to

generate various traffic conditions. The cell characteristics and experiment parameter values are provided in Table 4-1.

We label the IFPW speed in the direction of vehicular traversal as the forward IFPW speed. The IFPW speed opposite to the direction of vehicular traversal is defined as the backward IFPW speed. The IFPW speed is positive in the direction of traffic flow.

Table 4-1 Cell characteristics of the study network, and experiment parameters

Variables	Units	Value
Free flow speed ( $u_f$ )	(km/h)	108
Time interval ( $\tau$ )	(seconds)	0.5
Grid cell length ( $\Delta x$ )	(meters)	15
Number of lanes	-	1,2
Market penetration rate ( $\gamma$ )	(%)	50
Total number of cells	-	2,000
Critical density ( $k_c$ )	(vehicles/km/lane)	42
Jam density ( $k_j$ )	(vehicles/km/lane)	167
Frequency of communication ( $\beta$ )	(Hz)	2
Communication range ( $L$ )	(meters)	500

#### 4.5.2 Parameter calibration of communication kernel

This section discusses the calibration of the parameters of the communication kernel that describes the success rate of single-hop communication and the effect of interference caused by multiple transmissions in a network. To do so, we analyze how the success rate of V2V communication decays with the increase in interference for different demand levels and a specific market penetration rate (50%). Due to the lack of real-world data for various V2V communication

environments, we use a simulation-based approach. The aim of the simulation-based approach is to generate realistic synthetic data for the success rate of single-hop V2V communication under various demand levels. As we focus on the success rate of single-hop V2V communication at a time instant (of length 0.5 seconds), the impact of the dynamic changes in the vehicle positions is ignored.

Using the simulation-based approach, we analyze the success rate of communication from the sender equipped vehicle to the receiver equipped vehicle, by factoring the cumulative interference (see Section 4.2.2). Note that the inherent random effects on V2V communication from the real-world traffic and communication constraints are captured by the communication kernel, which is a key innovation of this study. To obtain the communication kernel, Monte Carlo simulations are performed that randomly locate vehicles based on the traffic density in each simulation run, and then apply the V2V communication constraints (range, interference and signal power). Through the simulation approach, we are able to leverage the macroscopic models to derive analytical properties and closed-form solutions for information flow propagation.

The approach is as follows. For a given density ( $k$ ), the sender is assumed to be located in the middle of a 2 km highway, and other equipped vehicles are randomly distributed along the highway. The 2km highway length is used because the communication range is 500 meters, and we incorporate the ranges of both the sender and receivers who are 500 meters on either side of the sender. The analysis is performed for the scenarios in which the receiver is assumed to be located at a distance between 5 meters and 500 meters from sender, at 5 meters space intervals. Suppose other equipped vehicles within communication range from the receiver simultaneously transmit information at a time instant, leading to some cumulative interference. The success (or lack of it) in receiving the transmitted information is determined using the SINR (Gupta and Kumar, 2000). For the communication from equipped vehicle  $a$  (sender) to equipped vehicle  $b$  (receiver), the SINR is defined as:

$$\frac{1}{\|\delta_a - \delta_b\|^2} / \sum_{\substack{h \in E \\ h \neq a}} \frac{1}{\|\delta_h - \delta_b\|^2} \geq \sigma \quad (20)$$

where  $\delta_h$  denotes the coordinates of an equipped vehicle  $h$  within communication range of equipped vehicle  $b$ . The transmitted information from vehicle  $a$  is successfully received by vehicle

$b$  if it satisfies the SINR threshold  $\sigma$  (the study experiments use  $\sigma = 0.15$ ). For each distance ( $v$ ) between the sender and receiver vehicles, 100 simulation runs are performed to account for the stochasticity in the locations of other equipped vehicles.

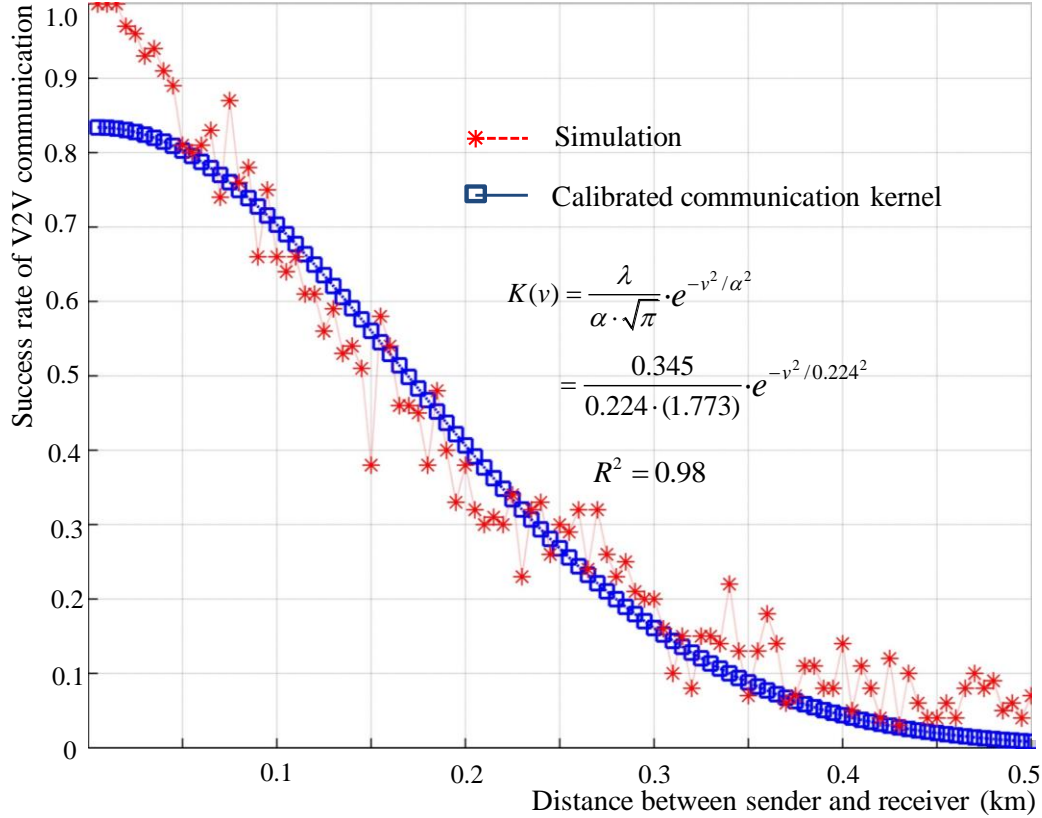


Figure 4-9 Parameter calibration for communication kernel (density: 50 veh./km, and market penetration rate: 50%)

The success rate of V2V communication with distance  $v$  under the vehicle density  $k$ ,  $P_k(v)$ , is obtained based on the simulation results as:

$$P_k(v) = C_k(v)/100, \quad (21)$$

where  $C_k(v)$  is the number of simulation runs in which information is successfully received under a distance  $v$  for density  $k$ . Figure 4-9 plots the  $P_{50}(v)$  values obtained from the simulation runs for various distances between the sender and receiver vehicles.

The simulation data is also used to calibrate the parameters  $\alpha$  and  $\lambda$  for the Gaussian communication kernel  $K(v) = \frac{\lambda}{\alpha \cdot \sqrt{\pi}} \cdot e^{-v^2/\alpha^2}$ . The Least Sum of Squared Errors (LSSE) is applied to calibrate the communication kernel. Figure 4-6 shows the calibrated communication kernel that indicates the probability of successful reception of information with respect to the distance between the sender and receiver vehicles for the density level 50 veh./km. Table 4-2 illustrates the calibrated values of the parameters  $\alpha$  and  $\lambda$  for various densities ( $k$ ) ranging from 10 veh./km to 480 veh./km, in discrete intervals of 10 veh./km, under the 50% market penetration rate.

Table 4-2 Calibrated communication kernel parameters for various densities, and the market penetration rate of 50%

Density ( $k$ ) (veh./km)	$\alpha$	$\lambda$	Density ( $k$ ) (veh./km)	$\alpha$	$\lambda$	Density ( $k$ ) (veh./km)	$\alpha$	$\lambda$
10	0.464	0.864	170	0.066	0.108	330	0.037	0.063
20	0.410	0.685	180	0.063	0.106	340	0.035	0.061
30	0.345	0.548	190	0.063	0.101	350	0.034	0.059
40	0.273	0.420	200	0.059	0.096	360	0.035	0.06
50	0.224	0.345	210	0.056	0.091	370	0.032	0.057
60	0.191	0.292	220	0.054	0.086	380	0.031	0.056
70	0.156	0.246	230	0.049	0.084	390	0.031	0.055
80	0.138	0.218	240	0.049	0.084	400	0.03	0.053
90	0.125	0.195	250	0.048	0.08	410	0.029	0.051
100	0.109	0.175	260	0.045	0.076	420	0.029	0.051
110	0.101	0.165	270	0.042	0.073	430	0.028	0.05
120	0.088	0.145	280	0.039	0.067	440	0.028	0.051
130	0.083	0.140	290	0.04	0.07	450	0.027	0.048
140	0.081	0.131	300	0.038	0.065	460	0.027	0.048
150	0.073	0.121	310	0.038	0.067	470	0.026	0.046
160	0.070	0.116	320	0.037	0.065	480	0.027	0.047

### 4.5.3 Comparison of the IFPW speeds of the closed-form and numerical solutions

#### 4.5.3.1 IFPW speed under homogeneous traffic conditions and unidirectional flow

We first consider a unidirectional one-lane highway under homogeneous traffic conditions (that is, constant density over the 30km highway). The results for the forward and backward IFPW speeds are illustrated in Figure 4-10. In the figure, solid curves represent the forward and backward IFPW speeds generated using the closed-form solution, and dashed curves show the numerical solutions. As the density of traffic flow increases, the IFPW speeds increase until  $k = 30$  veh./km and decrease thereafter. This is because while higher equipped vehicle densities provide more opportunities for communication, they also cause increasing interference due to the higher numbers of equipped vehicles. The IFPW speed variation patterns for the forward and backward IFPW speeds have a similar trend, and illustrate symmetry with respect to the traffic speed pattern.

Further, Figure 4-10 illustrates that the speeds generated by the closed-form solutions fit very closely to those of the numerical solutions. For example, when  $k= 30$  veh./km, the closed-form solution (14) of IDE (1) provides the value of  $\bar{c}_l$  as:

$$\sqrt{\frac{e}{2}} \cdot \alpha \cdot \beta \cdot \lambda \cdot E = \sqrt{\frac{e}{2}} \cdot 0.345 \cdot 2 \cdot 0.548 \cdot (0.45 \cdot 0.5) = 0.099 \text{ km/s} = 357 \text{ km/h}$$

Also, the speed for  $k= 30$  veh./km is the free flow speed (see Table 4-1), 108. The forward IFPW speed is then calculated as  $\bar{c}_l + c_T = 357 + 108 = 465$  km/h, which is close to the speed of 447 km/h provided by the numerical solution.

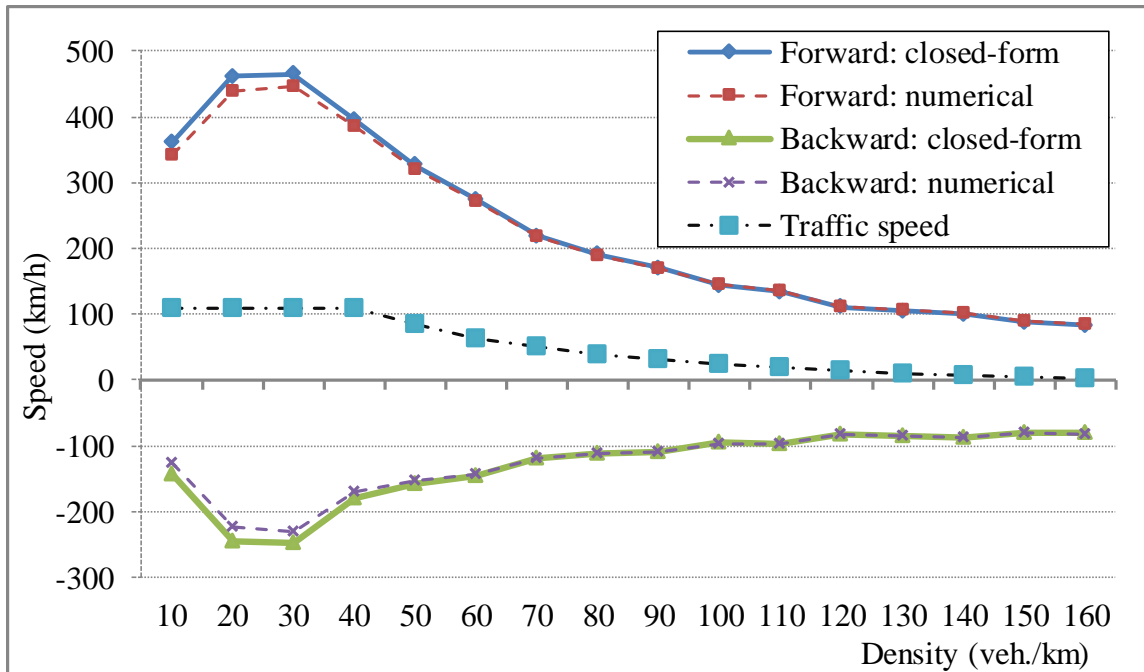


Figure 4-10 Speed of IFPWs under various densities (one-lane highway)

The forward and backward IFPW speeds in a unidirectional two-lane highway are illustrated in Figure 4-10. Note that the traffic flow propagation wave speeds are identical to those in Figure 4-9. Akin to Figure 4-9, the trends show that the forward and backward IFPW speeds decrease with increasing density, due to the increased interference. Figure 4-10 also illustrates that the closed-form solutions of the forward/backward IFPW speeds are similar to their numerical solutions.

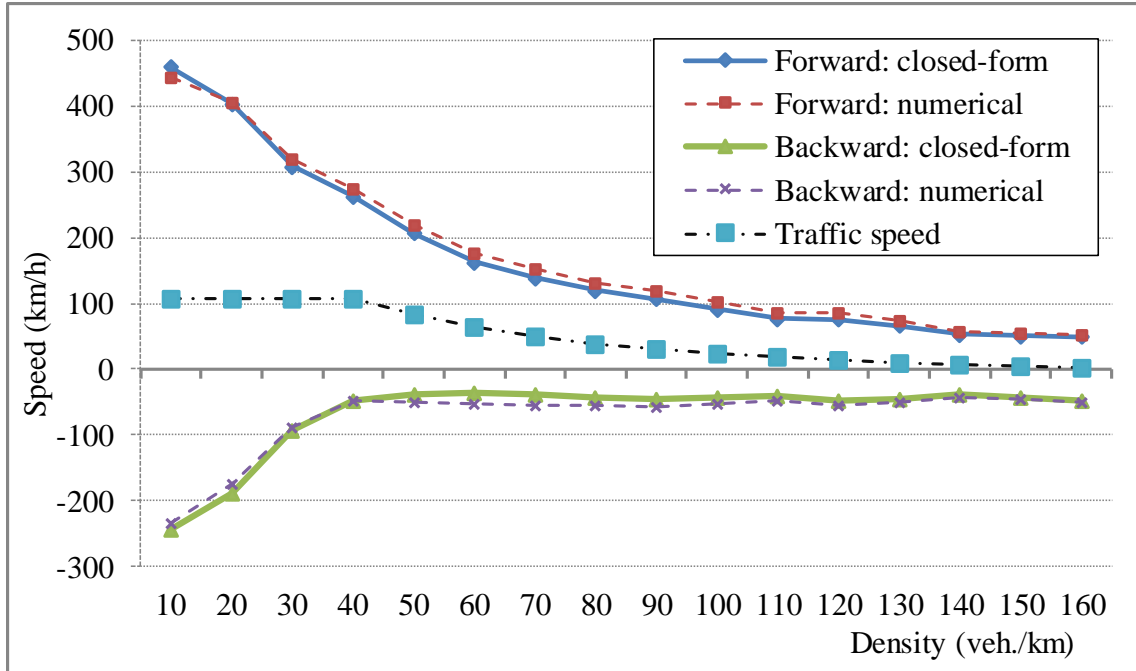


Figure 4-11 Speed of IFPWs under various densities (two-lane highway)

### 5.3.2 Sensitivity analysis of the IFPW speed

This section examines the sensitivity of the IFPW speed to the market penetration rate ( $\gamma$ ). The traffic density is set at 50 veh./km, and the associated speed is 84 km/h. We perform parameter calibration for the communication kernel for this density under different market penetration rates (10% to 100%). Figure 4-12 illustrates the variation of the IFPW speed with  $\gamma$ . The IFPW speeds vary with  $\gamma$  as the information dissemination speeds vary with  $\gamma$ . The IFPW speed variation pattern is symmetric with respect to the traffic flow speed (84 km/h) for the forward and backward IFPW speeds. Up to a  $\gamma$  of 50%, both IFPW speeds increase due to the increased opportunity for information dissemination under V2V communications. Beyond the  $\gamma$  of 50%, both forward and backward IFPW speeds decrease due to the increased interference.

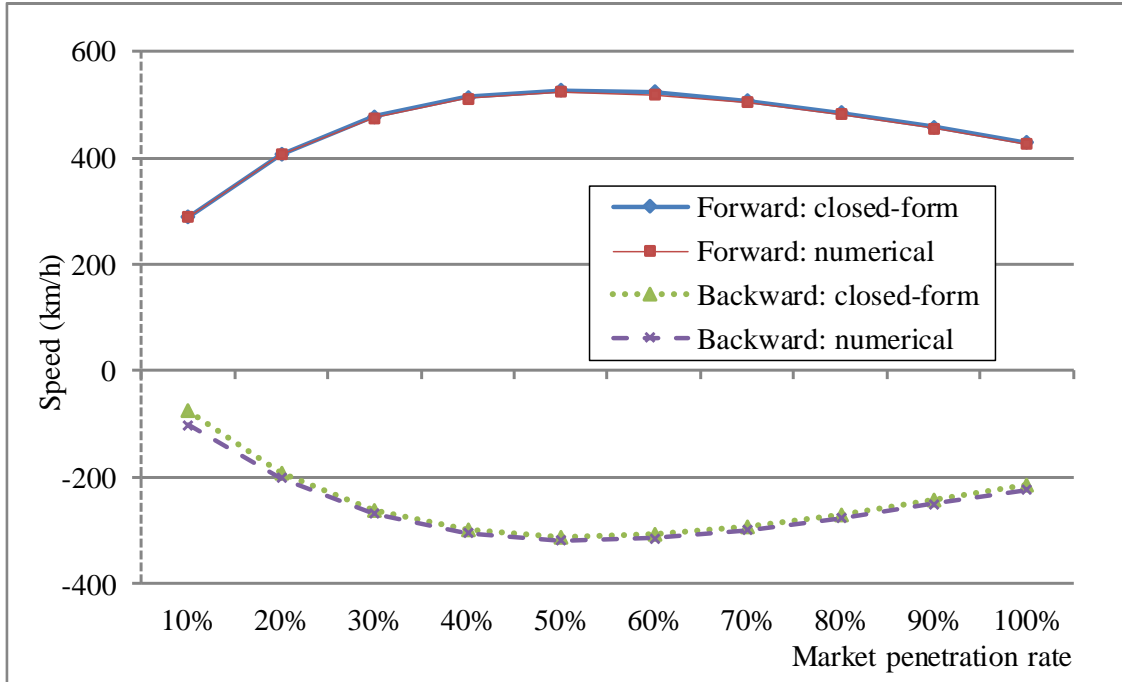


Figure 4-12 IFPW speeds for different market penetration rates

#### 4.5.4 Shape of the IFPW and its asymptotic speed

The forward and backward IFPWs under various densities are illustrated in Figure 4-13. The IDEs (equation (1)) and PDEs (equation (5)) generate IFPWs that preserve their shape and move across space at a constant speed. Figure 4-13 is obtained by plotting the forward and backward IFPW fronts every thirty iterations (15 seconds). To evaluate the IFPW shape and the speed at which traffic information propagates along a given unidirectional highway, we perform a numerical experiment based on equations (1) and (5). Each curve represents the density of informed vehicles at successive time intervals, and lines that are farther from the origin appear later in time.

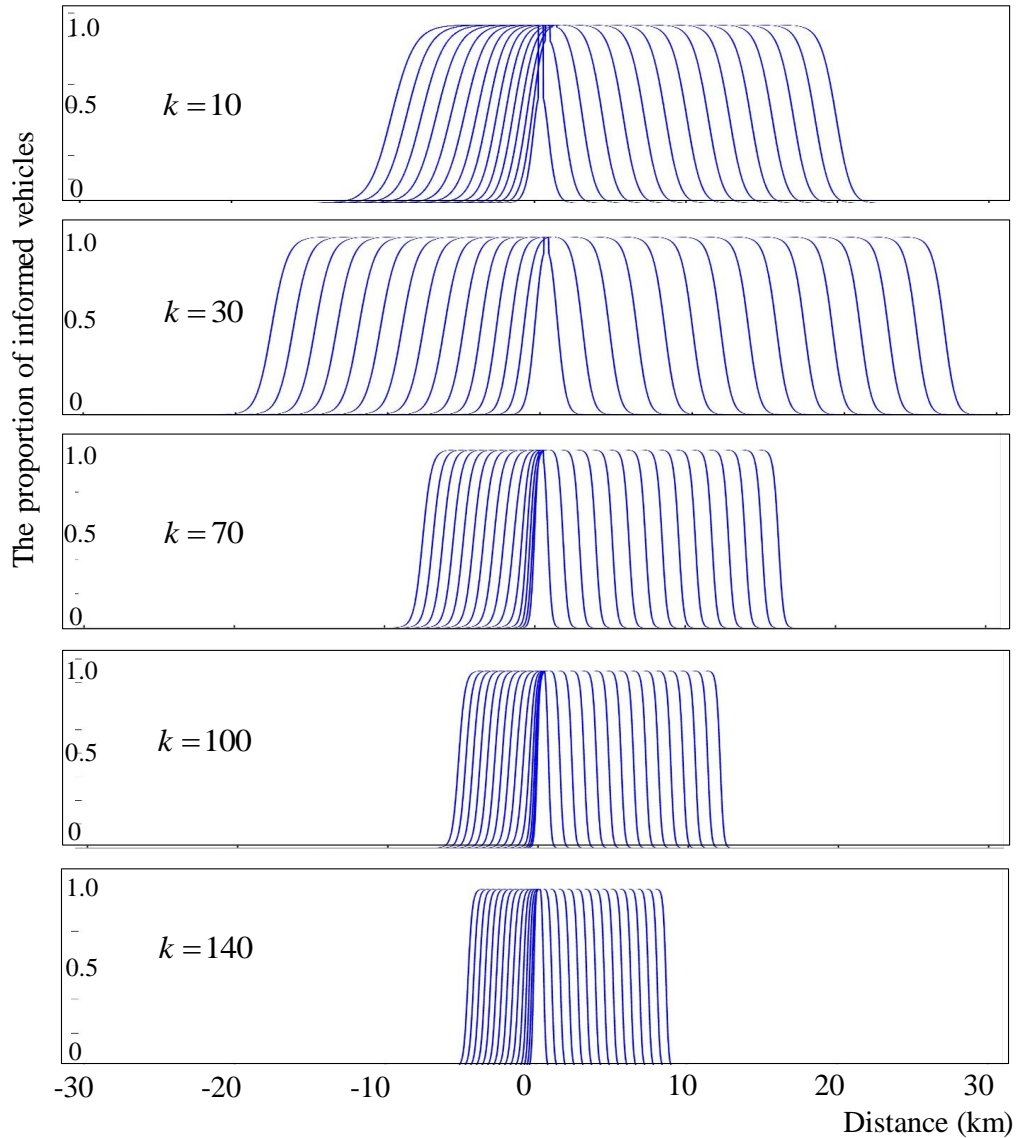


Figure 4-13 IFPWs under various densities

As illustrated by Figure 4-12, the forward and backward IFPW speeds are different under different traffic flow conditions. For light traffic conditions ( $k = 10$  veh./km), the IFPW speeds are slow due to the fewer opportunities to communicate in a low-density environment. As the density of traffic flow increases ( $k = 30$  veh./km), the IFPW speeds increase. At even higher densities (in the figure,  $k = 70$  veh./km, and beyond), the interference increases substantially and the traffic speed reduces, leading to the decrease in IFPW speeds. As informed vehicles carry and broadcast

the information, a boundary of informed region moves in the direction of vehicular traversal. These observations are consistent with those in Kim et al. (2016).

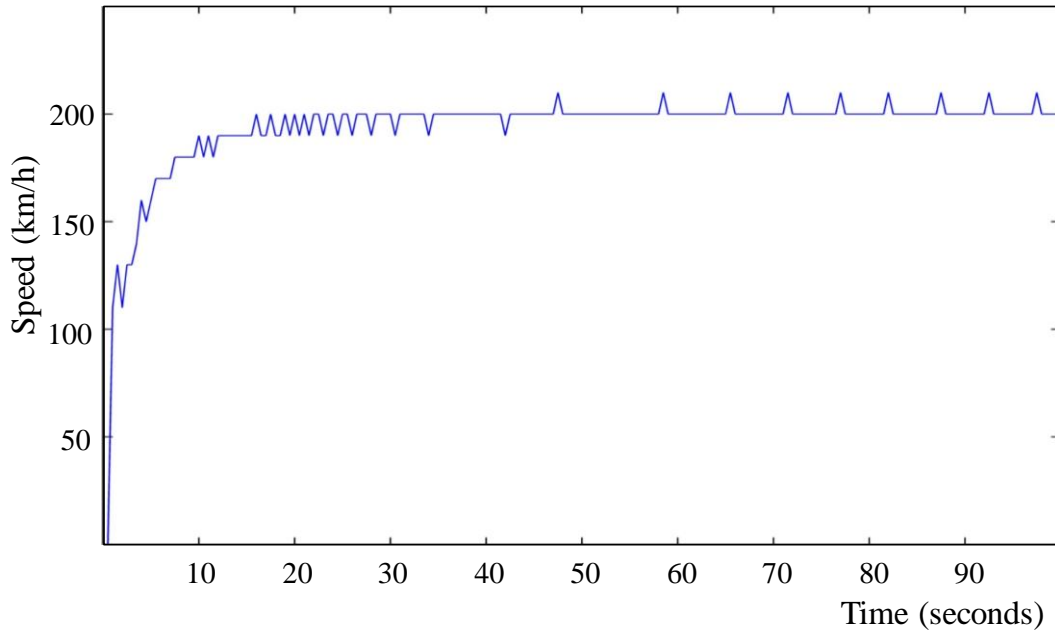


Figure 4-14 Illustration of asymptotic speed

Next, we illustrate the asymptotic property of the solution of the IDE model (equation (1)). Figure 4-14 indicates that the IFPW speed takes 15 seconds to increase from a low initial value to the asymptotic speed. This observation is consistent with the finding in epidemiology (Mollison, 1972a) that the initial speed of epidemic front is slower than its asymptotic speed.

#### 4.5.5 IFPW under bidirectional flow and/or heterogeneous traffic conditions

##### 4.5.5.1 Bidirectional flow

In this section, we address the bidirectional highway (one lane in each direction) case, where information can be propagated by vehicles traveling in both directions. The number of vehicles in the two lanes of the bidirectional highway is the same as for the case with unidirectional traffic flow and two lanes (see Section 4.5.3.1).

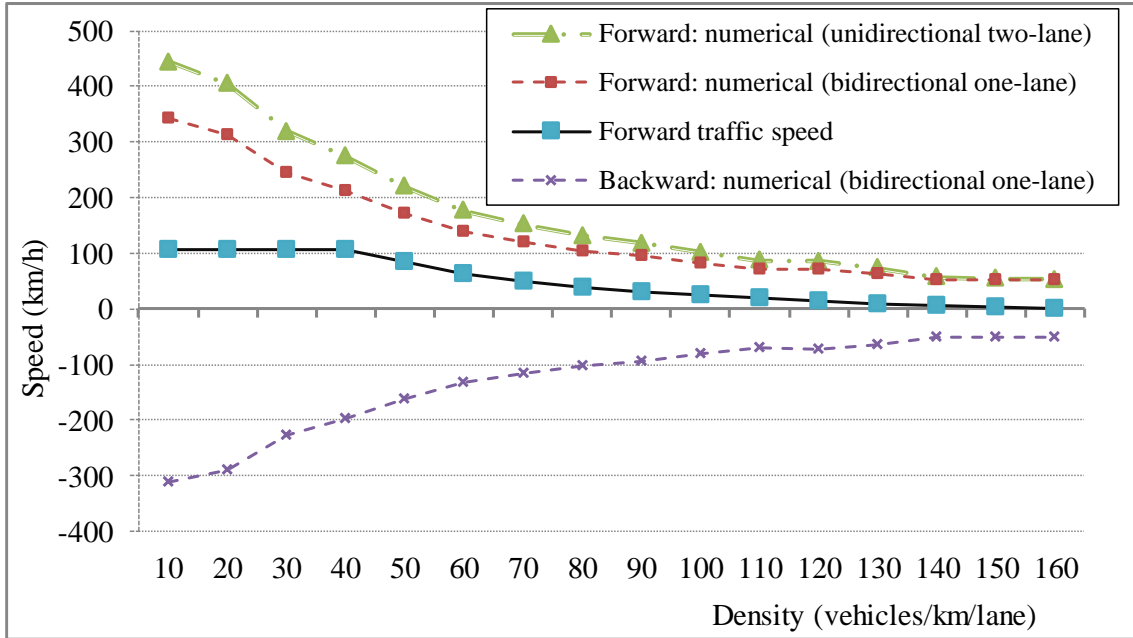


Figure 4-15 Speed of IFPWs under various densities (bidirectional two-lane highway)

The bidirectional (eastbound and westbound) traffic flow affects the forward and backward IFPW speeds in two ways. First, it can be observed that the pattern of the forward IFPW speed is similar to that of the unidirectional two-lane highway case, though the speed is lower. This is because vehicles moving in the opposite direction contribute to the IFPW, though they move in the direction opposite to that of the IFPW front. Hence, the unidirectional two-lane case provides an upper bound for the bidirectional forward IFPW speed, as shown in Figure 4-15. Second, as traffic flow conditions are identical for both directions, the backward and forward IFPW speeds in the bidirectional traffic case are symmetric with respect to the forward traffic speed.

#### 4.5.5.2 One-lane unidirectional highway with incident

Here, we examine the influence of traffic density heterogeneity in the traffic stream on the speed of IFPWs, by considering the effects of a traffic incident for a one-lane unidirectional highway with a traffic density of 50 veh./km. To account for the spatial variability in density due to the incident, the communication kernel function consistent with the density for a spatial segment

is used to capture the effects of interference. As illustrated in Figure 4-16 (a), an incident occurs at location A at  $t = 0$ , and is cleared at  $t = 4$  minutes (at point B in Figure 4-16 (a)).

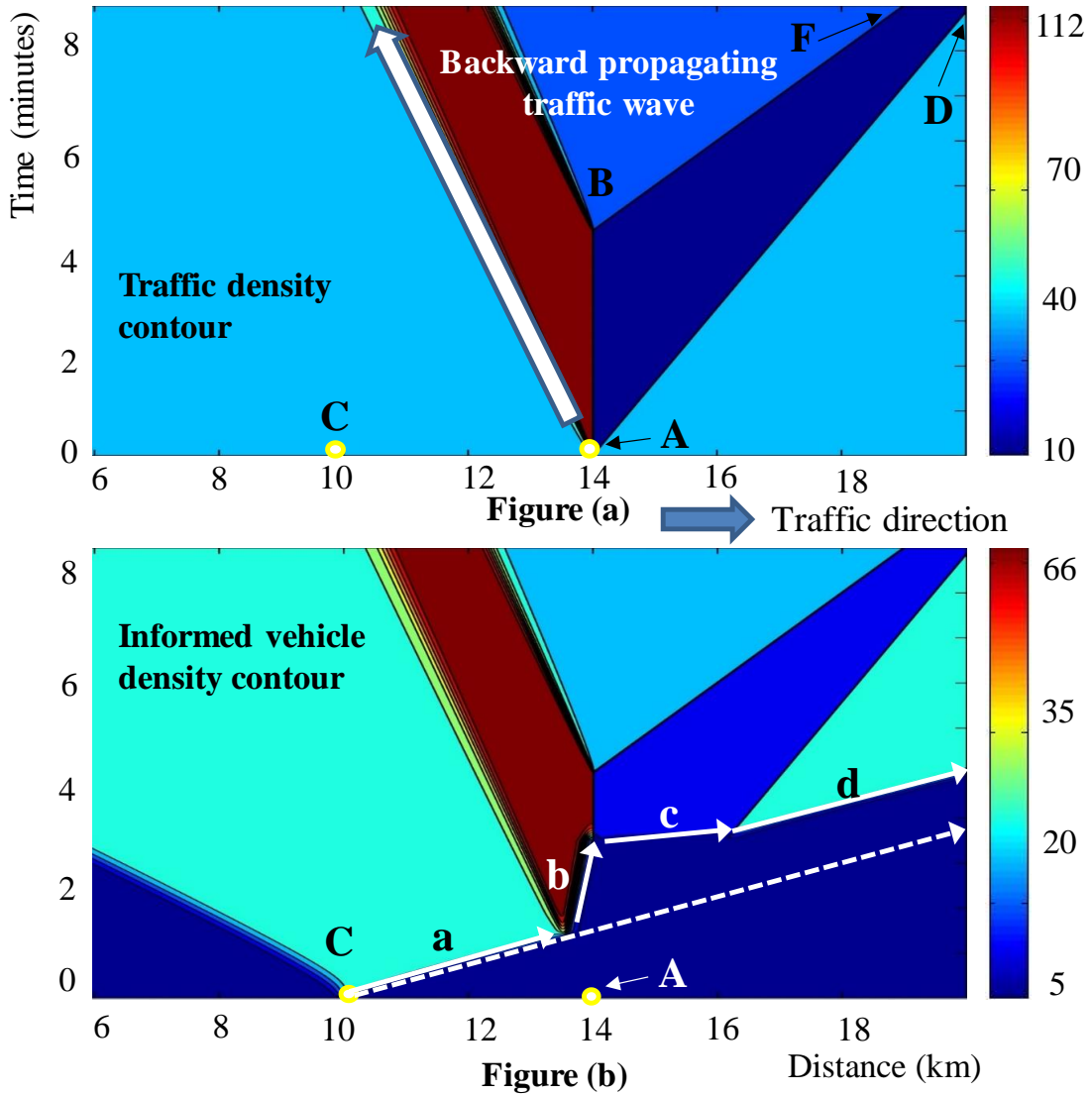


Figure 4-16 Contours of traffic density and information density

The incident reduces the highway capacity by  $1/3$  of its initial value for this duration. The line connecting points A and D in Fig. 4-16 (a) separates the congested area and the free flow traffic departing from the congested area. The information generated at  $t = 0$  at point C propagates in both directions. The resulting spatiotemporal contour plot of the traffic density and informed vehicle

density are shown in Figure 4-16. The forward IFPW speed changes as the downstream traffic density changes, and is represented by the arrows (a, b, c, and d) in Figure 4-16 (b).

As shown in Figure 4-16 (b), the forward IFPW speed (arrow b) decreases in the region of the backward propagating traffic shock wave. This is because a higher vehicle density implies unfavorable conditions for V2V communication due to the higher interference, resulting in the lower likelihood of V2V communications. By contrast, in the queue dissipation area (illustrated by ABFD in Figure 4-16 (a)), the forward IFPW speed (illustrated by arrow c) is faster than those of the other areas, as traffic is at free flow speed and V2V communications take place more frequently.

The effect of encountering the congested traffic area is illustrated by the difference between the solid and dashed arrows in Figure 4-16 (b), whereby the dashed arrow indicates the forward IFPW if no incident occurs. The speed decrease in the congested area (illustrated by arrow b) is more than the speed increase in the queue dissipation area (illustrated by arrow c). Hence, the average IFPW speed is reduced due to the traffic congestion associated with the incident, compared to the no-incident case (illustrated by the dashed arrow).

#### **4.6 Concluding comments**

Existing studies on information flow propagation typically ignore the relationships between traffic flow and information flow dynamics by assuming instantaneous propagation of information flow through multi-hop communications. To bridge this gap, this study proposes a macroscopic model which characterizes the relationship between V2V communications and traffic flow dynamics, to determine the IFPW speed while factoring constraints arising from traffic flow dynamics and V2V communications.

A primary contribution of the proposed model is its closed-form solution for the IFPW speed under certain conditions. The theoretical investigation provides useful insights into the IFPW speed and interdependencies with traffic flow dynamics. While this model is used to describe the dynamics of information flow propagation, it is worth noting that the proposed model and its closed-form solution can also aid in designing effective V2V-based traffic systems without relying on computationally expensive numerical methods. For example, from a communication viewpoint, it bridges the relationship between V2V communication constraints and the IFPW speed through

the specification of a communication kernel. Therefore, it enables communication engineers to choose the optimal V2V communication parameters (such as transmission power and data communication frequency) to satisfy a certain speed threshold for information flow propagation. From a transportation perspective, it can help to design prescriptive strategies to promote the propagation of useful information efficiently.

The study offers the possibility of developing more sophisticated information flow propagation models by leveraging well-developed mathematic theories in epidemiology and ecology. For example, while this study establishes a deterministic model based on the notion that the density is large enough to ignore stochastic effects, a more comprehensive study could include stochastic effects, which can be important when the vehicle density is especially low. Another interesting topic would be considering the congestion effects for IFPW. This study considers a situation where the size of data and data generation rate is less than a critical value, and the V2V communications would not exceed the available bandwidth capacity. Hence, when the large number of information is generated by multiple vehicles in a small space and a short time period, it would cause communication congestion that it may significantly affect the speed of IFPW.

## 5. COUPLED HIDDEN MARKOV MODEL FOR TWO-STAGE MANEUVER-BASED MULTI-ANTICIPATIVE FORWARD COLLISION WARNING SYSTEM

### 5.1 Introduction

Driving an automobile is a complex task that requires the driver to continuously scan the environment, interpret traffic situation, and interact with it. To aid safe driving and reduce accidents, innovative technologies have been leveraged in advanced driver assistance systems (ADASs). An ADAS labeled as forward collision warning (FCW) system is an advanced safety feature that provides a warning about an impending collision with the lead vehicle to refocus driver's attention to the roadway and elicit a safe maneuver response from the driver. While the function and performance of FCW systems can vary widely, several studies (Cicchino, 2016; Georgi et al., 2009; Wu et al., 2018) report that FCW systems may prevent a significant proportion of rear-end collisions by providing warnings to drivers of upcoming threats and potential collisions.

There are several ways in which FCW systems work, including variations in the method used to detect potential collisions. Currently, typical FCW systems employ an on-board sensor (Ammoun and Nashashibi, 2010; Benedetto et al., 2015) such as radar, LIDAR, vision-based system, or a fusion of different sensing technologies. Such systems offer varying degrees of capability for vehicle detection and tracking (Sun et al., 2006). However, these technologies are limited in their ability to detect multiple downstream vehicles due to line-of-sight problem. Recent technological developments in vehicle-to-vehicle (V2V) communications make it possible to perceive downstream traffic conditions beyond those enabled by on-board sensors (Biswas et al., 2006; Kim et al., 2018; Leontiadis et al., 2011; Monteil et al., 2013; Palazzi et al., 2010). Thereby, an FCW system can utilize trajectory-related information from multiple downstream vehicles through V2V communications as *a priori* knowledge to predict the lead vehicle trajectory with sufficient lead time.

The ability to provide a warning about an upcoming safety-critical situation with sufficient time for the driver to react is the most critical component of FCW systems. Such systems can include early warning, imminent warning, or both. Lerner et al. (1996) define an imminent warning as a warning requiring an immediate corrective action, while an early warning alerts the driver

about a situation that requires immediate attention and may require a corrective action. Depending on whether an early warning is included, the FCW system can be classified into single-stage and multi-stage warning systems. Multi-stage warning systems (Werneke et al., 2014; Winkler et al., 2016) include multiple early warnings and an imminent warning, while single-stage warning systems provide only imminent warning. With an early warning, drivers can react with much milder and stress-free control (Winkler et al., 2016). The National Highway Traffic Safety Administration (NHTSA, 2002) also reports that multi-stage warnings can evoke significantly faster reaction times at the imminent warning compared to single-stage warnings by directing driver's attention towards a possible collision situation through early warning. A driving simulator based study (Lee et al., 2002) shows that early warnings help to avoid more collisions compared to no-warning or imminent-warning only scenarios. The National Transportation Safety Board (NTSB, 2015) crash data study shows that if vehicles had been equipped with an FCW system that is capable of providing a sufficiently early warning, it may have prevented or reduced the severity of injuries in more than 90 percent of those crashes.

While the safety benefits of multi-stage FCW systems are widely acknowledged in the literature (Cicchino 2017), two key issues related to the uncertainty in predicting the trajectories of downstream vehicles still remain. First, as the time required to predict collision risk of the host vehicle increases, the likelihood of a false alarm, that is, a warning being issued for a non-threatening situation, increases (Brown et al., 2001). Second, and as a consequence of the first issue, excessive number of false alarms reduces the driver's trust in the FCW system which results in slower and less reliable reactions by the driver towards valid warnings (Bliss and Acton, 2003; Burgett and Miller, 2001), thereby reducing the effectiveness of the FCW system.

While traditional FCW systems do not handle false alarm-related issues, several motion models, which predict the evolution of vehicle trajectory with time, have been proposed to address the uncertainty in predicting the lead-vehicle trajectory. A detailed survey on motion models can be found in Lefèvre et al., (2014). They can be categorized into two broad methodological groups, physics-based and maneuver-based, depending on the level of driving decisions and control. In general, driving is usually considered as an activity that consists of three levels of decision and control: strategic (planning), maneuvering (tactical), and operational (control) (Michon, 1985). At the strategic level, the driver makes high-level travel decisions such as choices related to

destination, route, and departure time. At the maneuvering level, the driver makes controlled maneuvering decisions such as overtaking, stopping, turning and obstacle avoidance (Michon, 1985). The operational level relates to executing maneuvering-level decisions by taking control actions such as steering and pressing brake or gas pedal.

Physics-based motion models (Brunson et al., 2002; Burgett and Miller, 2001; Kiefer et al., 1999; Najm et al., 2003; Wang et al., 2016) have the lowest degree of abstraction with an operational level interpretation (e.g., constant speed and deceleration). They assume that the lead vehicle will continue its current rate of deceleration until it stops, and thereby allow efficient computation of its instantaneous trajectory. However, they are unable to provide a reliable long-term (i.e., in the order of several seconds) prediction of the lead-vehicle trajectory as they do not factor the possible changes in maneuvering level decisions of downstream vehicles' drivers. Hence, physics-based models fail to adequately capture the uncertainty associated with lead-vehicle trajectory prediction.

Maneuver-based motion models (Kumar et al., 2013; Toledo-Moreo and Zamora-Izquierdo, 2010) have primarily emerged to predict the maneuvers of the lead-vehicle driver. Maneuver-based motion models postulate that the motion of the lead vehicle depends on the maneuver that its driver intends to perform (Lefèvre et al., 2014). In these models, the driver is represented as a maneuvering entity that executes its intended maneuvers. However, the intent of a maneuver is not directly observable until the maneuver is performed. The general approach is to define a finite set of discrete maneuvers and analyze the driver's maneuvers as a classification problem or pattern recognition. Different machine learning methods such as support vector machine (Kumar et al., 2013), and Hidden Markov model (HMM) (Hou et al., 2011; Kumagai et al., 2003) have been used to develop maneuver-based motion models in the literature. However, most existing maneuver-based motion models used in FCW systems are "single process" models; that is, they use only the immediate lead-vehicle's trajectory-related information as they are built upon the assumption of on-board sensor technology that is limited by line-of-sight. In reality, the lead vehicle's trajectory depends on the interactions among multiple vehicles downstream of it and thus, single process motion models are not well-suited to describe FCW systems as they entail multiple interacting processes (Brand et al., 1997).

To address the aforementioned gaps, this study proposes a maneuver-based multi-anticipative motion (MBMAM) model that is embedded in a two-stage FCW system. “Multi-anticipative” implies here that trajectory-related information (such as location, speed, acceleration and direction) from multiple downstream vehicles through V2V communications is used in the model to anticipate their maneuvers. It predicts the lead-vehicle trajectory by considering its interactions with multiple downstream vehicles. Thereby, the proposed model takes into account the maneuver intentions of drivers of multiple downstream vehicles and their interdependencies to incorporate the uncertainty in anticipating their vehicle trajectories. Figure 5-1 illustrates the conceptual difference between the existing approaches and the proposed one. While existing approaches use only the lead-vehicle’s trajectory-related information using on-board sensors to predict the lead-vehicle’s trajectory, the proposed approach leverages V2V communications to obtain and use trajectory-related information of multiple downstream vehicles.

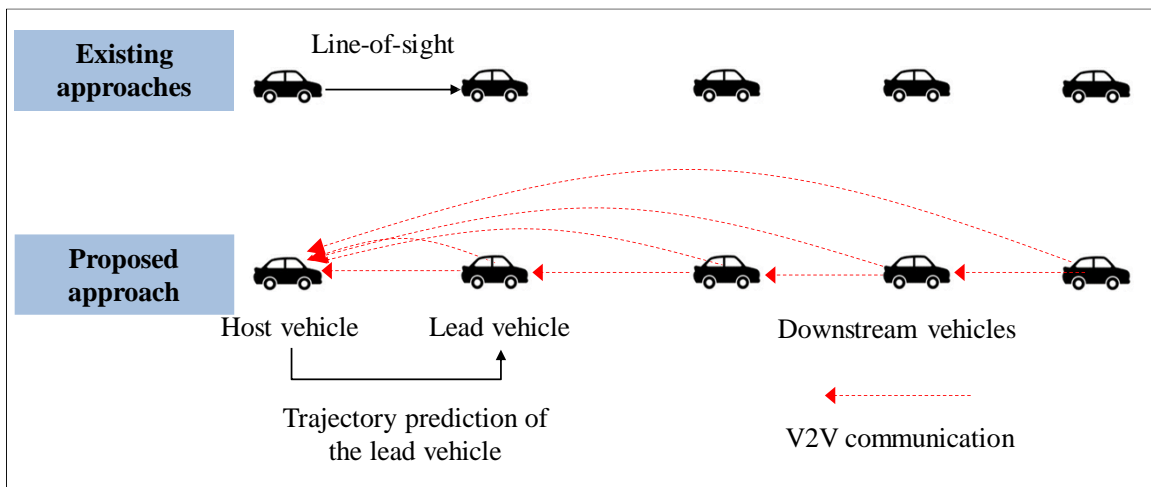


Figure 5-1 Conceptual comparison of the proposed approach with the current approaches

The MBMAM model is formulated as a coupled HMM (Brand et al., 1997) that models the maneuver intentions and their interdependencies as a causal relationship. This model is embedded in the two-stage FCW system that includes an early warning in the first stage and an imminent warning in the second stage. The collision risk of the host vehicle based on the lead-vehicle’s anticipated trajectory is used to determine the issuance of warning and the warning type. The proposed FCW system generates a more effective early warning in the first stage which reduces the frequency of false alarms. The performance of the coupled HMM-based two-stage FCW

system is evaluated using the Next Generation SIMulation (NGSIM) driving trajectory data (FHWA, 2005). The system performance is benchmarked against two existing FCW systems: (i) a two-stage FCW system embedded with NHTSA's physics-based motion model (Brunson et al., 2002), and (ii) a single stage FCW system embedded with a physics-based motion model (Knipling et al., 1993).

The primary contributions of this study are to: (i) develop a two-stage FCW system that provides an earlier first stage warning in potential collision situations, (ii) leverage V2V communications to incorporate trajectory-related information from multiple downstream vehicles to enhance prediction accuracy, and (iii) reduce the frequency of false alarms by decreasing the uncertainty associated with predicting the lead-vehicle's trajectory.

The remainder of the paper is organized as follows. Section 2 discusses the proposed two-stage maneuver-based multi-anticipative FCW system, including the embedded coupled HMM model. Section 3 describes the experiment design and the NGSIM data used for the experiments. Section 4 discusses numerical experiments to analyze the capabilities of the proposed FCW system and compares it to the two existing FCW systems. Section 5 summarizes the main findings and future research directions.

## **5.2 Two-stage MBMAM model-based FCW system**

Section 5.2.1 discusses the information propagation capabilities enabled by V2V communications. Section 5.2.2 elucidates the key capability enabled by the MBMAM model. Section 5.2.3 discusses the proposed MBMAM model. Section 5.2.4 describes the criticality assessment of collision risk that is used to determine the issuance of warning and the warning type.

### **5.2.1 V2V communications for the MBMAM model**

Suitably equipped vehicles can generate trajectory-related information, including location data using a Global Positioning System (GPS) and on-board kinematic data (speed, acceleration, and direction). Through V2V communications, V2V-equipped vehicles can propagate this information by relaying it from one vehicle to another through a multi-hop dissemination process (Kim et al., 2018). Thus, periodic transmission and acquisition of trajectory-related information enables V2V-

equipped vehicles to maintain up-to-date trajectory-related information of other V2V-equipped downstream vehicles.

This study assumes that all vehicles are V2V-equipped while developing the MBMAM model. While there will be a transition period during which V2V-equipped vehicles and unequipped vehicles would need to interact on the road, over the long-term all vehicles would be equipped with compatible V2V communication devices (Tan and Huang, 2006). In the U.S., the USDOT is seeking to mandate V2V communication technology for all new light-duty vehicles (NHTSA NPRM, 2018). Further, to keep the focus on the development of the proposed motion model, the study assumes that no communication failure or time lag would occur due to communication constraints (related to range, interference and bandwidth; see Kim et al., 2018).

### 5.2.2 Capability enabled by the MBMAM model

Figure 5-2 illustrates the key capability enabled by the proposed MBMAM model. It considers a potential collision situation involving multiple vehicles on a highway. The trajectories of vehicles A-D are shown in the space-time diagram where elapsed time is shown on the  $x$ -axis and the vehicle positions are shown on the  $y$ -axis. The figure illustrates a four-vehicle example with a host-vehicle (vehicle D), an immediate lead-vehicle (vehicle C) and two other downstream vehicles (vehicles A and B). Vehicle A is the most-downstream vehicle, and is followed by vehicles B, C, and D, in that order. Assume that vehicle A brakes abruptly at time  $\tau_0$ . For a FCW system that uses only on-board sensors, and hence only the immediate lead-vehicle information, vehicle B will detect vehicle A's braking cue at time  $\tau_0$ , and will begin to brake at time  $\tau_1$ . Similarly, vehicles C and D will detect the braking event of their immediate lead vehicle at times  $\tau_1$  and  $\tau_2$ , respectively, and will apply brakes at times  $\tau_2$  and  $\tau_3$  respectively, as shown in Figure 5-2(a). Hence, vehicle D will receive a warning only after vehicle C starts braking at time  $\tau_2$ , based on vehicle C's predicted trajectory. Depending on the space headway between vehicles C and D, this situation may result in a collision.

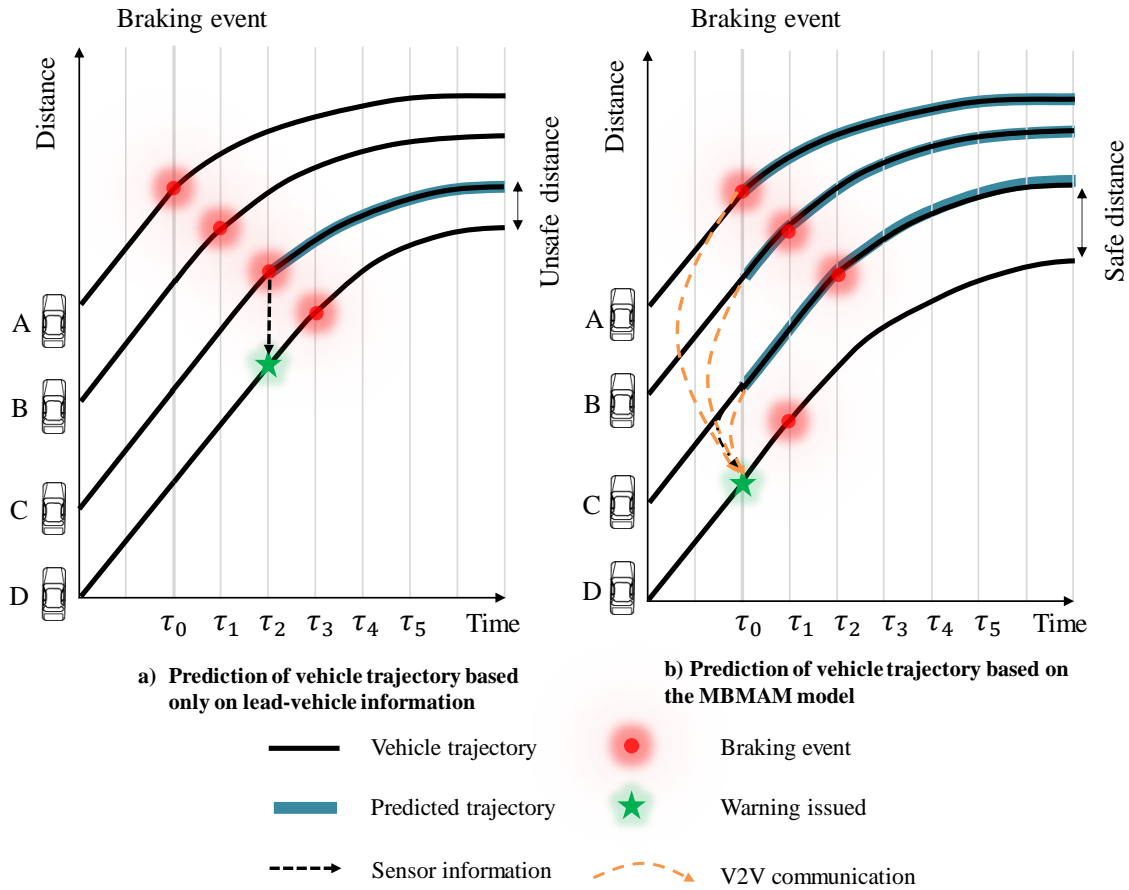


Figure 5-2 Capability of the MBMAM model to provide an earlier early warning

By contrast, Figure 5-2(b) illustrates the same potential collision situation handled by the proposed FCW system leveraging V2V communications capability. V2V communications allow vehicle D to receive information about vehicle A's braking event at time  $\tau_0$ , and use this information to predict the vehicle trajectories of vehicles B and C assuming that vehicle A will maintain its current deceleration rate. Then, using the MBMAM model, FCW system can provide an early warning to vehicle D at an earlier time (between  $\tau_0$  and  $\tau_2$ ) which can increase its likelihood of avoiding a collision with vehicle C due to the valuable additional time to act on the warning, as illustrated in Figure 5-2(b). Thus, the proposed system can be more effective than existing FCW systems as it provides more time to the host vehicle to react to potentially dangerous situations.

### 5.2.3 MBMAM model-based FCW system

Figure 5-3 shows the framework of the MBMAM model-based FCW system. The trajectory-related information of multiple downstream vehicles is provided to the host vehicle at every time instant (0.1 seconds in this study) through V2V communications. Using their trajectory-related information, the host vehicle predicts the driver maneuver intentions of these downstream vehicles through a coupled HMM at every time instant. The predicted maneuver intentions of these downstream vehicles are used to predict their trajectories.

Next, we perform a criticality assessment to determine if a warning should be issued to the host vehicle, and if so, the type of warning to be issued. To do so, we first project the host-vehicle's future trajectories under early and imminent warnings. Depending on the type of warning, the host-vehicle's driver will decelerate at a different rate after a specific reaction time. Then, the predicted lead-vehicle trajectory and the projected host-vehicle trajectories under the two types of warnings are used to estimate the collision risk. Finally, based on the estimated collision risk, the host-vehicle's FCW system determines the issuance of warning and its type.

The rest of this section is organized as follows. We first discuss the conceptual modeling of driver maneuver intention in Section 5.2.3.1. Next, in Section 5.2.3.2, we propose a coupled HMM to anticipate the lead-vehicle driver's maneuver intention by coupling the maneuver intentions of the drivers of multiple downstream vehicles. Finally, we discuss Gipps' car-following model in the study context in Section 5.2.3.3.

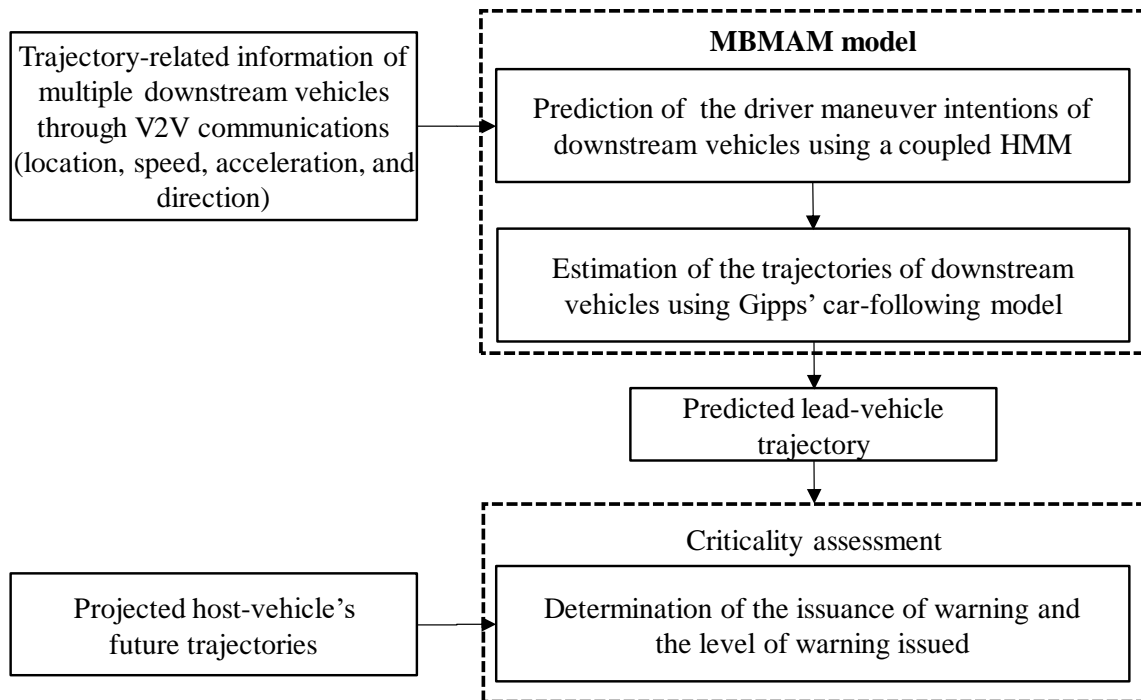


Figure 5-3 Framework of the MBMAM-based FCW system

### 5.2.3.1 Conceptual modeling of driver maneuver intention

The FCW system is designed to provide a warning on an upcoming high-risk situation if the host vehicle comes too close to the lead vehicle. Typically, such situations occur upon abrupt braking by a vehicle downstream that leaves little time for the host vehicle to react and maintain a safe distance from its leading vehicle. Another possible high-risk situation is when the lead vehicle slows down but the host vehicle does not adjust its speed accordingly due to its driver being inattentive or distracted. However, it should be noted here that there can be situations in which the lead vehicle maintains a certain speed, but the host vehicle accelerates, leading to tailgating. This is not addressed in FCW modeling as it indicates an intentional unsafe driving action on the part of the host-vehicle driver.

The maneuver intention is endogenous to the driver and may not be observed directly (that is, it is hidden) which makes its inference uncertain. HMMs offer a mathematically sound basis for making inference under uncertainties. They have been applied extensively to problems in speech recognition and computational biology due to their effectiveness in modeling uncertainties (Rabiner and Juang, 1986). The hidden maneuver intention is inferred from vehicle's observable trajectory-related information and its surrounding environment (e.g., speed limit, etc.). A HMM

can be used to model maneuver intention as a sequential Markov process over time with  $N$  possible discrete states,  $S = \{S_1, S_2, S_3, \dots, S_N\}$ .

In this study, four states (that is,  $N = 4$ ) are used to represent the possible maneuver intention: (i) normal driving ( $S_1$ ), (ii) hard braking ( $S_2$ ), (iii) very-hard braking ( $S_3$ ), and (iv) transitory driving; transitory driving is a transitory moment from normal driving for any circumstance that requires an evasive maneuver by the host vehicle. Among these, normal driving corresponds to a low-risk situation, and the other three states correspond to a high-risk situation. The state of driver maneuver intention at time instant  $t$ , denoted by  $q_t$ , is determined based on the previous maneuver state ( $q_{t-1}$ ), and the rolling average acceleration rate ( $w_{avg}$ ) in the previous  $T$  time instants (we use 30 time instants in this study).

We define the vehicle to be in state  $S_1$  if any of the following conditions is satisfied: (i)  $w_{avg}$  is greater than  $1\text{m/s}^2$  (*condition 1*), or (ii)  $w_{avg}$  is between  $-3\text{m/s}^2$  and  $1\text{m/s}^2$  when the previous state is  $S_1$  (*condition 2*), or (iii)  $w_{avg}$  is between  $-3\text{m/s}^2$  and  $1\text{m/s}^2$  after 3.0 seconds of being in  $S_4$  (*condition 3*). Conditions 1 and 2 correspond to the situations where the vehicle accelerates to achieve its desired speed or uses a low acceleration/deceleration rate to adjust its space headway, respectively. Condition 3 occurs when the vehicle resumes normal driving after being in a transitory driving state. Under the normal driving actions of the lead-vehicle driver, the FCW system will not issue a warning for the host vehicle.

State  $S_2$  corresponds to the driving situation when  $w_{avg}$  is between  $-5\text{m/s}^2$  and  $-3\text{m/s}^2$ , and state  $S_3$  corresponds to  $w_{avg}$  being less than  $-5\text{m/s}^2$ . These driving states are characterized based on the following considerations: (i) the maximum “comfortable” braking deceleration rate is generally accepted to be around  $-3\text{m/s}^2$  (ITE, 1992), (ii) the mean of unexpected deceleration rate is  $-5.39\text{ m/s}^2$  (Fambro et al., 1997), and (iii) the maximum deceleration rate for a typical passenger vehicle is around  $-9\text{m/s}^2$  (Punzo et al., 2011). A vehicle under states  $S_2$  or  $S_3$  transitions back to a normal driving state if it accelerates with  $w_{avg}$  greater than  $1\text{m/s}^2$ . We choose  $w_{avg}$  greater than  $1\text{m/s}^2$  to indicate normal driving since a nominal range for “comfortable” acceleration for speeds of 48km/h and above is  $0.6\text{m/s}^2$  to  $0.7\text{m/s}^2$  (AASHTO, 1990). The transition from states  $S_2$  or  $S_3$  to transitory driving is discussed after state  $S_4$  is described in detail next.

We define transitory driving ( $S_4$ ) as a short-term driving situation in which the lead vehicle is driving at a low acceleration/deceleration rate (between  $-3\text{m/s}^2$  and  $1\text{m/s}^2$ ) immediately after hard or very-hard braking. At that point, the host vehicle is still adjusting to the braking action of the lead vehicle as it requires some reaction time. This leads to a situation in which the headway between the lead and host vehicles is reduced because the lead vehicle uses a low acceleration/deceleration rate. The maximum duration of the transitory state ( $\rho$ ) is set to the 99<sup>th</sup> percentile value of reaction time under the unexpected lead-vehicle braking, which is 3.0 seconds (Lerner et al., 1995) or 30 time instants. This is because it is assumed that the host-vehicle driver will notice the slow-moving lead vehicle within  $\rho$  time instants and will react to this situation. Under state  $S_4$ , the issuance of a warning by the FCW system will be determined by the criticality assessment (discussed in Section 2.4).

The transition from states  $S_2$  or  $S_3$  to state  $S_4$  occurs when  $w_{avg}$  is between  $-3\text{m/s}^2$  and  $1\text{m/s}^2$ . However, if within 3.0 seconds the acceleration rate again goes below  $-3\text{m/s}^2$ , the state will revert back to  $S_2$  or  $S_3$  depending on the actual value of the acceleration rate. On the other hand, if a vehicle is in state  $S_4$  for at least 3 seconds, its driving state reverts to normal driving (condition 3). The set of all possible driver's maneuver intention states is illustrated in Figure 5-4.

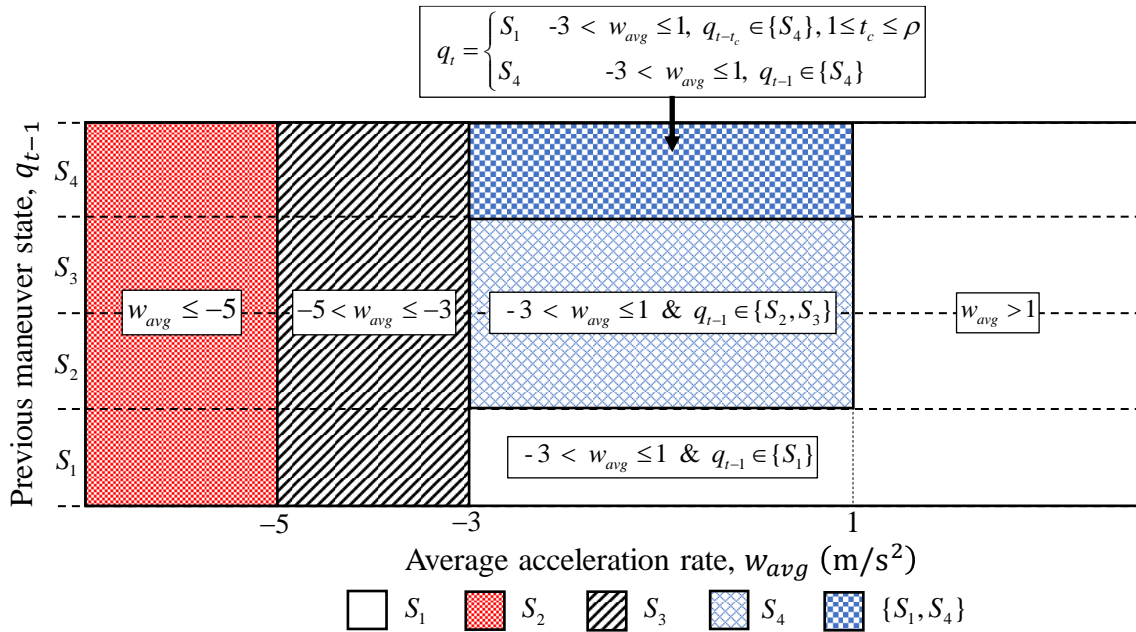


Figure 5-4 Set of the lead-vehicle driver's current maneuver intention ( $q_t$ ) states

Next, the conceptual modeling of the lead-vehicle driver's maneuver intention through the proposed coupled HMM is illustrated. A "coupled" HMM is proposed here because the driver's maneuver intention is determined by coupling trajectory-related information from multiple downstream vehicles.

### 5.2.3.2 Proposed coupled HMM

Assume that there are  $G$  consecutive moving vehicles, indexed by  $g = 1, \dots, G$ , from the upstream to the most-downstream vehicle. The maximum value of  $G$  in the study experiments is 5; that is, if there are more than 5 vehicles downstream of the host vehicle, only the 5 vehicles immediately downstream of the host vehicle are considered, starting with its lead vehicle. If  $G=1$ , it simply implies that only one vehicle is downstream of the host vehicle, at which point there is no coupling of trajectory-related information across multiple vehicles, and line-of-sight is the basis to determine the lead-vehicle driver's maneuver intention. Hence, in the discussion hereafter  $G$  has a minimum value of 2.

The proposed coupled HMM to anticipate the lead-vehicle driver's maneuver intention has three distinctive properties. First, the sequence of states of the most-downstream vehicle ( $g=G$ ) satisfies the Markov property that the probability of the current state depends only on the immediate previous state of that vehicle. From the perspective of the proposed FCW system, it implies that the most-downstream vehicle driver's previous maneuver state includes all information about the history of the process needed to predict the current maneuver intention of that vehicle. This state sequence is generated by a Markov model parametrized by a state transition matrix ( $A$ ).

Second, in HMMs, an underlying stochastic process is not observable before the current state occurs. However, it can be inferred through another set of stochastic processes that produce a sequence of observations. In the proposed FCW system, the current maneuver intentions of the drivers of the downstream vehicles are not observable before those maneuvers are performed. However, the current maneuver intention for each of these vehicles can be inferred through trajectory-related information on speed and acceleration for that vehicle, and the time headway between that vehicle and its lead vehicle. We model the probability of generating trajectory-related information as a function of the hidden state using an observation probability matrix ( $B$ ).

Third, the sequences of the states of the other downstream vehicles ( $g = 1, \dots, G-1$ ) satisfy the coupled Markov property that the probability of the current state of vehicle  $l$  at time instant  $t$  depends only on its immediate previous state and its lead vehicle's state at time instant  $(t-\delta)$ , where  $\delta$  denotes the reaction time. While a single-process HMM uses only the immediate previous state (matrix  $A$ ) to predict the lead-vehicle's maneuver intention, the proposed coupled HMM predicts the downstream-vehicles' maneuver intention by considering interactions with their lead-vehicle's state. The sequences of maneuver intentions of the downstream vehicles are generated by a driver interaction matrix ( $DI$ ). We use the value of 1.2 seconds for  $\delta$  in this study based on Green's (2000) report that response to unexpected, but common signals, such as a lead car's brake lights, is about 1.2 seconds.

Based on the aforementioned three distinctive properties of the proposed coupled HMM, at each time instant, a downstream driver's current maneuver state is determined as follows: (i) the current maneuver state for vehicle  $G$  is determined using the state transition matrix ( $A$ ) and the observation probability matrix ( $B$ ), and (ii) the current maneuver state for each of the other downstream vehicles ( $1, \dots, G-1$ ) is determined by the driver interaction matrix ( $DI$ ) and the observation probability matrix ( $B$ ).

The state transition matrix ( $A$ ) is a  $N \times N$  matrix of the transition probabilities ( $a_t^G(i, j)$ ) that the current (that is, at time instant  $t$ ) maneuver state of vehicle  $G$  is  $S_j$  if its previous maneuver state is  $S_i$ ; that is, based on the Markov property:

$$A = \{a_t^G(i, j)\} = P(q_t^G = S_j | q_{t-1}^G = S_i), \quad 1 \leq i, j \leq N \quad (1)$$

where  $q_t^G$  denotes the state of the driver maneuver intention of vehicle  $G$  at time instant  $t$  and  $N$  is 4 in this study. The state transition probability for vehicle  $G$ ,  $a_t^G(i, j)$ , has the following standard properties:

$$a_t^G(i, j) \geq 0 \quad (2)$$

$$\sum_{j=1}^N a_t^G(i, j) = 1. \quad (3)$$

The matrix  $A$  of state transition probabilities for the study experiments using NGSIM data is listed in Table I in the Appendix.

We infer the state of each vehicle through the observed trajectory-related information. To do so, the observation probability matrix ( $B$ ) encodes the probability of the hidden state generating

the trajectory-related information. The trajectory-related information on speed, deceleration rate, and time headway are discretized into three discrete categories (low, medium, and high). Speed is discretized into speed within a queue, queue discharge, and uncongested (Hall et al.1992). Deceleration rate is discretized by the comfortable (ITE, 1992), expected and the unexpected deceleration rates (Fambro et al., 1997). Time headway is discretized into the tailgating, normal, and sufficient following distance (Song and Wang, 2010). Table 5-1 shows three trajectory-related observations that have been discretized into three levels, where  $k_s$ ,  $k_d$ , and  $k_u$  denote the speed, deceleration rate, and time headway variables, respectively.

$V = \{v_1, v_2, v_3, \dots, v_E\}$  denotes the set of  $E$  distinct trajectory-related observations. Each observation is a combination of the three trajectory-related variables. For example,  $v_1 = \{k_s = L, k_d = L, k_u = L\}$  denotes that all three observations are at their low levels, where  $L$ ,  $M$ , and  $H$  denote low level, medium level and high level, respectively. The number of distinct trajectory-related observations ( $E$ ) in this study is 27. The complete set of possible combinations of observations is illustrated in Table II in the Appendix.

Table 5-1 Discrete trajectory-related observations

	Low ( $L$ )	Medium ( $M$ )	High ( $H$ )
Speed: $k_s$ (km/h)	$30 > k_s$	$30 \leq k_s \leq 50$	$50 < k_s$
Deceleration rate: $k_d$ (m/s <sup>2</sup> )	$-5 > k_d$	$-5 \leq k_d \leq -3$	$-3 < k_d$
Time headway: $k_u$ (seconds)	$3 > k_u$	$3 \leq k_u \leq 6$	$6 < k_u$

We denote the observation of vehicle  $g$  at time instant  $t$  as  $o_t^g$ . The observation probability matrix ( $B$ ) is defined by a  $N \times E$  matrix, containing the probabilities ( $b_t^g(j, k)$ ) of the current maneuver state of vehicle  $g$  ( $1, \dots, G-1$ ) at time instant  $t$ ,  $q_t^g$ , being  $S_j$  if the observation of vehicle  $g$  at time instant  $t$ ,  $o_t^g$ , is  $v_k$ ;

$$B = \{b_t^g(j, k)\} = P(o_t^g = v_k | q_t^g = S_j), \quad 1 \leq j \leq N, 1 \leq k \leq E. \quad (4)$$

The observation probability for vehicle  $g$  in state  $j$ ,  $b_t^g(j, k)$ , has the following standard properties:

$$b_t^g(j, k) \geq 0 \quad (5)$$

$$\sum_{k=1}^E b_t^g(j, k) = 1. \quad (6)$$

The matrix  $B$  of observation probabilities is listed in Table II in the Appendix.

The driver interaction matrix ( $DI$ ) is a  $4 \times 4 \times 4$  matrix containing the probabilities of the current maneuver state  $q_t^g$  of all downstream vehicles  $g$  ( $1, \dots, G-1$ ) other than the most-downstream vehicle. It contains the probability ( $c_t^g(h, i, j)$ ) of vehicle  $g$  being in state  $S_j$  if the immediate previous maneuver state of vehicle  $g$ ,  $q_{t-1}^g$ , is  $S_i$  and the maneuver state of its lead vehicle (vehicle  $g+1$ ) at time instant  $t-\delta$ ,  $q_{t-\delta}^{g+1}$  is  $S_h$ ; that is, based on the coupled Markov property:

$$DI = \{c_t^g(h, i, j)\} = P(q_t^g = S_j | q_{t-1}^g = S_i, q_{t-\delta}^{g+1} = S_h), \quad 1 \leq h, i, j \leq N \quad (7)$$

The  $DI$  for vehicle  $g$ ,  $c_t^g(h, i, j)$ , has standard properties based on probability theory:

$$c_t^g(h, i, j) \geq 0, \quad (8)$$

$$\sum_{j=1}^N c_t^g(h, i, j) = 1. \quad (9)$$

Finally, the initial state matrix that is the initial probability distribution over states at time ( $t=1$ ) is defined as:

$$\pi_i = P(q_1^g = S_i), \quad 1 \leq i \leq N. \quad (10)$$

The matrix  $DI$  and the initial state matrix are illustrated for the NGSIM data in Table III and IV in the Appendix, respectively.

Figure 5-5 shows the graphical representation of the proposed coupled HMM. A circular node denotes the state of maneuver intention of vehicle  $g$  at time instant  $t$ ,  $q_t^g$ . A square node represents the observation at time instant  $t$ ,  $o_t^g$  which is received by the host vehicle from vehicle  $g$  through V2V communications. The vertical links represent the observation probability matrix. The horizontal links for vehicle  $G$  represent the state transition matrix. The diagonal and horizontal links together represent the  $DI$  matrix for downstream vehicles  $g$  ( $g = 1, 2, 3, 4$ ). For example, the maneuver state  $q_t^4$  is updated based on  $q_{t-1}^4$  and  $q_{t-\delta}^5$ , as illustrated in Figure 5-5.

Given the graphical representation of proposed coupled HMM, a statistical inference algorithm is required to infer the most likely series of states given a series of trajectory-related observations. The message passing algorithm (Pearl, 1988) for exact inference in singly-connected networks (Suermondt and Cooper, 1990) has been developed to compute the marginal probabilities of all the variables to incorporate new observations. However, the proposed structure of coupled HMM in Figure 5-5 has a multiply-connected network in which there can be more than one directed path

between any two nodes. Suermondt and Cooper (1990) extend the message passing algorithm to enable it for multiply-connected networks. We adapt the extended message passing algorithm to update the maneuver intentions of the drivers of multiple downstream vehicle to incorporate new observations. Based on the aforementioned properties of the proposed coupled HMM, at each time instant, the maneuver intentions of multiple downstream vehicles are obtained. Next, the detailed trajectories of downstream vehicles are estimated using a car-following model.

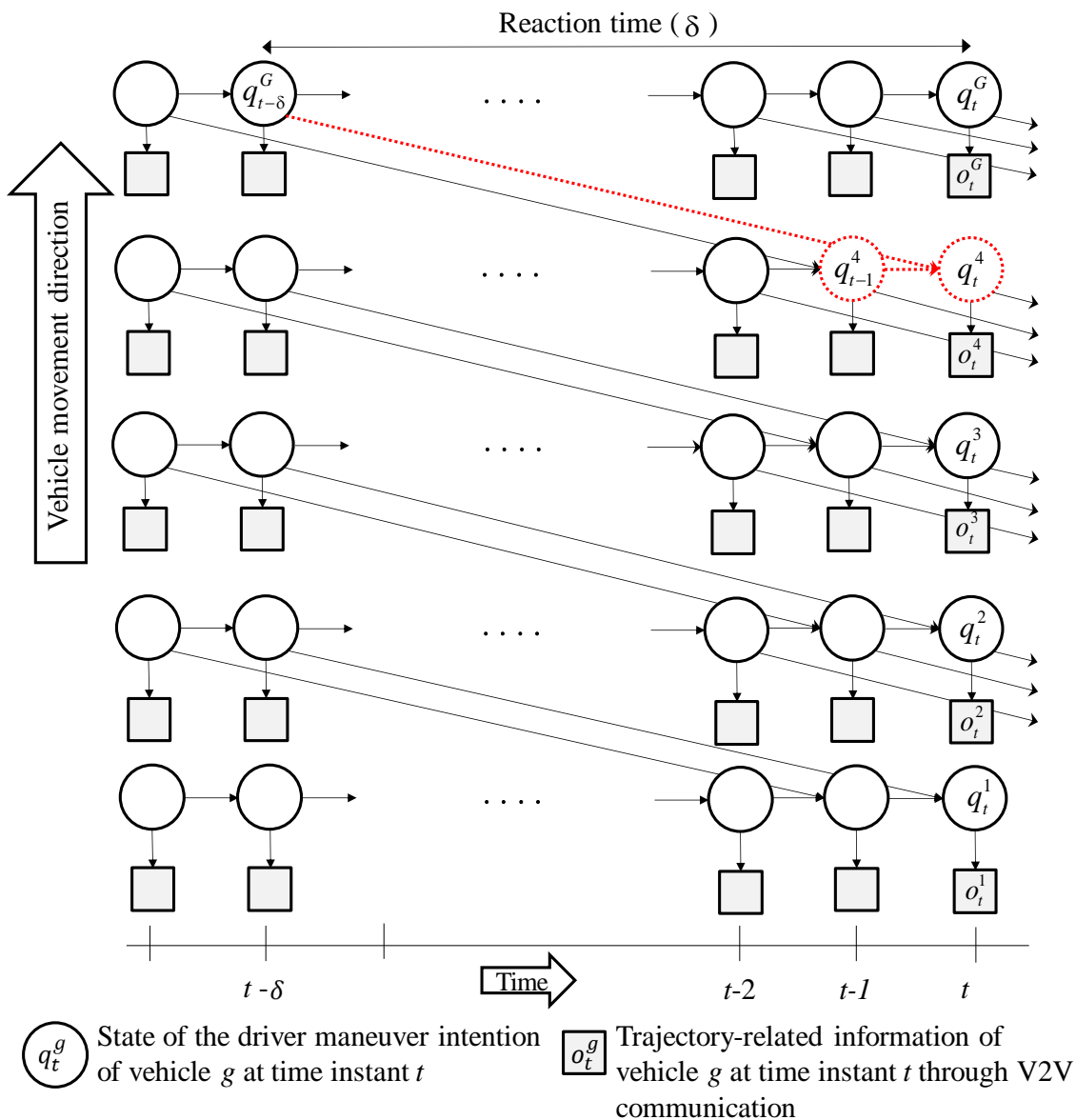


Figure 5-5 Graphical representation of the proposed coupled HMM

### 5.2.3.3 Trajectory estimation using Gipps' car-following model

The predicted maneuver intentions of downstream vehicles are used to predict their trajectories using a microscopic car-following model. We use the Gipps' car-following model (Gipps, 1981) to generate a detailed trajectories of downstream vehicles. After generating downstream vehicle trajectories, we generate the lead-vehicle's trajectory. Gipps' model is developed based on the notion that the following driver tends to keep a safe following distance. It is well-known from the literature that Gipps' model is able to reproduce essential traffic dynamics phenomena observed on freeways. If the coupled HMM produces the high-risk situations of hard braking, very-hard braking, and transitory driving of any downstream vehicle ( $g$ ), a feasible trajectory of vehicle  $g$  is calculated using the kinematic constraints, with a deceleration rate of  $-4\text{m/s}^2$  ( $s_2$ ),  $-7\text{m/s}^2$  ( $s_3$ ) and  $-1\text{m/s}^2$  ( $s_4$ ), respectively. For hard braking and very-hard braking, we assume that vehicle  $g$  will continue its current rate of deceleration until it stops. For transitory driving, we assume that the deceleration rate of  $-1\text{m/s}^2$  continues for 10 seconds. Then, Gipps' model predicts the trajectories of all vehicles downstream of the host vehicle (from vehicle  $g-1$  to the lead vehicle) using the following equation:

$$V_{g-1}(t + \delta) = b_{g-1} \cdot \delta + \sqrt{(b_{g-1} \cdot \delta)^2 - b_{g-1}[2[x_g(t) - s_g - x_{g-1}(t)] - v_{g-1}(t) \cdot \delta - \frac{v_g(t)^2}{\hat{b}_g}]}, \quad (11)$$

where  $b_g$  is the most severe braking rate that the driver of vehicle  $g$  wishes to undertake,  $s_g$  is the effective size of vehicle  $g$ ,  $\delta$  is the reaction time (that is, 1.2 seconds),  $\hat{b}_g$  is the value of  $b_{g-1}$  estimated by the driver of vehicle  $g$  who cannot know this value from direct observation, and  $x_g(t)$  and  $v_g(t)$  are the location and speed of vehicle  $g$  at time  $t$ , respectively. The parameters of Gipps' model in this study are from Gipps (1981).

### 5.2.4 Two-stage criticality assessment

The criticality assessment determines the issuance of warning and the level of warning (Knipling et al., 1993; Van Der Horst and Hogema, 1993). Two groups of approaches have been proposed in the literature based on the risk indicators; the time headway or time-to-collision (TTC), and the projected vehicle trajectory. An advantage of using risk indicators is their simplicity and

consistency with current driving-manual recommendations for safe driving (Taieb-Maimon and Shinar, 2001). Time headway is measured as the elapsed time between the lead vehicle and host vehicle reaching the same location. TTC is defined as the time until a collision between the lead vehicle and host vehicle would occur if their current trajectory and speed are maintained, if the host vehicle is moving faster than the lead vehicle (Minderhoud and Bovy, 2001).

The other approach that this study adopts is based on the projected minimum distance between the lead vehicle and host vehicle using their predicted trajectories (Brunson et al., 2002). As shown in Figure 5-6, the lead-vehicle trajectory is predicted using the proposed MBMAM model. It computes the projected host-vehicle trajectory at each time interval, based on the assumption that the driver of the host vehicle will respond to the warning with a specific reaction time and a specific decelerate rate. Here, we use different braking rates for the host-vehicle deceleration. The assumed host-vehicle braking rate for early warning is  $3.14 \text{ m/s}^2$  and for imminent warning is  $5.39 \text{ m/s}^2$  (Brunson et al., 2002). The reaction time is set as 1.2 seconds. The projected minimum distance is then compared with a predefined critical distance to determine whether a warning should be issued. The critical distance is defined as the physical length of a vehicle plus a margin into which the host vehicle is not willing to intrude.

When the projected minimum distance is less than or equal to the critical distance (5 meters in this study), a warning is issued. As the early warning uses a conservative value (less hard braking) for the assumed braking rate, it will be issued before the imminent warning. The decision to issue a warning is made every 0.1 seconds upon a new observation through V2V communications. A warning may be suppressed when the driver has recently braked or been warned. Once a warning is issued, the same warning level is maintained for a minimum of one second, unless an imminent warning is issued. The FCW system is specified to be active only when the host vehicular speed is greater than 30 km/h. This is because under stop-and-go driving or close-to-jam density, the FCW system is not effective (Brunson et al., 2002).

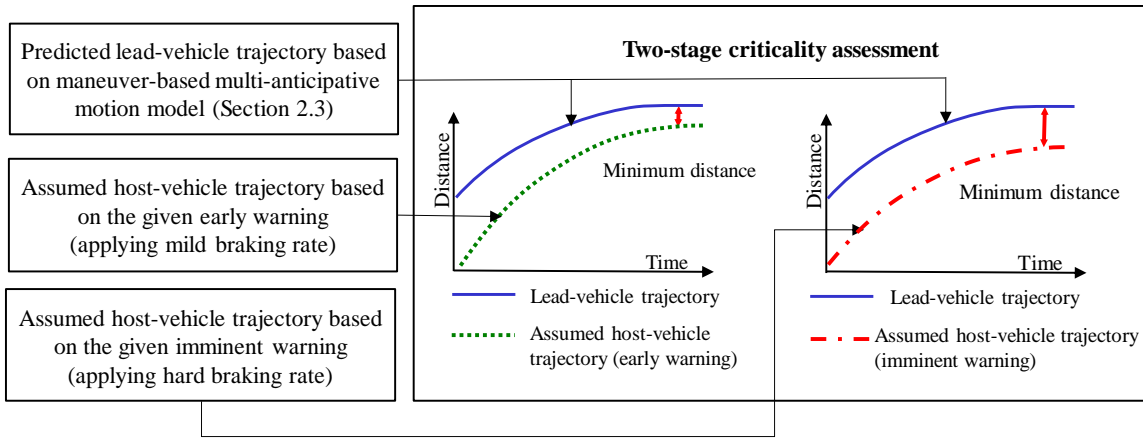


Figure 5-6 Illustration of the two-stage criticality assessment

## 5.3 Experiment design

### 5.3.1 Experiment scenario

The scenario which we consider for the study experiments is a string of vehicles on a highway. A time-series NGSIM (FHWA, 2005) data is used to reproduce the dynamics of vehicle trajectories and the trajectory-related information which the host vehicle will receive from multiple downstream vehicles. We make the following assumptions: (i) the current trajectory-related information is accurate (no measurement errors for on-board kinematic data and no communication failure), (ii) warnings are not issued when the host vehicle speed is below a threshold value (30 km/h in this study), (iii) all vehicles are equipped with GPS and V2V communications, and (iv) the host vehicle predicts the driver maneuver intentions of the five downstream vehicles through a coupled HMM. To analyze the performance of the proposed FCW system, we compare it with two commonly-benchmarked systems: (1) a two-stage FCW system embedded with NHTSA’s physics-based motion model (Brunson et al., 2002), and (2) a single stage FCW system embedded with a physics-based motion model (Knipling et al., 1993). Details of these two FCW systems are provided in Section 5.3.4.

### 5.3.2 NGSIM data

This study uses the NGSIM vehicle trajectory data to evaluate the performance of the FCW systems as well as to estimate the model parameters. The NGSIM data contains real-world vehicle trajectory data that provide opportunities to evaluate the performance of the FCW systems based

on realistic driving behaviors. The NGSIM vehicle trajectory data are from a segment of Interstate-80 in Emeryville, California collected between 4:00pm and 4:15pm, 5:00pm and 5:15pm, and 5:15pm and 5:30pm on April 13, 2005. This data was collected using several synchronized video cameras, mounted on a 30-story building adjacent to the roadway. The corridor is approximately 500 meters long and has an HOV lane and 5 regular lanes. Each dataset stores microscopic information on vehicle trajectories on the road segment. It includes vehicle ID,  $x$  and  $y$  location coordinates, speed, acceleration rate, and space headway at a resolution of 10 frames per second.

The reliability of the experiment is highly affected by the accuracy of empirical vehicle kinematic quantities, such as speed, acceleration, and time headway. Several papers have raised issues related to the accuracy of NGSIM vehicle trajectory data. Punzo et al. (2011) identify different types of errors including misidentification of vehicle, vehicle's lane ID, and lane-changing and merging behaviors. This may be due to errors in extracting vehicle trajectory data from video recordings (Montanino and Punzo, 2015). They suggest using a pre-processing step to filter several errors in order to obtain a consistent dataset. We filter the identified errors using the following two steps.

Step 1 modifies the outliers from acceleration data using the maximum and minimum acceleration rates. Thresholds of  $5 \text{ m/s}^2$  and  $-8 \text{ m/s}^2$  are adopted (Montanino and Punzo, 2015) for the maximum and minimum acceleration rates. Step 2 eliminates noise from the acceleration data. This can be done by smoothing the acceleration profile with moving average filters. The signal is filtered using 7-points moving average filters. The resulting acceleration profiles are shown in Figure 5-7. The speed is also changed as a result of modifying the acceleration data. Figure 5-8 illustrates the speed profiles resulting from the filtering.

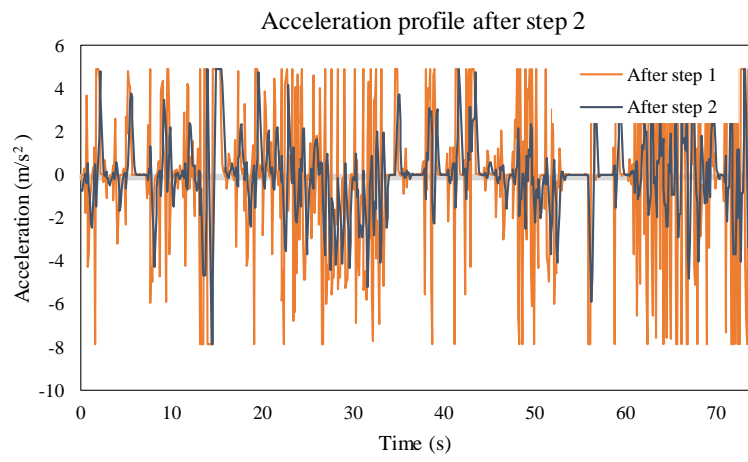
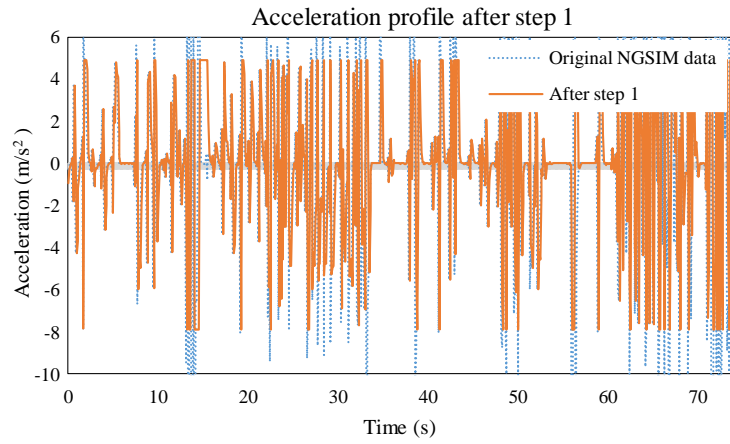


Figure 5-7 NGSIM acceleration data pre-processing

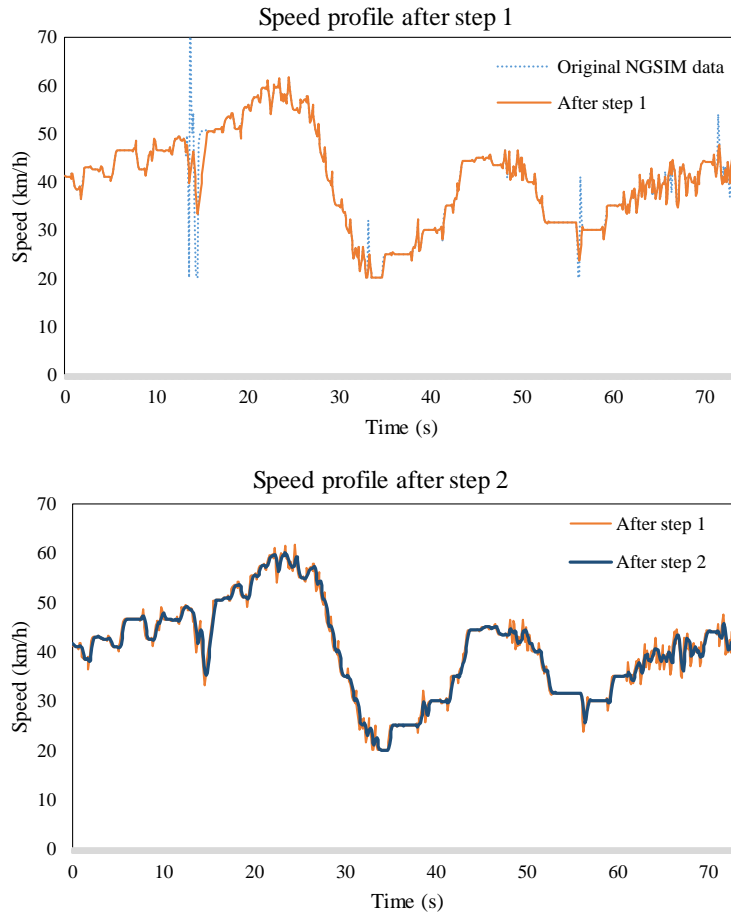


Figure 5-8 NGSIM speed data pre-processing

### 5.3.3 Generation of driver maneuver states using NGSIM data

Based on the NGSIM vehicle trajectory profiles, the sequences of driver maneuver states are estimated using the criteria described in Section 2.3.1. An example of estimated states based on vehicle trajectory data is shown in Figure 5-9. It starts with state 1, and changes to state 2 as the vehicle decelerates at time  $t=12.9$ . At  $t=27.6$ , the vehicle decelerates and the state changes from 1 to 2 and 3. At  $t=33.4$ , the state changes to 4.

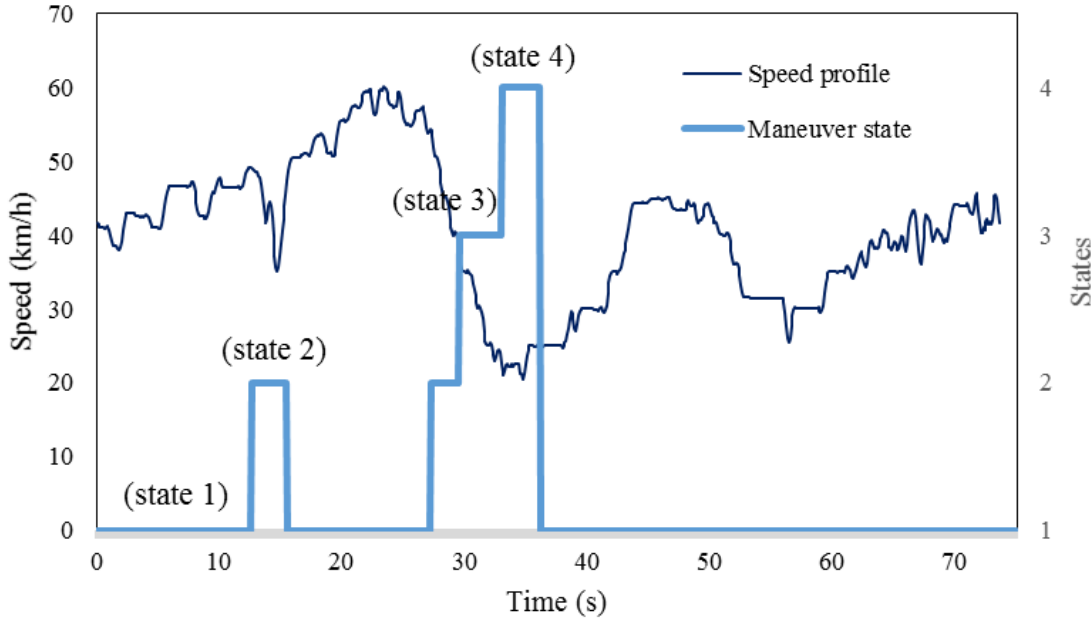


Figure 5-9 Estimation of maneuver states

### 5.3.4 The two benchmark FCW systems

#### 5.3.4.1 A single-stage FCW embedded with Knipling model

Knipling et al. (1993) develop a physics-based motion model that classifies rear-end crash scenarios into: lead-vehicle stationary (LVS) and lead-vehicle moving (LVM). The model uses a warning distance ( $r_w$ ) to determine the issuance of warning. A warning distance is the required minimum distance that allows the host vehicle to react and then decelerate to a stop just behind the stationary lead vehicle. The warning distance for the LVS case is:

$$r_w = t_d \cdot v_H + \frac{v_H^2}{2 \cdot a_H} \quad (12)$$

where  $t_d$ ,  $v_H$ , and  $a_H$  denote reaction time of the driver, host-vehicle speed, and acceleration rate of host vehicle, respectively. For the LVM case, the equation becomes:

$$r_w = t_d \cdot v_H + \frac{v_H^2}{2 \cdot a_H} - \frac{v_L^2}{2 \cdot a_L} \quad (13)$$

where  $v_L$  and  $a_L$  are the speed and acceleration of the lead vehicle, respectively. If the actual headway falls below the computed  $r_w$ , then the warning is issued. The modeling parameters  $t_d$

and  $a_L$  are set as 2.05 seconds and 5.88 m/s<sup>2</sup> (Knipling et al., 1993). This motion model is embedded in a single-stage FCW system.

### 5.3.5 NHTSA physics-based motion model based two-stage FCW system

The NHTSA physics-based motion model by Brunson et al. (2002) is developed based on the predicted minimum distance calculation. There are two cases for the calculation of minimum distance; either the lead vehicle stops prior to the host vehicle or host vehicle stops while the lead vehicle is still in motion. They are used to determine which set of equations should be used. To determine the case that applies, the time for the lead vehicle to stop ( $t_{L,S}$ ) and the time for the host vehicle to stop ( $t_{H,S}$ ) are calculated as follows and compared:

$$t_{L,S} = -v_L/a_L \quad (14)$$

and

$$t_{H,S} = t_R - (v_H + a_H \cdot t_R)/a_{Hmax} \quad (15)$$

where,  $v_L$  and  $v_H$  denote the speed of lead vehicle and host vehicle, respectively.  $a_L$  and  $a_H$  denote the acceleration of lead vehicle and host vehicle, respectively.  $a_{Hmax}$  refers the maximum brake rate of host vehicle, and  $t_R$  denotes reaction time of the host-vehicle driver.

When the lead vehicle comes to a stop first ( $t_{L,S} < t_{H,S}$ ), the minimum distance ( $D_{min}$ ) between the lead vehicle and host vehicle will occur when the host vehicle comes to a stop. This minimum distance can be calculated as follows:

$$D_{min} = r_h + 0.5 \cdot (a_H - a_{Hmax}) \cdot t_R^2 - 0.5 \cdot a_L \cdot t_{L,S}^2 - (a_H - a_{Hmax}) \cdot t_R \cdot t_{H,S} + r_r \cdot t_{H,S} + a_L \cdot t_{H,S} \cdot t_{L,S} - 0.5 \cdot a_{Hmax} \cdot t_{H,S}^2 \quad (16)$$

where,  $r_h$  is headway and  $r_r$  is range rate (the change rate of the headway between the lead vehicle and host vehicle). When the host vehicle comes to a stop first ( $t_{L,S} \geq t_{H,S}$ ),  $D_{miss}$  between the lead vehicle and host vehicle will occur when two vehicles' speed is same ( $t_M$ ). This minimum distance can be calculated as:

$$D_{min} = r_h + r_r \cdot t_M + 0.5 \cdot (a_L - a_{Hmax}) \cdot t_M^2 - (a_H - a_{Hmax}) \cdot t_M \cdot t_R + 0.5 \cdot (a_H - a_{Hmax}) \cdot t_R^2 \quad (17)$$

Warnings are issued when the calculated minimum distance is less than the predefined threshold in two of the last three time intervals. This motion model is embedded in a two-stage FCW system. It uses different brake rates for the two-stage FCW system. The assumed host-vehicle brake rates are  $3.14 \text{ m/s}^2$  for early warning and  $5.39 \text{ m/s}^2$  for imminent warning Brunson et al. (2002), respectively.

## **5.4 Numerical experiments**

This section discusses results of numerical experiments to investigate how the proposed FCW system performs compared to the two benchmarked FCW systems.

### **5.4.1 Performance index**

The performance of the three FCW systems can be evaluated based on missed alarm rates and false alarm rates computed using a confusion matrix. It describes the performance of a classification model. An illustration of the confusion matrix is shown in Table 5-2. The columns correspond to the true driving conditions and the rows correspond to the predicted driving conditions. Ground truth data, such as data on near-crash situations, is needed to create the confusion matrix. A near-crash is defined as a conflict situation requiring a rapid, severe evasive maneuver to avoid a crash (McLaughlin et al., 2009). Hence, in near-crash situations, the FCW system should provide an appropriate warning. However, the development of quantitative near-crash criteria is very limited (Klauer et al., 2006). This study uses all of the following criteria to define near-crash situations for the NGSIM data: (i) TTC is less than 3 seconds, (ii) average acceleration rate of the lead vehicle for 2 seconds is less than  $-3.5 \text{ m/s}^2$ , (iii) speed of the host vehicle is greater than the speed of lead vehicle, and (iv) speed of the host vehicle is greater than 30 km/h.

The A and D values of the confusion matrix in Table 5-2 give the correctly predicted driving conditions, while B and C values show the percentage of mislabeling for each driving condition. Therefore, the sum of A and D values divided by the total number of observation represents the overall accuracy. There are two error types: missed and false alarms. A missed alarm (false negative) is a situation in which the FCW system predicts no near-crash or crash but the traffic

situation is a near-crash situation. A false alarm (false positive) is a situation in which the FCW system has identified a near-crash or crash and gives a warning, but in reality poses no threat or danger to the driver. Excessive false warnings result in slower and less-reliable driver reactions. Missed alarm rates and false alarm rates are calculated based on Table 5-3.

Table 5-2 Confusion matrix

		Ground truth NGSIM data	
		Near-crash or crash	Safe
Prediction of FCW system	Warning	A	C
	No-warning	B	D

Table 5-3 Performance indices

Performance index	Definition
Missed alarm rate (false negative)	$B/(A+B)$
False alarm rate (false positive)	$C/(A+C)$

#### 5.4.2 Performance comparison

Tables 5-4 and 5-5 show the missed alarm rates and false alarm rates for the three FCW systems compared using the NGSIM data. Several observations can be made on the performance of these FCW systems.

Table 5-4 Missed alarm rates

FCW system	Missed alarm rate (%)	
Single-stage FCW system embedded with a physics-based motion model (Knipling model)	19.1	
Two-stage FCW system embedded with NHTSA's physics-based motion model (Brunson model)	Early warning	25.5
	Imminent warning	34.0
Proposed model	Early warning	12.8
	Imminent warning	21.3

Table 5-5 False alarm rates

FCW system		False alarm rate (%)
Single-stage FCW system embedded with a physics-based motion model (Knipling model)		24.0
Two-stage FCW system embedded with NHTSA's physics-based motion model (Brunson model)	Early warning	14.6
	Imminent warning	6.0
Proposed model	Early warning	4.7
	Imminent warning	2.6

While the Knipling model has a 19.1% missed alarm rate, it also has the highest false-alarm rate (24.0%). That is, it provides frequent warnings for situations that pose no threat to the driver. The NHTSA model provides fewer false alarm rates than the Knipling model, but its missed alarm rates are higher than those for other models. The proposed model provides 4.7 and 2.6 percent false alarm rates for early warning and imminent warning, respectively. It performs significantly better than the NHTSA model for both the missed alarm (37% to 50% better) and false alarm rates (57% to 68% better).

In general, early warnings using the NHTSA model and the proposed model have lower missed alarm rates than those of imminent warnings. However, they provide a higher rate of false alarms. To reduce the rate of missed alarms while maintaining an acceptable level of FCW false alarm rate, one method is to adjust the critical distance or host-vehicle braking rate in Section 5.2.4. This will aid in balancing missed alarm rate and false alarm rate. Second, the driver state information could be useful. If drivers are attentive to the driving task, it is likely that suppressing warnings when the driver is attentive can be effective in reducing false alarms.

### 5.4.3 Timing of warnings

The capability to provide earlier warnings is an important factor as earlier warnings allow sufficient time for the driver to react. Here, the time at which the downstream vehicle begins to brake at less than  $-5 \text{ m/s}^2$  is used as a primary reference and is defined as  $t = 0$ . The timings of the warnings are shown in Table 5-6 for the various FCW systems. The results show that the Knipling

(6.4 seconds) and NHTSA (5.6 and 6.8 seconds) models' warning timings occur later than those using the proposed model as they can provide warnings only after the lead vehicle starts to decelerate. By contrast, through V2V communications, imminent warning using the proposed model can be provided 2 seconds earlier than imminent warnings under the NHTSA and Knipling models. This provides sufficient time to react to a possible collision situation. These results indicate that the proposed model performs significantly better than the other two models in terms of providing an earlier warning.

Table 5-6 Timing of warnings

FCW system		Timing of warning from $t = 0$ (seconds)
Single-stage FCW system embedded with a physics-based motion model (Knipling model)		6.4
Two-stage FCW system embedded with NHTSA's physics-based motion model (Brunson model)	Early warning	5.6
	Imminent warning	6.8
Proposed model	Early warning	3.7
	Imminent warning	4.7

## 5.5 Concluding comments

This study proposes a two-stage MBMAM model to provide an effective early warning in the first stage while reducing the false alarm rate. The proposed FCW system leverages V2V communications to incorporate trajectory-related information from multiple downstream vehicles to enhance prediction accuracy. It provides a capability to alert the driver in an early stage. A coupled HMM is used to predict the lead-vehicle driver's unobservable maneuver intention, by taking into account the interactions of downstream vehicles with the lead vehicle. Thereby, the host-vehicle driver will have greater clarity on unfolding situations that require the driver to act to avoid a collision. Hence, by leveraging V2V connectivity, the proposed FCW system overcomes the limitations of existing physics-based motion models that assume that the lead vehicle will continue its current rate of deceleration, and of single process maneuver-based models that use

only the lead-vehicle information. Numerical results illustrate the effectiveness of proposed FCW system to provide early warnings while reducing false alarm rates. In addition to the enhanced anticipation for human-driven vehicles, this model can predict the evolution of ambient traffic conditions for partially and fully autonomous vehicles with V2V communication capabilities.

The study offers the possibility of developing even more sophisticated FCW systems. First, while we use a fixed deceleration rate and reaction time for the host-vehicle's trajectory prediction, they vary across different driver groups. Hence, it may be meaningful to develop a FCW system that integrates a learning mechanism for the host-vehicle's driving behavior, so that the system can adjust its settings by interacting with the host-vehicle's driver. Second, during a transition period with mixed traffic flows, V2V-equipped vehicles will interact with unequipped vehicles, which can be addressed by extending the proposed FCW system. Third, in addition to the heterogeneity in reaction times to predict the maneuver intention of the lead vehicle, there is the possibility of V2V communications failure in receiving downstream vehicle information. In this context, the proposed model can be extended by incorporating a stochastic modeling capability to enable more realism.

## **6. MODELING OF THE DYNAMIC FLOW PROPAGATION OF MULTIPLE UNITS OF INFORMATION UNDER V2V COMMUNICATIONS BASED ADVANCED TRAVELLER INFORMATION SYSTEMS**

### **6.1 Introduction**

Vehicle-to-vehicle (V2V) communications can facilitate a broad range of applications, including road safety (Sepulcre et al. 2013), cooperative driving (Ammoun and Nashashibi 2010), and advanced traveler information system (ATIS) applications. In the ATIS context, V2V communications can provide a capability for vehicles to exchange time-dependent information on the network traffic conditions. Thereby, suitably-equipped vehicles can generate data on their time-dependent locations, and consequently their experienced travel times on the links traversed on their routes. We refer to the time-dependent link travel time experienced by a vehicle as “a unit of information”. As vehicles generate their own link travel experience data over time and space, a V2V-based ATIS entails the propagation of multiple units of information. The vehicles carry such information and exchange it with other vehicles through V2V communications without any central coordination. Consequently, the traffic dynamics and inter-vehicle communication constraints lead the dynamic flow propagation of multiple units of information.

The dynamic flow propagation of multiple units of information leads to each vehicle having time-dependent knowledge on the traffic network conditions, labeled the “vehicle knowledge,” based on its own experienced link travel time data and similar data received from the other equipped vehicles. The current traffic state estimation of each equipped vehicle based on its time-dependent knowledge represents an input for the associated driver to determine his/her route choice. As the route choice decisions of all drivers lead to the traffic flow network evolution, the information flow evolution and propagation influences the dynamics of the network traffic flow. More broadly, an understanding of how the information evolves and propagates is critical to develop system-level strategies for information flow routing and vehicular route guidance.

The dynamic flow propagation of multiple units of information generates two challenges for the modeling of the V2V-based ATIS. First, the propagation of each unit of information depends on the vehicular traffic flow dynamics and the inter-vehicle communication constraints introduced

by the V2V communications technology and the ambient traffic flow characteristics. To address the complexity associated with modeling the propagation of multiple units of information under traffic flow dynamics and inter-vehicle communication constraints, simulation-based approaches (Schmidt-Eisenlohr et al. 2007; Schroth et al. 2005) have been proposed. Although these approaches can model the propagation of information flow, they lack insights to understand the characteristics of the information flow propagation and their interactions with the traffic flow and the inter-vehicle communication. To the best of our knowledge, there is no approach to address the propagation of multiple units of information flow.

Second, as multiple units of information in the network are dynamically exchanged across vehicles, it is necessary to track the propagation of multiple units of information flow in a computationally efficient manner. That is, we need to map what information is generated and when/where the information propagates. Kim and Peeta (2016) model a V2V-based ATIS as consisting of three interacting layers: physical traffic flow, inter-vehicle communication and information flow. They propose a graph-based multi-layer framework that enables the computationally efficient tracking of information propagation using a simple graph-based search algorithm and the computationally efficient storage of information through a single graph database.

The focus of that framework is to develop a computationally efficient graph mechanism to track and store the dynamic vehicle knowledge, and provide an explicit retrospective modeling capability to track how information flow evolves and propagates. However, it incorporates a simulation-based traffic flow model and a set of inter-vehicle communication constraints to determine the information flow propagation. That is, the simulation model is used to replicate the traffic flow dynamics as well as determine when and where inter-vehicle communication would occur subject to the inter-vehicle communication constraints. Similarly, past studies (Wu et al., 2005; Fitzgibbons et al., 2004; Schroth et al., 2005) use simulation-based approaches to analyze the feasibility and reliability of V2V-based traffic system for practical applications. They incorporate a traffic flow simulator (such as Paramics and CORSIM) and a wireless (inter-vehicle communication) network simulator (such as NS-2 and NS-3, or a simple analytical model) to derive some descriptive insights on the interactions between the traffic flow movement and the inter-vehicle communication. However, the key limitation of simulation-based approaches is the lack of theoretical insights. The use of such a simulation-based approach limits the understanding

of the dynamics of the information flow characteristics, such as the information forward/backward propagation wave speeds, spatial information propagation front, spatio-temporal density of informed vehicles and the spatio-temporal characteristics of vehicle knowledge.

This study proposes a multi-layer framework to address the propagation of multiple units of information flow by capturing the dynamics of the three interacting layers so as to generate the aforementioned insights. The physical traffic flow layer is represented using an analytical model (the Cell Transmission Model (CTM)) and the inter-vehicle communication layer is represented using the communication range and an aggregate function that links the inter-vehicle communication success rate and the density of the V2V-equipped vehicles. As graph structure is shown to be able to track the spatiotemporal characteristics of information flow explicitly in a computationally efficient manner (Kim and Peeta 2016), we adapt the graph-based representation of information flow propagation in the proposed multi-layer framework. The term “information flow” denotes the flow of raw traffic data (such as the time-dependent experienced link travel time) between vehicles, and not processed data through mechanisms such as data fusion. Hence, this study does not intend to determine how the information flow layer, through the information content, would affect the traffic flow layer. Rather, as stated earlier, it seeks to determine how the dynamics of multiple units of information flow (in terms of the information forward/backward propagation waves, spatial propagation fronts, spatiotemporal vehicular knowledge characteristics, etc.) can be mapped from the traffic flow dynamics (in terms of the traffic forward/backward propagating waves, etc.) and the inter-vehicle communication constraints. Therefore, adding CTM-based traffic dynamics in the physical traffic flow layer, and integrating it with the graph-based multi-layer framework (Kim and Peeta, 2016), does not add much computational burden in this study context.

While widely-used analytical models exist to characterize traffic flow dynamics in a network context, and inter-vehicle communications constraints associated with range, interference and bandwidth have been well-studied in the communications domain, existing analytical models to characterize the evolution and propagation of information under V2V communications have key limitations, especially for the V2V-based ATIS, and even more so when multiple units of information are considered.

First, analytical approaches (Wang 2007; Wu et al. 2004) to integrate the traffic flow and the inter-vehicle communication have limitations to characterize the underlying dynamics within a layer or the interactions among layers. From the traffic flow layer perspective, they do not describe several key phenomena of real-world traffic flow such as kinematic waves, and queue formation and dissipation. Instead, they focus on the instantaneous spatial propagation of information and do not consider the time dimension. To do so, they rely on the independent vehicle mobility assumption whereby the locations of vehicles are pre-determined based on statistical distributions of the spatial headway. Thereby, they lack realism in terms of modeling traffic flow dynamics. From the perspective of the interactions among layers, the V2V communication constraints are not well-captured in the inter-vehicle communication layer. The information propagation mechanism in these studies often assumes that the V2V communications can occur successfully up to a predefined distance representing the communication range, and none beyond it. Thereby, the interference and bandwidth are ignored in the modeling.

Second, most existing analytical approaches (Ukkusuri and Du 2008; Wang 2007) assume that information propagates instantaneously across multiple vehicles through a multi-hop process based on the perspective that the speeds at which vehicles move are negligible compared to the speed at which information propagates via inter-vehicle communication. A multiple hop implies a unit of information can propagate through an instantaneous relay process to all vehicles which are serially connected to the vehicle disseminating the information by being within communication range of any vehicle within this series. However, the instantaneous multi-hop assumption does not factor interference effects and the size of information, which are significant characteristics of the V2V-based ATIS where multiple vehicles frequently exchange or disseminate information. Further, due to the assumption of instantaneous information propagation, the traffic flow dynamics and its interactions with the inter-vehicle communication constraints are ignored. That is, the transfer of a unit of information from one vehicle to another that is not in its vicinity can entail some time, which requires the consideration of the traffic flow dynamics as vehicles move continuously. This aspect is significantly exacerbated when multiple units of information flow are exchanged. A consequence of this aspect is that information needs to be tracked in terms of when and where a vehicle receives the information to determine the spatiotemporal propagation of

information. So, while the assumption of instantaneous information propagation can be analytically convenient, it has limitations to model the V2V-based ATIS.

Third, most of the aforementioned analytical approaches analyze the propagation of a single unit of information. An example is the propagation of upstream collision warning information to allow other drivers approaching the affected location to be aware of the impending situation. By contrast, a V2V-based ATIS entails the propagation of multiple units of information. Extending a single unit of information propagation model to capture the propagation of multiple units of information in space and time is neither simple nor straightforward, in terms of determining how the information flow dynamics can be mapped from the traffic flow dynamics and the inter-vehicle communication constraints.

This paper seeks to bridge the aforementioned gaps in the literature in the V2V-based ATIS context by proposing a multi-layer framework to model the flow of multiple units of information as a complex system comprised of three interacting layers. Shown in Figure 6-1, these layers include the traffic flow, the inter-vehicle communication, and the information flow layers.

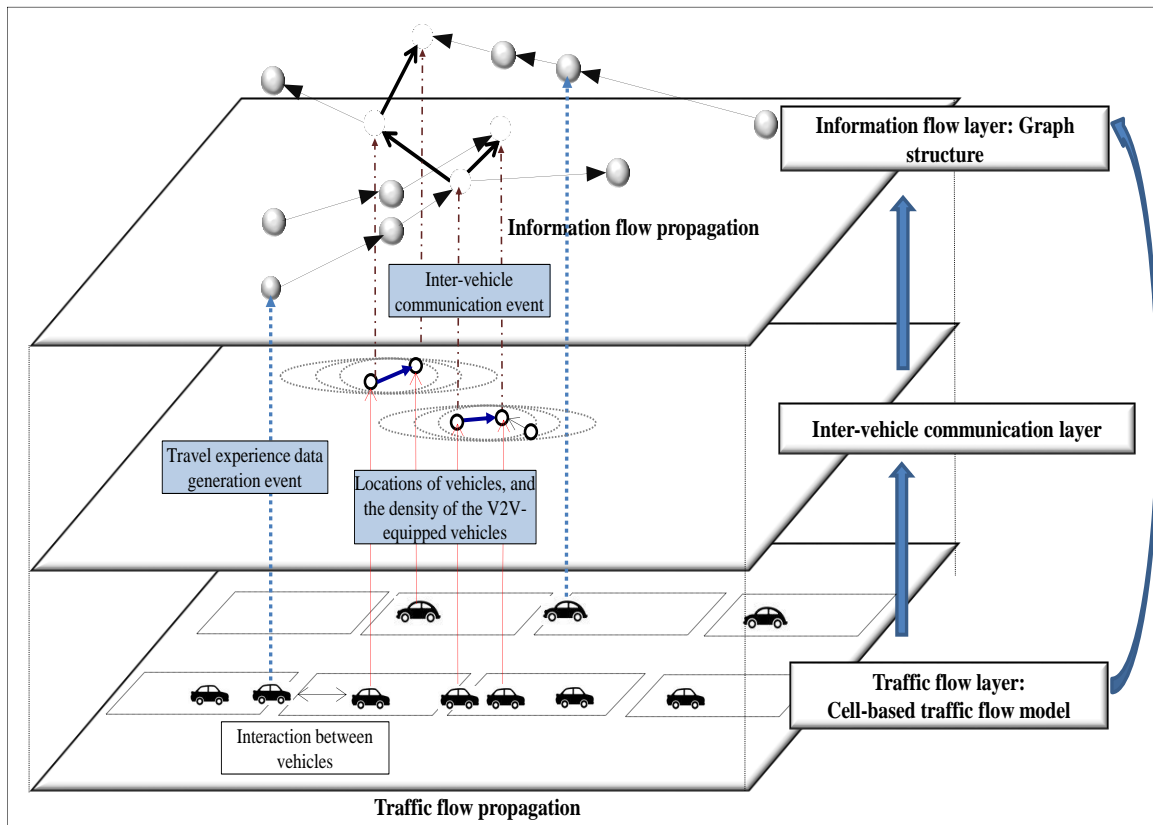


Figure 6-1 Conceptual overview of the multi-layer framework

The traffic flow dynamics are captured by a cell-transmission model (CTM) in the physical traffic flow layer. The inter-vehicle communication layer uses the time-dependent locations of vehicles and a traffic flow variable (the density of the V2V-equipped vehicles) in the traffic flow layer and inter-vehicle communication related constraints/function to determine the occurrence of inter-vehicle communications. The information flow layer depicts the flow of multiple units of information as a network whose nodes correspond to events of travel experience data generation and inter-vehicle communication, and links indicate the direction of information flow.

The contributions of this study are: (i) developing a model for the propagation of multiple units of information in space and time, (ii) mapping the information flow dynamics from the traffic flow dynamics and the inter-vehicle communication constraints, (iii) illustrating the information forward/backward propagation waves, the spatial information propagation front, and spatio-temporal density of informed vehicles, and (iv) modeling the spatio-temporal characteristics of vehicle knowledge as a building block for providing a descriptive capability and developing system-level strategies under V2V-based ATIS.

The remainder of the paper is organized as follows. Section 6-2 discusses proposed models to integrate the traffic flow and inter-vehicle communication layers. Section 6-3 describes the information flow layer using a graph-based information flow network to map the information flow dynamics based on the interactions involving the other two layers. Section 6-4 discusses the characteristics of the information flow dynamics. Section 6-5 discusses synthetic experiments and analyzes the capabilities of the proposed approach. Section 6 provides some concluding comments.

## **6.2 The physical traffic flow and inter-vehicle communication layers**

### **6.2.1 Physical traffic flow layer**

The physical traffic flow layer captures the spatiotemporal interactions between vehicles through a cell-transmission model (Daganzo 1994). It is a discrete approximation to the LWR model (Lighthill and Whitham 1955; Richards 1956) through the use of a trapezoidal flow-density relationship. The CTM captures several key congestion phenomena in an explicit manner, making it a suitable platform for modeling the traffic flow dynamics. In the proposed framework, the following traffic flow characteristics are identified from this layer: (i) dynamic traffic vehicular

movement, and the impacts of congested traffic such as the backward propagating traffic wave, and (ii) “travel experience data,” which represents the actual travel experiences of vehicles along their route trajectories.

Under V2V-based ATIS, a traffic flow layer consists of a physical traffic network  $G^T = (N, A)$  and vehicles ( $x, y \in x$ ) have an ability to communicate with each other. A set  $N$  of nodes corresponds to physical intersections or designated points, and a set  $A$  of directed links corresponds to road links. The link is further divided using the set of cells  $H$  with the cell length equal to the distance traveled at free flow speed in one time interval  $\Delta t$ , and the set of cell connectors  $E$ . The maximum number of vehicles that can be present in a cell  $a$  at time  $t \in T$  is  $N_a(t)$ , and the maximum flow from cell  $a-1$  to cell  $a$  is  $Q_a(t)$  for time interval  $(t, t+1)$ . The free-flow speed and traffic backward wave propagation speed are denoted as  $v$  and  $r$ , respectively. Further, denote  $n_a(t)$  as the number of vehicles in cell  $a \in H$  at time  $t \in T$ , and  $y_a(t)$  as the number of vehicles that are routed by cell connector  $(a-1, a) \in E$  for time interval  $(t, t+1)$ . The CTM is based on two main constraints on flow conservation and flow restriction:

$$n_a(t) = n_a(t-1) + y_{a-1}(t-1) - y_a(t-1), \quad \forall a-1, a \in H, t \in T, \quad (1)$$

$$y_a(t) = \min \{N_a(t), Q_a(t), \delta(N_a(t) - n_a(t))\}, \quad \forall a \in H, t \in T, \quad (2)$$

where the ratio  $\delta$  is determined by  $r/v$ . Equation (1) represents the flow conservation that indicates the cell occupancy at time  $t$  is equal to its occupancy at time  $t-1$  plus inflow and minus the outflow. Equation (2) represents the flow propagation that is restricted by the three traffic conditions of the underlying trapezoidal flow density relationship: (i) free flow, (ii) saturated flow, and (iii) congested flow.

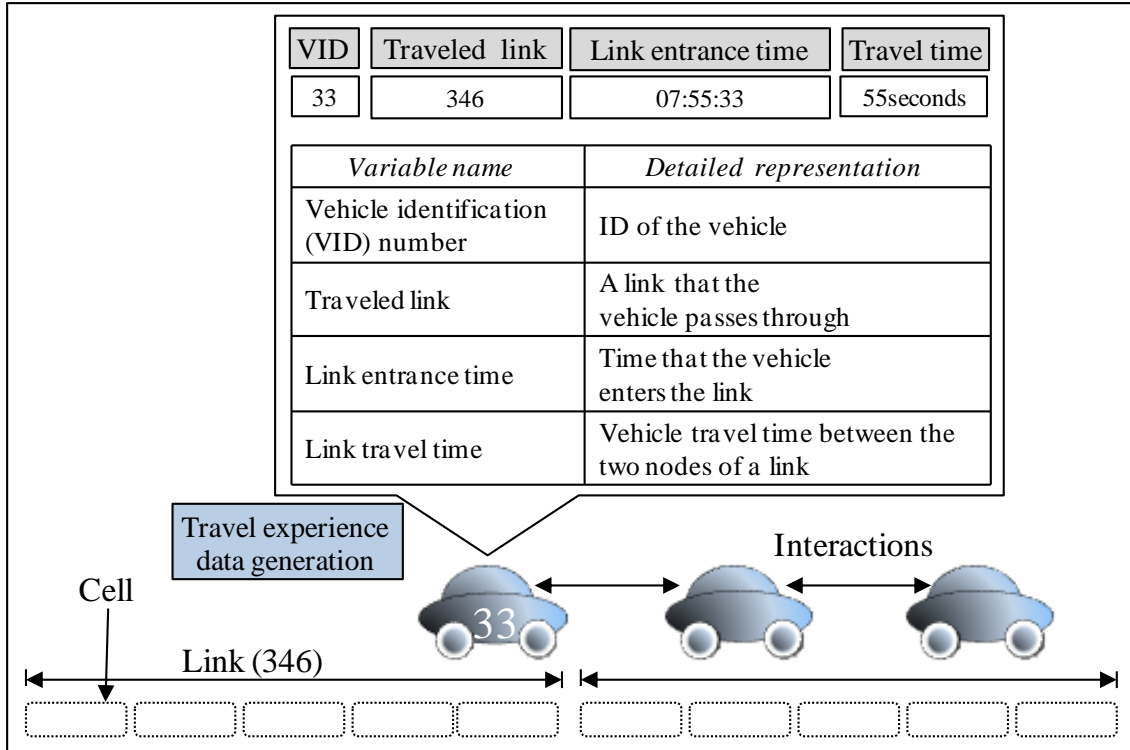


Figure 6-2 The travel experience data generation, and interactions among the vehicles

While the conventional CTM can track the traffic flow variables (density, flow, and speed), it cannot track the individual vehicles' locations. The proposed CTM is extended to track the individual vehicle's trajectory and the associated multiple units of travel experience data generation. The following steps are implemented similar to Cheu et al. (2009). First, the vehicle identification number is generated as a sequential number based on the order a vehicle enters the network. The vehicle arrival headways are assumed to be uniform within the time interval. For each time step, the CTM moves some vehicles from cell  $a$  to the downstream cell  $a+1$ , and the first and last entering vehicle IDs to cell  $a+1$  are updated and stored. In this manner, we assume that no overtaking is allowed within a cell and the First-In-First-Out (FIFO) property is preserved.

Similar to past analytical studies that only consider a single straight road topology for a V2V-based system, our approach also focuses on single road topologies. However, in our case, this is because we newly seek to incorporate traffic flow dynamics analytically to obtain a basic understanding of its impact on the propagation of multiple information units. We do so using an ordinary cell in CTM. Hence, the study experiments in Section 5 are conducted for a bi-directional

single highway. In future work, we aim to extend this to include different types of road geometry (e.g. merging and diverging nodes, and intersections).

As presented in Figure 6-2, the generated travel experience data contains its vehicle identification (VID) number, the identification number of the link traversed, the link entrance time, and the link travel time. As shown in Figure 6-1, the time-dependent locations of vehicles and the associated generation of the multiple units of information flow are used to construct the information flow layer. The time-dependent locations of vehicles and the density of the V2V-equipped vehicles are inputs for the determination of the success rate of inter-vehicle communication under the inter-vehicle communication constraints, as discussed next.

### **6.2.2 Inter-vehicle communication layer**

The occurrence of the inter-vehicle communication is subject to inter-vehicle communication related technical constraints such as communication range, interference and bandwidth. As discussed earlier, most existing analytical approaches only use a predefined communication range. Hence, they do not factor the interactions between the traffic flow dynamics (in terms of the density of the V2V-equipped vehicles) and the success rate of inter-vehicle communication. In this study, the time-dependent locations of vehicles and the density of the V2V-equipped vehicles in the traffic flow layer are used as key determinants of the inter-vehicle communication characteristics.

An issue that may arise in the integration of the physical traffic flow and the inter-vehicle communication layers is the different time scales to reflect the events in the two layers. Typically, inter-vehicle communication events can occur much more frequently compared to traffic-related events (such as travel experience data generation). In the study experiments, the traffic flow is updated in the CTM every 6 seconds for computational efficiency. Also, the frequency of inter-vehicle communication is assumed to be 2 Hz (Karagiannis et al., 2011) for data transfer due to the limited bandwidth. Then, the impacts of the dynamic changes in the vehicle positions cannot be captured within the traffic flow update interval. To reconcile this issue, we use the cumulative success rate of inter-vehicle communication  $Z$  which is defined as the probability that a vehicle communicates with another vehicle within communication range during the traffic flow update interval (6 seconds). The cumulative success rate of inter-vehicle communication is estimated

through the simulation of scenarios (Kim et al., 2014). The aim of the simulation is to derive an aggregate function for the cumulative success rate of inter-vehicle communication for different densities of V2V-equipped vehicles within communication range. To do so, a traffic flow simulator, DYNASMART (Mahmassani et al., 1998), is used to generate the movements of all vehicles under various scenarios with different demand levels and market penetration rates (of vehicles equipped for V2V communications), and track the trajectories of all equipped vehicles.

A pair of equipped vehicles within communication range (200 meters) can potentially communicate with each other at any time through V2V communications. However, multiple communications from vehicles within the communication range can cause interference and result in the failure of this inter-vehicle communication. The interference level can be measured by comparing the signal power of the specific inter-vehicle communication of interest with the signal powers of the other inter-vehicle communications within this communication range, as follows (Gupta and Kumar 2000):

$$\frac{\frac{T_x}{|\theta_x - \theta_y|^2}}{N + \sum_{\substack{k \in X \\ k \neq x}} \frac{T_k}{|\theta_k - \theta_y|^2}} \geq \beta \quad (3)$$

Let  $\theta_k$  denote the GPS location coordinate of an equipped vehicle  $k$  within communication range,  $k \in X$ , as illustrated in Figure 6-3. Suppose a subset of vehicles within the communication range simultaneously transmit information at some time instant, leading to possible interference. The signal power decays with distance from a broadcasting vehicle  $k$  as  $1/|\theta_k - \theta_y|^2$ . The transmitted information through the inter-vehicle communication of interest from a vehicle  $x$  is successfully received by a vehicle  $y$  if it satisfies the minimum signal-to-interference ratio of  $\beta$  (the study experiments use  $\beta = 2$  based on Gupta and Kumar, 2000). It is assumed that the power levels of vehicles ( $T_x$  and  $T_k$ ) are identical and the ambient noise power level ( $N$ ) is zero. Based on the interference level implied by equation (3), a simulation is conducted to check whether information is successfully transmitted between vehicles  $x$  and  $y$  every 0.5 seconds during a 6-second time interval. From the perspective of the cumulative success rate of inter-vehicle communication, information is successfully transmitted between vehicles  $x$  and  $y$

if it satisfies the minimum signal-to-interference ratio at least once during this 6-second time interval.

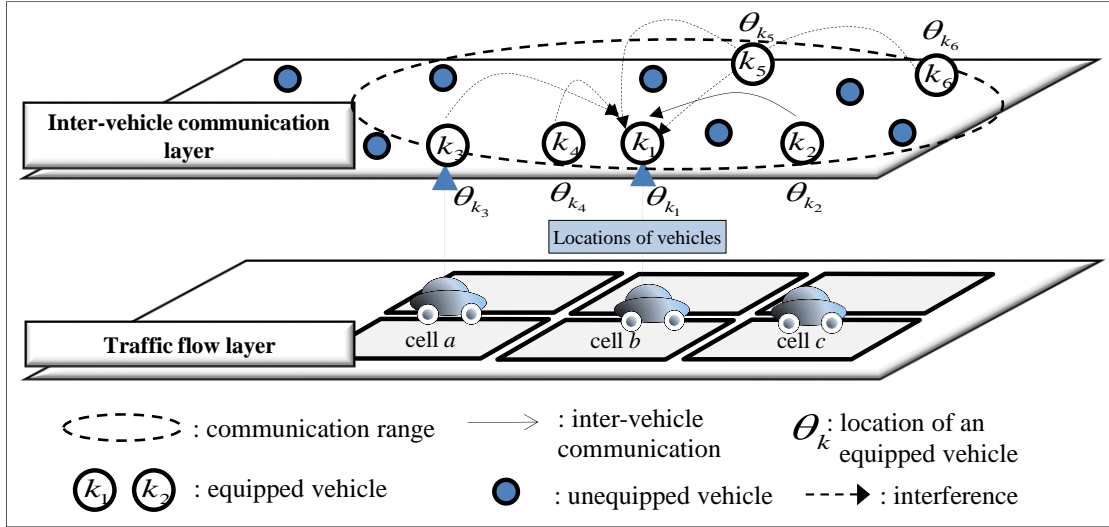


Figure 6-3 Interference among vehicles

Given a specific density,  $q$ , of equipped vehicles within the V2V communication range, 1,000 simulation runs are performed using different demand levels and market penetration rates that are randomly chosen from specific ranges. In the study experiments, we use demand levels between 1 veh./lane/mile to 160 veh./lane/mile in discrete units of 1 veh./lane/mile, and market penetration rates between 0.05 to 0.5 in discrete units of 0.05. Then,  $Z(q)$  is obtained based on the simulation results as:

$$Z(q) = s_q / 1000 \quad (4)$$

where  $s_q$  is the number of simulation runs in which information is successfully received under the scenario ( $q$ ). The estimation results provide an aggregate function, which is the cumulative success rate of inter-vehicle communication ( $Z$ ) for different densities is a negative exponential function of the density of equipped vehicles within V2V communication range as follows:

$$Z(q) = 0.9411 \cdot e^{-0.066 \cdot q} \quad (5)$$

Figure 6-4 shows that the cumulative success rate of inter-vehicle communication  $Z(q)$  decreases with the density of V2V-equipped vehicles. As the density of equipped vehicles varies across cells with time,  $z$  also varies. Therefore, the function  $z$  represents how the dynamics of

traffic flow (the density of the V2V-equipped vehicles) affect the success rate of inter-vehicle communication. The occurrence of events in the inter-vehicle communication layer represents one of the components used to construct the information flow layer, as discussed next.

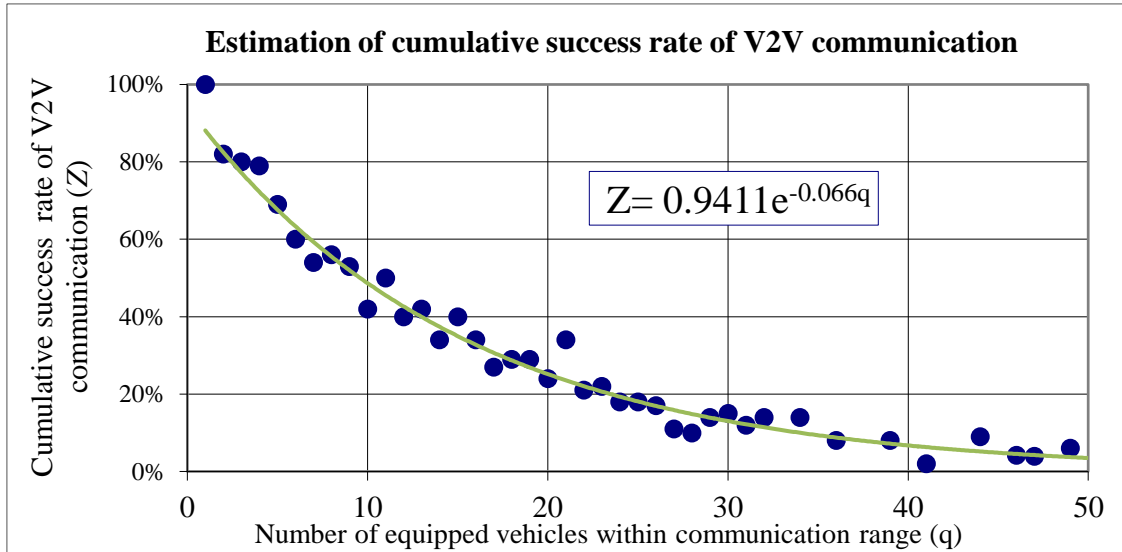


Figure 6-4 Estimation of cumulative success rate of V2V communication ( $Z(q)$ )

### 6.3 Information flow layer

As illustrated by Figure 6-1, based on the known events in the other two layers (the travel experience data generation and the occurrence of inter-vehicle communication, discussed in Section 6-2), the flow of multiple units of information is mapped using a graph-based representation (Kim and Peeta, 2016) of the information flow network.

#### 6.3.1 Information flow network construction

Table 1 shows the notation of variables for the graph-based representation of the information flow network, which is a dynamically evolving graph in which the nodes and links appear and disappear based on the time-dependent events in the traffic flow and inter-vehicle communication layers. Hence, driven by the events in the other two layers, the information flow network evolves over time in that new nodes are generated, some nodes gain new links, and some nodes and links are deleted. The information flow network  $G^1 = (N^1, C^1, A^1, M^1)$  consists of two types of nodes: (i) a “travel experience data (TED)” node  $\in N^1$ , and (ii) a pair of “virtual inter-vehicle communication

(VIC)” nodes  $\in C^I$  (one for broadcast and the other for receiving). Hence, nodes correspond to events of travel experience data generation and inter-vehicle communication.

Table 6-1 Notation to represent variables in the information flow layer

Information flow layer $G^I = (N^I, C^I, A^I, M^I)$	
$N^I$	the set of travel experience data (TED) nodes
$C^I$	the set of virtual inter-vehicle communication (VIC) nodes
$P^I$	the set of nodes in the information flow network, $P^I = \{N^I, C^I\}$ , $N^I \cap C^I = \emptyset$
$A^I$	the set of information flow propagation trajectory links (T-link) indicating the vehicle trajectory direction based on the traffic flow
$M^I$	the set of inter-vehicle communication based information flow propagation links (I-link) denoting the direction of information flow based on the inter-vehicle communication
$i_x^t$	travel experience data (TED) node indicating a travel experience data generated by vehicle $x$ at node $i$ at time $t$ , $\forall x \in X, \forall i \in N, i_x^t \in N^I$
$\lambda_x^t$	virtual inter-vehicle communication (VIC) node denoting that vehicle $x$ broadcasts travel experience data at time $t$ , $\lambda_x^t \in C^I$
$\bar{\lambda}_y^t$	virtual inter-vehicle communication (VIC) node denoting that vehicle $y$ receives travel experience data at time $t$ , $\bar{\lambda}_y^t \in C^I$
$p_x^t, q_x^t$	nodes in the information flow network associated with vehicle $x$ at time $t$ ; $p_x^t, q_x^t \in P^I$
$(p_x^{t_1}, q_x^{t_2})$	information flow propagation trajectory link associated with the trajectory direction of vehicle $x$ from time $t_1$ to time $t_2$ , $p_x^{t_1}, q_x^{t_2} \in P^I, \forall x \in X, t_1 < t_2$
$(\lambda_x^{t_1}, \bar{\lambda}_y^{t_2})$	inter-vehicle communication based information flow propagation link representing the direction of information flow (from vehicle $x$ to vehicle $y$ ), $(\lambda_x^{t_1}, \bar{\lambda}_y^{t_2}) \in C^I, x \neq y, t_1 = t_2$

The dynamics of information flow evolution and propagation are represented through two type of links: (i) the directed information flow propagation trajectory links (T-link)  $\in A^I$  representing the TED-TED, TED-VIC, VIC-TED or VIC-VIC node connections based on the trajectories of the vehicles, and (ii) the inter-vehicle communication based information flow propagation links (I-link)  $\in M^I$  connecting each pair of nodes (VIC-VIC) corresponding to inter-vehicle communication events. In terms of the VIC-VIC connections, the I-link connects a pair of VIC nodes between two vehicles to indicate inter-vehicle communication, while a T-link connects a pair of VIC nodes of the same vehicle based on the spatiotemporal trajectory of that vehicle. The details of the aforementioned graph-based representation of the information flow network are discussed in Sections 6.3.2 and 6.3.3.

### 6.3.2 Information flow generation/deletion

The event that a V2V communications equipped vehicle reaches a physical intersection in the traffic layer entails the generation of travel experience data for the link traversed. A TED node, denoted as  $i_x^t \in N^I$ , represents the travel experience data generated by vehicle  $x \in X$  at node  $i$  at time  $t$ .

Figure 6-5 shows that a vehicle  $x \in X$  reaches nodes  $i$  and  $j$  at times  $t_1$  and  $t_2$ , respectively. TED nodes  $i_x^{t_1}$  and  $j_x^{t_2}$  in  $G^I$  are generated at the corresponding intersections sharing the same topology as the physical nodes  $i, j \in N$ , but at times  $t_1$  and  $t_2$ , respectively.

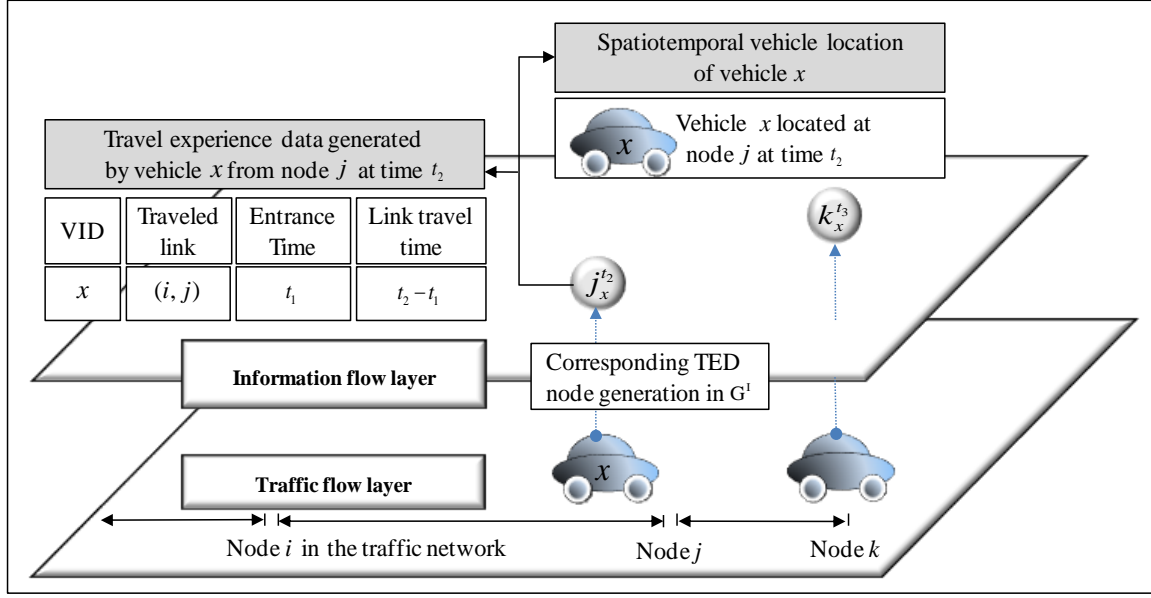


Figure 6-5 TED nodes in  $G^1$  corresponding to events of travel experience data generation

The definition of the TED node illustrates that it can also aid in characterizing the spatiotemporal location of vehicles. This is because the travel experience data generation for a vehicle follows its trajectory in the traffic flow layer. Thus,  $i_x^{t_1}$  represents the spatiotemporal vehicle trajectory for vehicle  $x \in X$ ; that it is located at node  $i$  at time  $t$ . For example, in Figure 6-5, the TED node  $j_x^{t_2}$  in the information flow network represents the travel experience data that is generated by  $x$  at the physical node and its time-dependent location.

### 6.3.3 Information flow evolution and propagation

Characteristics of the information flow evolution and propagation are captured through the VIC nodes and the directed link representations (T-links and I-links) in the  $G^1$ . First, the inter-vehicle communication by a vehicle with vehicles in its vicinity (communication range) leads to information being broadcast from that vehicle. When vehicle  $x$  communicates with vehicle  $y$  and shares its travel experience data, a pair of VIC nodes  $\lambda_x^{t_1}$  and  $\bar{\lambda}_y^{t_2} \in C^1$  is generated in  $G^1$

corresponding to the inter-vehicle communication event. The VIC node pairs are partitioned into two subsets: broadcasting VIC node  $C_b^I$  and receiving VIC node  $C_r^I$  ( $C_b^I, C_r^I \subset C^I$ ).

A set of inter-vehicle communication based information flow propagation links (I-links),  $(\lambda_x^{t_1}, \bar{\lambda}_y^{t_2}) \in M^I$  in  $G^I$ , is defined as follows:

$$M^I = \{(\lambda_x^{t_1}, \bar{\lambda}_y^{t_2}) \in C_b^I \times C_r^I \mid x \neq y, t_1 = t_2\} \quad (6)$$

A pair of VIC nodes is connected by a directed I-link, from the broadcasting VIC node  $\lambda_x^{t_1} \in C_b^I$  to the receiving VIC node  $\bar{\lambda}_y^{t_2} \in C_r^I$ , to represent the corresponding information flow evolution and propagation through the inter-vehicle communication. Given the instantaneous nature of a single inter-vehicle communication event, the broadcasting and receiving of information occur at the same time.

Figure 6-6 illustrates a traffic flow layer and an inter-vehicle communication layer with four vehicles ( $x, y, w,$  and  $z$ ), and the generation of the corresponding VIC nodes and I-links in the  $G^I$ . For example, a broadcasting VIC node  $\lambda_y^{t_7}$  and a receiving VIC node  $\bar{\lambda}_x^{t_7}$  represent the occurrence of the inter-vehicle communication from vehicle  $y$  to vehicle  $x$  at time  $t_7$ , and the directed I-link  $(\lambda_y^{t_7}, \bar{\lambda}_x^{t_7})$  connects them. These VIC nodes play the role of information flow propagation junctions, at which the information flow merges from another vehicle for the receiving node or diverges to another vehicle from the broadcasting node.

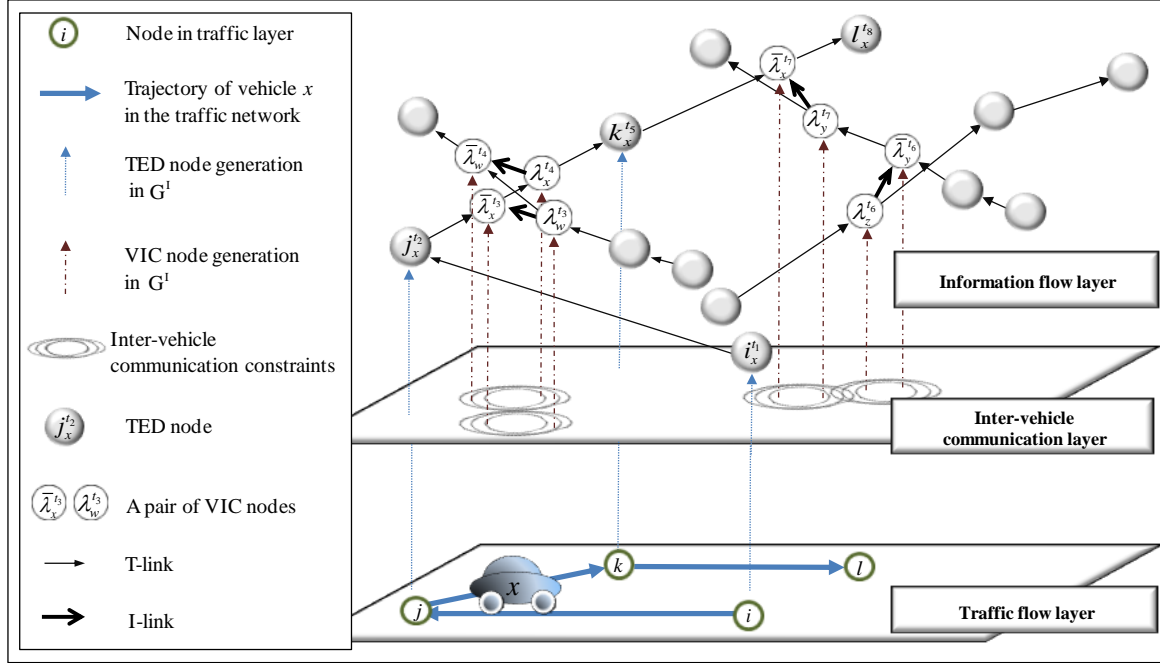


Figure 6-6 Information flow evolution and propagation

The travel experience data generation for a vehicle follows its trajectory in the traffic flow layer. The associated spatiotemporal dynamics are represented by a set of information flow propagation trajectory links (T-link). A set of T-links  $A^I$  is defined as follows:

$$A^I = \{(p_x^{t_1}, q_x^{t_2}) \in (P^I \times P^I) \mid \forall x \in X, t_1 < t_2\} \quad (7)$$

A directed T-link connects TED-TED, TED-VIC, VIC-TED or VIC-VIC nodes based on the trajectory of vehicle  $x$  from time  $t_1$  to time  $t_2$  ( $t_1 < t_2$ ). Figure 6-6 illustrates that the directed T-links in  $G^I$  connect the nodes based on each vehicle's trajectory direction. For example, T-links  $(i_x^{t_1}, j_x^{t_2})$ ,  $(j_x^{t_2}, \bar{\lambda}_x^{t_3})$  and  $(\bar{\lambda}_x^{t_3}, \lambda_x^{t_4})$  connect the TED-TED, TED-VIC, and VIC-VIC nodes based on the trajectory of vehicle  $x$  consistent with the evolution of time. These T-links explain how information flow propagates along with each vehicle's trajectory.

The graph structure of  $G^I$  is the result of the continuous generation/deletion of travel experience data that is represented by TED nodes and their propagation represented by the VIC nodes and the directed links. This graph structure can illustrate which vehicle's time-dependent travel experience data is propagated to a specific vehicle by traversing a connected subgraph of

the information flow network. Thereby, in the next section, a graph-based forward search algorithm is proposed to identify how information flow propagates, particularly in terms of linkage to the interactions with traffic flow and inter-vehicle communication.

## **6.4 Characterizing the information flow dynamics**

### **6.4.1 Graph structure of information flow network and the forward search algorithm to track the information flow propagation**

The graph structure of  $G^I$ , through the node and link representations, can map of what/when/where information is generated and how it propagates. In this context, the spatiotemporal propagation of a particular unit of information is represented by a connected group of TED nodes (interpreted as a vehicle's time-dependent locations) and the associated directed links from the specific TED node at which the travel experience data of interest is generated. Thereby, determining the TED nodes that are connected from a specific node in  $G^I$  provides an understanding of the characteristics of the information flow evolution and propagation. This is done using a graph-based forward search algorithm, by traversing the direction of the flow of information from the specific TED node where the unit of information (travel experience data of interest) is generated and identifying other vehicles' time-dependent locations at which this information is obtained.

Figure 6-7 conceptually shows the propagation of information flow generated by vehicles  $W$  and  $Z$  obtained from  $G^I$  using the forward search algorithm. Each unit of information propagation constitutes a different subgraph of  $G^I$  (blue and light red colored subgraphs in the figure). The encircled TED nodes in Figure 6-7 correspond to the generated travel experience data of interest, and TED nodes in each subgraph indicate the locations of vehicles. The VIC nodes enable the information flow propagation to other vehicles through the inter-vehicle communication. This graph structure illustrates the information flow evolution and propagation explicitly.

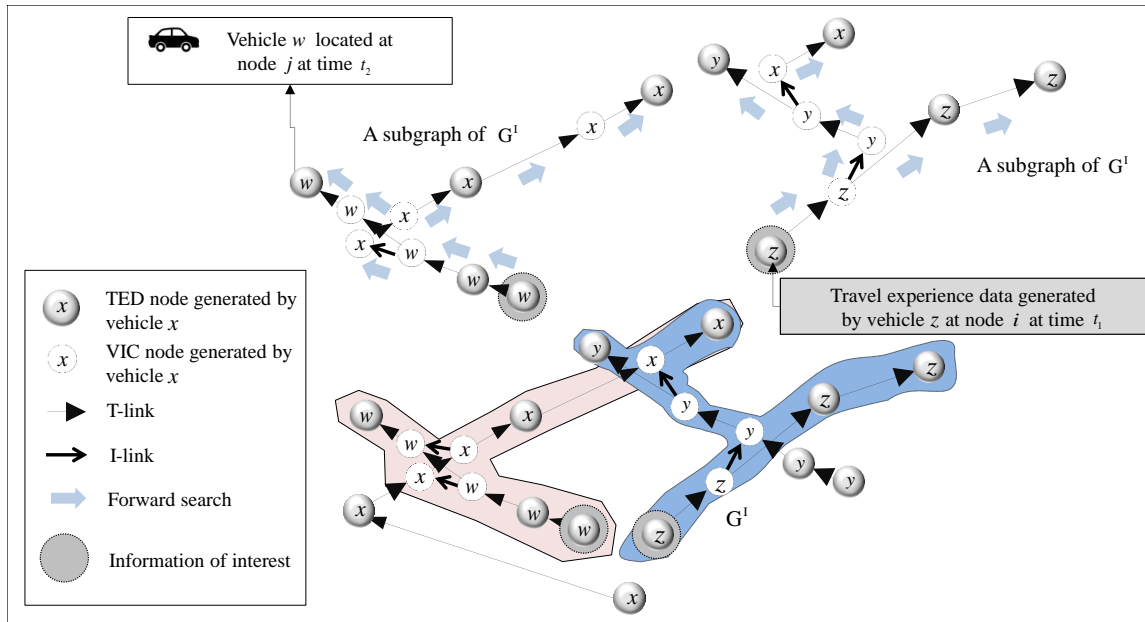


Figure 6-7 Subgraph of information flow network ( $G^1$ ) indicating information flow propagation

#### 6.4.2 Identification of information forward/backward propagation wave

This section illustrates the information forward/backward propagation waves, spatial propagation fronts, and the spatio-temporal density of informed vehicles to characterize the information flow dynamics. When a unit of information is spreading, an information propagation wave separates the traffic flow into the informed and uninformed regions and moves towards the uninformed region (Kim et al. 2014). Of particular interest is the rate of spread of the information propagation wave front; the wave front refers to the boundary between the informed and uninformed regions. Viewed over the entire network in Figure 6-8(a), the propagation of the information occurs as a spatial wave, with most cases of information propagation occurring near the information propagation wave front. It characterizes the spatiotemporal information flow propagation, describing how the traffic density changes lead to the dynamics of information flow.

Figure 6-8(b) illustrates how the propagation of a single unit of information is represented by a subgraph of  $G^1$ . The subgraph structure can explicitly address when and to which vehicle a specific unit of information propagates. For example, the flow of travel experience data generated by vehicle  $z$  to vehicles  $y$  and  $x$ , and the information propagation front locations, can be tracked using the TED nodes. Figure 6-8(a) illustrates an information forward propagation wave that is

moving in the direction of vehicular traversal. Since vehicles carry the information and the information can leap forward through V2V communications, the information propagation wave speed is always greater than or equal to a vehicle's speed.

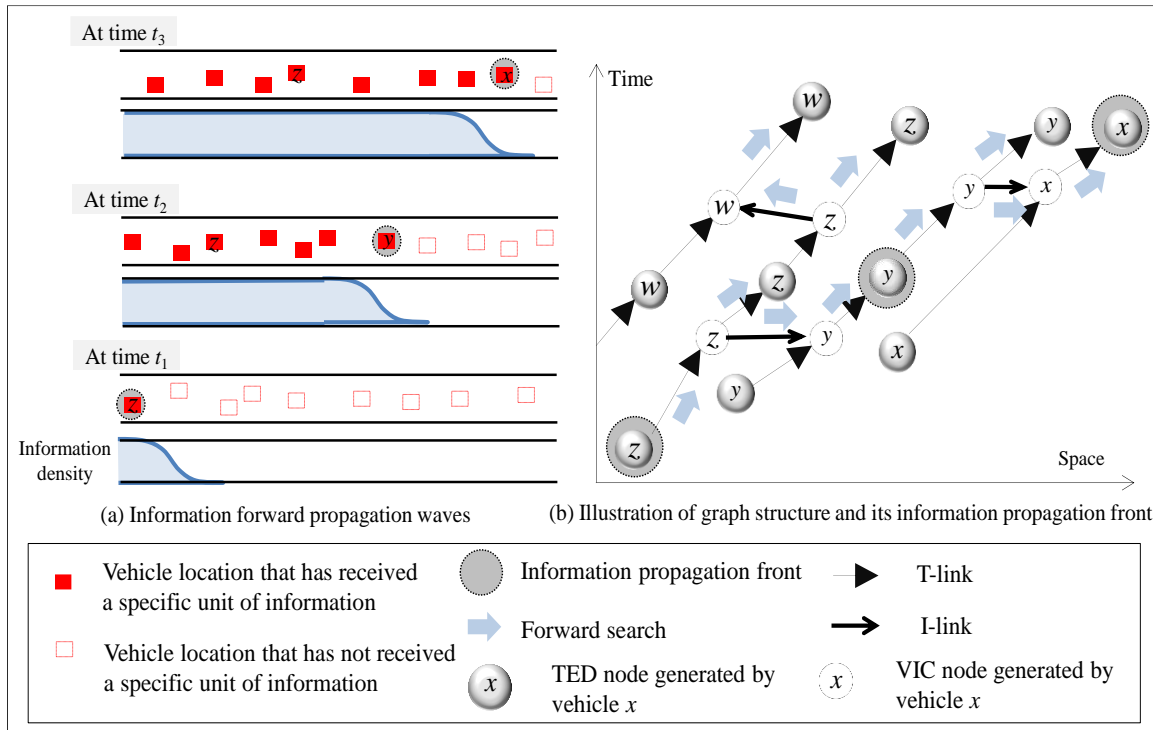


Figure 6-8 Illustration of the information forward propagation wave

## 6.5 Numerical experiments

### 6.5.1 Experiment setup

As shown in Figure 6-9(a), a bi-directional three-lane highway is considered for the experiments where all cells have homogeneous characteristics. Though experiments from heterogeneous environments (different road geometry or urban road network) may provide interesting topics for future work, for simplicity we confine our analysis to a homogeneous geometry environment. The traffic network consists of 100 cells and 99 cell connectors, which is equivalent to 11 miles of highway length. Each link consists of 10 cells. The cell length is 0.11 miles with a time step of 6 seconds. The cell parameters include backward propagating traffic wave speed of 22 mph, capacity of 2,350 vehicles per hour and free flow speed of 65 mph. A pre-defined

market penetration rate of 50% is assumed. Initially, the east bound (EB) traffic density is 40 veh./mile/lane and the west bound (WB) density is 13.3 veh./mile/lane.

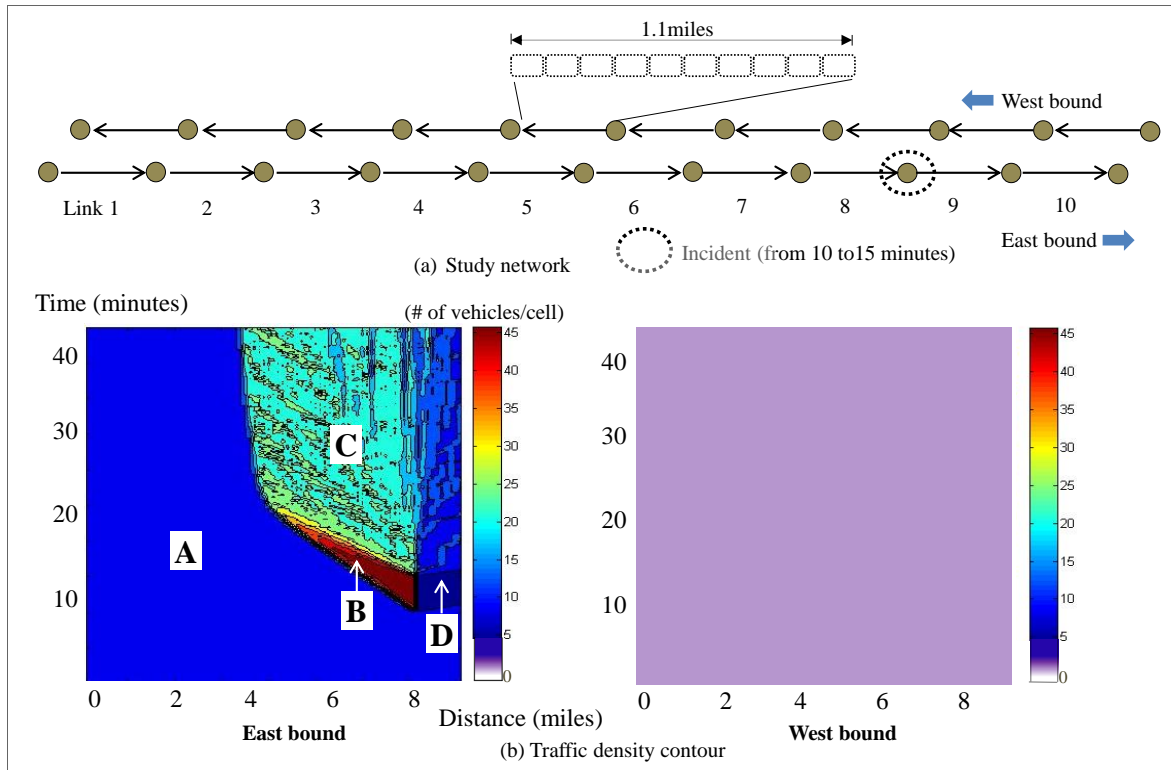


Figure 6-9 Study traffic network and traffic density contours

To consider the impact of traffic shock waves, we assume that an incident occurs on the EB highway on link 8 at time 10 minutes, and that its initial capacity is recovered at 15 minutes, as illustrated in Figure 6-9(a). The incident reduces the highway capacity by 1/3 of its initial value. A shock wave forms and travels backward at 22mph. The resulting spatio-temporal contour plot of the average traffic density is shown in Figure 6-9(b). Area A denotes a uniform traffic stream on the uncongested highway section. Area B is where the underlying traffic shock wave propagates backward due to the incident. Areas C and D denote the moving and discharging queue regions, respectively. The WB highway has a uniform traffic stream for all sections.

### 6.5.2 Interaction between the traffic flow and inter-vehicle communication layers

Figure 6-10 shows a heat map of the frequency of the inter-vehicle communication events under the different traffic conditions. The red color indicates higher frequency and blue color

indicates lower frequency of inter-vehicle communication events. It illustrates how different density levels of equipped vehicles affect the inter-vehicle communication frequency.

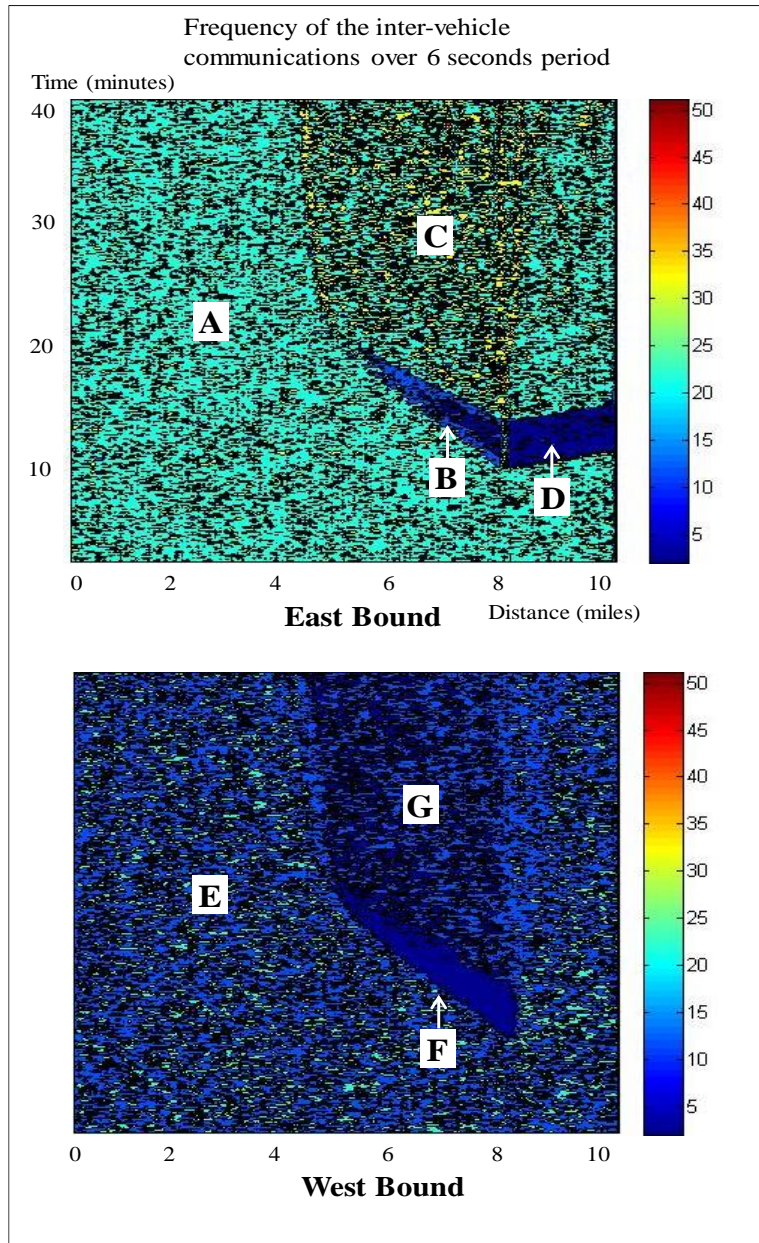


Figure 6-10 Heat map showing inter-vehicle communication frequency

A higher density level in the traffic network leads to a greater likelihood of communication with other vehicles under the same market penetration rate. As the interference level increases, it leads to lower success rate of communication. Specifically, for the EB highway, under the uncongested traffic condition in area A, successful inter-vehicle communications take place 15-25

times in a cell. As the density level increases in area C, vehicles are more likely to exchange information. However, as the density level increases further in the traffic shock wave region (area B), the success rate of V2V communications is reduced due to the much higher impact of interference, resulting in reduced inter-vehicle communication frequency. Also, since the traffic density is low in area D, the opportunity for V2V communications is limited.

For the WB case, though the traffic stream is uniform, the occurrence of inter-vehicle communications can be affected by interference arising from the opposite direction (EB). A high density level in the EB reduces the success rates of inter-vehicle communication in the WB context, as illustrated by areas F and G area.

### **6.5.3 Information forward propagation wave**

The graph structure of the information flow network provides a capability to determine how quickly and far the information forward/backward propagation wave can propagate, as discussed in Section 6.4.2. The trajectories of the information forward propagation wave front with the underlying traffic conditions are shown in Figure 6-11. Information generated at every minute from vehicles at point A propagates in the downstream direction.

The information forward propagation wave speed varies as the downstream traffic density changes. As the information is transported by moving vehicles and broadcasted, the speed of information flow propagation depends on the underlying traffic speed and information propagation characteristics. The information forward propagation wave speed reduces after encountering the traffic shock wave (B and C areas) because of the reduced traffic flow speed and the limited inter-vehicle communication occurrences due to the higher interference. These observations are consistent with Figure 6-10, which illustrates the likelihood of inter-vehicle communication at different density levels. In the queue dissipation area (area D), the information forward propagation wave speed is faster than that of the B and C areas, since traffic is at free flow speed and inter-vehicle communication takes place more frequently.

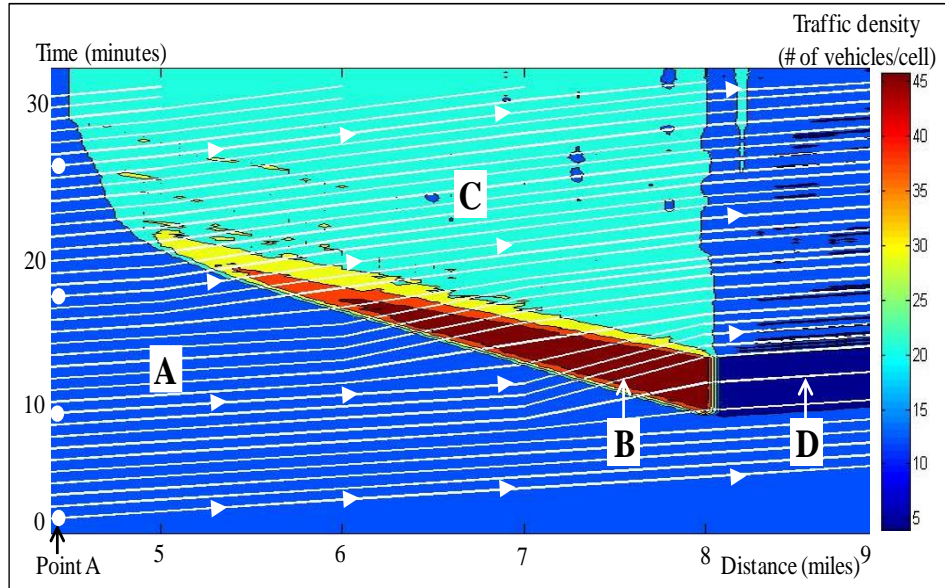


Figure 6-11 Trajectories of information forward propagation wave front

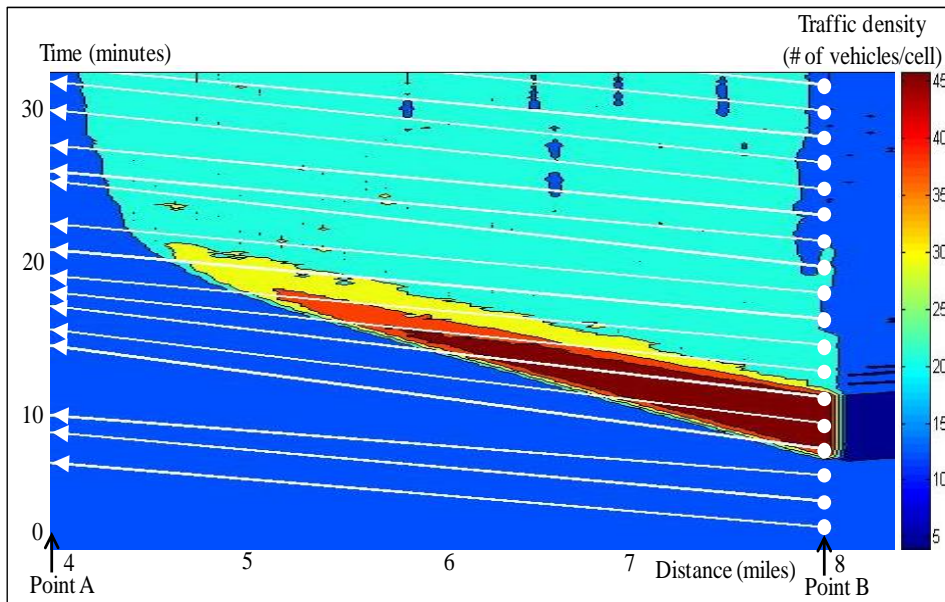


Figure 6-12 Information flow propagation speed

To be useful for V2V-based ATIS, the generated information has to propagate faster than the traffic backward propagating wave. Figure 6-12 illustrates how fast the information generated

downstream can reach the upstream traffic through the bi-directional traffic flow. The downstream traffic conditions on the EB facility are sensed by vehicles at point B and these travel experience data are received by the equipped vehicles in the opposite traffic direction (WB), and finally the EB vehicles at point A.

Each solid line in Figure 6-12 connects the spatiotemporal locations where travel experience data is generated and where vehicles receive that information. As vehicles in the opposite direction carry and transmit the information, the traffic flow and the interference in the opposite direction affect the information flow propagation speeds. This indicates that the vehicles located at point A can receive the most recent information faster than the speed of the backward traffic shock wave (22mph).

#### **6.5.4 Spatiotemporal characteristics of vehicle knowledge**

As discussed heretofore, a V2V-based ATIS is inherently a decentralized system where the dynamic flow propagation of multiple units of information depends on the interactions between the traffic and inter-vehicle communication constraints. This implies that, at any given time, the information available to each vehicle may differ, and hence the specific interpretation of the network state of each vehicle may also vary. In the multi-layer framework, the time-dependent vehicle knowledge of interest consists of a set of subgraphs in  $G^l$ . The evolution of the vehicle knowledge can be tracked from any point using the graph-based reverse search algorithm (Kim and Peeta, 2016).

Figure 6-13 shows the spatiotemporal knowledge of vehicles located on link 4 at different time points. The set of travel experience data on the downstream link 8 is received by vehicles on the upstream link 4, and each distribution graph shows a range of travel times at different times (17, 22, 27, and 32 minutes). Duplicate data (spatiotemporal data of the same vehicle) and older data (older than 15 minutes) are discarded. The figure indicates that each vehicle has different time-dependent knowledge of the traffic conditions due to the dynamics of multiple units of information flow propagation. This is because of the different information flow propagation speeds, which depend on the dynamics of traffic flow and inter-vehicle communication. Figure 6-14 illustrates

that the spatiotemporal knowledge of vehicles can be different for vehicles at the same location (link 4) at a given time (22 minutes).

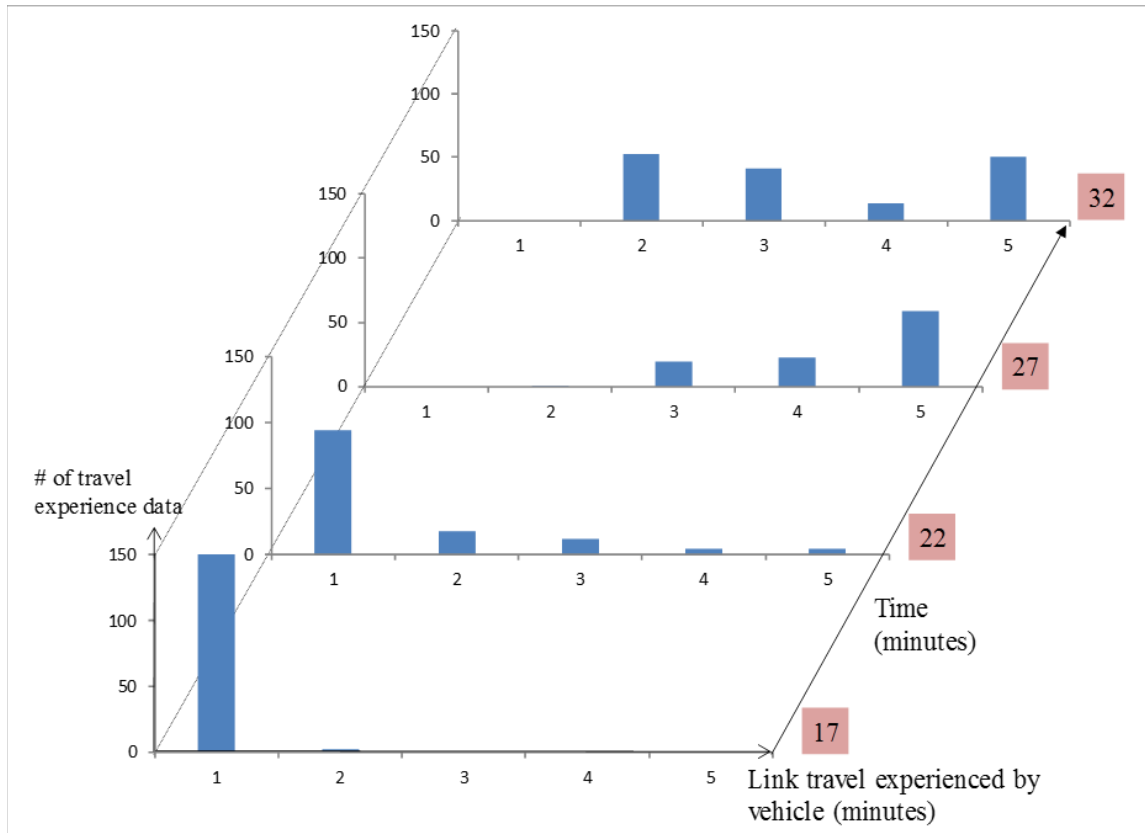


Figure 6-13 Illustration of the time-dependent knowledge of vehicles located on link 4

Some studies (Bauza and Gozávez 2013; Lee and Park 2008) highlight the limitations of most existing link travel time estimation or prediction methods to address the dynamic vehicle knowledge related challenges. For example, an inaccurate interpretation of the network conditions based on the time-dependent vehicle knowledge of each individual vehicle can cause travelers to experience worse trip conditions.

More broadly, ensuring some level of coordination of decision-making across vehicles through real-time traffic management is important for enhancing the network-level traffic performance rather than potentially being negatively affected by the myopic decisions of individual vehicles based on their individual spatiotemporal knowledge. This motivates the need to understand how multiple units of information flow propagate and contribute to the time-dependent vehicle

knowledge. Such an understanding is critical for the design of robust V2V-based ATIS architectures, especially to establish coordinated real time traffic management strategies and active control mechanisms to spread useful/important information.

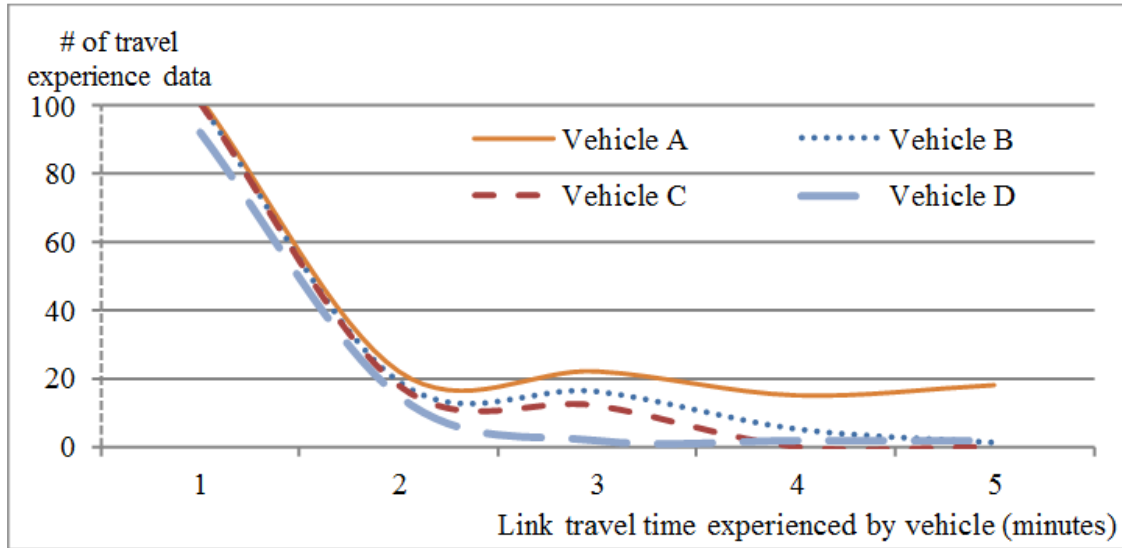


Figure 6-14 Illustration of the knowledge of vehicles located at link 4 at a given time point

## 6.6 Summary and discussion

Due to the multi-dimensional impacts of traffic flow dynamics and inter-vehicle communication constraints on information flow evolution and propagation, the need to understand their interdependencies is a fundamental problem for a V2V-based ATIS. The existing literature in this domain typically focuses on the propagation of a single unit of information. There is a key need for modeling frameworks to explain how multiple units of information flow evolve and propagate, particularly in terms of the linkage to the interactions with traffic flow and inter-vehicle communication dynamics.

This study proposes a multi-layer framework to model multiple units of information flow evolution and propagation by integrating a traffic flow model and an inter-vehicle communication model. Traffic flow dynamics are captured by the CTM in the physical traffic flow layer. The inter-vehicle communication layer uses the time-dependent locations of vehicles and the density of the V2V-equipped vehicles as inputs for an aggregate function (equation 5) of the inter-vehicle communication success rate. Then, the information flow evolution and propagation is modeled using a graph-based representation. The proposed modeling framework enables capturing the

information flow dynamics (in terms of the information forward/backward propagation waves, spatial propagation fronts, spatiotemporal vehicular knowledge characteristics, etc.) using the traffic flow dynamics (in terms of traffic forward/backward propagating waves and traffic flow variables) and the inter-vehicle communication events.

Synthetic experiments seek to map how the information flow dynamics are determined by the traffic flow dynamics and the inter-vehicle communication constraints. The occurrence of the inter-vehicle communication varies as the underlying traffic density changes. This leads to varying information forward/backward propagation wave speeds under different traffic conditions. The experiments also seek to understand the interactions involving information flow in terms of the spatiotemporal characteristics of the time-dependent vehicle knowledge. They illustrate that the proposed multi-layer framework can integrate the dynamics of traffic flow and inter-vehicle communication constraints to generate insights for the propagation of the multiple units of information flow.

This study offers the potential to develop a new generation of V2V communications based route guidance strategies with individual routing decisions. These include fully decentralized V2V communications based routing that relies solely on the vehicle-level knowledge, and more advanced hybrid systems that combine both centralized and decentralized information strategies under V2V-based ATIS.

## **7. EVALUATION OF DECENTRALIZED VEHICLE-TO-VEHICLE COMMUNICATIONS-BASED ADVANCED TRAVELER INFORMATION SYSTEM**

### **7.1 Introduction**

Intelligent transportation systems (ITS) leverage advanced technologies to improve the efficiency, reliability, and safety of a transportation system. Within the framework of ITS, advances in wireless and other communication technologies have enabled vehicle-to-vehicle (V2V) communications in traffic systems, which offer the potential for real-time traffic management and control in multiple, innovative ways. They include safety applications enabled by V2V communications that are effective in mitigating or preventing potential crashes (Harding et al., 2014); examples include warnings for blind spot, forward collision and lane change. Another mechanism for real-time traffic management leverages information propagation to improve system efficiency based on the exchange of travel-related information between vehicles through V2V communications. In such a system, vehicles are envisioned to generate and relay time-dependent information on traffic conditions in the absence of centralized coordination. Using such V2V-obtained information, the vehicle computes its own route so as to satisfy its travel-related objectives.

While the level of decentralization may vary, the potential for an infrastructure-based decentralized advanced traveler information system (ATIS) has been analyzed in past studies (Papageorgiou, 1990; Hawas and Mahmassani, 1996; Pavlis and Papageorgiou, 1999; Wang and Papageorgiou, 2000) to address the limitations of centralized systems (Chen and Underwood, 1991; Ben-Akiva et al., 1997; Bottom, 2000). Here, infrastructure refers to intrusive and non-intrusive sensors installed on roads, and associated communications infrastructure such as road-side units. Infrastructure-based decentralized ATIS is responsive to unfolding local traffic conditions, and can be more robust and resilient under disasters. This is because decentralized systems rely on nodal controllers and/or in-vehicle devices and are less likely to be affected by potential single-point failures.

Ziliaskopoulos and Zhang (2003) first discuss a decentralized real-time V2V-based ATIS and introduce the concept of a zero-infrastructure traffic information system through V2V-based

information-sharing. Such a decentralized system can be easily extended and is scalable without the need for elaborate system-level sensing and control infrastructure as the technology resides in the vehicles. Yang and Recker (2005, 2006, 2008) investigate the feasibility of a decentralized V2V-based ATIS in terms of the required market penetration rate (MPR) of V2V-equipped vehicles and information propagation speed using simulation-based modeling. Some preliminary analyses of V2V-based ATIS have been conducted to explore the impact of V2V-based ATIS on the traffic network. Minelli et al. (2015) evaluate the impacts of V2V-based ATIS on mode choice and the efficiency of transportation system. They show that travel time changes in the auto mode under various MPRs of V2V-equipped vehicles can cause changes in mode choice. Dai et al. (2019) investigate driver route choice behavior heterogeneity related to fuel consumption and travel time, and suggest that a traffic system with higher MPRs of V2V-equipped vehicles can enhance performance.

However, few studies have focused on the implications of the characteristics of the fully decentralized nature of information-sharing and routing decisions under an uncoordinated V2V-based ATIS. First, a V2V-based ATIS consists of traffic flow, V2V communications, information flow and vehicle-level computations. The relationships between these components are characterized by nonlinearity and interdependencies, as will be illustrated in Section 7.2. Analyzing the closed loop relationship among these components is critical to enhance the understanding of the characteristics of V2V-based ATIS. It will serve as a building block to design new strategies with some level of coordination in information-sharing and decision-making across vehicles to manage traffic conditions in congested networks.

Second, the quality and quantity of travel experience data can vary across links. As information spreads due to data from several vehicles, it may illustrate variability or have inconsistencies. For example, time-dependent travel times for a link may have a range even if vehicles traverse that link close to each other in time. Further, the vehicle knowledge may entail quality issues in terms of latency or the time gap between when data is collected and when it is used to estimate the traffic network state for that vehicle, labeled the time delay (Ziliaskopoulos and Zhang, 2003; Du et al., 2012). Existing models do not consider the quality and usefulness of information in the estimation of traffic network conditions over time.

Third, any information that is shared with other vehicles is subject to traffic flow dynamics and V2V communications constraints, including interference, signal attenuation over distance, bandwidth, etc. These lead to randomness in terms of which information is propagated to which vehicle. That is, at any given time, each individual vehicle has a specific interpretation of the network conditions, which is labeled as the “vehicle-level knowledge” based on its own experience and the information it has received up to that time (Kim and Peeta, 2017). Therefore, the spatiotemporal coverage/spread of vehicle knowledge in an area can vary with the locations of vehicles, origin-destination (O-D) demand profile, traffic flow pattern, V2V communications constraints, and MPR of V2V-equipped vehicles. Hence, understanding the relationship between vehicle-level knowledge and routing decisions is critical under an uncoordinated V2V-based ATIS.

Fourth, a V2V-based ATIS inherently implies that routing decisions are performed at the vehicle level. Since it lacks any level of formal coordination of decision-making across vehicles, the resulting routing decisions can be myopic. Therefore, it can potentially have a negative impact on the network performance. Chen and Du (2017) develop a local information provision strategy to address network traffic fluctuations which may occur when many vehicles are uniformly provided real-time traffic information based on global conditions.

In the context of V2V-based ATIS, the focus of this study is to explore the decentralized nature of information-sharing and routing decisions and their impacts on the performance of transportation system. Understanding its strengths and limitations will provide insights for effectively leveraging a V2V-based ATIS. The primary contributions of this study can be summarized as follows. First, this study systematically exploits the interdependencies among traffic flow dynamics, V2V communications, information flow propagation, routing decisions and network state evolution. To the authors’ knowledge, this is the first study to close the loop on understanding how information flow propagation affects network state evolution, and how network evolution affects information flow propagation. Second, to address information quality issues, information processing and routing decisions that are suitable for the V2V-based ATIS are proposed. Most existing models use a simple mechanism to estimate link travel time and provide shortest path information. Third, the proposed study explicitly factors several deployment constraints related to V2V communications and vehicle-level computation. Fourth, many studies use simple, hypothetical networks which may produce a limited number of alternate routes. The

proposed modeling framework is tested on a large-size network, the Borman Expressway network in northern Indiana. Due to the inherent complexity of V2V-based ATIS, a simulation-based approach is used to analyze the study objectives.

The remainder of this paper is organized as follows. The next section discusses the proposed modeling framework for the V2V-based ATIS. The modeling details of the decentralized V2V-based ATIS are discussed in Section 7.3. Section 7.4 discusses the design of the study experiments. Results from the experiments are discussed in Section 7.5. The paper concludes with some comments in Section 7.6.

## **7.2 Decentralized V2V-based ATIS modeling framework**

While various ATISs differ in their design and operation, they have key common elements. Three important common components are data collection, information processing, and routing decisions. We discuss these components for the decentralized V2V-based ATIS.

V2V-equipped vehicles have the ability to communicate with each other in the decentralized V2V-based ATIS. Each V2V-equipped vehicle generates data on its time-dependent location and experienced travel times on the links traversed on its route using a global positioning system (GPS) and a digital network mapping. The vehicles store such information and relay their own experience and obtain travel experience data of other V2V-equipped vehicles (data collection). The information available to a vehicle depends on network-level interactions. These network-level interactions include the vehicle's physical interactions with other vehicles in its vicinity and the V2V communications constraints, as illustrated on the left-hand side of Figure 7.1. This study adopts a multi-layer network framework to characterize the network-level interactions associated with information flow propagation dynamics resulting from traffic flow dynamics and V2V communications constraints (Kim and Peeta, 2016). It provides a computationally efficient mechanism to track the individual vehicle-level knowledge. It is important to note here that Kim and Peeta (2016) address only how traffic flow dynamics lead to the dynamics of information flow, but do not close the loop in terms of how information flow propagation affects traffic flow through routing decisions.

Based on its dynamic knowledge, a vehicle continuously estimates the network state by updating the link travel time distributions (information processing). Then, the routing decision is

determined at the vehicle level and provided to the driver. The right-hand side in Figure 7.1 shows the vehicle-level computational component that consists of information processing and routing decisions. We adapt an information discounting method (Koutsopoulos and Xu, 1993) to capture the quality of information. Then, the estimated link travel time distributions are used at the vehicle-level to compute the routing decisions. This study uses a reactive routing strategy in which the route is continuously updated en route. It enables the vehicle to react to evolving network conditions, including the occurrence of incidents, daily variation in demand, and/or traffic fluctuations.

The routing decisions of all V2V-equipped vehicles determine the traffic network state evolution, and the aforementioned components and processes are repeated as time progresses. Without loss of generality, it is assumed that all V2V-equipped vehicles have identical equipment. While V2V-equipped vehicles may switch from their initial paths based on updated vehicle-level knowledge as time progresses, we assume that unequipped vehicles rely on their past experience throughout the entire period and affect only the traffic flow dynamics.

In summary, the primary focus of this study is on how information flow propagation affects routing decisions and vice versa.

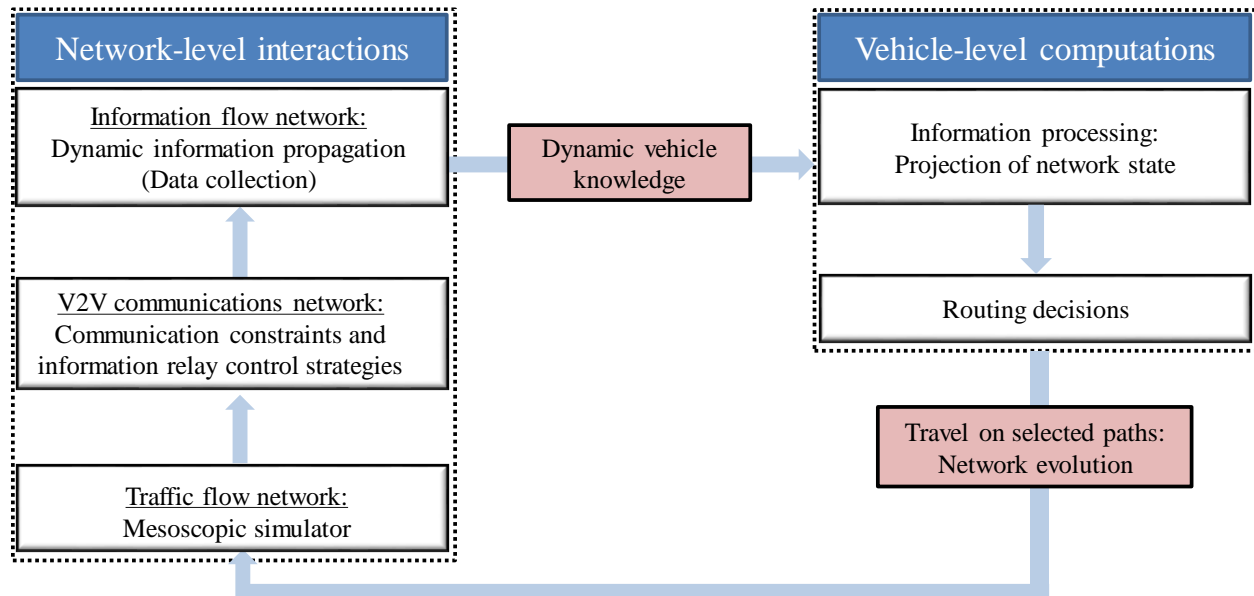


Figure 7-1 Elements of a decentralized V2V-based ATIS

### **7.3 Modeling of the decentralized V2V-based ATIS components**

#### **7.3.1 Multi-layer framework for network-level interactions**

The dynamics of traffic flow and V2V communications lead to time-dependent vehicle-level knowledge on network traffic conditions. Kim and Peeta (2016) propose a graph-based multi-layer network framework to model dynamic information flow propagation in V2V-based ATIS as a complex system comprised of three coupled network layers: physical traffic flow network, V2V communications network and information flow network. These layers have dependencies in terms of shared physical networks, and dynamics of traffic flow and V2V communications constraints (based on location of vehicles and feasibility of V2V communications). The consideration of the three layers simultaneously enables addressing their interactions.

##### **7.3.1.1 Physical traffic flow network**

The physical traffic flow network captures the spatiotemporal interactions between vehicles and travel experience data generation. When a V2V-equipped vehicle reaches the end of a link, it generates travel experience data that includes vehicle identification number, identification number of the link traversed, link entrance time, and link travel time. These travel experience data are stored in the temporary memory onboard the vehicle's system to communicate with other vehicles. Duplicate and/or older data (data older than 20 minutes in the study experiments here) are discarded.

##### **7.3.1.2 V2V communications network**

Most existing models represent V2V communications constraints in an abstract manner; that each vehicle has a fixed communication success rate. The V2V communications network in this study receives all V2V-equipped vehicles' time-dependent positions as input from the traffic flow network, and then determines the occurrence of information flow propagation among the V2V-equipped vehicles. The V2V communications network uses an interference model from Gupta and Kumar (2000) to calculate V2V communications connectivity between vehicles. Two V2V-equipped vehicles whose physical distance is less than the communication range (250 meters in this study) can potentially communicate with each other at any time through V2V communications. However, multiple communications from vehicles within communication range can cause a high

degree of mutual interference, which may result in the failure of V2V communications. The interference rate is defined as follows (Gupta and Kumar, 2000):

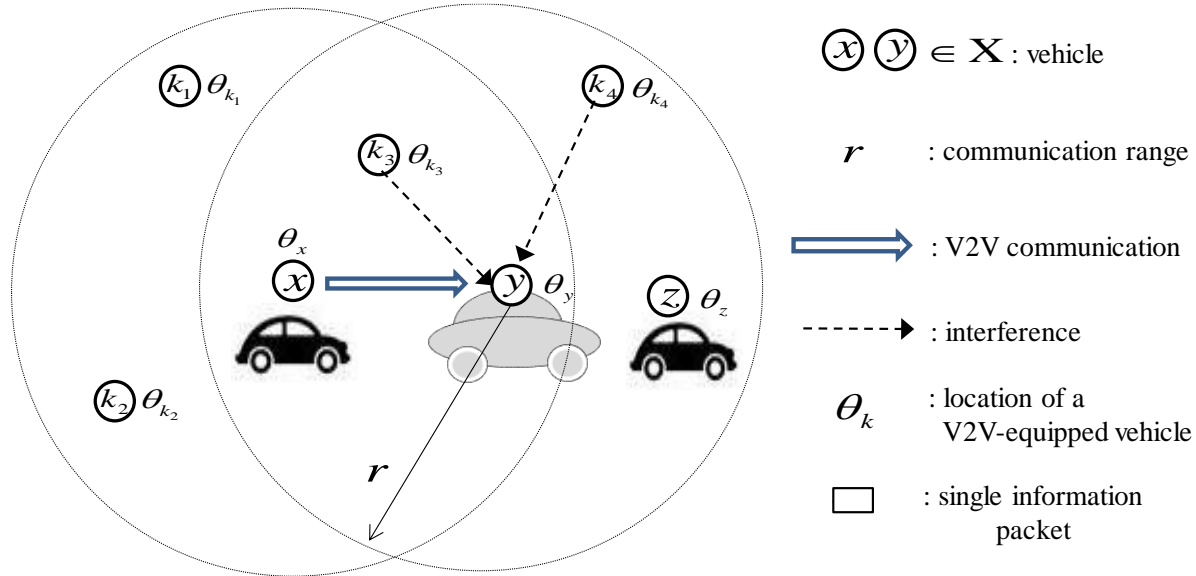
$$\frac{\frac{T_x}{|\theta_x - \theta_y|^2}}{N + \sum_{\substack{k \in X \\ k \neq x}} \frac{T_x}{|\theta_x - \theta_y|^2}} \geq \beta \quad (1)$$

where,  $\theta_k$  denote the coordinates of a V2V-equipped vehicle  $k$  within communication range,  $k \in X$ , where  $X$  is the set of V2V-equipped vehicles within communication range. Consider the situation shown in Figure 7.2 where vehicle  $x$  is broadcasting, and  $y$  is a receiving vehicle. Suppose a subset of vehicles ( $k_3$  and  $k_4$ ) within communication range of vehicle  $y$  simultaneously transmit information at the same time instant, it can lead to possible interference.

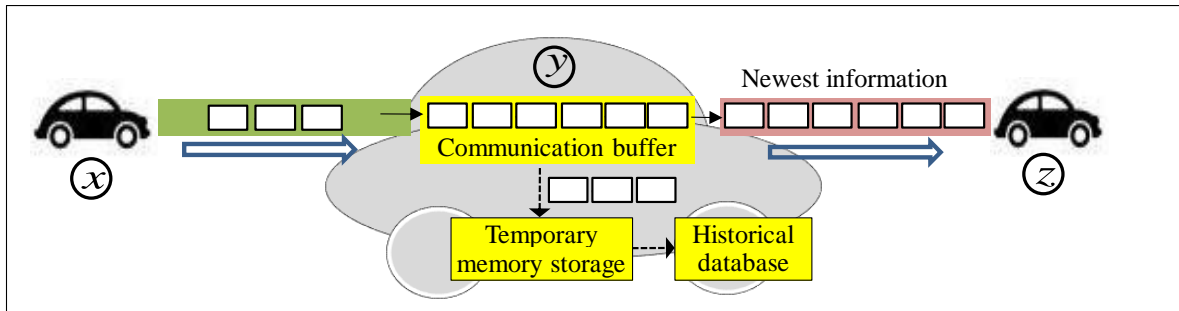
Signal power decays with distance from a broadcasting vehicle  $k$  at the rate  $1/|\theta_x - \theta_y|^2$ . The transmitted vehicle-level knowledge from vehicle  $x$  is successfully received by vehicle  $y$  if it satisfies the minimum signal-to-interference ratio of  $\beta$  ( $\beta = 2$  in the study experiments here). Specifically, all V2V-equipped vehicles' positions within communication range of vehicle  $y$  in the traffic network are tracked. The accomplishment of V2V communications between  $y$  and those vehicles is checked every 0.5 seconds based on the distances between it and the other V2V-equipped vehicles in its vicinity to determine the interference level. It is assumed that the power levels of vehicles ( $T_x$ ) are identical and the ambient noise power level ( $N$ ) is zero. The study experiments also assume that the available bandwidth is 3Mbps with the data communication frequency (2Hz) (Karagiannis et al., 2011).

Wang et al. (2018) show that several communication factors (e.g. information packet generation rate, communication frequency, and communication buffer size) also significantly affect the characteristics of information flow propagation. This is because a large number of information packets generated by multiple vehicles in a small space and a short time period can lead to congestion in the information flow network. It necessitates an information relay control strategy to prevent packet collisions, so that the limited communication capacity can be efficiently shared by all information packets (Wang et al., 2018). How these buffers store information depends on which traffic information has a higher priority (usefulness) for a V2V-based ATIS. We use a strategy that seeks to keep the newest information (in terms of when the information is generated) in the communication buffer, to be relayed if the communication buffer is congested as shown in

Figure 7.2(b). All of the information received by a vehicle goes into its vehicle-level temporary memory storage in Figure 7.2(b) to generate the historical database, which will be discussed in Section 7.3.2.1.



(a) Interference among vehicles



(b) Illustration of information relay control strategy from communication buffer

Figure 7-2 Illustration of V2V communications-related constraints

### 7.3.1.3 Graph-based representation of information flow network

Based on the travel experience data generation in the traffic flow network, and the occurrence of V2V communications in the V2V communications network, the flow of information is mapped using a graph-based representation of the information flow network (Kim and Peeta, 2016).

The graph structure can illustrate which vehicle's time-dependent travel experience data is propagated to a specific vehicle by traversing a connected subgraph of the information flow

network. A simple graph-based search algorithm by Kim and Peeta (2016) is used to identify how information flow propagates and how vehicle-level knowledge evolves, particularly in terms of the interactions with traffic flow and V2V communications constraints. In this study, we modify the graph-based search algorithm to incorporate the limited channel capacity by limiting the number of information packets being relayed. It seeks to identify the vehicle knowledge of all equipped vehicles in space and time to explain what information is obtained by each V2V-equipped vehicle.

A key benefit of the graph-based multi-layer framework is that it provides the capability to track the spatiotemporal characteristics of information flow and evolution of vehicle-level knowledge explicitly. An explicit model for information flow propagation in the graph-based approach enables an understanding of the dynamic interactions among the three layers, and the evolution of vehicles' knowledge in time and space. Therefore, it can explain how vehicle-level knowledge is shaped by the events from the other two layers. Further, the graph-based approach provides retrospective information to track the spatiotemporal characteristics of information flow directly through a connected graph structure. For a detailed discussion on the multi-layer framework, see Kim and Peeta (2016).

### **7.3.2 Vehicle-level computations**

The computational components reside onboard the vehicle. With its dynamic knowledge, the vehicle performs information processing and routing decisions.

#### **7.3.2.1 Information processing**

When the vehicle reaches the end of a link, it updates the link travel time distribution to estimate the traffic network state. In this study, an information discounting model (Koutsopoulos and Xu, 1993) is modified to incorporate the quality of information. The proposed information discounting model combines real-time information available from vehicle-level knowledge and data from the associated historical database. This is because it is likely that the real-time information will not provide full coverage on traffic conditions for the entire network (Toledo and Beinaker, 2007). The historical database does not capture day-to-day variability that may be caused by fluctuations in demand and by events (such as incidents and maintenance work). Thus, it is desirable to leverage real-time information with the historical database.

The information discounting model (Koutsopoulos and Xu, 1993) involves the explicit recognition of accuracy in real-time information to update the long-term historical distribution. It is reasonable to assume that travel experience data with less time delay is reliable. Further, when the standard deviation of travel time data is large, the information on current travel time will soon be dated. Therefore, the larger the values of time delay and variability, the lesser the value of information on current travel times. So, the estimated travel time should be appropriately adjusted (discounted) with respect to the quality of information.

The historical database is represented as a discrete distribution. Let  $H_a(t)$  denote the discrete historical travel time distribution on link  $a$  at time  $t$ . Travel time state  $S_a^i$  is defined as  $i^{\text{th}}$  travel time interval with lower and upper bounds  $[l_a^i, u_a^i]$  with associated probability  $p_a^i(t)$ . The corresponding probability density function is given below:

$$H_a(t) = \{S_a^i, p_a^i(t)\}_{i=1}^{I_a}, \quad S_a^i = [l_a^i, u_a^i] \quad (2)$$

where  $I_a$  is the total number of intervals in the discrete travel time distribution of link  $a$ . The associated standard deviation of the historical travel time of link  $a$  is defined as  $\sigma_a$ .

Consider a set of real-time link travel experience data  $R_a^i(t)$  on link  $a$ , obtained using the vehicle knowledge at time  $t$ . The data latency is  $\delta = t - t_0$ . The updating mechanism for link  $a$  is as follows:

$$F_a^i(t) = p_a^i(t) + \varphi \cdot \sum_{m=1}^{[R_a^i(t)]} e^{-\sigma_a \cdot \delta_m}, \quad (3)$$

where  $F_a^i(t)$  is updated probability of  $p_a^i(t)$ ,  $\varphi$  is a weighting coefficient, and  $[R_a^i(t)]$  is the number of real-time link travel time data on travel time state  $S_a^i$ . To account for the lesser reliability of outdated data, it is discounted using an exponential function of time delay. Further, the real-time information is discounted by the standard deviation ( $\sigma_a$ ) of historical travel time on that link. Then,  $F_a^i(t)$  is normalized to  $\bar{F}_a^i(t)$ , so that normalized values satisfy  $\sum_{i=1}^{I_a} \bar{F}_a^i(t) = 1$ . If there is no information available on a link, its historical database will be used. This study uses an updated travel time distribution on link  $a$  for time interval  $t$ ,  $C_a(t)$ , with lower and upper bounds  $[l_a^i, u_a^i]$  and associated updated probability  $\bar{F}_a^i(t)$ .

### 7.3.2.2 Routing decisions

As traffic information (either real-time or with latency) is available to vehicles en route through V2V communications, this study assumes that travelers make routing decisions using routing policies. Given the location of the vehicle and the short-term link travel time distribution, a routing policy determines only the link that should be traversed next, rather than computing a complete path with the objective of minimizing the expected travel time. Such a routing strategy takes into account current as well as future availability of travel time information based on possible realization of link travel time. This study adapts an online stochastic routing strategy (Du et al., 2013) for the proposed V2V-based ATIS. In it, the optimal routing decision is adaptively updated en route using vehicle-level knowledge. Thereby, based on the prevailing traffic state information, V2V-equipped vehicles may be re-routed to less congested paths.

Let the set of links incident from node  $g$  be denoted by  $\delta^-(g)$ , and  $o$  and  $s$  denote the origin and destination nodes, respectively. In the proposed routing policy, the traveler will be suggested the next link such that the associated route has the expected minimum travel time from his/her current node  $v$  to the destination  $s$  given the network conditions at the current time. It can be expressed as:

$$a^*(t) = \operatorname{argmin}\{E[C_a(t)] + G_{qs}(t) | \forall a = (v, q) \in \delta^-(v)\} \quad (4)$$

where  $a^*(t)$  denotes the next link suggested to the traveler at time  $t$ .  $E[C_a(t)]$  is the expected travel time on link  $a$  at time  $t$ .  $G_{qs}(t)$  is the expected minimum travel time from node  $q$  to destination  $s$  at time  $t$  given that the vehicle arrives at node  $q$  and continues to be routed under the provided policy. It can be expressed as:

$$G_{qs}(t) = E[\min\{C_a(t) + G_{ws}(t) | \forall a = (q, w) \in \delta^-(q)\}] \quad (5)$$

It is formulated as a recurrent relationship. Therefore, equation (6) also holds.

$$G_{ss}(t) = 0 \quad (6)$$

To find the optimal next link, a modified label-correcting routing algorithm that proceeds in a backward manner (Du et al., 2012) is used to identify the optimal next node.

Several past studies have focused on capturing the network-level interactions associated with the traffic dynamics resulting from assumed behaviors of travelers under information provision (Peeta and Mahmassani, 1995a, 1995b; Peeta and Ziliaskopoulos, 2001), and the routing decision behavior of travelers under information provision and consequent network-level traffic evolution

(Peeta and Yu, 2002, 2004, 2005, 2006). Nevertheless, for simplicity, we assume that all vehicles which receive routing information comply with the recommended routes.

The vehicle-level routing decisions of the V2V-equipped vehicles affect the traffic network flow evolution. Hence, the impacts of dynamic routing decisions based on vehicle-level knowledge are explicitly considered in the proposed V2V-based ATIS.

## **7.4 Case study**

This section discusses the setup for the simulation-based experiments to analyze the performance of the proposed V2V-based ATIS.

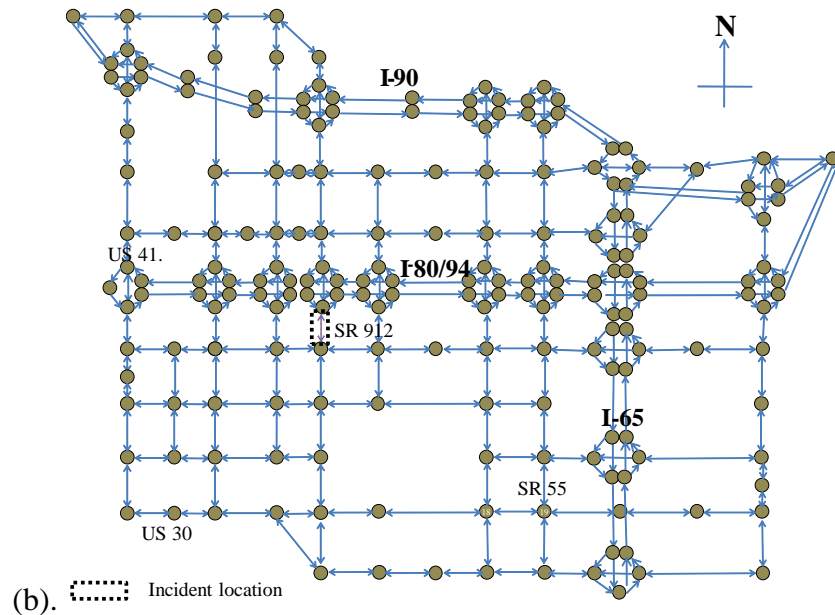
### **7.4.1 Experiment setup**

A mesoscopic traffic simulator, DYNASMART-P (Mahmassani et al, 2009), is used to replicate the traffic flow dynamics and to track the vehicle positions in the traffic network. In the simulator, as vehicles are generated, they are randomly designated as V2V-equipped or unequipped based on the MPR. Both V2V-equipped and unequipped vehicles are assigned to initial paths at the beginning of their trips based on a time-dependent  $K$ -shortest path algorithm using current traffic conditions at those times (Jayakrishnan et al., 1994). However, V2V-equipped vehicles may change their initial paths en route based on updated vehicle-level knowledge, while unequipped vehicles do not.

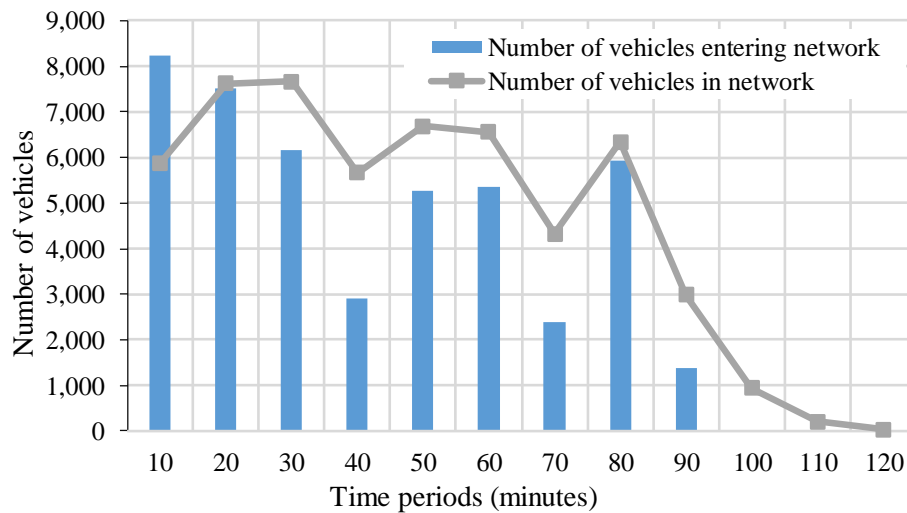
### **7.4.2 Test network and characteristics**

The Borman Expressway network in northern Indiana, which includes interstates 80/94 and 65, and the surrounding arterials, is used as the study network. It consists of 197 nodes and 460 links. Dynamic origin-destination demand (in 10-minute intervals) comprising a total of 45,143 vehicles and various MPRs (10%, 25%, 50%, 75% and 100%) are considered for analysis over a 120-minute period of interest. Performance statistics are collected only for the vehicles generated between the 30<sup>th</sup> and 90<sup>th</sup> minutes to ensure that results are not biased by the warm-up or end periods of the simulation. Figure 7.3 shows the Borman Expressway network and its demand profile.

An incident scenario is modeled in which the incident lasts for 1 hour, from the 15<sup>th</sup> minute to the 75<sup>th</sup> minute, and reduces the capacity to 1/4 of the original capacity for that period. Figure 7.3 (a) shows the location of the incident on State Road 912. The time-dependent number of vehicles entering the network and the number of vehicles present in the network are shown in Figure 7.3



(a) Study network



(b) Demand profile and network conditions

Figure 7-3 Study network and associated characteristics

### **7.4.3 Historical database for link travel time distribution**

A historical database is generated for the link travel time distribution by simulating 50 days of network conditions for the 2-hour period of interest using randomly generated origin-destination demands from a range that is  $\pm 50\%$  from the base demand (45,143 vehicles). Based on these 50 simulation runs, the link travel time distributions are generated for each link for 10-minute time intervals. The historical database is stored as a discrete link travel time distribution. All V2V-equipped vehicles are assumed to access the same historical database before the start of their trips.

### **7.4.4 Baseline and system optimal scenarios**

Baseline and system optimal (SO) scenarios are used to benchmark the effectiveness and robustness of the proposed V2V-based ATIS. The baseline scenario represents the situation without the V2V-based ATIS. Therefore, the MPR is zero for this scenario. The SO solution corresponds to the best system performance and is used as benchmark for real-time deployment strategies.

## **7.5 Results**

The experiments mainly seek to analyze the performance of the routing decisions provided by the V2V-based ATIS. The system performance depends on the dynamic vehicle-level knowledge and many factors such as origin-destination demand, MPR, V2V communications constraints, and the presence of incidents in the network. Thus, we analyze the relationship between these factors and the system performance. Section 7.5.1 discusses the results related to the V2V communications and evolution of vehicle-level knowledge. Section 7.5.2 illustrates the performance of the baseline and SO scenarios. Sections 7.5.3 and 7.5.4 analyze the performance of the V2V-based ATIS under incident-free and incident scenarios, respectively.

### **7.5.1 V2V communications efficiency and vehicle-level knowledge**

The performance of V2V-based ATIS depends on the timely dissemination of travel-related information and the accurate estimation/prediction of prevailing traffic conditions. First, we analyze the V2V communications efficiency by focusing on the success rate of communication under different MPRs. The success rate  $\mu$  is calculated as follows:

$$\mu = s / (s + f), \quad (7)$$

where  $s$  is the number of communications that successfully transmit information to other V2V-equipped vehicles, and  $f$  is the number of communications that fail to transmit information due to the communication constraints.

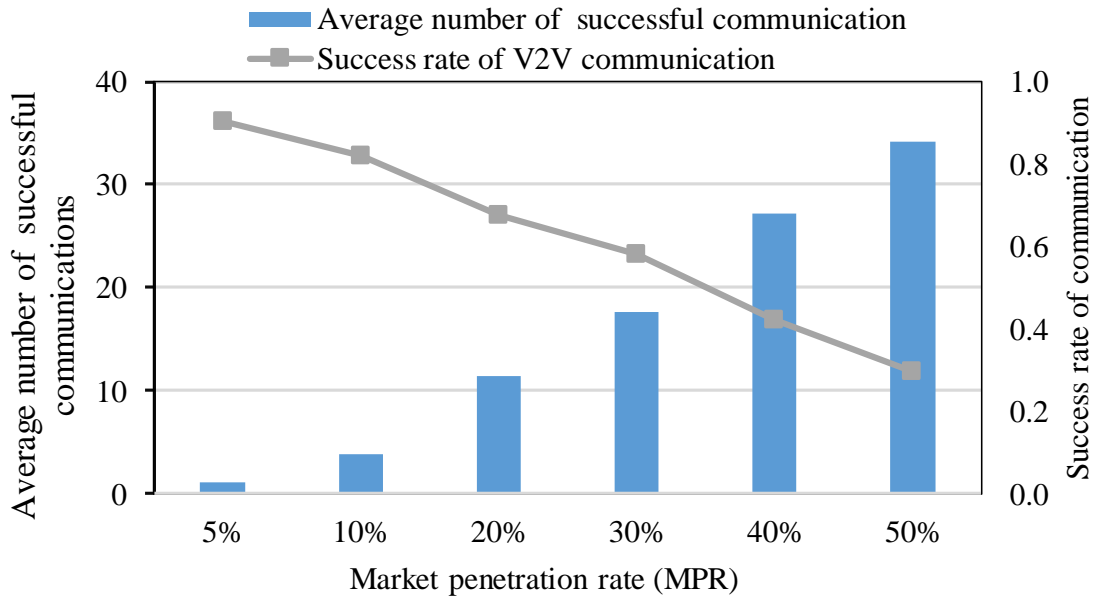


Figure 7-4 Efficiency of V2V communications under different MPR

Figure 7.4 shows the values of  $\mu$  under different MPRs. The success rate of V2V communications decreases as MPR increases, though the number of successful communications increases. It implies that the larger number of V2V-equipped vehicles within communication range increases the potential for interference, but also increases the opportunities for communications among V2V-equipped vehicles.

The amount of information obtained by V2V-equipped vehicles is measured by the number of obtained travel experience data during the trip. Figure 7.5 shows the number of obtained travel experience data during the equipped vehicles' trips under a 25% MPR. It indicates that the number of obtained travel experience data increases as vehicles are closer to their destinations and/or for longer trips. Also, the number of travel experience data is stable after 30 minutes of trip time; this is because as vehicles are closer to their destinations, they may discard older (20 minutes old and beyond) and duplicate data from the vehicle's onboard memory storage.

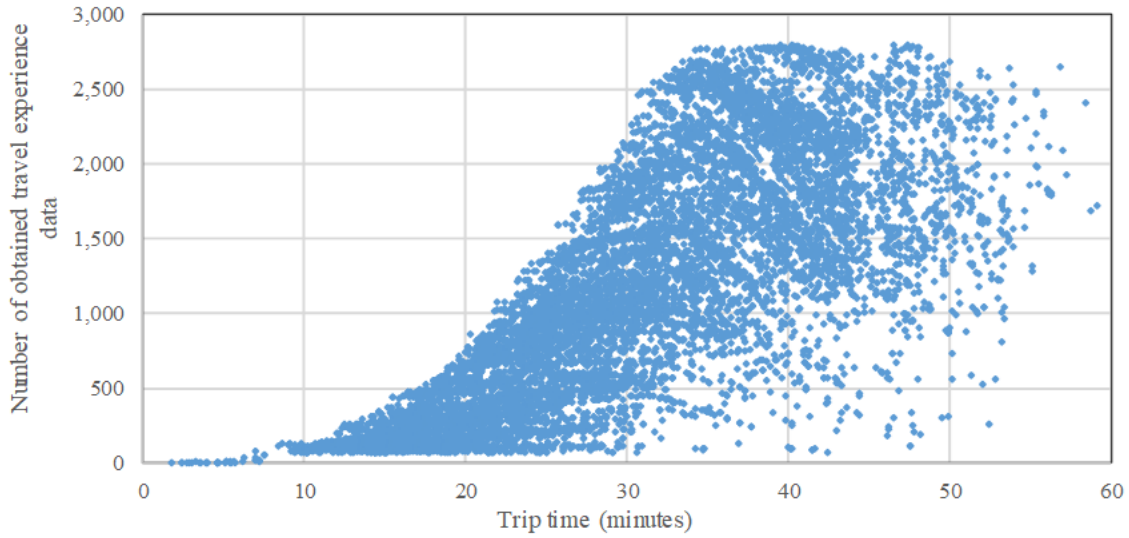


Figure 7-5 Number of obtained travel experience data during trips

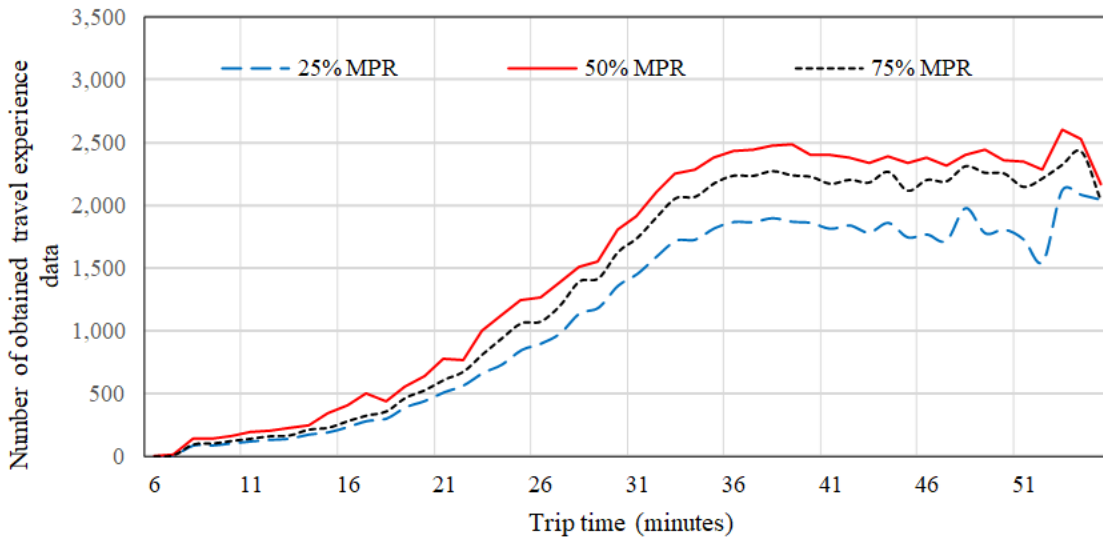


Figure 7-6 Number of obtained travel experience data during trips for different MPRs

Figure 7.6 shows that the performance in terms of the number of obtained travel experience data is the best for 50% MPR, and reduces for 75% MPR. This is due to the communications bandwidth constraint as the available capacity is shared by more equipped vehicles under 75% MPR. This illustrates that congestion in a V2V communications environment can lead to congestion effects for information flow propagation.

## 7.5.2 Baseline and SO scenarios

Table 7.1 summarizes the performance of the baseline and SO scenarios in terms of travel time under the incident-free and incident scenarios. The average travel time of vehicles under SO decreases by 22% in the incident-free scenario and 16% in the incident scenario compared to the baseline. The presence of the incident increases travel time by approximately 15% in the baseline scenario.

Table 7-1 Comparison to baseline and SO scenarios

Scenarios	Baseline		System optimal (SO)	
	Average travel time (minutes)	Total system travel time (hours)	Average travel time (minutes)	Total system travel time (hours)
Incident-free	13.23	7,775	13.23	7,775
Incident	15.28	9,702	15.28	9,702

## 7.5.3 Incident-free scenario

### 7.5.3.1 Analysis of network performance

The system performance is analyzed in two aspects: (i) fraction of V2V-equipped vehicles that change routes en route due to updated vehicle-level knowledge, and (ii) network performance. As shown in Table 7.2, the number of V2V-equipped vehicles that change routes en route increases as the MPR increases. However, the fraction changing routes en route increases until MPR 50% and then decreases with higher MPRs. As shown in Figure 7.6, this could be due to the size of the obtained travel experience data whereby due to congestion effects on information flow propagation, the efficiency of V2V-based ATIS is reduced.

We analyze the average travel times of V2V-equipped, unequipped, and all vehicles as the primary measure of effectiveness of the proposed V2V-based ATIS. Figure 7.7 illustrates that V2V-based ATIS offers the potential for travel time savings. The average travel time for V2V-equipped vehicles decrease up to an MPR of 50%. For 75% and 100% MPRs, V2V-equipped vehicles experience higher travel times than under 50% MPR. This is possibly because many V2V-equipped vehicles shift to the same route en route, and the travel time of that route increases

accordingly. Further, the average travel times under the different MPRs (12.6 to 13.2 minutes) are much higher than for SO (10.33 minutes). These results suggest that a V2V-based ATIS can be leveraged through coordinated traffic management strategies involving a central controller to generate additional savings over the uncoordinated individual vehicle-level V2V-based ATIS.

It is also insightful to examine the effect of MPRs on the unequipped vehicles. Figure 7.7 illustrates that a V2V-based ATIS can be beneficial for unequipped vehicles, though V2V-equipped vehicles benefit much more than the unequipped vehicles. The average travel time for all vehicles reduces as the MPR of V2V-equipped vehicles increases.

Table 7-2 V2V-equipped vehicles changing routes en route for different MPRs

MPR	Number of V2V-equipped vehicles	Vehicles that change routes en route	Vehicles that do not change routes en route	Fraction of vehicles changing routes en route
10%	4,514	1,129	3,385	0.25
25%	11,286	3,273	8,013	0.29
50%	22,572	7,900	14,672	0.35
75%	33,857	10,834	23,023	0.32
100%	45,143	13,994	31,149	0.31

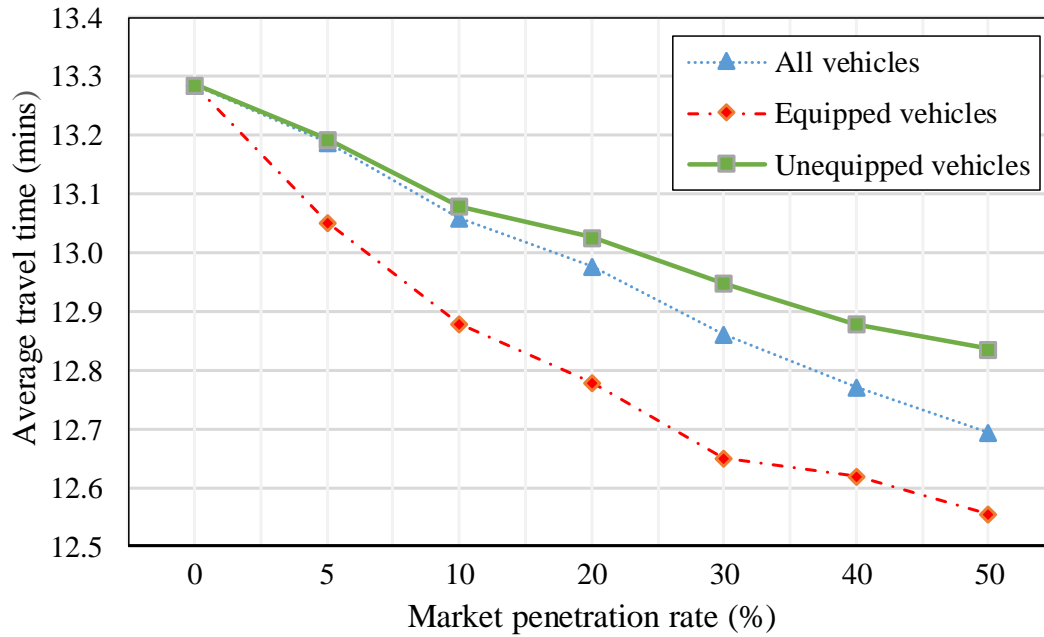


Figure 7-7 Effects of MPR on average travel time under the incident-free scenario

### 7.5.3.2 Analysis of individual vehicle performance

Figure 7-8 compares the individual vehicles' travel times under the V2V-based ATIS to those under the baseline scenario for 25% MPR. It can be noted that in several cases the V2V-equipped vehicles experience negative benefits (increased travel time), implying that information quality can impact the performance of a V2V-based ATIS. However, these cases are dominated by V2V-equipped vehicles with trip times less than 30 minutes (shorter trips).

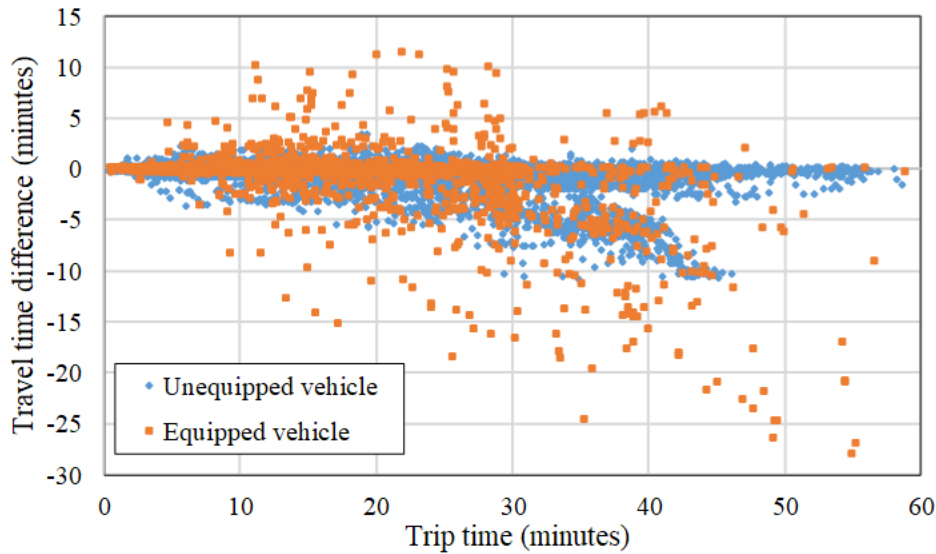


Figure 7-8 Distribution of travel time differences for different trip time (under 25% MPR)

It can be noted that more travel time savings occur for longer trips under the V2V-based ATIS compared to the baseline scenario. This is because longer trips may provide better travel time estimates due to the larger number of obtained travel experience data as illustrated by Figure 7.5 in Section 7.5.1. Further, Figure 7.8 suggests that while unequipped vehicles also benefit under a V2V-based ATIS, their share of travel time savings is significantly less than that of V2V-equipped vehicles.

#### 7.5.4 Incident scenario

This experiment investigates the performance of a V2V-based ATIS under an incident (State Road 912 in Figure 7.3). While unequipped vehicles remain on their initial routes, V2V-equipped vehicles may shift routes to avoid the temporary bottleneck due to the incident. Figure 7.9 illustrates that the average travel time is reduced up to 5.8% under the 50% MPR for the incident scenario. This illustrates a superior performance than under the incident-free scenario (2.7% reduction in Figure 7.7). This improvement is due to the incident response enabled by using a reactive algorithm which can respond quickly to changing network conditions. Similar to the incident-free scenario, V2V-equipped vehicles experience higher travel times for 100% MPR compared to those under 50% and 75% MPRs.

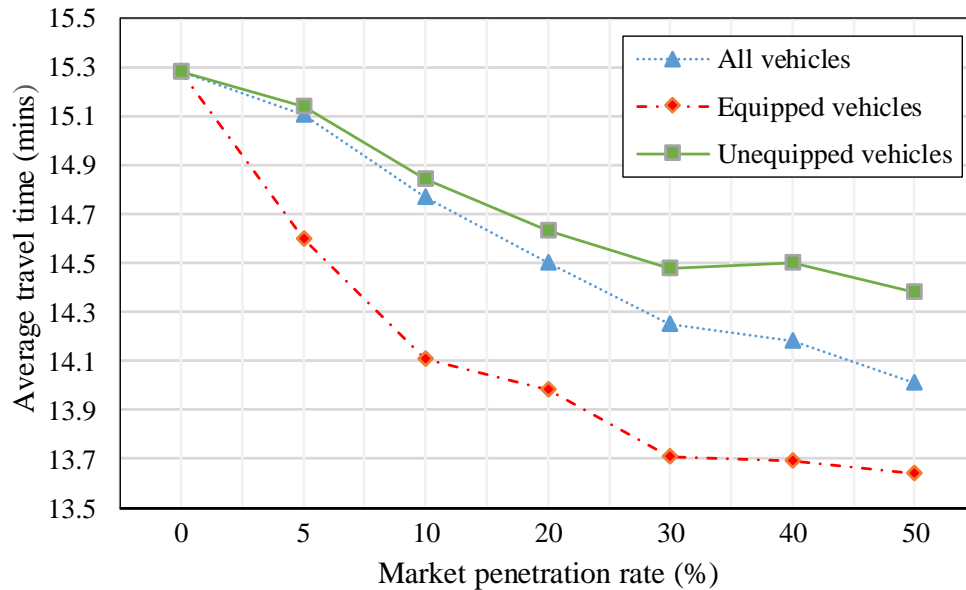


Figure 7-9 Effects of MPR on average travel time under incident scenario

## 7.6 Concluding comment

This study analyzes a fully decentralized V2V-based ATIS which leverages spatiotemporal vehicle-level knowledge and entails vehicle-level computation. The interdependencies between traffic flow dynamics, V2V communications constraints, and information flow propagation impact traveler routing decisions, thereby determining the performance of the V2V-based ATIS. A simulation-based approach is used to capture the impacts of the interdependencies between information flow propagation and travelers' routing decisions on the network state evolution and the performance of the V2V-based ATIS. Hence, this study closes the loop on understanding how information flow propagation affects network state evolution through routing decisions, and how network evolution affects information flow propagation in terms of obtained travel experience data.

The study results show that as a consequence of information propagation, the level of vehicle knowledge may vary. That is, informed routing decisions depend on traffic flow dynamics, V2V communications constraints, and MPR of V2V-equipped vehicles. A V2V-based ATIS can lead to travel time savings under both incident-free and incident scenarios. Travel time benefits are higher for incident scenarios, possibly due to rapid incident response. The study also suggests that a V2V-based ATIS can provide benefits to both V2V-equipped and unequipped vehicles.

Experiment results also indicate that enabling some level of formal coordination of decision-making across V2V-equipped vehicles through a centralized controller can enhance network-level traffic performance, especially under high MPRs to counteract the effects of communications-related constraints. The proposed V2V-based ATIS framework can be expanded to implement a hybrid centralized system that has some level of coordination of decision-making across vehicles in addition to individual vehicle-level knowledge for routing decisions.

## 8. CONCLUSIONS

This chapter summarizes the study and the research contributions and suggests directions for future research. Section 8.1 summarizes the research and discusses associated conclusions. Section 8.2 highlights the significance of the research, and Section 8.3 discusses possible extensions for future research.

### 8.1 Summary and conclusions

This dissertation proposes a systematic framework of V2V-based traffic system that is integrated with the information flow propagation with physical traffic flow, vehicle-to-vehicle communications, and V2V applications. The V2V-based traffic system is characterized by non-linearity, interdependencies, and feedback structure. Due to the multi-dimensional impacts of traffic flow dynamics and inter-vehicle communication constraints on information flow propagation, the need to model and understand their interdependencies is a fundamental problem for a V2V-based traffic system. While widely-used analytical models exist to characterize the influencing factors in the communication and transportation domains, their interdependencies have not fully explored within the framework of V2V-based traffic system. The research focuses on understanding how information flow propagate in space and time while capturing the dependency with the underlying traffic flow.

This study proposes a graph-based multi-layer framework to model multiple units of information flow evolution and propagation by integrating traffic flow model and vehicle-to-vehicle communications model. It illustrates the potential benefits of the retrospective capability to identify the spatiotemporal characteristics of vehicle knowledge. Synthetic experiments illustrate how the proposed framework maps how the information flow dynamics are determined by the traffic flow dynamics and inter-vehicle communication constraints. As graph structure is shown to be able to track the spatiotemporal characteristics of information flow explicitly, the graph-based multi-layer framework is extended to develop the analytical multi-layer framework. They illustrate that the proposed analytical multi-layer framework can integrate the dynamics of traffic flow and inter-vehicle communication constraints to generate insights for the propagation of the multiple units of information flow.

This study develops a discrete analytical model to track dynamic information flow propagation by integrating a traffic flow model and an epidemic model. This study defines the information flow propagation wave (IFPW) to address the macroscopic behavior of information flow propagation. The proposed model characterizes the single-hop communication to reflect the details of communication constraints. Incorporated into a multi-hop information dissemination process through integro-differential equations, the proposed model allows to derive a closed-form solution for the IFPW speed. A theoretical investigation provides useful insights into the qualitative properties of information flow propagation speed and a better understanding of the fundamental relationship between traffic flow dynamics and information flow propagation that enable broader applications based on V2V communications.

This thesis has integrated the key influencing factors for applications of traffic safety and management and control. The comprehensive coverage through V2V communications brings a possible benefit that information of multiple vehicles ahead can be used as a priori knowledge to predict the collision risk associated with a lead-vehicle. This study proposes a multi-anticipative FCW system that predicts the driver maneuver intention to incorporate the uncertainty of motion prediction. The multiple vehicle motion prediction is modeled by a coupled Hidden Markov model, motivated by statistical machine learning techniques. It overcomes the limitation of the currently available sensor-based kinematic model for addressing the uncertainty associated with future motion prediction.

An assessment of V2V-based ATIS on vehicular traffic efficiency requires consideration of multiple units of information flow propagation and thus a large number of communications and reacting vehicles. In this context, this study focuses on modeling the information flow evolution and propagation that leads to the dynamics of vehicle knowledge in V2V-based ATIS as a building block to develop coordinated information provision strategies that additionally would require an understanding of how the vehicle knowledge would affect the driver actions.

## **8.2 Research Contributions**

As information flow propagation entails complex interdependent processes, an explicit understanding of their linkages for design, planning, and operation is important. This dissertation suggests the use of the concept of an integrated multi-layer network modeling framework that can

describe the network-wide spatiotemporal propagation of information while capturing the interdependencies with traffic flow dynamics and V2V communications. An important practical implication of the proposed methodology is the ability to generate effective traffic control strategies under V2V-based ATIS. The proposed methodology can serve as a platform to address several other applications and modeling needs related to V2V-based ATIS; they include routing strategies for specific classes of vehicles, targeted information propagation strategies to alleviate local traffic situations, rapid information communication strategies to address emergent safety problems, seamless communication of pricing strategies, etc.

This study proposes a macroscopic model that characterizes the multi-hop process of information flow propagation based on the broadcasting method rather than the widely-used assumption of instantaneous multi-hop propagation while characterizing the single-hop communication to reflect the details of communication constraints. The proposed model and the closed-form solution of IFPW speed can help in designing effective V2V-based systems, without relying on computationally expensive numerical methods. From a communication point of view, it bridges the relationship between wireless network characteristics and the information flow propagation speed through communication kernel. Therefore, it enables communication engineers to choose the best wireless communication parameters to satisfy a certain speed threshold of information flow propagation. From a transportation point of view, the proposed model can be used to design prescriptive strategies that promote the propagation of useful information efficiently. Further, it can be used to develop a vehicle to infrastructure (V2I) placement strategy where the average delay to reach a vehicle at any location is bounded by a prescribed threshold. To enable these V2V-based applications and associated design, a wide range of research questions need to be answered by researchers in electrical engineering, computer science, and information communication. Therefore, this research would introduce great research opportunities in such an interdisciplinary research domain.

From a practical standpoint, the proposed graph-based approach can efficiently model the V2V-based ATIS by leveraging a single graph database. It provides memory efficiency through the use of a graph database and computational efficiency through the use of a simple reverse search algorithm to update the vehicle knowledge by traversing a connected subgraph of the information

flow network. Hence, graph-based modeling to identify vehicle knowledge can provide powerful capabilities to leverage efficient graph-based methods and algorithms.

### **8.3 Future Research**

This section discusses several possible extensions of the proposed models. The study offers the possibility of developing more sophisticated information flow propagation models by leveraging well-developed mathematical theories in epidemiology and ecology. This study applies a spatially structured model that is quite flexible and can be extended to a spectrum of models. One advantage of the spatially structured model is that it is particularly amenable to mathematical analysis. The analysis can lead to many important insights into the characteristics of IFPW. A stochastic modeling capability to generate greater realism can be incorporated. This study establishes a deterministic model upon the basic assumption that the population is large enough to ignore stochastic effects. A more comprehensive study could include stochastic effects, which are particularly important when vehicle density is low.

In addition, we present the effects of spatial heterogeneity on the information flow wave speed using the numerical experiments. Although it is confirmed that numerical solution is realized as an analytical solution, we have not developed analytical solutions for the heterogeneous environment. This problem needs further investigation.

On the application of V2V-based system, vehicles need to autonomously choose the wireless network parameters (such as transmission power, communication frequency, and data rate) that best fit an application's needs, for example, satisfying the minimum information flow propagation speed threshold for safety applications (Killat and Hartenstein, 2009). To do so, it is required to understand the relationship between wireless network parameters and information flow propagation speed. The complexity of the numerous influencing factors, however, impedes the determination of an appropriate relationship in general. If such linkages are identified in the planning stage, it can be formulated and solved as a corresponding optimization problem to achieve the maximum speed. The proposed model is a suitable approach that maintains accuracy and flexibility without relying on computational expensive simulation.

The study offers the possibility of developing a more sophisticated FCW system. While we use a fixed parameters FCW system (non-adaptive), disagreement between the human drivers and

system response always exists. Therefore, the development of the adaptive FCW system is important. The most preferable tradeoff between false alarms and miss alarm is arguably varying from situation-to-situation and across different driver groups. Driver behavior in the presence of the collision warning/avoidance system, is usually the additional input of these algorithms, in order to make the system effective and acceptable to the driver. A system that integrates machine learning mechanism with predictive FCW algorithm, so that the system can adjust its settings by interacting with the driver is promising.

It may be synergistic with a hybrid system which combines a predictive, behavior-consistent logic of a centralized system with the decentralized, reactive logic of the proposed V2V-based ATIS. The design of the hybrid system is focused on the effectiveness and quality of hybrid guidance logic by addressing the strengths and weaknesses of centralized and decentralized systems. The capabilities of the hybrid framework can leverage behavioral realism and the synergies of the centralized and decentralized systems.

## REFERENCES

- Ammoun, S., and Nashashibi, F. (2010). "Design and efficiency measurement of cooperative driver assistance system based on wireless communication devices." *Transportation research part C: emerging technologies*, Elsevier, 18(3), 408–428.
- Batz, T., Watson, K., and Beyerer, J. (2009). "Recognition of dangerous situations within a cooperative group of vehicles." *IEEE Intelligent Vehicles Symposium, Proceedings*, 907–912.
- Bauza, R., and Gozávez, J. (2013). "Traffic congestion detection in large-scale scenarios using vehicle-to-vehicle communications." *Journal of Network and Computer Applications*, Elsevier, 36(5), 1295–1307.
- Benedetto, F., Calvi, A., D'Amico, F., and Giunta, G. (2015). "Applying telecommunications methodology to road safety for rear-end collision avoidance." *Transportation research part C: emerging technologies*, Elsevier, 50, 150–159.
- Biswas, S., Tatchikou, R., and Dion, F. (2006a). "Vehicle-to-vehicle wireless communication protocols for enhancing highway traffic safety." *IEEE Communications Magazine*, 44(1), 74–82.
- Biswas, S., Tatchikou, R., and Dion, F. (2006b). "Vehicle-to-vehicle wireless communication protocols for enhancing highway traffic safety." *IEEE Communications Magazine*, 44(1), 74–82.
- Bliss, J. P., and Acton, S. A. (2003). "Alarm mistrust in automobiles: how collision alarm reliability affects driving." *Applied ergonomics*, Elsevier, 34(6), 499–509.
- Bottom, J. A. (2000). "Consistent anticipatory route guidance" *PhD thesis, Massachusetts Institute of Technology*.
- Bottom, J., Bierlaire, M., Chabini, I., Koutsopoulos, H., and Yang, Q. (1999). "Investigation of Route Guidance Generation Issues by Simulation with DynaMIT." *14th International Symposium on Transportation and Traffic Theory*, 577–600.
- Brand, M., Oliver, N., and Pentland, A. (1997). "Coupled hiddenMarkov models for complex action recognition." *International Conference on Computer Vision and Pattern Recognition*, 1–6.
- Briesemeister, L., Schäfers, L., and Hommel, G. (2000). "Disseminating messages among highly mobile hosts based on inter-vehicle communication." *Intelligent Vehicles Symposium, 2000. IV 2000. Proceedings of the IEEE*, 522–527.

- Brown, T. L., Lee, J. D., and McGehee, D. V. (2001). "Human Performance Models and Rear-End Collision Avoidance Algorithms." *Human Factors: The Journal of the Human Factors and Ergonomics Society*, 43(3), 462–482.
- Brunson, S. J., Kyle, E. M., Phamdo, N. C., and Preziotti, G. R. (2002). Alert algorithm development program: NHTSA rear-end collision alert algorithm.
- Burgett, A., Carter, A., and Preziotti, G. (2001). "Algorithm for Rear-End Collision Avoidance Warning Systems." *Proceedings of the 17th ESV Conference*, 1–8.
- Burgett, A. L., and Miller, R. J. (2001). A new paradigm for rear-end crash prevention driving performance.
- Chen, K., and Underwood, S. E. (1991). "Research on anticipatory route guidance." *SAE Technical Papers*, (P-253 pt 1), 427–439.
- Chen, T. M., and Robert, J.-M. (2004). "Worm epidemics in high-speed networks." *Computer*, 37(6), 1–14.
- Chen, Z., Gao, L., and Kwiat, K. (2003). "Modeling the spread of active worms." INFOCOM 2003. Twenty-Second Annual Joint Conference of the IEEE Computer and Communications. IEEE Societies, 1890–1900.
- Cheu, R., Martinez, J., and Duran, C. (2009). "A cell transmission model with lane changing and vehicle tracking for port of entry simulations." *Transportation Research Record: Journal of the Transportation Research Board*, Transportation Research Board of the National Academies, (2124), 241–248.
- Choffnes, D. R., and Bustamante, F. E. (2005). "An integrated mobility and traffic model for vehicular wireless networks." *Proceedings of the 2nd ACM international workshop on Vehicular ad hoc networks*, 69–78.
- Cole, R. G., Phamdo, N., Rajab, M., Terzis, A., and others. (2005). "Requirements on worm mitigation technologies in MANETS." *Principles of Advanced and Distributed Simulation, 2005. PADS 2005. Workshop on*, 207–214.
- Daganzo, C. F. (1994). "The cell transmission model: A dynamic representation of highway traffic consistent with the hydrodynamic theory." *Transportation Research Part B: Methodologica*, 28(4), 269–287.
- Daganzo, C. F. (1995). "The cell transmission model, part II: Network traffic." *Transportation Research Part B: Methodological*, 29(2), 79–93.

- Dingus, T. a., Klauer, S. G., Neale, V. L., Petersen, A., Lee, S. E., Sudweeks, J., Perez, M. a., Hankey, J., Ramsey, D., Gupta, S., Bucher, C., Doerzaph, Z. R., Jermeland, J., and Knippling, R. R. (2006). "The 100-Car naturalistic driving study phase II – Results of the 100-Car field experiment." *Dot Hs 810 593*, (April), No. HS-810 593.
- Du, L., and Dao, H. (2015). "Information dissemination delay in vehicle-to-vehicle communication networks in a traffic stream." *IEEE Transactions on Intelligent Transportation Systems*, 16(1), 66–80.
- Du, L., Peeta, S., and Kim, Y. H. (2012). "An adaptive information fusion model to predict the short-term link travel time distribution in dynamic traffic networks." *Transportation Research Part B: Methodological*, Elsevier Ltd, 46(1), 235–252.
- Du, L., Peeta, S., and Kim, Y. H. (2013). "Online Stochastic Routing Incorporating Real-Time Traffic Information." *Transportation Research Record: Journal of the Transportation Research Board*, 2334(1), 95–104.
- Eichler, S., Ostermaier, B., Schroth, C., and Kosch, T. (2005). "Simulation of car-to-car messaging: Analyzing the impact on road traffic." *Proceedings - IEEE Computer Society's Annual International Symposium on Modeling, Analysis, and Simulation of Computer and Telecommunications Systems, MASCOTS, 2005*, 507–510.
- Fitzgibbons, B., Fujimoto, R., Guensler, R., Hunter, M., Park, A., and Wu, H. (2004). "Distributed Simulation Test Bed for Intelligent Transportation Systems Design and Analysis." *Proceedings of the 2004 Annual National Conference on Digital Government Research*, dg.o '04, Digital Government Society of North America, 32:1--32:2.
- Fujimoto, R., Riley, G., Wu, H., Fujimoto, R., and Riley, G. (2004). "Analytical models for information propagation in vehicle-to-vehicle networks." *IEEE 60th Vehicular Technology Conference, 2004. VTC2004-Fall. 2004*, 6(C), 4548–4552.
- Grenfell, B. T., Bjørnstad, O. N., and Kappey, J. (2001). "Travelling waves and spatial hierarchies in measles epidemics." *Nature*, Nature Publishing Group, 414(6865), 716–723.
- Gupta, P., and Kumar, P. R. (2000). "The capacity of wireless networks." *Information Theory, IEEE Transactions on*, IEEE, 46(2), 388–404.

- Han, L., Ukkusuri, S., and Doan, K. (2011). “Complementarity formulations for the cell transmission model based dynamic user equilibrium with departure time choice, elastic demand and user heterogeneity.” *Transportation Research Part B: Methodological*, Elsevier, 45(10), 1749–1767.
- Hastings, A. (1996). “Models of spatial spread: a synthesis.” *Biological Conservation*, Elsevier, 78(1), 143–148.
- Hawas, Y., and Mahmassani, H. (1996). “Comparative Analysis of Robustness of Centralized and Distributed Network Route Control Systems in Incident Situations.” *Transportation Research Record*, 1537(1), 83–90.
- Van Der Horst, R., and Hogema, J. (1993). “Time-to-collision and collision avoidance systems.” *proceedings of The 6th Workshop of the International*, 1–12.
- Hou, H., Jin, L., Niu, Q., Sun, Y., and Lu, M. (2011). “Driver Intention Recognition Method Using Continuous Hidden Markov Model.” *International Journal of Computational Intelligence Systems*, 4(3), 386–393.
- Jacquet, P., Mans, B., and Rodolakis, G. (2010). “Information propagation speed in mobile and delay tolerant networks.” *Information Theory, IEEE Transactions on*, IEEE, 56(10), 5001–5015.
- Jayakrishnan, R., Mahmassani, H. S., and Hu, T.-Y. (1994). “An evaluation tool for advanced traffic information and management systems in urban networks.” *Transportation Research Part C: Emerging Technologies*, 2(3), 129–147.
- Jiang, D., Chen, Q., and Delgrossi, L. (2008). “Optimal data rate selection for vehicle safety communications.” *Proceedings of the fifth ACM international workshop on VehiculAr Inter-NETworking*, 30–38.
- Jin, W.-L., and Recker, W. W. (2006). “Instantaneous information propagation in a traffic stream through inter-vehicle communication.” *Transportation Research Part B: Methodological*, Elsevier, 40(3), 230–250.
- Jin, W., and Recker, W. W. (2010). “Transactions Papers An Analytical Model of Multihop Connectivity of Inter-Vehicle Communication Systems.” 9(1), 106–112.
- Jinyang Li, Blake, C., De Couto, D. S. J., Lee, H. I., and Morris, R. (2001). “Capacity of Ad Hoc wireless networks.” *Proceedings of the 7th annual international conference on Mobile computing and networking - MobiCom '01*, (1), 61–69.

- Karagiannis, G., Altintas, O., Ekici, E., Heijenk, G., Jarupan, B., Lin, K., and Weil, T. (2011). “Vehicular networking: A survey and tutorial on requirements, architectures, challenges, standards and solutions.” *IEEE Communications Surveys and Tutorials*, 13(4), 584–616.
- Keeling, M. J. (1999). “The effects of local spatial structure on epidemiological invasions.” *Proceedings. Biological sciences / The Royal Society*, 266(1421), 859–67.
- Keeling, M. J., and Rohani, P. (2008). *Modeling infectious diseases in humans and animals*. Princeton University Press.
- Kermack, W. O., and McKendrick, A. G. (1927). “A contribution to the mathematical theory of epidemics.” *Proceedings of the Royal Society of London A: Mathematical, Physical and Engineering Sciences*, 700–721.
- Kesting, A., Treiber, M., and Helbing, D. (2010). “Connectivity statistics of store-and-forward intervehicle communication.” *IEEE Transactions on Intelligent Transportation Systems*, 11(1), 172–181.
- Khelil, A., Becker, C., Tian, J., and Rothermel, K. (2002). “An epidemic model for information diffusion in MANETs.” *Proceedings of the 5th ACM international workshop on Modeling analysis and simulation of wireless and mobile systems*, 54–60.
- Kiefer, R., LeBlanc, D., Palmer, M., Salinger, J., Deering, R., and Shulman, M. (1999). “Development and Validation of Functional Definitions and Evaluation Procedures For Collision Warning/Avoidance Systems.”
- Killat, M., and Hartenstein, H. (2009). “An empirical model for probability of packet reception in vehicular ad hoc networks.” *Eurasip Journal on Wireless Communications and Networking*, 2009(1).
- Kim, H. (2007). A simulation framework for traffic information dissemination in ubiquitous vehicular ad hoc networks. ProQuest.
- Kim, Y. H. and Peeta, S. (2016). “Modeling the information flow propagation wave under vehicle-to-vehicle communications.” *Transportation Research Part C*, (85).
- Kim, Y. H., and Peeta, S. (2016). “Graph-Based Modeling of Information Flow Evolution and Propagation under V2V Communications-Based Advanced Traveler Information Systems.” *Computer-Aided Civil and Infrastructure Engineering*, (31).

- Kim, Y. H., Peeta, S., and He, X. (2014). “An analytical model to characterize the spatiotemporal propagation of information under vehicle-to-vehicle communications.” *2014 17th IEEE International Conference on Intelligent Transportation Systems, ITSC 2014*, 1142–1147.
- Knipling, R. R., Mironer, M., Hendricks, D. L., Tijeripa, L., and Everson, J. (1993). “Assessment of IVHS Countermeasures for Collision Avoidance: Rear-End Crashes.” (May), DOT HS 807 995.
- Koutsopoulos, H. N. (1993). “An information discounting routing for advanced traveler information discounting routing for advanced traveler information.” *Transportation Research, Part C: Emerging Technologies*, 1(3), 249–264.
- Kumagai, T., Sakaguchi, Y., Okuwa, M., and Akamatsu, M. (2003). “Prediction of Driving Behavior through Probabilistic Inference.” *Engineering Applications of Neural Networks, Eighth International Conference on*, (September), 8–10.
- Kumar, P., Perrollaz, M., Laugier, C., Kumar, P., Perrollaz, M., Kumar, P., and Perrollaz, M. (2013). “Learning-based approach for online lane change intention prediction To cite this version : Learning-Based Approach for Online Lane Change Intention Prediction.”
- Lee, J., and Park, B. (2008). “Evaluation of route guidance strategies based on vehicle-infrastructure integration under incident conditions.” *Transportation Research Record: Journal of the Transportation Research Board*, Transportation Research Board of the National Academies, (2086), 107–114.
- Lee, K., and Peng, H. (2005). “Evaluation of automotive forward collision warning and collision avoidance algorithms.” *Vehicle System Dynamics*, 43(10), 735–751.
- Lefèvre, S., Vasquez, D., and Laugier, C. (2014). “A survey on motion prediction and risk assessment for intelligent vehicles.” *ROBOMECH Journal*, 1(1), 1.
- Leontiadis, I., Marfia, G., MacK, D., Pau, G., Mascolo, C., and Gerla, M. (2011). “On the effectiveness of an opportunistic traffic management system for vehicular networks.” *IEEE Transactions on Intelligent Transportation Systems*, 12(4), 1537–1548.
- Lerner, N. D., Dekker, D. K., Steinberg, G. V, Huey, R. W., and Hs, D. (1996). “Inappropriate Alarm Rates and Driver Annoyance.” *Citeseer*, (February 1996).
- Li, L., and Wang, F.-Y. (2007). “Advanced vehicle longitudinal motion control.” *Advanced Motion Control and Sensing for Intelligent Vehicles*, Springer, 135–184.

Lighthill, M. J., and Whitham, G. B. (1955). "On Kinematic Waves. I. Flood Movement in Long Rivers." *Proceedings of the Royal Society A: Mathematical, Physical and Engineering Sciences*, 229(1178), 281–316.

Lin, W.-H., and Ahanotu, D. (1995). "Validating the basic cell transmission model on a single freeway link." *PATH technical note; 95-3*.

Mahmassani, H. S., Hawas, Y. E., Abdelghany, K., Abdelfatah, A., Chiu, Y. C., Kang, Y., Chang, G. L., Peeta, S., Taylor, R., and Ziliaskopoulos, A. (1998). "DYNASMART-X; Volume II: analytical and algorithmic aspects." *Technical Rep. ST067*, 85.

McLaughlin, S. B., Hankey, J. M., Dingus, T. a, and Klauer, S. G. (2009). "Development of an FCW algorithm evaluation methodology with evaluation of three alert algorithms." *National Highway Traffic Safety Administration, DOT HS*, 811(June), 145.

Michon, J. (1985). "A critical view of driver behavior models: what do we know, what should we do?" *Human behavior and traffic safety*, 485–520.

Minderhoud, M. M., and Bovy, P. H. L. (2001). "Extended time-to-collision measures for road traffic safety assessment." *Accident Analysis & Prevention*, Elsevier, 33(1), 89–97.

Mollison, D. (1972a). "The rate of spatial propagation of simple epidemics." *Proceedings of the sixth berkeley symposium on mathematical statistics and probability*, 579–614.

Mollison, D. (1972b). "Possible Velocities for a Simple Epidemic." *Advances in Applied Probability*, 4(2), 233–257.

Mollison, D. (1977). "Spatial contact models for ecological and epidemic spread." *Journal of the Royal Statistical Society. Series B (Methodological)*, JSTOR, 283–326.

Montanino, M., and Punzo, V. (2015). "Trajectory data reconstruction and simulation-based validation against macroscopic traffic patterns." *Transportation Research Part B: Methodological*, Elsevier Ltd, 80, 82–106.

Monteil, J., Billot, R., Sau, J., Armetta, F., Hassas, S., and El Faouzi, N.-E. (2013). "Cooperative Highway Traffic: Multiagent Modeling and Robustness Assessment of Local Perturbations." *Transportation Research Record: Journal of the Transportation Research Board*, Transportation Research Board of the National Academies, (2391), 1–10.

Muñoz, L., Sun, X., Sun, D., Gomes, G., and Horowitz, R. (2004). "Methodological calibration of the cell transmission model." *American Control Conference, 2004. Proceedings of the 2004*, 798–803.

- Najm, W. G., Sen, B., Smith, J. D., and Campbell, B. N. (2003). "Analysis of Light Vehicle Crashes and Pre-Crash Scenarios Based on the 2000 General Estimates System." *The National Academies of Sciences, Engineering, and Medicine*, 80 p.
- Nekovee, M. (2006). "Modeling the spread of worm epidemics in vehicular ad hoc networks." *Vehicular Technology Conference, 2006. VTC 2006-Spring. IEEE 63rd*, 841–845.
- Newman, M. E. J. (2002). "Spread of epidemic disease on networks." *Physical review E, APS*, 66(1), 16128.
- Ng, M., and Travis Waller, S. (2010). "A static network level model for the information propagation in vehicular ad hoc networks." *Transportation Research Part C: Emerging Technologies*, Elsevier Ltd, 18(3), 393–407.
- Palazzi, C. E., Rocchetti, M., and Ferretti, S. (2010). "An intervehicular communication architecture for safety and entertainment." *IEEE Transactions on Intelligent Transportation Systems*, 11(1), 90–99.
- Papageorgiou, M. (1990). "Dynamic modeling, assignment, and route guidance in traffic networks." *Transportation Research Part B*, 24(6), 471–495.
- Papageorgiou, M., and Messmer, A. (1991). "Dynamic network traffic assignment and route guidance via feedback regulation." *Transportation Research Record: Journal of the Transportation Research Board*, (1306), 49–58.
- Pavlis, Y., and Papageorgiou, M. (1999). "Simple Decentralized Feedback Strategies for Route Guidance in Traffic Networks." *Transportation Science*, 33(3), 264–278.
- Peeta, S., and Anastassopoulos, I. (2002). "Automatic Real-Time Detection and Correction of Erroneous Detector Data with Fourier Transforms for Online Traffic Control Architectures." *Transportation Research Record*, 1811(1), 1–11.
- Peeta, S., and Mahmassani, H. S. (1995a). "System optimal and user equilibrium time-dependent traffic assignment in congested networks." *Annals of Operations Research*, Springer, 60(1), 81–113.
- Peeta, S., and Mahmassani, H. S. (1995b). "Multiple user classes real-time traffic assignment for online operations: a rolling horizon solution framework." *Transportation Research Part C: Emerging Technologies*, Elsevier, 3(2), 83–98.

- Peeta, S., and Yu, J. W. (2004). "Adaptability of a hybrid route choice model to incorporating driver behavior dynamics under information provision." *Systems, Man and Cybernetics, Part A: Systems and Humans, IEEE Transactions on*, IEEE, 34(2), 243–256.
- Peeta, S., and Yu, J. W. (2005). "A hybrid model for driver route choice incorporating en-route attributes and real-time information effects." *Networks and Spatial Economics*, Springer, 5(1), 21–40.
- Peeta, S., and Yu, J. W. (2006). "Behavior-based consistency-seeking models as deployment alternatives to dynamic traffic assignment models." *Transportation Research Part C: Emerging Technologies*, Elsevier, 14(2), 114–138.
- Polychronopoulos, A., Tsogas, M., Amditis, A. J., and Andreone, L. (2007). "Sensor fusion for predicting vehicles' path for collision avoidance systems." *IEEE Transactions on Intelligent Transportation Systems*, 8(3), 549–562.
- Polychronopoulos, G. H., and Tsitsiklis, J. N. (1996). "Stochastic Shortest Path Problems with Recourse." *Networks*.
- Punzo, V., Borzacchiello, M. T., and Ciuffo, B. (2011). "On the assessment of vehicle trajectory data accuracy and application to the Next Generation SIMulation (NGSIM) program data." *Transportation Research Part C: Emerging Technologies*, Elsevier Ltd, 19(6), 1243–1262.
- Richards, P. I. (1956). "Shock waves on the highway." *Operations research*, INFORMS, 4(1), 42–51.
- Robinson, I., Webber, J., and Eifrem, E. (2013). *Graph databases*. "O'Reilly Media, Inc."
- Rvachev, L. A., and Longini, I. M. (1985). "A mathematical model for the global spread of influenza." *Mathematical biosciences*, Elsevier, 75(1), 3–22.
- Sakr, S., and Pardede, E. (2012). *Graph data management: techniques and applications*. Information Science Reference.
- Santa, J., Toledo-Moreo, R., Zamora-Izquierdo, M. A., Úbeda, B., and Gómez-Skarmeta, A. F. (2010). "An analysis of communication and navigation issues in collision avoidance support systems." *Transportation Research Part C: Emerging Technologies*, Elsevier Ltd, 18(3), 351–366.
- Schmidt-Eisenlohr, F., Torrent-Moreno, M., Mittag, J., and Hartenstein, H. (2007). "Simulation platform for inter-vehicle communications and analysis of periodic information exchange." *2007 Fourth Annual Conference on Wireless on Demand Network Systems and Services, WONS'07*, 50–58.

- Schroth, C., Dötzer, F., Kosch, T., Ostermaier, B., and Strassberger, M. (2005). “Simulating the traffic effects of vehicle-to-vehicle messaging systems.” *Proceedings of the 5th International Conference on ITS Telecommunications*, 4.
- Sepulcre, M., Gozalvez, J., and Hernandez, J. (2013). “Cooperative vehicle-to-vehicle active safety testing under challenging conditions.” *Transportation research part C: emerging technologies*, Elsevier, 26, 233–255.
- Spaho, E., Barolli, L., Mino, G., Xhafa, F., and Kolici, V. (2011). “VANET simulators: A survey on mobility and routing protocols.” *Proceedings - 2011 International Conference on Broadband and Wireless Computing, Communication and Applications, BWCCA 2011*, 1–10.
- Spyropoulou, I. (2007). “Simulation Using Gipps’ Car-Following Model—an in-Depth Analysis.” *Transportmetrica*, 3(3), 231–245.
- Tan, H. S., and Huang, J. (2006). “DGPS-based vehicle-to-vehicle cooperative collision warning: Engineering feasibility viewpoints.” *IEEE Transactions on Intelligent Transportation Systems*, 7(4), 415–427.
- Toledo, T. (2007). “Driving Behaviour: Models and Challenges.” *Transport Reviews*, 27(1), 65–84.
- Torrent-Moreno, M., Mittag, J., Santi, P., and Hartenstein, H. (2009). “Vehicle-to-vehicle communication: fair transmit power control for safety-critical information.” *Vehicular Technology, IEEE Transactions on*, IEEE, 58(7), 3684–3703.
- Trullols-Cruces, O., Fiore, M., and Barcelo-Ordinas, J. M. (2013). “Understanding, modeling and taming mobile malware epidemics in a large-scale vehicular network.” *World of Wireless, Mobile and Multimedia Networks (WoWMoM), 2013 IEEE 14th International Symposium and Workshops on a*, 1–9.
- Ukkusuri, S., and Du, L. (2008). “Geometric connectivity of vehicular ad hoc networks: Analytical characterization.” *Transportation Research Part C: Emerging Technologies*, Elsevier, 16(5), 615–634.
- Vuyyuru, R., and Oguchi, K. (2007). “Vehicle-to-vehicle ad hoc communication protocol evaluation using realistic simulation framework.” *Wireless on Demand Network Systems and Services, 2007. WONS’07. Fourth Annual Conference on*, 100–106.

- Wang, B. X., Yin, K., and Zhang, Y. (2012). “An exact markov process for multihop connectivity via intervehicle communication on parallel roads.” *IEEE Transactions on Wireless Communications*, 11(3), 865–868.
- Wang, J., Hoon, Y., He, X., and Peeta, S. (2016). “ScienceDirect Analytical model for information flow propagation wave under an information relay control strategy in a congested vehicle-to-vehicle communication environment.” 0, 1–20.
- Wang, X. (2007). “Modeling the process of information relay through inter-vehicle communication.” *Transportation Research Part B: Methodological*, Elsevier, 41(6), 684–700.
- Wang, Y., Papageorgiou, M., and Messmer, A. (1856). “Strategy for Freeway Network Traffic.” (3), 62–73.
- Werneke, J., Kleen, a., and Vollrath, M. (2013). “Perfect Timing: Urgency, Not Driving Situations, Influence the Best Timing to Activate Warnings.” *Human Factors: The Journal of the Human Factors and Ergonomics Society*, 56(2), 249–259.
- Winkler, S., Werneke, J., and Vollrath, M. (2016). “Timing of early warning stages in a multi stage collision warning system: Drivers’ evaluation depending on situational influences.” *Transportation Research Part F: Traffic Psychology and Behaviour*, Elsevier Ltd, 36, 57–68.
- Wu, C., Peng, L., Huang, Z., Zhong, M., and Chu, D. (2014). “A method of vehicle motion prediction and collision risk assessment with a simulated vehicular cyber physical system.” *Transportation Research Part C: Emerging Technologies*, Elsevier Ltd, 47(P2), 179–191.
- Wu, H., Fujimoto, R. M., Riley, G. F., and Hunter, M. (2009). “Spatial propagation of information in vehicular networks.” *IEEE Transactions on Vehicular Technology*, 58(1), 420–431.
- Wu, H., Fujimoto, R., and Riley, G. (2004). “Analytical models for information propagation in vehicle-to-vehicle networks.” *Vehicular Technology Conference, 2004. VTC2004-Fall. 2004 IEEE 60th*, 4548–4552.
- Wu, H., Lee, J., Hunter, M., Fujimoto, R., Guensler, R., and Ko, J. (2005a). “Efficiency of simulated vehicle-to-vehicle message propagation in Atlanta, Georgia, I-75 corridor.” *Transportation Research Record: Journal of the Transportation Research Board*, Transportation Research Board of the National Academies, (1910), 82–89.
- Wu, H., Lee, J., Hunter, M., Fujimoto, R. M., Guensler, R. L., and Ko, J. (2005b). “Simulated vehicle-to-vehicle message propagation efficiency on Atlanta’s I-75 corridor.” *Transportation Research Board Conference Proceedings, Washington DC*.

- Xu, H., and Barth, M. (2006). "Travel time estimation techniques for traffic information systems based on intervehicle communications." *Transportation Research Record: Journal of the Transportation Research Board*, (1944), 72–81.
- Yang, X., and Recker, W. (2005). "Simulation studies of information propagation in a self-organizing distributed traffic information system." *Transportation Research Part C: Emerging Technologies*, Elsevier, 13(5), 370–390.
- Yang, X., and Recker, W. (2006). "Modeling Dynamic Vehicle Navigation in a Self-Organizing, Peer-to-Peer, Distributed Traffic Information System." *Journal of Intelligent Transportation Systems*, 10(4), 185–204.
- Yang, X., and Recker, W. (2008). "Evaluation of information applications of a self-organizing distributed traffic information system for a large-scale real-world traffic network." *Computer-Aided Civil and Infrastructure Engineering*, 23(8), 575–595.
- Yin, K., Wang, X. B., and Zhang, Y. (2013). "Vehicle-to-vehicle connectivity on two parallel roadways with a general headway distribution." *Transportation Research Part C: Emerging Technologies*, Elsevier, 29, 84–96.
- Zhang, P., and Peeta, S. (2011). "A generalized modeling framework to analyze interdependencies among infrastructure systems." *Transportation Research Part B: Methodological*, Elsevier Ltd, 45(3), 553–579.
- Ziliaskopoulos, A., and Zhang, J. (2003). "A zero public infrastructure vehicle based traffic information system." *Transportation Research Board (TRB) Annual Meeting CD-ROM*, (July 2002).